

EX. A

# AAV2 Gene Therapy Readministration in Three Adults with Congenital Blindness

Jean Bennett,<sup>1,2,\*†</sup> Manzar Ashtari,<sup>3,\*†</sup> Jennifer Wellman,<sup>2</sup> Kathleen A. Marshall,<sup>2</sup> Laura L. Cyckowski,<sup>3</sup> Daniel C. Chung,<sup>1,2</sup> Sarah McCague,<sup>2</sup> Eric A. Pierce,<sup>1,4#</sup> Yifeng Chen,<sup>2</sup> Jeannette L. Bennicelli,<sup>1</sup> Xiaosong Zhu,<sup>4</sup> Gui-shuang Ying,<sup>5</sup> Junwei Sun,<sup>2</sup> J. Fraser Wright,<sup>2</sup> Alberto Auricchio,<sup>6,7</sup> Francesca Simonelli,<sup>6,8</sup> Kenneth S. Shindler,<sup>1</sup> Federico Mingozzi,<sup>2</sup> Katherine A. High,<sup>2,9</sup> Albert M. Maguire<sup>1,2,4</sup>

Demonstration of safe and stable reversal of blindness after a single unilateral subretinal injection of a recombinant adeno-associated virus (AAV) carrying the *RPE65* gene (AAV2-hRPE65v2) prompted us to determine whether it was possible to obtain additional benefit through a second administration of the AAV vector to the contralateral eye. Readministration of vector to the second eye was carried out in three adults with Leber congenital amaurosis due to mutations in the *RPE65* gene 1.7 to 3.3 years after they had received their initial subretinal injection of AAV2-hRPE65v2. Results (through 6 months) including evaluations of immune response, retinal and visual function testing, and functional magnetic resonance imaging indicate that readministration is both safe and efficacious after previous exposure to AAV2-hRPE65v2.

## INTRODUCTION

Leber congenital amaurosis (LCA) is a group of hereditary retinal dystrophies characterized by profound impairment in retinal and visual function in infancy and early childhood followed by progressive deterioration and loss of retinal cells in the first few decades of life (1–3). LCA is usually inherited as an autosomal recessive trait, and mutations in 15 different genes have been reported so far (4, 5). One of the more common forms of LCA, LCA2, is due to mutations in the *RPE65* gene (6, 7). This gene encodes an all-*trans*-retinyl ester isomerase, an enzyme critical to the function of the retinoid cycle (8, 9). Without RPE65, very little 11-*cis*-retinal, the vitamin A derivative that is the chromophore of rod and cone photoreceptor opsins, is made (8, 9). Without 11-*cis*-retinal, opsins cannot capture light and relay this into electrical responses to initiate vision (8, 10). Successful proof-of-principle studies in LCA2 murine and canine animal models using a replication-defective adeno-associated viral vector (rAAV) (11–14) demonstrated that the biochemical blockade of the visual cycle due to RPE65 deficiency could be overcome through gene augmentation. Safety and dosing studies in large animals then provided the pre-

clinical safety and efficacy data that formed the impetus to test this approach in human clinical trials (15–17).

We reported safe and stable amelioration in retinal and visual function in all 12 patients treated in a phase 1/2 study at The Children's Hospital of Philadelphia (CHOP) (16, 18–20). These individuals had been injected subretinally in the eye with worse vision in a dose-escalation study with doses ranging from  $1.5 \times 10^{10}$  to  $1.5 \times 10^{11}$  vector genomes (vg) of the AAV2 vector carrying the *RPE65* gene (AAV2.hRPE65v2) (16, 18). Each one of the subjects showed improvement in multiple measures of retinal and visual function in the injected eye. Most of the subjects showed improvement in full-field light sensitivity and pupillary light reflex (PLR). About half of the subjects showed significant improvement in visual acuity, and all showed a trend toward improvement in visual fields. Five of the 12 patients (including all pediatric subjects age 8 to 11 years) developed the ability to navigate a standardized obstacle course (16, 18). The improvements were observed as early as 1 month after treatment and persisted through the latest time point (now 4 years for the initial subjects) (16, 18, 20). Functional magnetic resonance imaging (fMRI) studies carried out in subjects after they had received the injection also showed that the visual cortex became responsive to retinal input after this unilateral gene therapy, even after prolonged visual deprivation (20). Both the retina and the visual cortex became far more sensitive to dim light and lower-contrast stimuli.

The success of the unilateral injections begged the question of whether additional visual function could be further gained in the contralateral eye of these patients. Because the immune consequences of subretinal readministration of rAAV2 were unknown, we carried out contralateral eye readministration studies in two different large-animal models. Readministration resulted in efficacy in both eyes in the affected dogs and appeared safe in both affected dogs and unaffected nonhuman primates (21). However, there is little precedent for the ability to safely readminister rAAV in humans and obtain a therapeutic effect. There was also a concern that immune responses after readministration would diminish the benefits that the subjects had obtained in their previously injected eye. We therefore proceeded cautiously to test safety and efficacy of administration to the contralateral eye in three adult subjects

<sup>1</sup>F. M. Kirby Center for Molecular Ophthalmology, Scheie Eye Institute, University of Pennsylvania, 309 Stellar-Chance Labs, 422 Curie Boulevard, Philadelphia, PA 19104, USA. <sup>2</sup>Center for Cellular and Molecular Therapeutics at The Children's Hospital of Philadelphia, Colket Translational Research Building, 3501 Civic Center Boulevard, Philadelphia, PA 19014, USA. <sup>3</sup>Department of Radiology, The Children's Hospital of Philadelphia, Philadelphia, PA 19014, USA. <sup>4</sup>Department of Ophthalmology, Children's Hospital of Philadelphia, Philadelphia, PA 19014, USA. <sup>5</sup>Scheie Eye Institute, Center for Preventive Ophthalmology and Biostatistics, Department of Ophthalmology, University of Pennsylvania, 3535 Market Street, Suite 700, Philadelphia, PA 19104, USA. <sup>6</sup>Telethon Institute of Genetics and Medicine, Via P. Castellino 111, 80131 Naples, Italy. <sup>7</sup>Medical Genetics, Department of Pediatrics, "Federico II" University, Via S. Pansini 5, 80131 Naples, Italy. <sup>8</sup>Department of Ophthalmology, Seconda Università degli Studi di Napoli, Via S. Pansini 5, 80131 Naples, Italy. <sup>9</sup>Howard Hughes Medical Institute, 3615 Civic Center Boulevard, Philadelphia, PA 19104, USA.

\*These authors contributed equally to this work.

†To whom correspondence should be addressed. E-mail: jebennet@mail.med.upenn.edu (J.B.); ashtari@email.chop.edu (M.A.)

#Present address: Ocular Genomics Institute, Massachusetts Eye and Ear Infirmary, Boston, MA 02114, USA.

who had already undergone unilateral subretinal injection in our phase 1/2 dose-escalation study (16, 18).

Through comparison of pre- and postsurgical testing, we demonstrate that delivery of AAV2-hRPE65v2 to the contralateral eye is safe even if years have passed since the initial treatment. Further, before and after comparisons of psychophysical data and fMRI results provide additional evidence for the effectiveness of gene therapy readministration in LCA2 patients and also reveal the magnitude and pattern of improvement. Results in two patients receiving different doses in each eye suggest a possible dose-response effect of the gene therapy vector.

## RESULTS

### Follow-on enrollment and study design

The readministration study was carried out as a “follow-on” (FO) study to the original phase 1/2 protocol (NCT01208389). The original protocol entailed injection into each subject’s more impaired eye (16, 18). The Institutional Review Board (IRB) had given approval for the contralateral eye administration as long as the first three subjects were adults. The first three adults enrolled in the FO study were CH12, CH11, and NP01, all of whom have missense mutations in *RPE65* (Table 1), and these individuals self-selected on the basis of availability. The disease was advanced in each one of these subjects, the degree of which correlated with their age due to the degenerative nature of LCA2. These individuals had received their initial injection 1.7 to 3.4 years earlier and were enrolled sequentially (with an 8-week interval between each enrollment). After providing informed consent, the subjects underwent “FO baseline” immunological and retinal/visual testing before the readministration. The schedule of tests in the FO study was similar to but not identical to the schedule in the initial study (table S1). Some tests that had been used in the initial study were dropped (for example, electroretinograms). Other analyses had been added during the course of the initial study, and these were maintained in the FO study including the full-field light sensitivity threshold (FST) test. Subjects also consented separately to participate in an fMRI study.

As with the initial injection, the area targeted in the readministration was selected on the basis of the results of clinical evaluations and retinal imaging studies indicating that the tissue in that region had sufficient numbers of viable retinal cells. Although the subjects had received different doses and volumes of AAV2-hRPE65v2 in their ini-

tial administration, they all received  $1.5 \times 10^{11}$  vg in 300  $\mu$ l for the readministration study in their previously uninjected (second) eye (Fig. 1A and Table 1). This was the same dose/volume that 46-year-old patient CH12 had received initially. The other two subjects (NP01 and CH11, 29 and 27 years, respectively) had previously received lower doses ( $1.5 \times 10^{10}$  and  $4.8 \times 10^{10}$  vg, respectively) in a volume of 150  $\mu$ l (Table 1). Post-injection safety, retinal/visual function, and fMRI imaging studies were carried out serially at prescribed FO time points through the latest evaluation time point, FO day 180 (FOd180) (table S1).

### Safety of subretinal readministration

There were no surgical complications resulting from vector readministration. Vector was delivered to the superotemporal retina, including the macular region superior to the fovea, in all three individuals (Table 1, Fig. 1, and Supplementary Methods). Although the regions of the retina that were targeted in the initially injected eye and the FO eye were similar, they were not entirely symmetrical except for patient CH12. The central retina of CH12 was scarred, and thus, the superior portions of the macula and retina were targeted. CH11’s second eye injection was slightly superior to the fovea, whereas the first injection encompassed the fovea; NP01’s second eye injection occupied the superior portion of the macula, whereas her first injection was superotemporal to the macula (16, 18). AAV readministration was well tolerated, and there was no inflammation in either eye of the subjects observed by clinical exam at any of the post-readministration time points (Fig. 1).

There were no serious adverse events related to vector readministration in any of the subjects. Adverse events included surface irritation of the eye between FOd30 and FOd60 (CH12), a sprained ankle in week 4 (CH11), and a headache on FOd2 (NP01). All were deemed minor.

Similar to previous results (18), blood and tear samples were positive at low levels for vector DNA sequences at early post-injection time points (table S2). Some of the polymerase chain reaction (PCR) results were nonquantitative. All samples were negative after FOd3. There was no clear relationship between leakage of vector into the blood and immune responses (Tables 2 and 3). There were no significant detectable T cell responses to either vector or transgene product (Table 2). Two subjects in this study had a transient positive enzyme-linked immunospot (ELISpot) result at a single time point (CH11, week 6, for AAV2 and RPE65; NP01, week 5, for RPE65). In both instances, the finding was isolated and was not confirmed in any other peripheral blood mononuclear cell (PBMC) samples collected subsequently from these

**Table 1.** Subject enrollment characteristics and injection details. Subjects are listed in the order that they were enrolled in the FO study. Eye #1, retina that was initially injected; Eye #2, retina that received the FO injection. All subjects were followed through FOd180.

Visual acuity is expressed in LogMAR (log of the minimum angle of resolution). Higher values indicate poorer vision (see Supplementary Methods). Hand motion vision was assigned a conservative LogMAR of 2.6.

Patient ID	Age at readministration	Sex	Follow-up after initial injection (years)	AAV2-hRPE65v2 dose (vg)/volume ( $\mu$ l)		Visual acuity (pre/post)		RPE65 mutation
				Eye #1	Eye #2	Eye #1	Eye #2	
CH12	46	F	2.1	$1.5 \times 10^{11}/300$ (high/high)	$1.5 \times 10^{11}/300$ (high/high)	2.6/2.16	2.6/2.0	K303X/W431C
CH11	27	F	2.3	$4.8 \times 10^{10}/150$ (medium/low)	$1.5 \times 10^{11}/300$ (high/high)	0.76/0.77	0.64/0.58	V473D/V473D
NP01	29	F	3.7	$1.5 \times 10^{10}/150$ (low/low)	$1.5 \times 10^{11}/300$ (high/high)	1.5/1.6	1.83/1.6	E102K/E102K

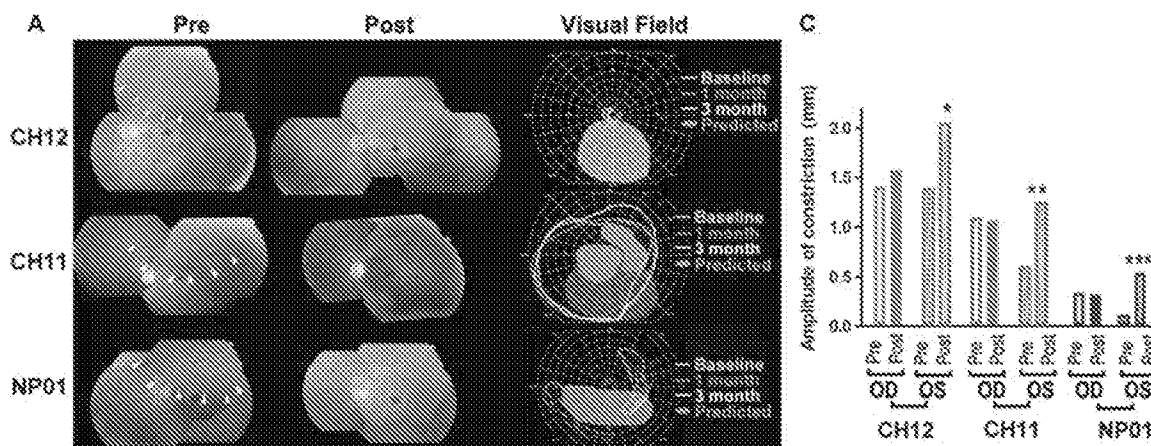


**Fig. 1. (A)** Images of fundus photos compare the baseline (“Pre”) and d60 (“Post”) appearance and the predicted pre- and post-readministration visual field. There is extensive disease at baseline, with retinal pigment epithelial disturbance and geographical atrophy in the macula in patient CH12. Arrowheads indicate the lower border of the subretinal injection site, which was supratemporal and included the superior aspect of the macula in all three subjects. The lower border of the bleb was closer to the superior vascular arcade in CH12, whereas the lower borders for patients CH11 and NP01 were closer to the fovea. On the far right are the pre- and post-readministration visual fields. The predicted visual field changes based on the injection sites (and assuming a healthy retina) were similar for the three subjects (yellow shaded areas). Gray shaded areas denote scotomas (spots in the visual field in

which vision is absent or decreased) that were altered in location at each different FO exam (only baseline scotomas are shown). **(B)** Full-field sensitivity threshold testing shows an increase in retinal light sensitivity (y axis shows sensitivity thresholds) in the left eyes of NP01 and CH11 by d30 persisting through the latest time point (d180), but no change in sensitivity of the previously injected eye for the three patients. There was no change in FST test results for either eye of patient CH12. **(C)** Improved PLR in the second eye to receive an injection of AAV2-hRPE65v2. Average pre-readministration PLR amplitudes of constriction are compared with those of post-readministration amplitudes (FOd30 to FOd180). PLR amplitudes were measured after illumination with light at 10 lux (CH12) or 0.4 lux (CH11 and NP01). \* $P = 0.08$ ; \*\* $P = 0.009$ ; \*\*\* $P = 0.01$ .

subjects. Additionally, higher than normal background [ $>50$  spot-forming units (SFUs) per  $10^6$  PBMCs plated in the assay] may have influenced the readout of the ELISpot, making the relevance of these findings unclear. Neutralizing antibody (NAb) responses to AAV2 and RPE65 protein remained at or close to baseline in the postoperative period in each subject (Table 2). The minor variations were most likely due to the variability of the assay used to measure NAb. By comparison, NAb after the systemic administration of an AAV2 vector in humans increased by several logs (4). In summary, readministration of AAV2-hRPE65v2 to the contralateral eye appeared safe based on both clinical examination and immunological response.

**Readministration and retinal/visual function**

Each subject reported improvements in vision in the second (FO) eye extending over the entire period of observation beginning as early as FOd14. Testing revealed a trend toward improvement in visual acuity of the second eye in all three subjects, with the highest level of improve-

ment in CH12. This patient also showed a trend toward improvement in the initially injected eye (Table 1). There was no change in the visual acuity of the previously injected eye of patients CH11 and NP01. There was a trend in improvement of the visual field correlating with the area of retina injected (Fig. 1A), although there was a high degree of intra-subject and intervisit variability in these subjects with low vision and nystagmus (involuntary, oscillating movements of the eyes). For CH12, the pre- and postvisual fields were limited to a very small central island. For CH11, the outer border of the FOd90 post-readministration visual fields was expanded compared to the FO baseline and FOd30 visual fields. For NP01, the visual fields showed expansion at FOd45 and FOd90 compared to baseline (Fig. 1A). There was also a trend regarding a decrease in the amplitude of nystagmus in the initially injected eye of all three subjects and in the newly injected eye of CH11 and NP01 (table S5). Two of the subjects (CH12 and NP01) showed reduced frequency of nystagmus, whereas CH11 showed increased frequency of nystagmus in both eyes after readministration (table S5).



**Table 2.** Analysis of anti-AAV2 and anti-RPE65 Nab and responses over time after initial injection (bold) and after readministration. The exact time points evaluated differed for the initial and the FO study (table S1). There were no detectable anti-RPE65 Nabs detected after the initial injection (18). However, these data are not included in Table 2 because the assay was modified for the FO study measurements. Results are indicated as reciprocal dilutions of serum samples (see Supplementary Methods). Anti-AAV2 titers after the first injection were previously reported (18) and are

shown here for comparison with the FO titers. The titers remained low throughout the course of the study, with a minor increase at week 8 for CH12 (italicized) followed by a return to baseline. High FO baseline Nabs directed against RPE65 protein were detectable in subjects CH12 and CH11. The positivity may have been due to cross-reaction with another RPE65-like protein or that the subject may produce a dysfunctional but immunologically detectable protein. The positive responses detected early on decreased slightly over time. NA, sample not available.

Subject ID	Antibody assay	Baseline/FO baseline	FOd7	d28/FOd28	FOd60	d90	d180/FOd180	d365
CH12	AAV2	<b>Neat-1:3.16/1:1</b>	1:1	<b>Neat-1:3.16/1:1</b>	<i>1:3.16-1:10</i>	<b>Neat-1:3.16</b>	1:1	<b>Neat-1:3.16</b>
	RPE65	1000	1000	1000	1000		100	
CH11	AAV2	<b>1:3.16-1:10/1:3.16-1:10</b>	1:1	<b>1:3.16-1:10/1:3.16-1:10</b>	1:3.16-1:10	<b>1:3.16-1:10</b>	1:1	<b>1:3.16-1:10</b>
	RPE65	1000	1000	100	100		100	
NP01	AAV2	<b>&lt;1:3.16/1:3.16-1:10</b>	1:1	<b>&lt;1:3.16/1:1</b>	1:1	<b>&lt;1:3.16</b>	1:1-1:3.16	<b>1:3.16-1:10</b>
	RPE65	100	<100	<100	<100		NA	

**Table 3.** Analysis of T cell responses performed by IFN-γ ELISpot after initial injection (bold) and after readministration. The time points for study are described in table S1. Most of the samples tested for T cell responses to the AAV capsid or the RPE65 transgene product were negative throughout the initial (18) and FO studies. A few samples tested positive in the assay (for example, CH12, FO week 6); however, these samples were negative the following week, suggesting either that the positive readings were false pos-

itives or that there was weak or transient T cell activation. Thus, there were no cell-mediated T cell responses detectable in peripheral blood, a result in agreement with the lack of local inflammation. Pos, positive (>50 SFUs per million cells plated) and at least threefold the medium-only control; Neg, negative (<50 SFUs per million cells plated) or less than threefold the medium-only control; Bkg, high background/not interpretable (medium control >100 SFUs per million cells plated).

Subject	Antigen	d0/FOd0	FO week 1	Week 2/FO week 2	FO week 3	Week 4/FO week 4	FO week 5	FO week 6	FO week 7	FO week 8	d90/FOd90
CH12	AAV	<b>Neg/Neg</b>	Neg	<b>Neg/Neg</b>	Neg	<b>Neg/Neg</b>	Neg	Neg	Neg	Neg	<b>Neg*/Neg</b>
	RPE65	<b>Neg/Neg</b>	Neg	<b>Neg/Neg</b>	Neg	<b>Neg/Neg</b>	Neg	Neg	Neg	Neg	<b>Neg*/Neg</b>
CH11	AAV	<b>Neg/Bkg</b>	Bkg	<b>Neg/Bkg</b>	Bkg	<b>Neg<sup>†</sup>/Bkg</b>	Bkg	Pos <sup>†</sup>	Neg	Neg	<b>Neg/Neg</b>
	RPE65	<b>Neg/Bkg</b>	Bkg	<b>Neg/Bkg</b>	Bkg	<b>Neg<sup>†</sup>/Bkg</b>	Bkg	Pos <sup>†</sup>	Neg	Neg	<b>Neg/Neg</b>
NP01	AAV	<b>Neg/Neg</b>	Neg	<b>Neg/Bkg</b>	Neg	<b>Neg/Bkg</b>	Neg	Neg	Bkg	Neg	<b>Neg/Bkg</b>
	RPE65	<b>Neg/Neg</b>	Neg	<b>Neg/Bkg</b>	Neg	<b>Neg/Bkg</b>	Pos <sup>†</sup>	Neg	Bkg	Neg	<b>Neg/Bkg</b>

\*Poor viability of cells. †Positive result likely due to high background reactivity.

The most significant improvements pertained to light sensitivity. Full-field light sensitivity, a subjective test of light perception, revealed sustained improvement in both white and chromatic (blue) light sensitivity in two of the three subjects (CH11 and NP01; Fig. 1B). One of these subjects (NP01) also showed increased sensitivity to red stimuli. The initially injected eyes retained their baseline white and blue light sensitivity with the exception of CH11, in whose initially injected eye there was diminished blue (but not white) light sensitivity after injection. The significance of this isolated finding is unknown. Similarly, there were fluctuations in sensitivity in the initially injected eyes of CH11 and NP01 between baseline and FOD30, but levels eventually returned to baseline.

Increases in light sensitivity for the newly injected eyes were also detected with pupillometry. The PLR test provides objective data relating to retinal function and the integrity of a major component of the retinal/central nervous system circuitry. We previously demonstrated that after unilateral injection of AAV2-hRPE65v2, the injected eye

showed an improved PLR, whereas the noninjected eye remained defective (16, 18, 19). Here, we show that there is an increased amplitude of constriction after readministration in each of the three FO eyes (Fig. 1C). There were minimal changes in the amplitude of constriction of the initially injected eye after readministration at this same level of illuminance. Using pupillometry, we also show that in all three subjects after readministration, the second eye gains responses (fig. S1). Further, in at least two of the subjects, CH12 and CH11, the initially injected eye retains its PLRs at the previous threshold sensitivity. The net result was that with threshold or subthreshold illumination, the PLR waveform changed from one suggesting a relative afferent pupillary defect (rAPD; where the initially injected eye had a robust response, whereas the uninjected eye did not) to one that was more symmetrical for the left and right eyes (fig. S1). Although amelioration of the rAPD was apparent as early as FOD14, it can take months for patterns to stabilize and for symmetry to develop between the left and the right eyes. Additional follow-up testing will be necessary in these and other

subjects to determine the long-term effects of the intervention on the pupillary responses of both eyes.

The ability of the subjects to accurately navigate a standardized course was also evaluated (16, 18). At and before the FO baseline, none of the subjects had been able to successfully negotiate an obstacle course using either eye. After readministration, both NP01 and CH11 avoided collisions with objects using their left, FO-injected eyes even in dim (10 lux) light for CH11 ( $P = 0.002$  and  $0.015$ , respectively; movies S1 to S4) and down to 5 lux for NP01 ( $P = 0.005$ ). Improvements in navigation were noted within 1 month after injection and persisted throughout the course of the study. There were no improvements in navigation using the initially injected eye.

### Readministration and cortical responses

fMRI analyses were performed with the general linear model and the contrast of active blocks (checkerboard stimuli) minus the rest blocks (black screen) (fig. S2) using the BrainVoyager QX software (22). To account for variability in the disease stage among subjects, we analyzed fMRI individually for each participant (20) (and not grouped as in most fMRI analyses). A single-subject analysis approach was especially suitable based on the fact that the three subjects differed by age and disease progression and thus differed in the area of the retina in which there was evidence of sufficient (albeit unhealthy) retinal cells. This approach also makes the correlation of fMRI results and clinical outcomes possible for each individual. All analyses were carried out to obtain significant results at high statistical thresholds that were corrected for false detection of any activation due to multiple-comparison type I errors (23); the thresholds were lowered if no activation was detected. At a lower statistical threshold, there was frontal activation responsible for eye movement (frontal eye fields), anterior cingulate (decision-making for button press), and premotor and sensory motor cortex (for button press).

### fMRI results for newly treated eyes

fMRI after gene therapy readministration showed significant cortical activation in and around the visual cortex for all three LCA2 subjects for full-field contrast-reversing (8 Hz) checkerboard stimuli at high and medium contrasts (Figs. 2 to 4). Presentation of the same stimuli at baseline, before readministration, did not result in significant cortical activation for either the high- or the medium-contrast stimulus. The results for each subject are as follows.

CH12's untreated eye before readministration was unresponsive to the high- and medium-contrast stimuli (Fig. 2, A and B) even at liberal statistical threshold levels. Significant bilateral cortical responses to the high-contrast stimulus were observed: false discovery rate (fdr) was  $<5\%$  with a corrected  $P$  value ( $P_c$ ) of  $<0.002$  and continuously connected area (cca) of  $\geq 100$  mm<sup>2</sup>; no response to medium contrast was recorded at FOD30 (Fig. 2, C and D, respectively). Even though her FO baseline and posttreatment visual fields were limited to a very small central area (Fig. 1), CH12's cortical responses to the high-contrast stimulus markedly increased at FOD90 (Fig. 2, E and F), especially for the high-contrast stimulus (fdr  $< 5\%$ ,  $P_c < 0.005$ , cca  $\geq 1000$  mm<sup>2</sup>). The medium-contrast stimulus showed unilateral but significant (fdr  $< 5\%$ ,  $P_c < 0.0002$ , cca  $\geq 25$  mm<sup>2</sup>) cortical activation.

CH11 showed no cortical activation, regardless of visual stimulus presented to her untreated (left) eye at FO baseline (Fig. 3, A and B). However, widespread bilateral activation was observed for the fMRI obtained on FOD30 in response to the high- and medium-contrast stimuli (fdr  $< 5\%$ ,  $P_c < 0.003$ , cca  $> 1000$  mm<sup>2</sup>) (Fig. 3, C and D), and the areas

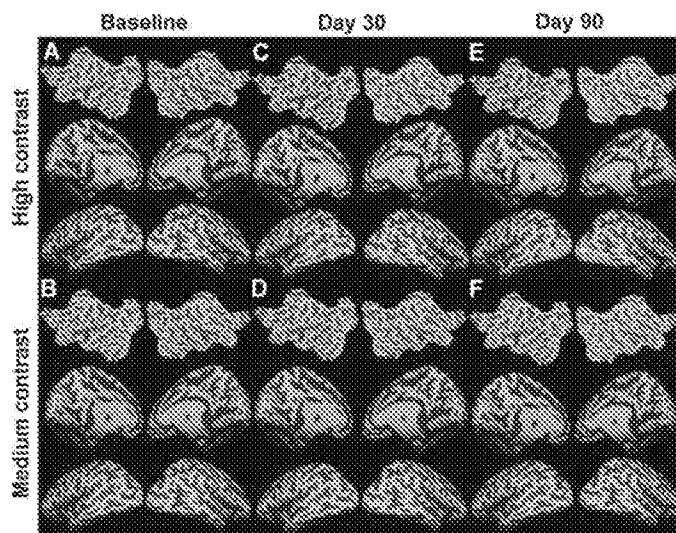


**Fig. 2.** Subject CH12 fMRI results at baseline, FOD30, and FOD90. (A and B) Subject CH12 showed no cortical activation at baseline for high- and medium-contrast stimuli. (C and D) At FOD30, significant bilateral cortical activations were observed in response to the high-contrast stimulus (C), whereas no response was recorded for the medium-contrast stimulus (D). (E and F) At FOD90, CH12's cortical responses to the same stimuli markedly increased especially for the high-contrast stimulus. Smaller clusters of activations are observed in response to medium-contrast stimulus at FOD90 (F).

of activation increased by FOD90 (Fig. 3, E and F). At FOD90 (Fig. 3E), there was greater bilateral cortical activation for the high-contrast stimulus (fdr  $< 5\%$ ,  $P_c < 0.003$ , cca  $\geq 1000$  mm<sup>2</sup>). Marked activation was also present in response to the medium-contrast stimulus (fdr  $< 5\%$ ,  $P_c < 0.003$ , cca  $\geq 1000$  mm<sup>2</sup>) (Fig. 3F). As depicted in Fig. 3, CH11's FO visual activations were symmetrically distributed in both hemispheres as well as in the upper and lower banks of the calcarine fissure, comparable to a pattern predicted from her visual field distribution and the location of the subretinal injection (Fig. 1), given that the cells in the injected region were viable.

Similar to CH11 and CH12, NP01 did not present with any activation in response to the high- or medium-contrast stimuli for her untreated eye at FO baseline (Fig. 4, A and B). At FOD45, there was a response to the high-contrast stimulus (Fig. 4C; fdr  $< 5\%$ ,  $P_c < 0.001$ , cca  $\geq 50$  mm<sup>2</sup>), but not to the medium-contrast stimulus (Fig. 4D). The clusters of activation were bilaterally distributed and mainly located in the lateral and basal areas of the visual cortex, generally reflective of a pattern predicted by the FO visual fields (Fig. 1). At FOD90, NP01 showed increased bilateral activation in response to both the high-contrast (fdr  $< 5\%$ ,  $P_c < 0.0003$ , cca  $\geq 100$  mm<sup>2</sup>) and the medium-contrast (fdr  $< 5\%$ ,  $P_c < 0.001$ , cca  $\geq 25$  mm<sup>2</sup>) stimuli as depicted in Fig. 4, E and F, respectively.

Qualitative fMRI temporal changes for the FO studies of all three subjects are summarized in table S3. Results show that cortical responses increased in all subjects from baseline to FOD30 and continued to FOD90. Quantification of the fMRI results (areas of activation, mm<sup>2</sup>) for each hemisphere and total visual cortex for the FO studies are presented in table S4. Results show that the areas of visual cortex activation after visual stimulation increased in all three subjects through FOD90 ( $P < 0.0001$ , table S4). Steady increases in total cortical activation areas through FOD90 for all three subjects agreed with the increased

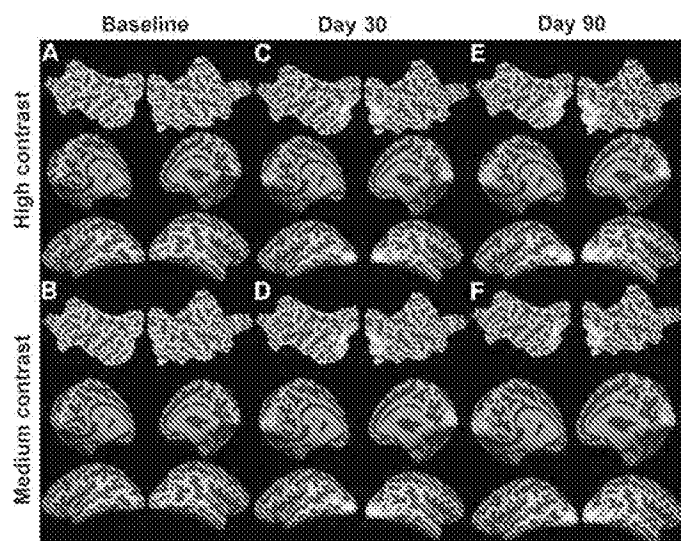


**Fig. 3.** Subject CH11 fMRI results at baseline, FOD30, and FOD90. (A and B) Subject CH11 showed no baseline cortical activation to the high- or medium-contrast checkerboard stimuli. (C and D) Highly significant and widespread bilateral activation at FOD30 in response to both high- and medium-contrast stimuli, respectively. (E and F) A more marked increase in cortical activation was present at FOD90 for high-contrast (E) and medium-contrast (F) stimuli.

light sensitivity measured with PLR testing and, for two of the subjects, with FST testing, in the same time frame (fig. S1 and Fig. 1C). This may reflect increasing expression of the *RPE65* transgene over this time period. The largest relative gains were observed in CH12 and NP01, the oldest of the three subjects. All subjects presented with greater bilateral activation at FOD90. This is not surprising because the subretinal injections spanned the midline of the posterior pole of the eye and thus should affect both hemispheres. There was good correlation between the fMRI findings and the results of retinal and visual function testing. In particular, the incremental increase in total cortical activation areas through FOD90 correlated with average postsurgical pupil constriction amplitudes ( $P < 0.049$ ).

In summary, results from fMRI showed an increase in cortical activation after readministration of gene therapy, and the pattern of visual cortex activation roughly correlated with the location of injection and visual field distribution. Temporal increases in cortical activation also generally correlated in time and magnitude with those that were measured using psychophysical testing.

#### fMRI results for previously treated eye

In addition to the newly treated eye, fMRI was also performed on the eye that had been initially injected at least 1.7 years earlier (see Table 1). This experiment was carried out to evaluate the functionality of the contralateral eye and to evaluate any potential toxicity associated with readministration of gene therapy. fMRI for the contralateral eye was carried out at FO baseline and FOD90.

As shown in Fig. 5, fMRI results at FO baseline for CH12 showed bilateral activation, distributed more extensively in the lateral aspects of the visual cortex, in response to high-contrast stimuli ( $\text{fdr} < 5\%$ ,  $P_c < 0.01$ ,  $\text{cca} > 25 \text{ mm}^2$ ) and at an uncorrected statistical level ( $P < 0.01$ ,  $\text{cca} > 25 \text{ mm}^2$ ) for medium-contrast stimuli. CH11 showed bilateral

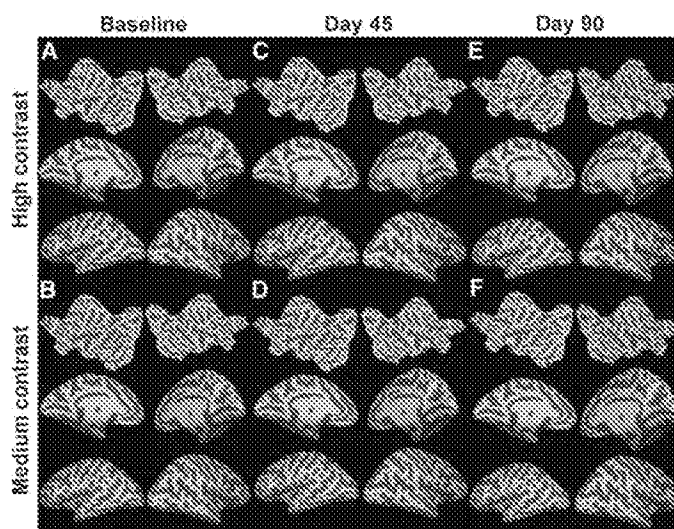


**Fig. 4.** Subject NP01 fMRI results at baseline, FOD45, and FOD90. (A and B) Subject NP01 showed no visual activation at baseline. (C and D) At FOD45, although significant cortical responses for the high-contrast stimulus were recorded (C), no response was observed for the medium-contrast stimulus (D). (E and F) At FOD90, NP01 showed significant activation for high-contrast (E) and medium-contrast (F) stimuli. Areas of activation at FOD90 were distributed in closer proximity to the primary visual cortex compared to FOD45 fMRI results [compare (E) and (C)].

activation for high-contrast stimuli ( $\text{fdr} < 5\%$ ,  $P_c < 0.01$ ,  $\text{cca} > 100 \text{ mm}^2$ ) and no activation for medium-contrast stimuli. The fMRI results for NP01 were observed at an uncorrected  $\text{fdr}$  statistical level for high-contrast stimuli ( $P < 0.01$ ,  $\text{cca} > 25 \text{ mm}^2$ ), with no activation detected for medium-contrast stimuli.

The fMRI results for the initially injected eyes at FOD90 are presented in Fig. 6. All three subjects demonstrated bilateral activation in response to the high- and medium-contrast stimuli in and around the visual cortex. The fMRI results for CH12 demonstrated bilateral activation in response to high-contrast ( $\text{fdr} < 5\%$ ,  $P_c < 0.003$ ,  $\text{cca} > 100 \text{ mm}^2$ ) and medium-contrast ( $\text{fdr} < 5\%$ ,  $P_c < 0.004$ ,  $\text{cca} > 100 \text{ mm}^2$ ) stimuli. CH11 also showed widespread activation for high-contrast ( $\text{fdr} < 5\%$ ,  $P_c < 0.004$ ,  $\text{cca} > 100 \text{ mm}^2$ ) and medium-contrast ( $\text{fdr} < 5\%$ ,  $P_c < 0.003$ ,  $\text{cca} > 100 \text{ mm}^2$ ) stimuli. NP01 showed activation at significant but  $\text{fdr}$  uncorrected statistical levels for high-contrast ( $P < 0.008$ ,  $\text{cca} > 25 \text{ mm}^2$ ) and medium-contrast ( $P < 0.008$ ,  $\text{cca} > 25 \text{ mm}^2$ ) stimuli. NP01 presented with lower cortical activation compared to CH12 and CH11.

Overall, the subjects demonstrated more extensive cortical activation for their initially treated eye after readministration of gene therapy to the second eye. Thus, the first injected eye retains and even shows ameliorated visual cortex activity after readministration. These results demonstrate that not only did each of the subjects retain retinal and visual function after injection of the first eye, but may have possibly gained retinal and visual function in both eyes.

#### DISCUSSION

Here, three adults who had each previously received a single, unilateral, subretinal injection of AAV2-hRPE65v2 underwent a repeat subretinal administration in their contralateral (previously uninjected)

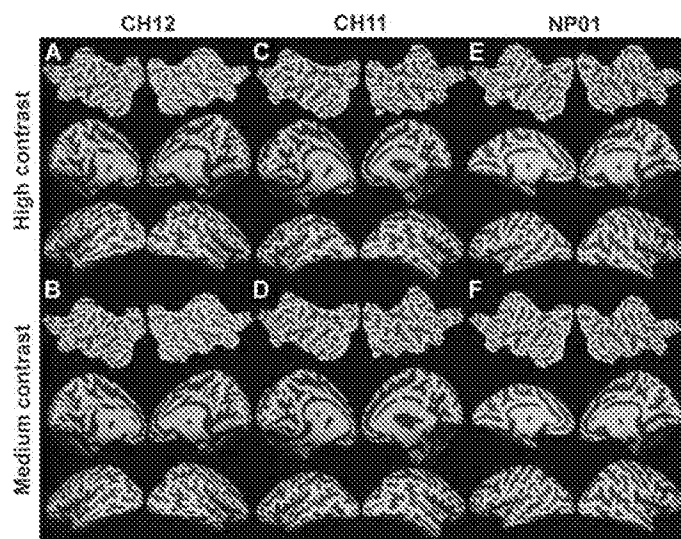


**Fig. 5.** fMRI results for initially injected eyes in response to high- and medium-contrast stimuli at FO baseline, before injection of the contralateral eyes. (A and B) CH12's fMRI results for the high- and medium-contrast stimuli showed bilateral activation. (C and D) CH11 showed activation to the high-contrast stimuli (C) but did not respond to medium-contrast stimuli (D). (E and F) Similar to CH11, NP01 responded to the high-contrast but not to the medium-contrast stimulus. The lower cortical activation for NP01 may be due to the fact that subject received the lowest dose of AAV2-hRPE65v2 for her initial subretinal injection and that subject is a chronic smoker (smoking is known to abate cortical blood flow and thus the fMRI signal).

eye. After injection, each of these “second” eyes became far more sensitive to dim light as shown by full-field sensitivity testing, pupillometry, and fMRI even though they had been severely impaired for more than 2.5 decades (and more than 4.5 decades in one individual). Two of these individuals also developed greatly improved navigational abilities using the newly injected eye. The results may reflect an age effect whereby the individuals who were younger (and thus whose retinas had not undergone as much degeneration) showed larger gains than the older individual. The gains were stable through at least the FOd180 time point, and the treatment appeared safe in all subjects. Efficacy was due to AAV-mediated delivery of wild-type RPE65 into the retinal pigment epithelium (RPE) and subsequent restoration of the retinoid cycle.

The improvements in retinal and cortical responses after subretinal delivery of AAV2-hRPE65v2 are not instantaneous because the transgene delivered by the single-stranded AAV2 vector must become double-stranded to be competent for transcription. Similar to earlier results in large animals and also to results after injection of the first eye in humans, there is a gradual ramp-up period that plateaus between 1.5 and 3 months after subretinal delivery (14, 16, 18, 24). Similar temporal gains in subjective and objective measures of retinal and visual function and in the activation of the visual cortex are found over this same time frame after readministration in humans. Here, we have also evaluated the spatial pattern of activation of the visual cortex after readministration and have found that the activation patterns mirror the improvements identified through subjective and objective clinical testing of retinal and visual function. Until now, no one has measured the temporal-spatial patterns of improvement in retinal and visual function after gene therapy using fMRI.

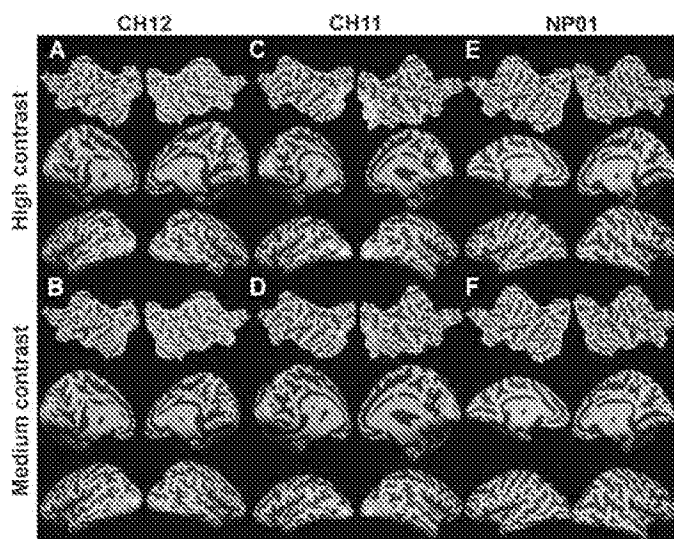


**Fig. 6.** fMRI results for initially injected eyes 90 days after readministration of the contralateral eyes. (A and B) CH12's fMRI results to high- and medium-contrast stimuli demonstrated significant bilateral cortical activation. (C and D) CH11 also showed widespread activation for high- and medium-contrast stimuli. (E and F) Although NP01 also showed activation in response to the high- and medium-contrast stimuli, they were at an uncorrected statistical threshold. Lower activation in NP01 may be due to a lower dose of AAV2-hRPE65v2 for the initial subretinal injection and the fact that this subject is a chronic smoker.

Given the gains in retinal and visual function that these and nine other individuals have enjoyed since injection of their first eye, one may have predicted the same level and time course of improvement after injection of the second eye. However, there are several variables that might have interfered with successful additional transduction events. These individuals were exposed, during the first injection, to antigens on the AAV capsid as well as RPE65 protein encoded by the AAV cargo. The concern with readministration was that previous exposure could “vaccinate” the individual and result in an inflammatory response upon repeat exposure. Although harmful immune responses were not observed in affected dogs and unaffected nonhuman primates in preclinical readministration studies (21), efficacy after readministration of AAV in humans has only been described in one study (25). This was a study where AAV was used to produce an immune response to vaccinate against HIV (25). A modest number of the HIV patients indeed developed (the desired) immune responses after injection and readministration. Our study in LCA2 subjects describes efficacy after readministration of gene therapy in a genetic disease—a response that was not accompanied by a significant (and potentially damaging) immune response. In addition, test results showed that the gains in retinal and visual function that had resulted from the initial injection were maintained after the second eye was injected.

Most of the results of the preclinical studies were predictive of results of the human readministration studies. However, there was one result that we had not observed in earlier studies. This was that one of the subjects showed improved light sensitivity responses to red stimuli in the second eye after readministration. Red stimuli selectively stimulate cone photoreceptors. This result suggests that the chromophore generated with the help of RPE65 can activate cone photoreceptors.

Previously, we had only observed improvements in rod photoreceptor responses (which were also stimulated by blue light) (16, 18). In general, there is a strong bias toward improvement in the short-wavelength (blue) spectrum, demonstrating greatest improvement in rod photoreceptors. This is analogous to the “Purkinje phenomenon,” which occurs during dark adaptation wherein the peak sensitivity of the retina shifts from the red (cone) to the blue (rod) photoreceptor population (26).

There were also some unexpected findings. The first relates to fMRI results in the initially injected eye. A concern before the study was that immune responses to readministration would dampen the gains in retinal and visual function of the initially injected eye. Surprisingly, the function of the initially injected eye was improved after readministration. Psychophysical testing did not reveal any change in function of the first injected eye. The improvement in cortical function may reflect plasticity of the neuronal connections in the brain. An increase in cortical activation at FOD90 for the initially injected eye may also be due to reduced nystagmus in the newly injected eye (improved eye movement synchrony) and a better ability to fixate the gaze during fMRI. Further study is necessary to unravel the role of nystagmus in the improvement of visual function. However, in support of this hypothesis, all three subjects showed a reduced amplitude of nystagmus in the eye receiving readministration after injection.

A second unexpected finding pertained to dose effects. In our studies of effects of unilateral “first eye” injection in subjects with LCA2, a dose response was not identified. Here, an interocular comparison of different doses was carried out because two of the subjects had previously received a lower dose than was administered in the readministration (Table 1). The responses in the second eye were significantly greater than those in the first injected eye in the two subjects who had previously received lower doses. This strongly argues for a dose/volume response. Such a response is difficult to elicit between subjects with different mutations, stages of disease, amblyopia (a condition wherein visual input is not recognized by the brain due to interference with retinal-cortical communication during development), and other complicating variables. Increases in both the dose and the volume likely contributed to the extent of improvement in the readministered eye of these two individuals. A third set of unexpected findings were variations in the timeline for improvement. As in our previous studies using psychophysical measures, fMRI showed improvements in cortical activation by the first month after injection, and there was a general ramp-up of improvement through FOD90. In CH11, the area of cortical activation was more extensive at d30 compared to the level of activation in the other two subjects. Another timeline anomaly was that there appeared to be improvement in light sensitivity in the previously injected eye at the FOD30 time point as shown through FST testing in two of the subjects (Fig. 1). This finding, which may have been a nonspecific effect of corticosteroids taken during the perioperative period, was transient, however, and the levels of light sensitivity returned to their FO baseline levels thereafter.

Finally, an unexpected finding that is more difficult to explain is the dichotomy between fMRI and the psychophysical results for CH12. With CH12, the fMRI responses were larger than would have been predicted on the basis of her improvements in visual acuity and light sensitivity (as judged by the PLR test). CH12 reported (through button press) seeing the stimuli during the period when responses were detected, and so, these responses were not an artifact. We can only speculate at this point why the fMRI responses in this subject appear to be more sensitive than the other outcome measures, at least

with this individual. Cortical activation in this individual may reflect additional aspects of vision (such as motion detection or depth perception) that would not be recognized in the other test results, or these responses may reflect a heightened level of attention. Alternatively, in this individual who had received the same dose in each eye and had also received those doses in a symmetrical fashion, there may have been a binocular summation, where the previously treated eye becomes a better driver of the visual cortex when it is better correlated with signals from the other eye.

In summary, this study provides the first demonstration of improved retinal and visual function after gene therapy readministration in a genetic disease and also the first demonstration of efficacy after readministration to the contralateral eye. Two of the three subjects can now navigate in dim light, arguably a clinically meaningful result. The fMRI data also provide the first evaluation of cortical responses to visual stimuli before and after gene therapy and is the first demonstration of the temporal-spatial changes in retinal and cortical activation in humans, as reflected by response of the visual cortex. The strong safety profile in this readministration study is likely to be due, at least in part, to the immune-privileged nature of the target tissue, the low dose of vector used, and the use of a vector preparation from which empty capsid had been removed, resulting in a lower antigen load. Although longer periods of follow-up and evaluation in these and additional subjects will be required to determine with certainty that readministration is safe in humans, the current data confirm the results of preclinical laboratory studies (21), which demonstrated that subretinal administration to the contralateral eye in animals previously exposed to intraocular AAV2-hRPE65v2 is both safe and efficacious. The current data provide evidence for the safety of vector readministration in humans of up to  $1.5 \times 10^{11}$  vg but cannot be extrapolated to higher doses or to vector with higher antigen load.

## MATERIALS AND METHODS

### Surgery and retinal/visual function testing

All recombinant DNA and human studies were carried out in compliance with local and federal guidelines. The transgene cassette in the AAV2-hRPE65v2 vector carries a chicken  $\beta$ -actin promoter driving expression of the human *RPE65* complementary DNA with an optimized Kozak sequence (14). The vector was manufactured by The Center for Cellular and Molecular Therapeutics at CHOP with current good manufacturing practices (16, 18). Surgery was performed as previously described (16, 18) with a standard three-port pars plana vitrectomy with removal of the posterior cortical vitreous (Supplementary Methods).

As per request by the IRB, the first three subjects were adults and the selection/order of these subjects was based on their availability. Subjects were evaluated before and at designated time points after surgery as was described (16, 18, 19). Efficacy for each subject was monitored with objective and subjective measures of vision (16, 18, 19). Statistical significance of mobility test results was evaluated with Fisher's exact test. *P* values of  $<0.05$  were considered significant.

### NAb assay and anti-AAV2 antibody ELISA

Anti-AAV NAb titer, anti-RPE65 antibody titer, and interferon- $\gamma$  (IFN- $\gamma$ ) ELISpot assay results were determined as previously described (Supplementary Methods) (16, 18).

## SUPPLEMENTARY MATERIAL

www.sciencetranslationalmedicine.org/cgi/content/full/4/120/120ra15/DC1

Materials and Methods

Results

Discussion

Table S1. Summary of the visual tests done at baseline before injection of the first eye, baseline before injection of the second eye [follow-on (FO), baseline], as well as after treatment of the first and then the second eye.

Table S2. Biodistribution data for subjects CH12 (A), CH11 (B), and NP01 (C) comparing results after injection in the first eye with those after readministration to the contralateral eye.

Table S3. Qualitative temporal changes in fMRI activation.

Table S4. Quantification of fMRI.

Table S5. Nystagmus parameters over time.

Fig. S1. Pupillary light reflex (PLR) testing shows an improved left eye response after readministration in all three subjects.

Fig. S2. fMRI stimuli and design.

Movie S1. NP01, follow-on baseline.

Movie S2. NP01, post-readministration.

Movie S3. CH11, follow-on baseline.

Movie S4. CH11, post-readministration.

References

## REFERENCES AND NOTES

1. T. S. Aleman, S. G. Jacobson, J. D. Chico, M. L. Scott, A. Y. Cheung, E. A. Windsor, M. Furushima, T. M. Redmond, J. Bennett, K. Palczewski, A. V. Cideciyan, Impairment of the transient pupillary light reflex in *Rpe65*<sup>-/-</sup> mice and humans with Leber congenital amaurosis. *Invest. Ophthalmol. Vis. Sci.* **45**, 1259–1271 (2004).
2. B. Lorenz, P. Gyürüs, M. Preising, D. Bremser, S. Gu, M. Andrassi, C. Gerth, A. Gal, Early-onset severe rod-cone dystrophy in young children with *RPE65* mutations. *Invest. Ophthalmol. Vis. Sci.* **41**, 2735–2742 (2000).
3. F. Simonelli, C. Ziviello, F. Testa, S. Rossi, E. Fazzi, P. E. Bianchi, M. Fossarello, S. Signorini, C. Bertone, S. Galantuomo, F. Brancati, E. M. Valente, A. Ciccodicola, E. Rinaldi, A. Auricchio, S. Banfi, Clinical and molecular genetics of Leber's congenital amaurosis: A multicenter study of Italian patients. *Invest. Ophthalmol. Vis. Sci.* **48**, 4284–4290 (2007).
4. A. I. den Hollander, A. Black, J. Bennett, F. P. Cremers, Lighting a candle in the dark: Advances in genetics and gene therapy of recessive retinal dystrophies. *J. Clin. Invest.* **120**, 3042–3053 (2010).
5. A. I. den Hollander, R. Roepman, R. K. Koenekeop, F. P. Cremers, Leber congenital amaurosis: Genes, proteins and disease mechanisms. *Prog. Retin. Eye Res.* **27**, 391–419 (2008).
6. H. Morimura, G. A. Fishman, S. A. Grover, A. B. Fulton, E. L. Berson, T. P. Dryja, Mutations in the *RPE65* gene in patients with autosomal recessive retinitis pigmentosa or Leber congenital amaurosis. *Proc. Natl. Acad. Sci. U.S.A.* **95**, 3088–3093 (1998).
7. D. A. Thompson, P. Gyürüs, L. L. Fleischer, E. L. Bingham, C. L. McHenry, E. Apfelstedt-Sylla, E. Zrenner, B. Lorenz, J. E. Richards, S. G. Jacobson, P. A. Sieving, A. Gal, Genetics and phenotypes of *RPE65* mutations in inherited retinal degeneration. *Invest. Ophthalmol. Vis. Sci.* **41**, 4293–4299 (2000).
8. T. M. Redmond, S. Yu, E. Lee, D. Bok, D. Hamasaki, N. Chen, P. Goletz, J. X. Ma, R. K. Crouch, K. Pfeifer, *Rpe65* is necessary for production of 11-*cis*-vitamin A in the retinal visual cycle. *Nat. Genet.* **20**, 344–351 (1998).
9. T. M. Redmond, E. Poliakov, S. Yu, J. Y. Tsai, Z. Lu, S. Gentleman, Mutation of key residues of *RPE65* abolishes its enzymatic role as isomerohydrolase in the visual cycle. *Proc. Natl. Acad. Sci. U.S.A.* **102**, 13658–13663 (2005).
10. S. M. Gu, D. A. Thompson, C. R. Srikumari, B. Lorenz, U. Finckh, A. Nicoletti, K. R. Murthy, M. Rathmann, G. Kumaramarickavel, M. J. Denton, A. Gal, Mutations in *RPE65* cause autosomal recessive childhood-onset severe retinal dystrophy. *Nat. Genet.* **17**, 194–197 (1997).
11. G. M. Acland, G. D. Aguirre, J. Bennett, T. S. Aleman, A. V. Cideciyan, J. Bencicelli, N. S. Dejneka, S. E. Pearce-Kelling, A. M. Maguire, K. Palczewski, W. W. Hauswirth, J. Bennett, Long-term restoration of rod and cone vision by single dose rAAV-mediated gene transfer to the retina in a canine model of childhood blindness. *Mol. Ther.* **12**, 1072–1082 (2005).
12. G. M. Acland, G. D. Aguirre, J. Ray, Q. Zhang, T. S. Aleman, A. V. Cideciyan, S. E. Pearce-Kelling, V. Anand, Y. Zeng, A. M. Maguire, S. G. Jacobson, W. W. Hauswirth, J. Bennett, Gene therapy restores vision in a canine model of childhood blindness. *Nat. Genet.* **28**, 92–95 (2001).
13. N. S. Dejneka, E. M. Surace, T. S. Aleman, A. V. Cideciyan, A. Lyubarsky, A. Savchenko, T. M. Redmond, W. Tang, Z. Wei, T. S. Rex, E. Glover, A. M. Maguire, E. N. Pugh Jr., S. G. Jacobson, J. Bennett, In utero gene therapy rescues vision in a murine model of congenital blindness. *Mol. Ther.* **9**, 182–188 (2004).
14. J. Bencicelli, J. F. Wright, A. Komaromy, J. B. Jacobs, B. Hauck, G. Zelenia, F. Mingozzi, D. Hui, D. Chung, T. S. Rex, Z. Wei, G. Qu, S. Zhou, C. Zeiss, V. R. Arruda, G. M. Acland, L. F. Dell'Osso, K. A. High, A. M. Maguire, J. Bennett, Reversal of blindness in animal models of Leber congenital amaurosis using optimized AAV2-mediated gene transfer. *Mol. Ther.* **16**, 458–465 (2008).
15. J. W. Bainbridge, A. J. Smith, S. S. Barker, S. Robbie, R. Henderson, K. Balaggan, A. Viswanathan, G. E. Holder, A. Stockman, N. Tyler, S. Petersen-Jones, S. S. Bhattacharya, A. J. Thrasher, F. W. Fitzke, B. J. Carter, G. S. Rubin, A. T. Moore, R. R. Ali, Effect of gene therapy on visual function in Leber's congenital amaurosis. *N. Engl. J. Med.* **358**, 2231–2239 (2008).
16. A. M. Maguire, F. Simonelli, E. A. Pierce, E. N. Pugh Jr., F. Mingozzi, J. Bencicelli, S. Banfi, K. A. Marshall, F. Testa, E. M. Surace, S. Rossi, A. Lyubarsky, V. R. Arruda, B. Konkle, E. Stone, J. Sun, J. Jacobs, L. Dell'Osso, R. Hertle, J. X. Ma, T. M. Redmond, X. Zhu, B. Hauck, O. Zelenia, K. S. Shindler, M. G. Maguire, J. F. Wright, N. J. Volpe, J. W. McDonnell, A. Auricchio, K. A. High, J. Bennett, Safety and efficacy of gene transfer for Leber's congenital amaurosis. *N. Engl. J. Med.* **358**, 2240–2248 (2008).
17. W. W. Hauswirth, T. S. Aieman, S. Kaushal, A. V. Cideciyan, S. B. Schwartz, L. Wang, T. J. Conlon, S. L. Boye, T. R. Flotte, B. J. Byrne, S. G. Jacobson, Treatment of Leber congenital amaurosis due to *RPE65* mutations by ocular subretinal injection of adeno-associated virus gene vector: Short-term results of a phase I trial. *Hum. Gene Ther.* **19**, 979–990 (2008).
18. A. M. Maguire, K. A. High, A. Auricchio, J. F. Wright, E. A. Pierce, F. Testa, F. Mingozzi, J. L. Bencicelli, G. S. Ying, S. Rossi, A. Fulton, K. A. Marshall, S. Banfi, D. C. Chung, J. I. Morgan, B. Hauck, O. Zelenia, X. Zhu, L. Raffini, F. Coppieters, E. De Baere, K. S. Shindler, N. J. Volpe, E. M. Surace, C. Acerra, A. Lyubarsky, T. M. Redmond, E. Stone, J. Sun, J. W. McDonnell, B. P. Leroy, F. Simonelli, J. Bennett, Age-dependent effects of *RPE65* gene therapy for Leber's congenital amaurosis: A phase 1 dose-escalation trial. *Lancet* **374**, 1597–1605 (2009).
19. F. Simonelli, A. M. Maguire, F. Testa, E. A. Pierce, F. Mingozzi, J. L. Bencicelli, S. Rossi, K. Marshall, S. Banfi, E. M. Surace, J. Sun, T. M. Redmond, X. Zhu, K. S. Shindler, G. S. Ying, C. Ziviello, C. Acerra, J. F. Wright, J. W. McDonnell, K. A. High, J. Bennett, A. Auricchio, Gene therapy for Leber's congenital amaurosis is safe and effective through 1.5 years after vector administration. *Mol. Ther.* **18**, 643–650 (2010).
20. M. Ashtari, L. L. Cyckowski, J. F. Monroe, K. A. Marshall, D. C. Chung, A. Auricchio, F. Simonelli, B. P. Leroy, A. M. Maguire, K. S. Shindler, J. Bennett, The human visual cortex responds to gene therapy-mediated recovery of retinal function. *J. Clin. Invest.* **121**, 2160–2168 (2011).
21. D. Amado, F. Mingozzi, D. Hui, J. L. Bencicelli, Z. Wei, Y. Chen, E. Bote, R. L. Grant, J. A. Golden, K. Narfstrom, N. A. Syed, S. E. Orlin, K. A. High, A. M. Maguire, J. Bennett, Safety and efficacy of subretinal readministration of a viral vector in large animals to treat congenital blindness. *Sci. Transl. Med.* **2**, 21ra16 (2010).
22. R. Goebel, F. Esposito, E. Formisano, Analysis of functional image analysis contest (FIAC) data with brainvoyager QX: From single-subject to cortically aligned group general linear model analysis and self-organizing group independent component analysis. *Hum. Brain Mapp.* **27**, 392–401 (2006).
23. T. Nichols, S. Hayasaka, Controlling the familywise error rate in functional neuroimaging: A comparative review. *Stat. Methods Med. Res.* **12**, 419–446 (2003).
24. J. Bennett, A. M. Maguire, A. V. Cideciyan, M. Schnell, E. Glover, V. Anand, T. S. Aieman, N. Chirmule, A. R. Gupta, Y. Huang, G. P. Gao, W. C. Nyberg, J. Tazelaar, J. Hughes, J. M. Wilson, S. G. Jacobson, Stable transgene expression in rod photoreceptors after recombinant adeno-associated virus-mediated gene transfer to monkey retina. *Proc. Natl. Acad. Sci. U.S.A.* **96**, 9920–9925 (1999).
25. E. Vardas, P. Kaleebu, L. G. Bekker, A. Hoosen, E. Chomba, P. R. Johnson, P. Anklesaria, J. Birungi, B. Barin, M. Boaz, J. Cox, J. Lehman, G. Stevens, J. Gilmour, T. Tarragona, P. Hayes, S. Lowenbein, E. Kizito, P. Fast, A. E. Heald, C. Schmidt, A phase 2 study to evaluate the safety and immunogenicity of a recombinant HIV type 1 vaccine based on adeno-associated virus. *AIDS Res. Hum. Retroviruses* **26**, 933–942 (2010).
26. H. Davson, in *Physiology of the Eye* (Pergamon Press, Elmsford, NY, 1990), pp. 395–396.

**Acknowledgments:** We thank O. Zelenia, B. Hauck, F. Bennett, K. Maguire, J. Tress, K. Brint, L. Pollack-Johnson, A. Faella, J. Rundio, P. Lam, R. Golemboski, and X. Zhu for expert technical assistance; L. Raffini and A. Fossough for expert clinical support; and E. Traboulsi for clinical input. **Funding:** Center for Cellular and Molecular Therapeutics at CHOP; Foundation Fighting Blindness-sponsored CHOP-PENN Pediatric Center for Retinal Degenerations; Clinical Translational Science Award NIH/National Center for Research Resources UL1-RR-024134, 1R21EY020662, and 1R01EY019014-01A2; Transdisciplinary Award Program in Translational Medicine and Therapeutics (TAPITMAT) from University of Pennsylvania; Research to Prevent Blindness; Hope for Vision; Howard Hughes Medical Institute; Paul and Evania Mackall Foundation Trust at Scheie Eye Institute; anonymous donors; Italian Telethon Foundation; and F. M. Kirby Foundation. **Author contributions:** A.M.M., J.B., J.W., M.A., F.M., and K.A.H. participated in the study design. A.M.M., J.B., K.A.M., S.M., D.C.C., X.Z., E.A.P., M.A., and L.L.C. carried out the surgical, clinical, and research procedures. J.L.B. and J.F.W. generated the AAV2-hRPE65v2 preclinical plasmid and vector, respectively. J.W., M.A., and L.L.C. obtained regulatory approvals. J.B., F.M., J.L.B., M.A., and L.L.C. participated in the design of specific assays.

Y.C. and F.M. carried out the NAb and T cell assays. A.M.M., K.A.H., S.M., G.-s.Y., M.A., L.L.C., K.S.S., and J.B. reviewed some or all of the primary data. J.B., M.A., and L.L.C. wrote the manuscript. All authors reviewed the manuscript. **Competing interests:** J.B. and A.M.M. are co-inventors on a pending patent (2797-11-US) for a method to treat or slow the development of blindness, but both waived any financial interest in this technology in 2002. K.A.H. and J.F.W. are co-inventors on a patent regarding methods of making AAV vectors for clinical studies (U.S. patent 61/299,184, 2010). J.B. and J.F.W. serve on the scientific advisory board for Avalanche Technologies. J.B. served on a scientific advisory board for Sanofi-Aventis in 2010 to 2011. J.B. has consulted for GlaxoSmithKline. J.F.W. has consulted for Tacere Therapeutics, Genzyme, Novartis, and Genetix Inc. The other authors declare that they have no competing interests.

Submitted 6 July 2011  
Accepted 19 January 2012  
Published 8 February 2012  
10.1126/scitranslmed.3002865

**Citation:** J. Bennett, M. Ashtari, J. Wellman, K. A. Marshall, L. L. Cyckowski, D. C. Chung, S. McCague, E. A. Pierce, Y. Chen, J. L. Bennicelli, X. Zhu, G.-s. Ying, J. Sun, J. F. Wright, A. Auricchio, F. Simonelli, K. S. Shindler, F. Mingozzi, K. A. High, A. M. Maguire, AAV2 gene therapy readministration in three adults with congenital blindness. *Sci. Transl. Med.* **4**, 120ra15 (2012).



# Science Translational Medicine

## AAV2 Gene Therapy Readministration in Three Adults with Congenital Blindness

Jean Bennett, Manzar Ashtari, Jennifer Wellman, Kathleen A. Marshall, Laura L. Cyckowski, Daniel C. Chung, Sarah McCague, Eric A. Pierce, Yifeng Chen, Jeannette L. Bennicelli, Xiaosong Zhu, Gui-shuang Ying, Junwei Sun, J. Fraser Wright, Alberto Auricchio, Francesca Simonelli, Kenneth S. Shindler, Federico Mingozzi, Katherine A. High and Albert M. Maguire

*Sci Transl Med* 4, 120ra15120ra15.  
DOI: 10.1126/scitranslmed.3002865

### Shining a Light with Gene Therapy

Gene therapy has great potential for treating certain diseases by providing therapeutic genes to target cells. Administration of a gene therapy vector carrying the *RPE65* gene in 12 patients with congenital blindness due to *RPE65* mutations led to improvements in retinal and visual function and proved to be a safe and stable procedure. In a follow-up study, the same group of researchers led by Jean Bennett set out to discover whether it would be possible to safely administer the vector and the therapeutic transgene to the contralateral eye of the patients. A big concern was whether the first gene therapy injection might have primed the patients' immune system to respond to the adeno-associated virus (AAV) vector or the product of the therapeutic transgene that it had delivered.

To test the safety and efficacy of a second administration of gene therapy to the second eye, the authors demonstrated that readministration was both safe and effective in animal models. Then, they selected 3 of the original 12 patients and readministered the AAV vector and its *RPE65* transgene to the contralateral eye. They assessed safety by evaluating inflammatory responses, immune reactions, and extraocular exposure to the AAV vector. Efficacy was assessed through qualitative and quantitative measures of retinal and visual function including the ability to read letters, the extent of side vision, light sensitivity, the pupillary light reflex, the ability to navigate in dim light, and evidence from neuroimaging studies of cortical activation (which demonstrated that signals from the retina were recognized by the brain). The researchers did not discover any safety concerns and did not identify harmful immune responses to the vector or the transgene product. Before and after comparisons of psychophysical data and cortical responses provided the authors with evidence that gene therapy readministration was effective and mediated improvements in retinal and visual function in the three patients. The researchers report that the lack of immune response and the robust safety profile in this readministration gene therapy study may be due in part to the immune-privileged nature of the eye, and the low dose and very pure preparation of the AAV vector.

ARTICLE TOOLS	<a href="http://stm.sciencemag.org/content/4/120/120ra15">http://stm.sciencemag.org/content/4/120/120ra15</a>
SUPPLEMENTARY MATERIALS	<a href="http://stm.sciencemag.org/content/suppl/2012/02/08/4.120.120ra15.DC1">http://stm.sciencemag.org/content/suppl/2012/02/08/4.120.120ra15.DC1</a>
RELATED CONTENT	<a href="http://stm.sciencemag.org/content/scitransmed/5/194/194ra92.full">http://stm.sciencemag.org/content/scitransmed/5/194/194ra92.full</a> <a href="http://stm.sciencemag.org/content/scitransmed/5/175/175fs8.full">http://stm.sciencemag.org/content/scitransmed/5/175/175fs8.full</a> <a href="http://stm.sciencemag.org/content/scitransmed/5/189/189ra76.full">http://stm.sciencemag.org/content/scitransmed/5/189/189ra76.full</a> <a href="http://stm.sciencemag.org/content/scitransmed/5/202/202ra122.full">http://stm.sciencemag.org/content/scitransmed/5/202/202ra122.full</a> <a href="http://stm.sciencemag.org/content/scitransmed/1/1/492/eaav4523.full">http://stm.sciencemag.org/content/scitransmed/1/1/492/eaav4523.full</a>
REFERENCES	This article cites 25 articles, 8 of which you can access for free <a href="http://stm.sciencemag.org/content/4/120/120ra15#BIBL">http://stm.sciencemag.org/content/4/120/120ra15#BIBL</a>

Use of this article is subject to the Terms of Service

*Science Translational Medicine* (ISSN 1946-6242) is published by the American Association for the Advancement of Science, 1200 New York Avenue NW, Washington, DC 20005. The title *Science Translational Medicine* is a registered trademark of AAAS.

Copyright © 2012, American Association for the Advancement of Science



PERMISSIONS

<http://www.sciencemag.org/help/reprints-and-permissions>

Downloaded from <http://sttm.sciencemag.org/> at REPRINTS DESK on December 10, 2019

Use of this article is subject to the Terms of Service

---

*Science Translational Medicine* (ISSN 1946-6242) is published by the American Association for the Advancement of Science, 1200 New York Avenue NW, Washington, DC 20005. The title *Science Translational Medicine* is a registered trademark of AAAS.

Copyright © 2012, American Association for the Advancement of Science

EX. B

# Dosage Thresholds for AAV2 and AAV8 Photoreceptor Gene Therapy in Monkey

Luk H. Vandenberghe,<sup>1\*</sup> Peter Bell,<sup>1</sup> Albert M. Maguire,<sup>2,3</sup> Cassia N. Cearley,<sup>4,5</sup> Ru Xiao,<sup>1</sup> Roberto Calcedo,<sup>1</sup> Lili Wang,<sup>1</sup> Michael J. Castle,<sup>4,5</sup> Alexandra C. Maguire,<sup>2†</sup> Rebecca Grant,<sup>1</sup> John H. Wolfe,<sup>4,5</sup> James M. Wilson,<sup>1‡</sup> Jean Bennett<sup>2,3‡</sup>

Published 22 June 2011; revised 7 December 2011

Gene therapy is emerging as a therapeutic modality for treating disorders of the retina. Photoreceptor cells are the primary cell type affected in many inherited diseases of retinal degeneration. Successfully treating these diseases with gene therapy requires the identification of efficient and safe targeting vectors that can transduce photoreceptor cells. One serotype of adeno-associated virus, AAV2, has been used successfully in clinical trials to treat a form of congenital blindness that requires transduction of the supporting cells of the retina in the retinal pigment epithelium (RPE). Here, we determined the dose required to achieve targeting of AAV2 and AAV8 vectors to photoreceptors in nonhuman primates. Transgene expression in animals injected subretinally with various doses of AAV2 or AAV8 vectors carrying a green fluorescent protein transgene was correlated with surgical, clinical, and immunological observations. Both AAV2 and AAV8 demonstrated efficient transduction of RPE, but AAV8 was markedly better at targeting photoreceptor cells. These preclinical results provide guidance for optimal vector and dose selection in future human gene therapy trials to treat retinal diseases caused by loss of photoreceptors.

## INTRODUCTION

There is an unmet clinical need for approaches to treat both inherited monogenetic and complex retinal degenerative disorders in which the disease originates in photoreceptor cells of the retina. The eye is an attractive target organ for gene therapy because of its accessibility, small size, compartmentalized structure, well-defined blood-retina barrier, and its characteristic of being an immune-privileged site. Because of these features, a gene delivery agent can be administered in low doses and has limited systemic distribution. In recent successful Phase I and II clinical trials for a childhood-onset blindness called Leber congenital amaurosis, a recombinant adeno-associated virus serotype 2 (AAV2) targeting vector was used to deliver a therapeutic transgene to cells of the retinal pigment epithelium (RPE). In this form of Leber congenital amaurosis, mutations in the *RPE65* gene result in lack of production of a key enzyme in the vitamin A cycle, the side effects of which include the inability of rod photoreceptors to initiate the process leading to vision as well as toxicity to the RPE cells secondary to buildup of retinyl esters. RPE cell atrophy leads to secondary toxicity to photoreceptor cells, which are located above the RPE layer (1–3). Gene therapy could also be applied to diseases of retinal degeneration that are due to primary loss of photoreceptor cells such as most forms of retinitis pigmentosa (RP), a heterogeneous group of diseases with a wide spectrum of genotypes and phenotypes that affect up to 100,000 people in the United States. RP includes dis-

ease subsets such as congenital blindness (Leber congenital amaurosis), syndromes in which RP is a component (Usher syndrome, RP and deafness; Bardet-Biedl syndrome, polydactyly, mental retardation, and RP), and inherited macular degeneration (Stargardt disease) (4, 5). The feasibility of therapeutic gene delivery to treat these diseases will depend on the nature and degree of degeneration of the diseased retina as well as the capabilities and properties of the gene delivery vector. Tropism for the therapeutic target, appropriate amounts of transgene product, and restriction of therapeutic gene expression to the relevant cell types are factors that affect the safety and efficacy profile of any gene delivery tool (5).

The first AAV serotype considered as a vehicle for gene transfer was AAV2, which was developed from a cloned wild-type virus in the 1980s (6). One of the early applications of AAV2 was in settings of in vivo gene transfer in the eye. In the retina, outer retinal cells (photoreceptors and RPE cells) were transduced most efficiently after a subretinal route of injection (7–9), whereas inner retinal cells were transduced after injection into the vitreous humor (10, 11). These encouraging findings led to the exploration of other AAV serotypes for in vivo gene transfer (12). Many AAV serotypes have been described, and studies in the retina have demonstrated that tropism, onset of transgene expression, and specificity of transduction can vary according to serotype and host species (13–15). Here, we compare AAV2 and AAV8 across a wide dose range in the cynomolgus macaque, an animal that, like humans, has a macula. This large-animal model also allowed the use of surgical maneuvers that are similar to those used in humans. Further, most large-animal studies describe the effects of exposure to doses higher than  $1.5 \times 10^{11}$  genome copies per eye, which to date is the maximum subretinal dose used in any of the AAV2 retinal gene therapy clinical trials (16). Studies in large animals with various AAV serotypes demonstrate consistent targeting of the RPE and, for most serotypes except AAV4, transduction of rod photoreceptor cells. Beltran *et al.* have highlighted the importance of the relationship of dose, gene transfer efficiency, and cellular specificity (17), which is not known for many AAV serotypes (18–21). There are conflicting reports on the ability of

<sup>1</sup>Gene Therapy Program, Department of Pathology and Laboratory Medicine, University of Pennsylvania, Philadelphia, PA 19104, USA. <sup>2</sup>F. M. Kirby Center for Molecular Ophthalmology, Scheie Eye Institute, University of Pennsylvania, Philadelphia, PA 19104, USA. <sup>3</sup>Center for Cellular and Molecular Therapeutics, Children's Hospital of Philadelphia, Philadelphia, PA 19104 USA. <sup>4</sup>W. F. Goodman Center for Comparative Medical Genetics, School of Veterinary Medicine and Department of Pediatrics, School of Medicine, University of Pennsylvania, Philadelphia, PA 19104, USA. <sup>5</sup>Stokes Research Institute, Children's Hospital of Philadelphia, Philadelphia, PA 19104, USA.

\*Present address: F. M. Kirby Center for Molecular Ophthalmology, Scheie Eye Institute, University of Pennsylvania, Philadelphia, PA 19104, USA.

†Present address: Princeton University, Princeton, NJ 08155, USA.

‡To whom correspondence should be addressed. E-mail: wilsonjm@mail.med.upenn.edu (J.M.W.); jebennet@mail.med.upenn.edu (J.B.)

**Table 1.** Experimental design and surgical and ophthalmoscopic findings. GFP expression intensities graded ophthalmoscopically correlate with AAV2 and AAV8 dose. Injection of AAV8 results in greater GFP expression than injection of AAV2 dose per dose. Gray shaded areas indicate exclusion from quantitative postmortem analysis because of injection anomalies or complications, including leakage into the vitreous humor (cf. notes). Percent of subretinal (SR) and intravitreal (IV) spaces reflect estimates of vector

deposits in these areas. GFP expression scores range from 0 (no visible expression) to 4 (broad, intense staining). They reflect a subjective composite of both intensity and area of transduction as observed by indirect ophthalmoscopy. F, foveal; V, 135- $\mu$ l volume injected instead of 150  $\mu$ l; B, blood (intraretinal or subretinal); ID, animal identification number; IR, intraretinal; I, injector defect required a second successful retinal application; GFP, green fluorescent protein; GC, genome copies.

	Animal ID	Weight (kg)	Sex	Duration (days)	Dose ( $10^4$ GC)	Right			Left									
						SR (%)	IV (%)	Notes	GFP score			Dose ( $10^4$ GC)	SR (%)	IV (%)	Notes	GFP score		
									1 week	1 month	4 months					1 week	1 month	4 months
AAV8	18216	5.60	♂	155	10	100	0	F	0	4	4	8	100	0		0	0	1
	18173	3.80	♀	153		15	85		0	3.5	3		100	0		0	0	3
	18204	5.60	♂	153		100	0	F	2	4	3		100	0		0.5	0	2
	18234	4.35	♂	155		90	10	V	0	3.5	4		100	0	B (IR)	0	0.5	0
	18238	3.50	♂	155		100			1	4	4		100	0		0	0	0
	18217	4.85	♂	162	11	100	0		0	4F	4F	9	87	13		0	2	2
	18155	3.50	♀	160		87	13		0.5	4F	4		100	0		0	2	3
	18180	3.25	♀	160		40	60	B (SR)	0	4F	4F		100	0		0	2	2
	18199	5.80	♂	162		100	0	I	0.5	4F	4F		100	0		0	2	4
	18208	5.20	♂	162		100	0	B (SR)	0	4F	4F		100	0		0	2	2
AAV2	18144	4.50	♀	139	11	100	0		0	4	4F	10	100	0		0	3	0
	18168	2.80	♀	139		100	0		0	3	4		100	0		0	2	4
	18226	5.75	♂	140		100	0	B (SR); F	0	3F	4F		13	87	F	0	4	2F
	18221	4.85	♂	140		100	0	F	0	1	3		100	0		0	1	0

AAV2 to transduce cone photoreceptors (20, 22), but recent studies suggest that AAV5 at elevated doses can target cone photoreceptor cells (17, 23). The availability of vectors that can transduce rod and cone photoreceptors efficiently will expand the opportunities for treating or preventing blindness due to degeneration of these cells. AAV8 has emerged as a highly effective vector with broad tropism for many tissues and a favorable immunological profile (24–26).

Here, we selected AAV2 and AAV8 for qualitative and quantitative comparison of transgene expression in the monkey retina. In addition, the relationship of dose and variables related to subretinal delivery of AAV was studied using clinical examination, systemic indicators of inflammation, and extraocular neuronal expression. The use of a non-human primate model was important because cellular transduction details can differ depending on the species. Given that the eye of non-human primates is similar anatomically to the human eye and that these animals physiologically resemble humans in other characteristics such as immune response, this animal model is likely to be more predictive of the utility of these targeting vectors in humans.

**RESULTS**

**Reporter gene expression after subretinal injection of AAV2 and AAV8 at different doses**

Both eyes of 14 cynomolgus macaques were injected with either AAV2 or AAV8 expressing the enhanced green fluorescent protein (GFP) under control of the early cytomegalovirus promoter. The study design, specifics

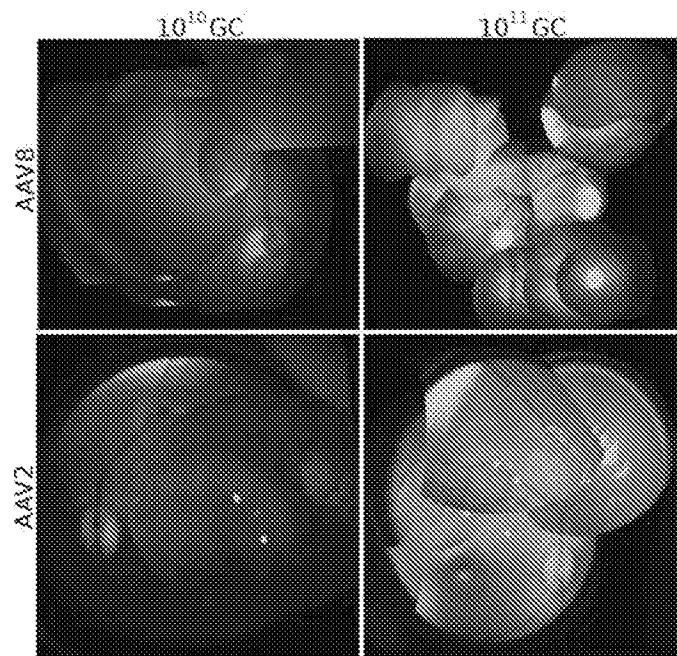


**Fig. 1.** GFP expression in monkey retina. Montages of photographs taken in vivo of monkey retinas 1 month after subretinal injection of AAV2 or AAV8 at  $10^{10}$  or  $10^{11}$  genome copy (GC) doses. Blue light was used for GFP excitation; GFP expression, green areas. Clockwise from top left: animal 18204, right eye; 18155, left eye; 18221, right eye; 18226, left eye.

Downloaded from <http://stm.sciencemag.org/> by guest on March 11, 2019

of injection, and clinical observations are summarized in Table 1. Briefly, both eyes were injected with the same virus serotype but at different doses:  $10^8$ ,  $10^9$ ,  $10^{10}$ , and  $10^{11}$  genome copies per eye for AAV8, and  $10^{10}$  and  $10^{11}$  genome copies per eye for AAV2. Other animal models have suggested that AAV8 has higher efficiency (13), and so to reduce animal use, we performed the AAV2 study after the AAV8 study in a dose de-escalating manner, and we terminated it at a dose of  $10^{10}$  genome copies per eye because this dose yielded expression levels quantitatively comparable to that of AAV8. The subretinal injection was always in a similar site located on the superior temporal quadrant of the retina. In some cases, the AAV injection area extended through the fovea, the central point of the macula within the retina that contains exclusively cone photoreceptor cells (Table 1).

All animals tolerated the surgical delivery of AAV well, regardless of whether most of the material was retained under the retina or whether it leaked into the vitreal space. Leakage of blood into the subretinal space was observed during the intraoperative procedure in three of the eyes, and intraretinal blood was observed postoperatively in an additional eye (Table 1). Ocular media (fluid in the anterior and posterior segments within the eye) remained clear throughout the study, and no significant inflammatory reaction was observed at any time. Visual behavior testing after surgery confirmed that all of the animals had good visual acuity (videos S1 to S4 and Supplementary Results) even after administration of vector directly to the fovea (videos S1 and S2). However, the visual acuity of an animal that did not receive a foveal injection (animal 18180) was slightly less than that of the other animals. In four eyes (18144 right and left; 18199 right and 18208 right), retinal thinning in the center of the area correlating with the injection site was observed by ophthalmoscopy starting at 28 days after injection and was later confirmed by histology (see below).

After 7 days, the highest doses of AAV8 led to the earliest evidence of transgene expression by ophthalmoscopy (Table 1). All eyes injected with AAV2 at both doses showed GFP expression 21 days after injection, with increasing intensities through day 28 (Fig. 1). Two of the eyes showed reduced GFP expression thereafter (Table 1). The right eye of animal 18221 had received  $10^{11}$  genome copies of AAV2 and showed moderate and broad expression in the superior temporal retina with increased focal

GFP intensity in the fovea at days 21 and 28 (Fig. 1). However, from the second month after injection, expression was restricted to the fovea exclusively and disappeared entirely 4 months after injection (Table 1). GFP expression in the left eye of animal 18144 injected with  $10^{10}$  genome copies of AAV2 was maximal after 1 month with a diffuse but broad pattern of transduction, but waned to a small GFP-positive area at month 3 with no visible GFP expression 4 months after injection (Table 1). Four months after injection, GFP expression from the  $10^8$  genome copy dose of AAV8 was detectable in three of five eyes, whereas all other AAV8-injected eyes had detectable GFP expression before the end of the first month (Table 1 and Fig. 1).

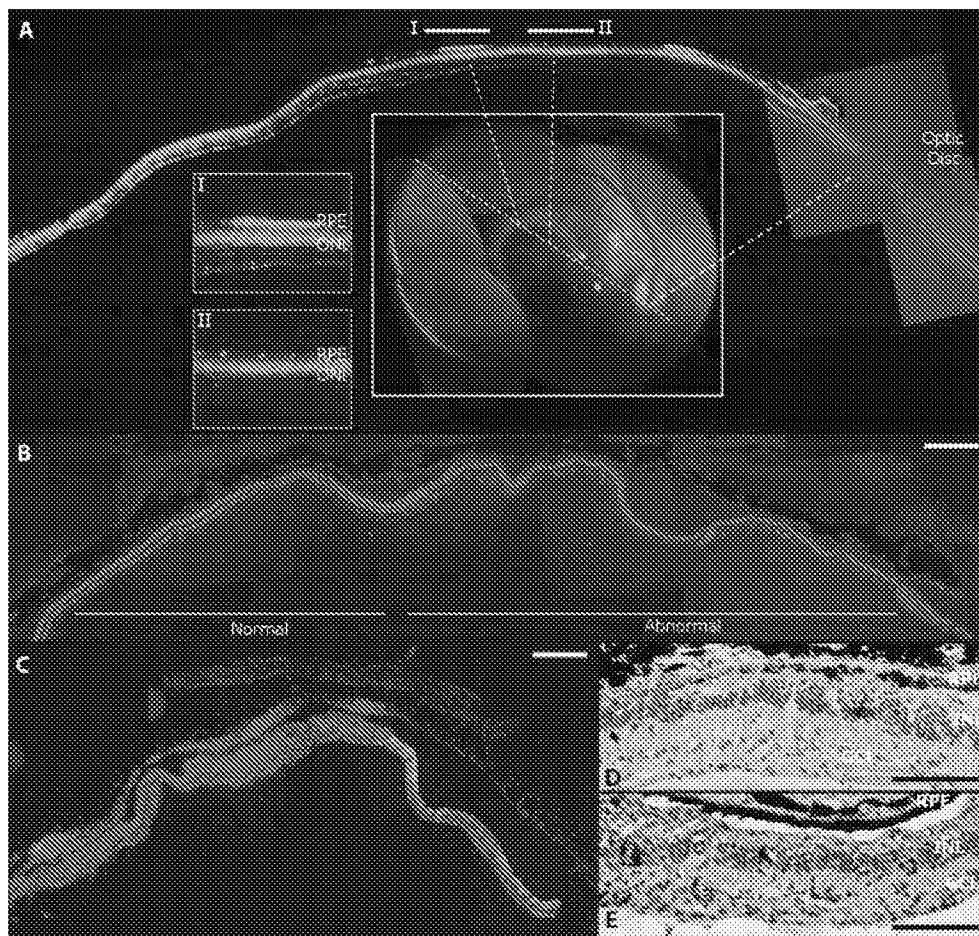


**Fig. 2.** Retinal pathology after highest-dose vector injection in monkey retina. (A) Correlating histology and live retinal imaging identifies heterogeneous GFP expression in the vector-exposed part of the retina. A halo-like GFP pattern (green rim) was observed by imaging of the retina (center inset) after a  $10^{11}$  genome copy dose injection of the AAV2 vector subretinally (animal 18226, right eye). Histology along an axis (center inset, dotted lines) that traverses the bleb, the optic disc, and the halo pattern (I and II) shows that the rims of the GFP halo (see inset I) are defined by GFP-positive RPE (green), whereas adjacent RPE does not express GFP (inset II) (GFP, green; DAPI staining of nuclei, blue). (B) DAPI staining (blue) of a section from a monkey eye injected subretinally with AAV2 (animal 18144, right eye) showing normal outer and inner nuclear layers with only minimal GFP fluorescence (green; left). This section is adjacent to a region where the nuclear layers are disturbed (abnormal; right). (C) Retina from the right eye of monkey 18199 after subretinal injection of AAV8 showing DAPI-stained nuclei (blue) and GFP expression (green) illustrates loss of retinal architecture and GFP on the left while retaining some GFP expression but abnormal retinal structure on the right. (D) Retinal section from animal 18144 (right eye) showing the abnormal portion in (B) stained with H&E. (E) H&E-stained section corresponding to the right part of the retina shown in (C) (animal 18199, right eye). Scale bars, 500  $\mu$ m [(A) to (C)] and 100  $\mu$ m [(D) and (E)].

After administration of  $10^{10}$  and  $10^{11}$  genome copies of AAV2 or AAV8, GFP expression was widespread but not always homogeneous. At  $10^{10}$  and  $10^{11}$  genome copy doses of either serotype, a circular rim of bright GFP expression enclosing an area of dim or hardly visible GFP signal (“halo”) was observed in a few eyes (Figs. 1 and 2A). Thus, comparison studies revealed a slightly earlier onset of GFP expression after delivery of AAV8 compared to AAV2 and similar patterns of GFP distribution, although GFP concentrations appeared higher dose for dose with AAV8 than with AAV2.

**Retinal cell tropism and AAV serotype**

At the lower doses of both targeting vectors ( $10^{10}$  genome copies for AAV2 and  $10^8$  and  $10^9$  genome copies for AAV8), the primary target was the RPE. Higher doses targeted greater numbers and a wider variety of cells in the neuronal retina, particularly photoreceptor cells (Fig. 3, A and B). As illustrated in Fig. 3A,  $10^{11}$  genome copies of

AAV2 and  $10^{10}$  and  $10^{11}$  genome copies of AAV8 resulted in widespread and bright GFP expression in photoreceptor cells and the RPE. Notably, at these doses, several regions of GFP-positive photoreceptor cells were identified that lacked GFP in the adjacent RPE. In these areas, regardless of GFP positivity, the RPE and photoreceptors appeared healthy and viable as determined by 4',6-diamidino-2-phenylindole (DAPI) staining.

Transduction of photoreceptor cells with AAV2 and AAV8 was essentially relegated to rod photoreceptors as judged by the well-defined shape and retinal locations of those cells. In the periphery of the retina, peanut agglutinin and cone arrestin immunofluorescence, used to stain cone photoreceptors, identified only limited GFP expression in this cell type, in terms of both the number of positive cells and the intensity of expression (fig. S1). The one notable exception was foveal photoreceptors, which consist entirely of cones. In the fovea, transduction was observed for AAV8 at  $10^{10}$  genome copies but not

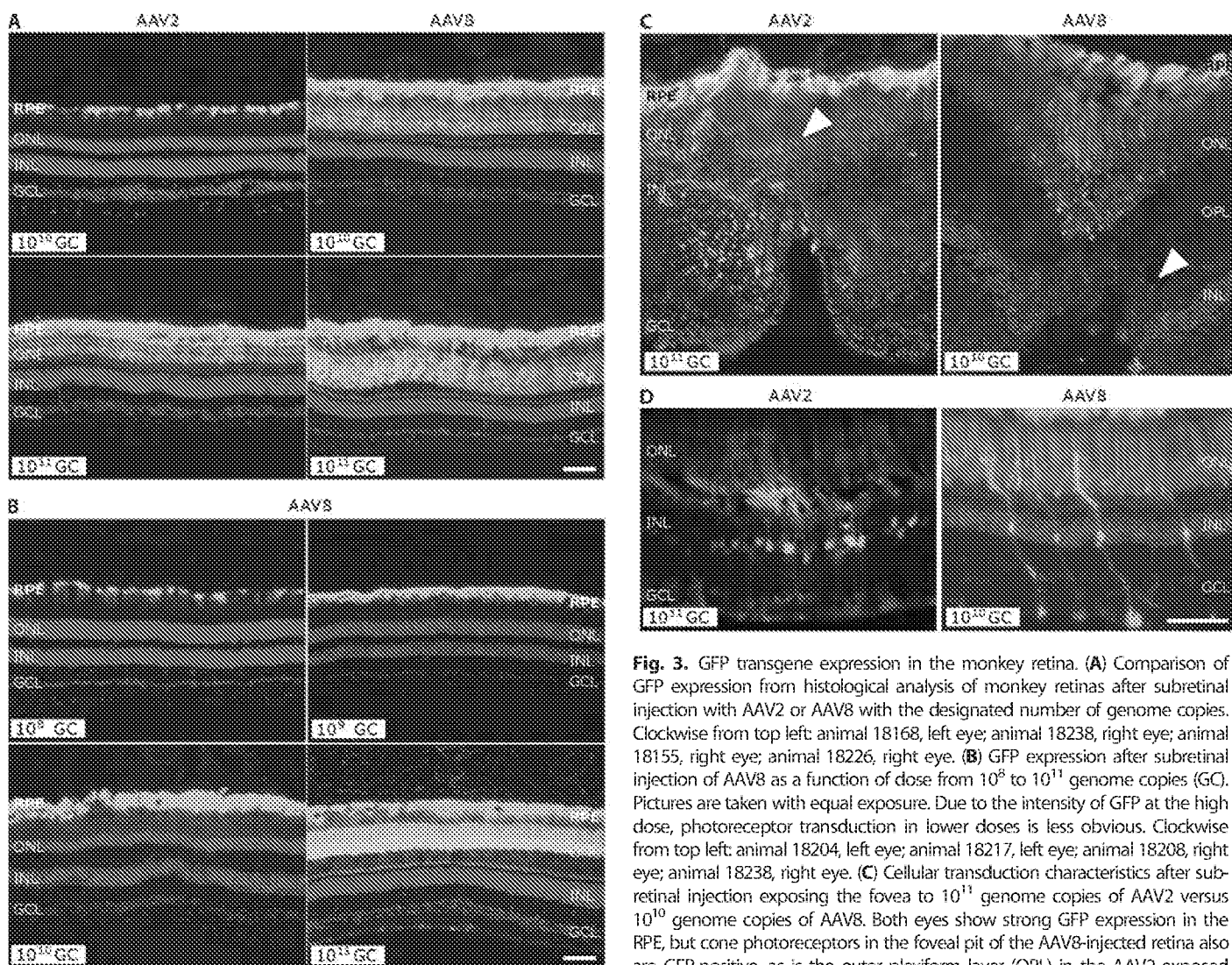


**Fig. 3.** GFP transgene expression in the monkey retina. (A) Comparison of GFP expression from histological analysis of monkey retinas after subretinal injection with AAV2 or AAV8 with the designated number of genome copies. Clockwise from top left: animal 18168, left eye; animal 18238, right eye; animal 18155, right eye; animal 18226, right eye. (B) GFP expression after subretinal injection of AAV8 as a function of dose from  $10^8$  to  $10^{11}$  genome copies (GC). Pictures are taken with equal exposure. Due to the intensity of GFP at the high dose, photoreceptor transduction in lower doses is less obvious. Clockwise from top left: animal 18204, left eye; animal 18217, left eye; animal 18208, right eye; animal 18238, right eye. (C) Cellular transduction characteristics after subretinal injection exposing the fovea to  $10^{11}$  genome copies of AAV2 versus  $10^{10}$  genome copies of AAV8. Both eyes show strong GFP expression in the RPE, but cone photoreceptors in the foveal pit of the AAV8-injected retina also are GFP-positive, as is the outer plexiform layer (OPL) in the AAV2-exposed retina (indicated by white arrowhead). (D) Transduction of Müller glial cells [with nuclei in the inner nuclear layer (INL)] after injection of AAV2 or AAV8. DAPI stain (blue) shows nuclear layers. Animal 18226, right eye (AAV2); animal 18204, right eye (AAV8). Scale bars, 100  $\mu$ m. RPE, retinal pigment epithelium; ONL, outer nuclear layer; GCL, ganglion cell layer.

Downloaded from <http://stm.sciencemag.org/> by guest on March 11, 2019

for AAV2 (Fig. 3C). In monkey retinas where the fovea was exposed to vector, AAV8 transduced up to 30% of foveal cones at the  $10^{10}$  genome copy dose; AAV2 achieved similar targeting but only at the  $10^{11}$  genome copy dose. Neither vector demonstrated prominent cone transduction in the perifoveal regions, highlighting the overall low permissiveness of cones compared to rods for vector transduction even at this elevated dose (fig. S1). Müller cells, glial cells embedded in and critical for the sustenance of the neuronal retina, were also frequent targets of AAV2 and AAV8 transduction (Fig. 2D), with qualitatively more of those cells transduced with AAV8 than with AAV2 at the same doses.

Through correlative analysis of retinal imaging and histological data, we reconstructed the entire cross section of the transduced areas of each retina, including the regional differences noted by ophthalmoscopic observation (such as the halo patterns of transduction described above). These analyses illustrate GFP-positive photoreceptor cells throughout the vector-exposed area and that the halo patterns correspond to small portions of the RPE expressing GFP as shown in Fig. 2A for an eye injected with  $10^{11}$  genome copies of AAV2 (animal 18226, right eye). In areas that showed histopathology (see below), there was reduced GFP expression noted both ophthalmoscopically and by microscopy. Within monkey retinas in which subretinal blood had been noted during the injection procedure, we identified areas that totally lacked GFP expression but were exposed to vector (Fig. 2, B and C). Those areas were also evaluated histopathologically in more detail (see below). Thus, both AAV2 and AAV8 transduce RPE efficiently at lower doses. At higher doses, AAV8 is more efficient than AAV2 at transducing photoreceptor cells. Targeting is largely restricted to rod photoreceptors; however, less efficient transduction of cone photoreceptors does occur particularly in the fovea at the highest doses.

### Quantitative assessment of transduction

To quantitatively assess the relationship between vector dose and serotype and retinal transduction efficiency, we measured total retinal fluorescence and performed detailed morphometric analyses on histological sections. Eyes with noted injection problems such as intravitreal leakage or retinal bleed were excluded from these analyses (Table 1). Using post-mortem whole retinal imaging, we detected GFP expression for all eyes injected with AAV8 at the two highest doses but not for the two lowest AAV8 doses. GFP expression was detected in only one of the  $10^{10}$  genome copy and two of the  $10^{11}$  genome copy AAV2-dosed eyes (Fig. 4, A and B). For the  $10^{10}$  genome copy dose, AAV8 resulted consistently in higher GFP expression than did AAV2. AAV2 can deliver similar transgene expression levels as AAV8, but it requires a 10-fold higher dose to do so.

Next, transduction intensity (Fig. 4C) and efficiency (Fig. 4D) in photoreceptors and RPE within the vector-exposed area of the retina were quantified per vector dose and serotype by morphometry of the fluorescent signal in the micrographs. Analyses were restricted to eyes that had received the entire vector dose subretinally in the absence of injection problems as noted in Table 1. Only  $10^9$  and  $10^{10}$  genome copy dose groups were analyzed quantitatively because of the marginal signal at the lowest dose and the incidence of toxicity at the highest dose, which complicated quantification. AAV8 transduction in both photoreceptor and RPE cells is equally intense at the  $10^{10}$  genome copy dose, whereas at  $10^9$  genome copies the GFP signal in photoreceptors is markedly reduced. The AAV2 transduction profile at  $10^{10}$  genome copies is similar to that of AAV8 at a 10-fold lower dose.

Within the vector-exposed subretinal space, the  $10^{10}$  genome copy dose of AAV2 and AAV8 targets 30 and 70%, respectively, of RPE and photoreceptor cells (Fig. 4D). AAV2 transduces photoreceptors at this dose, albeit at a much lower relative intensity compared to AAV8 (Fig. 4, C and D). Fifty percent of the RPE cells and 20% of photoreceptor cells are transduced with a  $10^9$  genome copy dose of AAV8. In the RPE, the relationship of AAV8 dose to transduction efficiency is nonlinear; a 10-fold higher dose realizes only a limited increase in GFP expression (Fig. 4, C and D). In contrast, a dose-related increase in photoreceptor transduction is apparent.

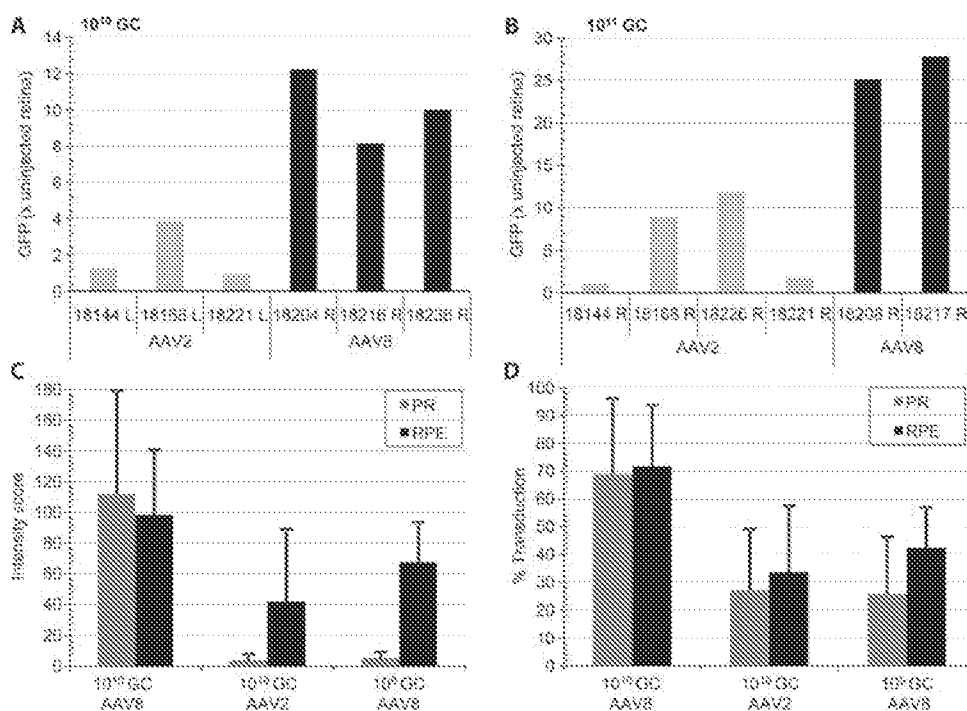


**Fig. 4.** Quantitative analysis of retinal transduction with AAV2 and AAV8. (A and B) Whole-mount retinal fluorescence after necropsy. Eyeballs were fixed, and the cornea, lens, and vitreous humor were removed to expose the posterior eye cup. Relative fluorescence was measured in a Xenogen Lumina IVIS imager and normalized to the fluorescence signal from an uninjected control eye. Eyes injected with 150  $\mu$ l of  $10^{10}$  genome copies (A) and  $10^{11}$  genome copies (B) of AAV2 or AAV8 vector are shown. (C and D) Morphometric analysis of RPE and photoreceptor (PR) transduction by AAV2 and AAV8. Relative intensity (C) and relative area (D) of the GFP expression signal in RPE and PR were established at doses of  $10^9$  and  $10^{10}$  genome copies based on morphometric histological analysis within the vector-exposed area. Numbers shown identify the animal used. L, left eye; R, right eye.

In summary, both AAV2 and AAV8 target the RPE efficiently at low doses. Substantial photoreceptor transduction is achieved at higher doses starting at 10<sup>9</sup> genome copies for AAV8 and at a 10-fold higher dose for AAV2.

**Immune responses to GFP and the AAV capsid**

Humoral and cellular immune responses to the capsid of the viral vector may affect the success of gene transfer. We therefore monitored several parameters of the host immune response to subretinal administration of AAV2 and AAV8 delivering GFP. Neutralizing antibody responses to the vector capsid were evaluated in anterior chamber fluid as well as in peripheral blood at time points before and after vector administration and at the time of necropsy. All animals in the study were negative for AAV-neutralizing antibodies at enrollment to minimize the impact of preexisting immunity on gene transfer. The host immune data are summarized in Table 2 and demonstrate a dose-related increase in neutralizing antibodies that is more pronounced in the serum than in the anterior chamber of the eye. With the exception of one eye dosed with 10<sup>10</sup> genome copies of AAV2, only eyes injected with the highest dose of the vector had detectable levels of neutralizing antibodies in the anterior chamber fluid. In serum, at a dose of 10<sup>10</sup> genome

copies, two of five animals had a titer of 1:80, whereas seven of nine animals that received 10<sup>11</sup> genome copies had titers of 1:80 to 1:640. There was no obvious correlation between eyes that developed anti-AAV-neutralizing antibodies in the anterior chamber fluid and increased intravitreal exposure to AAV (Table 1) or the presence of blood in the eye. Similarly, there was no obvious correlation between animals that showed increased anti-AAV-neutralizing antibodies in serum and increased intravitreal exposure to AAV. One animal (18226) that developed high anti-AAV-neutralizing antibodies did have blood exposure in one eye (Table 1), but two others (18180 and 18208) did not.

Cellular immune responses to both the GFP transgene product and the vector capsid were assessed by the enzyme-linked immunospot (ELISPOT) assay and intracellular cytokine staining for interferon-γ in peripheral blood mononuclear cells at day 14 after injection and in leukocytes from blood, liver, and spleen at the time of necropsy. Before AAV injection, 9 of 14 animals demonstrated detectable T cell activation in response to the AAV capsid upon amplification in the cultured ELISPOT assay, an indication of memory T cell responses. However, all animals were negative in the ex vivo assay (Table 2). Before this study, animals had not been exposed to GFP antigen. After vector administration, ex vivo ELISPOT data from peripheral blood mono-

**Table 2.** Host immune responses and toxicology. Neutralizing antibodies (NABs) directed at the AAV capsid trend upward with higher dosing in both intraocular fluid and serum. A T cell response (detected by ELISPOT assay) directed at GFP developed in two animals exposed to the highest dose of either AAV2 or AAV8. Histopathological analyses showed retinal infiltrates (observed in H&E-stained sections) in the retinas of those animals as well as in the retina of one animal that had experienced a retinal hemorrhage during the injection procedure (“hemorrhage”). Analyses of NAB responses com-

pared baseline levels of anterior chamber (AC) fluid and serum with samples at the termination of the experiment. The T cell-mediated immune response to GFP compared baseline measurements (“Pre-ex. capsid T”) with measurements taken 2 weeks after injection of AAV (“Capsid T 2w”) and at the termination of the study at 20 weeks (“GFP T 20w”). There was no correlation between expression of GFP in the optic nerve or optic chiasm and an immune response. Animals are identified by number. L, left eye; R, right eye; GFP, green fluorescent protein.

Vector serotype	AAV8										AAV2			
	10 <sup>8</sup> genome copies					10 <sup>9</sup> genome copies					10 <sup>10</sup> genome copies			
Dose	18238L	18234L	18173L	18216L	18204L	18199L	18155L	18217L	18208L	18180L	18144L	18168L	18221L	18226L
Retinal degeneration	-	-	-	-	-	-	-	-	-	-	+	-	-	-
Retina infiltrates	-	-	-	-	-	-	-	-	-	-	+	-	-	-
Optic nerve GFP	-	-	-	-	-	-	-	-	-	-	-	-	-	-
AC NAB	<1:20	<1:20	<1:20	<1:20	<1:20	<1:20	<1:20	<1:20	<1:20	<1:20	<1:20	1:20	<1:20	<1:20
Hemorrhage			+											+
Dose	10 <sup>10</sup> genome copies					10 <sup>11</sup> genome copies					10 <sup>11</sup> genome copies			
ID	18238R	18234R	18173R	18216R	18204R	18199R	18155R	18217R	18208R	18180R	18144R	18168R	18221R	18226R
Retinal degeneration	-	-	-	-	-	+	-	-	+	-	+	-	-	-
Retina infiltrates	-	-	-	-	-	+	-	-	+	-	+	-	-	-
Optic nerve GFP	+	-	-	-	-	+	+	+	+	+	+	+	+	+
AC NAB	<1:20	<1:20	<1:20	<1:20	<1:20	<1:20	1:160	<1:20	1:80	<1:20	1:80	1:20	<1:20	1:40
Hemorrhage									+	+				
Chiasm GFP	-	-	-	-	-	+	+	+	+	+	+	+	+	+
Pre-ex. capsid T	+	+	+	+	-	-	+	+	+	-	-	-	+	+
Capsid T 2w	-	-	-	-	-	-	-	-	-	-	-	-	-	-
GFP T 20w	-	-	-	-	-	+	-	-	-	-	+	-	-	-
Serum NAB	<1:20	<1:20	1:80	<1:20	1:80	<1:20	1:320	1:160	1:80	1:80	1:640	1:160	<1:20	1:320

Downloaded from <http://stm.sciencemag.org/> by guest on March 11, 2019



nuclear cells demonstrated no evidence of T cell activation in response to vector capsid either at 2 weeks after vector administration or at necropsy. Animal 18144 that received  $10^{10}$  and  $10^{11}$  genome copies per eye of AAV2 presented with T cell reactivity to GFP at necropsy in the spleen and peripheral blood mononuclear cells. T cell activation in response to the GFP transgene product was also detected in the blood, liver, and spleen of an animal (18199) given a high dose of AAV8 vector. Thus, retinal delivery of high doses of AAV2 or AAV8 carrying GFP can lead to increases in anti-AAV-neutralizing antibodies locally and systemically and can also lead to a systemic T cell response to GFP.

### Histopathology after subretinal injection of AAV2 and AAV8

Serial sections were taken throughout the area of the original retinal detachment where the AAV vectors were delivered. All sections were analyzed by DAPI staining of nuclei to evaluate retinal architecture. Hematoxylin and eosin (H&E) staining and immunohistochemistry were performed in areas where architecture was disrupted. Table 2 summarizes the results. Both retinas in the AAV2-injected animal 18144 showed retinal thinning in large portions of the exposed retina (Fig. 2B) due to loss of photoreceptor cells. Histopathology also showed foci of inflammatory cells within the retina and choroid (Fig. 2D). Pathological changes were also observed in animals 18199 and 18208 but were restricted to the right eye (Fig. 2, C and E), which received the highest dose ( $10^{11}$  genome copies) of vector. Here, too, foci of inflammatory cells, retinal thinning, and loss of the layered retinal structure in AAV-exposed regions were observed. Toxicity correlated with increased numbers of T cells in response to GFP in the periphery for animals 18144 and 18199, whereas no systemic inflammation was detected in animal 18208 (Table 2). Thus, exposure of the retina to high doses of AAV2 or AAV8 and/or high levels of GFP can lead to inflammatory changes that damage the retina.

### AAV2 and AAV8 transduction of the optic pathway

Histological analysis for positive staining for GFP along the visual pathway leading from the ganglion cells in the retina to the central nervous system (optic nerve, optic chiasm, and the lateral geniculate nuclei) was evaluated directly by fluorescence microscopy. Transduction of the optic disc was apparent in all eyes injected with  $10^{11}$  genome copies, irrespective of vector serotype or the extent to which the vitreous humor was exposed to vector, and in one eye injected with  $10^{10}$  genome copies of AAV8 (Table 2). GFP was also detected in the optic chiasm and both the ipsilateral and the contralateral lateral geniculate nucleus for all animals in the highest-dose cohort, irrespective of vector serotype. Exceptions were animals 18144 and 18199, which showed a T cell response to GFP (Table 2). Overall, there appeared to be more GFP-positive axons in animals injected with the higher doses of AAV8 compared to animals injected with the same doses of AAV2. No neuronal cell bodies in the lateral geniculate nuclei appeared to be positive for GFP, and there was no GFP detectable in the visual cortex (which is postsynaptic to the lateral geniculate nuclei). For each serotype, sections of the lateral geniculate nuclei from the animals with the greatest GFP expression in the lateral geniculate nuclei were stained with neutral red to visualize the layered structure of this region. Overlays of GFP staining and staining of cell organelles with neutral red stain are shown in fig. S2. The location of GFP-positive axons within the lateral geniculate nuclei directly correlated with known retinal projections and the retinal topography of the injection site in that the regions of the lateral genic-

ulate nuclei with the most GFP expression in axons were the regions receiving retinal projections from the eye injected with the highest titer of AAV8 or AAV2. The greatest number of GFP-positive axons was found in layer 2 of the right lateral geniculate nuclei and layer 1 of the left lateral geniculate nuclei. These layers receive inputs from the right eye, which received the highest titer of AAV8 or AAV2. GFP-positive axons were not observed in layers 3, 4, 5, or 6 of the lateral geniculate nuclei. Thus, retinal exposure to high doses of AAV2 or AAV8 can lead to transduction of a specific class of retinal ganglion cells.

### DISCUSSION

Recent results from three concurrent Phase I clinical trials for the treatment of Leber congenital amaurosis type II showed the potential for gene therapies based on subretinally delivered AAV for treating other retinal degeneration disorders (27). Broader clinical application of AAV technology will require an expanded vector toolkit along with a deeper understanding of the pharmacological, immunological, and toxicological effects of vectors and other safety aspects. For Leber congenital amaurosis, reconstitution of the RPE65 protein in the RPE was necessary and sufficient to restore retinal function. Other therapeutic approaches will require more efficient gene transfer into other cell types, particularly photoreceptor cells. There is also a need for new technologies to be investigated in animal models that more closely resemble humans with respect to anatomy, size, and host immune response. To this end, nonhuman primates are a unique and necessary resource because only primates (including humans) have both a macula and a fovea. Host immune responses to the viral vector and transgene are thought to be similar in nonhuman primates and humans because both populations are genetically heterogeneous and AAV is endemic in both (25). Here, AAV2 and AAV8 viral vectors expressing a GFP reporter transgene under control of the cytomegalovirus promoter were injected subretinally in nonhuman primates. Vector transduction of photoreceptor cells and the host immune response were evaluated as a function of vector type and dose.

The data show that the RPE is exceptionally permissive for uptake of both AAV2 and AAV8 vectors. Although it is unclear how AAV2 performs at lower doses, the relative efficiency of RPE transduction by AAV8 at  $10^9$  genome copies is similar to that of AAV2 at a 10-fold higher dose. RPE transduction does not increase linearly at higher doses, and heterogeneous patterns of GFP expression are seen in the fundus, indicating a loss of GFP transgene expression in an otherwise healthy RPE. Although these findings remain unexplained and have not been described previously in the retina, they could be attributable to RPE-specific epigenetic changes affecting the cytomegalovirus promoter leading to silencing of transgene expression (28).

Many retinal degeneration disorders affect cell types other than the RPE. Photoreceptor cells, the primary cell type involved in most retinal diseases, are a difficult cellular target for gene therapy, although progress has been made in mouse (13–15, 29), dog (17, 19, 21), and primate (20, 21) using improved vectors. Here, the relative efficiency of photoreceptor cell transduction by AAV2 and AAV8 was evaluated as a function of dose. AAV2 is less efficient compared to AAV8 at targeting photoreceptors with an ~10-fold dose differential. AAV8, at a dose of  $10^{10}$  genome copies, transduces most rod photoreceptors but not cone photoreceptors within the vector-exposed area. Cones are poorly transduced, particularly in extrafoveal areas. In the fovea, targeting

of cones is more efficient with AAV8 but can be achieved with AAV2 by increasing the vector dose. Previously, AAV5-mediated transduction was shown by Mancuso *et al.* to enhance color perception in a primate model of red-green color blindness (23, 30), which was presumed to result from cone-specific expression of the transgene. Lotery *et al.* (31) did not observe AAV5-mediated cone transduction in nonhuman primates, whereas Beltran *et al.* (17) did see this in dogs. The different conclusions of these studies may be attributable to differences in vector dose and promoter. An alternative explanation for the Mancuso *et al.* results is that rod photoreceptors were induced to behave like cones (because of transfer of L-opsin); such a possibility could be evaluated using an immunohistochemical label that is independent of the transgene. An AAV5 dosing study in nonhuman primates would also be helpful for evaluating the relative cone targeting efficiency of AAV5 compared to AAV2 or AAV8.

One vector-related concern is the extraocular distribution of the vector and transgene. The lateral geniculate nuclei carry visual information to the cerebral cortex and are the sites of the first synapse for 90% of axons coming from retinal ganglion cells. We and others have described transduction of retinal ganglion cells after intraocular administration of AAV (10, 11). Thus, it was not surprising in our new study to find GFP-positive axons that synapse with the lateral geniculate nuclei after delivery of the highest vector dose. However, unexpectedly, all of the synapses were in the lateral geniculate nuclei layers 1 and 2. These layers contain projections from M-type retinal ganglion cells, which are a minority (5 to 10%) of the ganglion cells in the retina (32). AAV2 and AAV8 may have a specific tropism for M-type retinal ganglion cells. Alternatively, M-type ganglion cells may be more accessible to vector leaking into the vitreous humor because they cover a large area of the retina owing to their extensively branched dendrites. It is less likely that vector diffuses from the subretinal space through the neuronal retina given the tight junctions between the cells. A third point of access may be the injection site in the peripheral macula, an area with denser M-type cells. Regardless of the route, it is clear that transduction of M-cells is favored and occurs efficiently at higher doses of AAV vectors. We did not observe transduction after the first synapse, which is similar to results reported in mice and dogs injected with AAV (10, 11) but different from studies in dogs using AAV8 (18). Nevertheless, these data support the use of cell-specific promoters for restricting transgene expression to primary outer retinal cellular targets.

Another safety aspect for AAV gene therapy targeting tissues including the eye is the immunological response to the AAV capsid and the transgene product. Several ocular compartments are immune-privileged based on their ability to accept foreign tissue grafts (33). But immune privilege could be breached through delivery of AAV and a foreign transgene. Immune responses and inherent toxicity to GFP could potentially contribute to the host immune response, although GFP was tolerated in previous studies in the nonhuman primate eye (20, 21). Here, intraocular administration of AAV2 and AAV8 led to increases in neutralizing antibodies to the vector capsid in a dose-related fashion. Potentially destructive T cell responses to the AAV capsid were not identified. However, evidence for responses to the GFP transgene product was found in two animals that had received the highest AAV dose. These particular animals demonstrated focal spots of retinal inflammation, retinal thinning, and disrupted retinal architecture (Table 2 and Fig. 2, B to E). For a few eyes, retinal bleeding was observed during the surgical delivery of vector. In one eye, which received the highest vector dose, inflammation was associated with leakage of

blood under the retina. Retinal degeneration is a well-known consequence of exposure of photoreceptors to blood components (34, 35). Fortunately, toxicity has not been observed in AAV-treated Leber congenital amaurosis patients, even though similar vector doses were injected into these patients. Several factors may contribute to the dissimilar findings including differences between the animal model and clinical settings in terms of vector quality and surgical procedures. The use of a reporter transgene product, GFP, which is foreign to the host, is different from the clinical setting. For example, in the AAV-Leber congenital amaurosis clinical trials, patients were injected with an AAV vector carrying a human *RPE65* complementary DNA (cDNA). The studies in this report may reflect a worst-case scenario in which a transgene product is foreign to the host, as would be the case in gene addition strategies to correct *null* mutations.

Our studies describe the dose relationship between AAV2 and AAV8 vectors and immunotoxicity in the nonhuman primate retina. Although the monkeys in this study weigh only 5 to 10% of an average human, the axial length of the eye is comparable (~70% of the axial length of the human eye). This, together with the high degree of anatomical similarity, makes nonhuman primates a relevant model for evaluating vector dosing for clinical translation of retinal gene therapies. Our data indicate the existence of dosage thresholds that need to be met to safely and efficiently target cells in the outer retina such as RPE cells and rod and cone photoreceptors. Whereas AAV2 and AAV8 efficiently transduce RPE at moderate to low doses, AAV-mediated expression of a foreign transgene in rod and cone photoreceptors was reached only at higher dosages. Substantial transduction of rods was obtained with moderate doses of AAV8 (doses that are similar to those currently used in experimental clinical protocols; <http://www.clinicaltrials.gov>). Targeting cones with AAV2 or AAV8 is less efficient than rod transduction but can be achieved at higher doses. However, at higher doses, some animals in both vector groups showed histopathological evidence of inflammatory foci and retinal degeneration. This pathology is likely attributable to transgene-specific immune responses and a transient breach of the retina-blood barrier, resulting in exposure of vector and retina to blood products. Our data suggest that AAV8, because of its ability to efficiently and safely target both RPE and photoreceptors at moderate doses, is an attractive gene transfer vehicle for gene therapy targeting the retina in patients with retinal degenerative diseases.

## SUPPLEMENTARY MATERIAL

[www.sciencetranslationalmedicine.org/cgi/content/full/3/88/88ra54/DC1](http://www.sciencetranslationalmedicine.org/cgi/content/full/3/88/88ra54/DC1)

Materials and Methods

Results

Fig. S1. Cone and rod foveal and extrafoveal tropism of AAV2 and AAV8.

Fig. S2. Colocalization of GFP and neutral red in the lateral geniculate nucleus.

Video S1 to S4. Visual behavior 4 months after subretinal injection of AAV2 versus AAV8.

References

## REFERENCES AND NOTES

1. J. W. Bainbridge, A. J. Smith, S. S. Barker, S. Robbie, R. Henderson, K. Balaggan, A. Viswanathan, G. E. Holder, A. Stockman, N. Tyler, S. Petersen-Jones, S. S. Bhattacharya, A. J. Thrasher, F. W. Fitzke, B. J. Carter, G. S. Rubin, A. T. Moore, R. R. Ali, Effect of gene therapy on visual function in Leber's congenital amaurosis. *N. Engl. J. Med.* **358**, 2231–2239 (2008).
2. W. W. Hauswirth, T. S. Aleman, S. Kaushal, A. V. Cideciyan, S. B. Schwartz, L. Wang, T. J. Conlon, S. L. Boye, T. R. Flotte, B. J. Byrne, S. G. Jacobson, Treatment of Leber congenital amaurosis due to *RPE65* mutations by ocular subretinal injection of adeno-associated virus gene vector: Short-term results of a phase I trial. *Hum. Gene Ther.* **19**, 979–990 (2008).

3. A. M. Maguire, F. Simonelli, E. A. Pierce, E. N. Pugh Jr., F. Mingozzi, J. Bencicelli, S. Banfi, K. A. Marshall, F. Testa, E. M. Surace, S. Rossi, A. Lyubarsky, V. R. Arruda, B. Konkle, E. Stone, J. Sun, J. Jacobs, L. Dell'Osso, R. Hertle, J. X. Ma, T. M. Redmond, X. Zhu, B. Hauck, O. Zelenia, K. S. Shindler, M. G. Maguire, J. F. Wright, N. J. Volpe, J. W. McDonnell, A. Auricchio, K. A. High, J. Bennett, Safety and efficacy of gene transfer for Leber's congenital amaurosis. *N. Engl. J. Med.* **358**, 2240–2248 (2008).
4. W. Berger, B. Kloeckener-Gruissem, J. Neidhardt, The molecular basis of human retinal and vitreoretinal diseases. *Prog. Retin. Eye Res.* **29**, 335–375 (2010).
5. E. M. Surace, A. Auricchio, Versatility of AAV vectors for retinal gene transfer. *Vision Res.* **48**, 353–359 (2008).
6. R. J. Samulski, K. I. Berns, M. Tan, N. Muzyczka, Cloning of adeno-associated virus into pBR322: Rescue of intact virus from the recombinant plasmid in human cells. *Proc. Natl. Acad. Sci. U.S.A.* **79**, 2077–2081 (1982).
7. R. R. Ali, M. B. Reichel, A. J. Thrasher, R. J. LeVinsky, C. Kinnon, N. Kanuga, D. M. Hunt, S. S. Bhattacharya, Gene transfer into the mouse retina mediated by an adeno-associated viral vector. *Hum. Mol. Genet.* **5**, 591–594 (1996).
8. J. Bennett, D. Duan, J. F. Engelhardt, A. M. Maguire, Real-time, noninvasive in vivo assessment of adeno-associated virus-mediated retinal transduction. *Invest. Ophthalmol. Vis. Sci.* **38**, 2857–2863 (1997).
9. J. G. Flannery, S. Zolotukhin, M. I. Vaquero, M. M. LaVail, N. Muzyczka, W. W. Hauswirth, Efficient photoreceptor-targeted gene expression in vivo by recombinant adeno-associated virus. *Proc. Natl. Acad. Sci. U.S.A.* **94**, 6916–6921 (1997).
10. L. Dudus, V. Anand, G. M. Acland, S. J. Chen, J. M. Wilson, K. J. Fisher, A. M. Maguire, J. Bennett, Persistent transgene product in retina, optic nerve and brain after intraocular injection of rAAV. *Vision Res.* **39**, 2545–2553 (1999).
11. J. Guy, X. Qi, N. Muzyczka, W. W. Hauswirth, Reporter expression persists 1 year after adeno-associated virus-mediated gene transfer to the optic nerve. *Arch. Ophthalmol.* **117**, 929–937 (1999).
12. L. H. Vandenberghe, J. M. Wilson, G. Gao, Tailoring the AAV vector capsid for gene therapy. *Gene Ther.* **16**, 311–319 (2009).
13. M. Allocca, C. Mussolino, M. Garcia-Hoyos, D. Sanges, C. Iodice, M. Pettilo, L. H. Vandenberghe, J. M. Wilson, V. Marigo, E. M. Surace, A. Auricchio, Novel adeno-associated virus serotypes efficiently transduce murine photoreceptors. *J. Virol.* **81**, 11372–11380 (2007).
14. C. Leberher, A. Maguire, W. Tang, J. Bennett, J. M. Wilson, Novel AAV serotypes for improved ocular gene transfer. *J. Gene Med.* **10**, 375–382 (2008).
15. M. Natkunarajah, P. Trittbach, J. McIntosh, Y. Duran, S. E. Barker, A. J. Smith, A. C. Nathwani, R. R. Ali, Assessment of ocular transduction using single-stranded and self-complementary recombinant adeno-associated virus serotype 2/8. *Gene Ther.* **15**, 463–467 (2008).
16. A. M. Maguire, K. A. High, A. Auricchio, J. F. Wright, E. A. Pierce, F. Testa, F. Mingozzi, J. L. Bencicelli, G. S. Ying, S. Rossi, A. Fulton, K. A. Marshall, S. Banfi, D. C. Chung, J. I. Morgan, B. Hauck, O. Zelenia, X. Zhu, I. Raffini, F. Coppieters, E. De Baere, K. S. Shindler, N. J. Volpe, E. M. Surace, C. Acerra, A. Lyubarsky, T. M. Redmond, E. Stone, J. Sun, J. W. McDonnell, B. P. Leroy, F. Simonelli, J. Bennett, Age-dependent effects of *RPE65* gene therapy for Leber's congenital amaurosis: A phase 1 dose-escalation trial. *Lancet* **374**, 1597–1605 (2009).
17. W. A. Beltran, S. L. Boye, S. E. Boye, V. A. Chiodo, A. S. Lewin, W. W. Hauswirth, G. D. Aguirre, rAAV2/5 gene-targeting to rods: Dose-dependent efficiency and complications associated with different promoters. *Gene Ther.* **17**, 1162–1174 (2010).
18. K. Stieger, M. A. Colle, L. Dubreil, A. Mendes-Madeira, M. Weber, G. Le Meur, J. Y. Deschamps, N. Provost, D. Nivard, Y. Chérel, P. Moulrier, F. Rolling, Subretinal delivery of recombinant AAV serotype 8 vector in dogs results in gene transfer to neurons in the brain. *Mol. Ther.* **16**, 916–923 (2008).
19. S. M. Petersen-Jones, J. T. Bartoe, A. J. Fischer, M. Scott, S. L. Boye, V. Chiodo, W. W. Hauswirth, AAV retinal transduction in a large animal model species: Comparison of a self-complementary AAV2/5 with a single-stranded AAV2/5 vector. *Mol. Vis.* **15**, 1835–1842 (2009).
20. J. Bennett, A. M. Maguire, A. V. Cideciyan, M. Schnell, E. Glover, V. Anand, T. S. Aleman, N. Chirmule, A. R. Gupta, Y. Huang, G. P. Gao, W. C. Nyberg, J. Tazelaar, J. Hughes, J. M. Wilson, S. G. Jacobson, Stable transgene expression in rod photoreceptors after recombinant adeno-associated virus-mediated gene transfer to monkey retina. *Proc. Natl. Acad. Sci. U.S.A.* **96**, 9920–9925 (1999).
21. M. Weber, J. Rabinowitz, N. Provost, H. Conrath, S. Folliot, D. Briot, Y. Chérel, P. Chenuaud, J. Samulski, P. Moulrier, F. Rolling, Recombinant adeno-associated virus serotype 4 mediates unique and exclusive long-term transduction of retinal pigmented epithelium in rat, dog, and nonhuman primate after subretinal delivery. *Mol. Ther.* **7**, 774–781 (2003).
22. J. W. Bainbridge, A. Mistry, F. C. Schlichtenbrede, A. Smith, C. Broderick, M. De Alwis, A. Georgiadis, P. M. Taylor, M. Squires, C. Sethi, D. Charteris, A. J. Thrasher, D. Sargan, R. R. Ali, Stable rAAV-mediated transduction of rod and cone photoreceptors in the canine retina. *Gene Ther.* **10**, 1336–1344 (2003).
23. K. Mancuso, A. E. Hendrickson, T. B. Connor Jr., M. C. Mauck, J. J. Kinsella, W. W. Hauswirth, J. Neitz, M. Neitz, Recombinant adeno-associated virus targets passenger gene expression to cones in primate retina. *J. Opt. Soc. Am. A Opt. Image Sci. Vis.* **24**, 1411–1416 (2007).
24. R. Calcedo, L. H. Vandenberghe, G. Gao, J. Lin, J. M. Wilson, Worldwide epidemiology of neutralizing antibodies to adeno-associated viruses. *J. Infect. Dis.* **199**, 381–390 (2009).
25. G. Gao, L. H. Vandenberghe, J. M. Wilson, New recombinant serotypes of AAV vectors. *Curr. Gene Ther.* **5**, 285–297 (2005).
26. L. H. Vandenberghe, L. Wang, S. Somanathan, Y. Zhi, J. Figueredo, R. Calcedo, J. Sanmiguel, R. A. Desai, C. S. Chen, J. Johnston, R. L. Grant, G. Gao, J. M. Wilson, Heparin binding directs activation of T cells against adeno-associated virus serotype 2 capsid. *Nat. Med.* **12**, 967–971 (2006).
27. K. Roy, L. Stein, S. Kaushal, Ocular gene therapy: An evaluation of recombinant adeno-associated virus-mediated gene therapy interventions for the treatment of ocular disease. *Hum. Gene Ther.* **21**, 915–927 (2010).
28. G. Grassi, P. Maccaroni, R. Meyer, H. Kaiser, E. D'Ambrosio, E. Pascale, M. Grassi, A. Kühn, P. Di Nardo, R. Kandolf, J. H. Klüpper, Inhibitors of DNA methylation and histone deacetylation activate cytomegalovirus promoter-controlled reporter gene expression in human glioblastoma cell line U87. *Carcinogenesis* **24**, 1625–1635 (2003).
29. A. Auricchio, G. Kobinger, V. Anand, M. Hildinger, E. O'Connor, A. M. Maguire, J. M. Wilson, J. Bennett, Exchange of surface proteins impacts on viral vector cellular specificity and transduction characteristics: The retina as a model. *Hum. Mol. Genet.* **10**, 3075–3081 (2001).
30. K. Mancuso, W. W. Hauswirth, Q. Li, T. B. Connor, J. A. Kuchenbecker, M. C. Mauck, J. Neitz, M. Neitz, Gene therapy for red-green colour blindness in adult primates. *Nature* **461**, 784–787 (2009).
31. A. J. Lotery, G. S. Yang, R. F. Mullins, S. R. Russell, M. Schmidt, E. M. Stone, J. D. Lindbloom, J. A. Chiorini, R. M. Kotin, B. L. Davidson, Adeno-associated virus type 5: Transduction efficiency and cell-type specificity in the primate retina. *Hum. Gene Ther.* **14**, 1663–1671 (2003).
32. V. H. Perry, R. Oehler, A. Cowey, Retinal ganglion cells that project to the dorsal lateral geniculate nucleus in the macaque monkey. *Neuroscience* **12**, 1101–1123 (1984).
33. J. Stein-Streilein, Immune regulation and the eye. *Trends Immunol.* **29**, 548–554 (2008).
34. H. Glatt, R. Machemer, Experimental subretinal hemorrhage in rabbits. *Am. J. Ophthalmol.* **94**, 762–773 (1982).
35. H. E. Grossniklaus, D. J. Wilson, S. B. Bressler, N. M. Bressler, C. A. Toth, W. R. Green, P. Miskala, Clinicopathologic studies of eyes that were obtained postmortem from four patients who were enrolled in the submacular surgery trials: SST Report No. 16. *Am. J. Ophthalmol.* **141**, 93–104 (2006).
36. **Acknowledgments:** We thank T. Cronin and P. Sulaiman for assistance with confocal microscopy, P. Macleish (Morehouse School of Medicine, Atlanta, GA) for the 7G6 cone arrestin antibody, and T. Irvin and E. Bote for support with the animal work. **Funding:** Supported by grants to J.M.W. from GlaxoSmithKline Pharmaceuticals Inc.; to J.B. from Research to Prevent Blindness, Foundation Fighting Blindness, the Paul and Evanina Mackall Foundation Trust, and the F. M. Kirby Foundation; to J.H.W. from the National Institute of Neurological Disorders and Stroke (NS038690) and training support for C.N.C. (NS007180) and M.J.C. (NS007413); and to L.H.V. by grant UL1RR024134 from the National Center for Research Resources and the Institute for Translational Medicine and Therapeutics at the University of Pennsylvania. **Author contributions:** L.H.V., J.M.W., and J.B. designed the research approach. R.G., L.H.V., J.B., and J.M.W. obtained regulatory approvals. A.M.M. carried out the surgery with assistance from J.B., L.H.V., and R.G. R.G. provided veterinary oversight and obtained tissue samples. J.B. and A.M.M. carried out in vivo evaluations of GFP expression and performed fundus photography. L.W. and R.C. performed immunologic studies. P.B., L.H.V., R.X., J.M.W., and J.B. carried out ocular histologic evaluations. C.N.C., M.J.C., and J.H.W. performed lateral geniculate nuclei histology and the interpretation thereof. A.C.M. did visual behavior studies and video editing. L.H.V., J.M.W., and J.B. wrote the paper. **Competing interests:** J.M.W. is a consultant to ReGenX Holdings and is a founder of, holds equity in, and receives a grant from affiliates of ReGenX Holdings. J.M.W. is an inventor on a patent licensed to various biopharmaceutical companies (adeno-associated virus serotype 8 sequences, vectors containing same, and uses thereof; USPTO 20080075740, WO/2003/052051). A.M.M. and J.B. are co-inventors on a pending patent for a method to treat or slow the development of blindness (WO/2002/082904, PCT/US2002/011314), both waived any financial interest in this technology in 2002. J.B. served on a scientific advisory board for Sanofi-Aventis and as a consultant for GlaxoSmithKline in 2010. The other authors declare that they have no competing interests.

Submitted 4 January 2011

Accepted 3 June 2011

Published 22 June 2011

10.1126/scitranslmed.3002103

**Citation:** L. H. Vandenberghe, P. Bell, A. M. Maguire, C. N. Cearley, R. Xiao, R. Calcedo, L. Wang, M. J. Castle, A. C. Maguire, R. Grant, J. H. Wolfe, J. M. Wilson, J. Bennett, Dosage thresholds for AAV2 and AAV8 photoreceptor gene therapy in monkey. *Sci. Transl. Med.* **3**, 88ra54 (2011).

# Science Translational Medicine

## Dosage Thresholds for AAV2 and AAV8 Photoreceptor Gene Therapy in Monkey

Luk H. Vandenberghe, Peter Bell, Albert M. Maguire, Cassia N. Cearley, Ru Xiao, Roberto Calcedo, Lili Wang, Michael J. Castle, Alexandra C. Maguire, Rebecca Grant, John H. Wolfe, James M. Wilson and Jean Bennett

*Sci Transl Med* 3, 88ra5488ra54.  
DOI: 10.1126/scitranslmed.3002103

### Gene Therapy Shines Light on Darkness

Using gene therapy to treat diseases of retinal degeneration is feasible because the human eye is compact, easy to access, and is an immune-privileged site. Phase I and II clinical trials using an adeno-associated virus serotype 2 (AAV2) viral vector to deliver a gene encoding RPE65 to retinal pigment epithelium (RPE) in children with congenital blindness due to Leber congenital amaurosis disease have shown the feasibility of using gene therapy to restore retinal function and partial vision. Other diseases of retinal degeneration are caused primarily by loss of the rod and cone photoreceptor cells rather than degeneration of RPE. Photoreceptor cells are more difficult to target with a vector carrying a therapeutic gene. As a first step toward using gene therapy to treat diseases caused by degeneration of photoreceptors, Vandenberghe *et al.* experiment with the dose of two AAV vectors (AAV2 and AAV8) in a nonhuman primate model.

The researchers injected either AAV2 or AAV8 vectors subretinally in cynomolgus macaques across a range of doses (from  $10^8$  to  $10^{11}$  genome copies). The vectors carried a transgene encoding green fluorescent protein (GFP), and the researchers used this marker to discern at which dose both RPE and photoreceptor cells could be transduced with the vector and express GFP. After injection, the monkeys were examined for any retinal damage due to surgery and for any immune response to the vector or to GFP. Both vector serotypes were efficient at transducing RPE, but AAV8 was also able to transduce photoreceptor cells (primarily rods but also some cones); AAV2 could only transduce photoreceptor cells at the highest dose. With respect to an immune response, anti-vector-neutralizing antibodies and a T cell response directed at GFP were detected at the highest doses of AAV2 and AAV8 leading to retinal inflammation and thinning. Thus, the authors conclude that using AAV8 at intermediate doses will be the best approach for using gene therapy to transduce photoreceptor cells with a therapeutic gene. These preclinical studies pave the way toward using gene therapy to treat a variety of retinal degeneration diseases caused by loss of photoreceptor cells.

ARTICLE TOOLS	<a href="http://stm.sciencemag.org/content/3/88/88ra54">http://stm.sciencemag.org/content/3/88/88ra54</a>
SUPPLEMENTARY MATERIALS	<a href="http://stm.sciencemag.org/content/suppl/2011/06/20/3.88.88ra54.DC1">http://stm.sciencemag.org/content/suppl/2011/06/20/3.88.88ra54.DC1</a>
RELATED CONTENT	<a href="http://stm.sciencemag.org/content/scitransmed/5/189/189ra76.full">http://stm.sciencemag.org/content/scitransmed/5/189/189ra76.full</a> <a href="http://stm.sciencemag.org/content/scitransmed/5/175/175fa3.full">http://stm.sciencemag.org/content/scitransmed/5/175/175fa3.full</a> <a href="http://stm.sciencemag.org/content/scitransmed/5/202/202ra122.full">http://stm.sciencemag.org/content/scitransmed/5/202/202ra122.full</a> <a href="http://stm.sciencemag.org/content/scitransmed/5/203/203ra127.full">http://stm.sciencemag.org/content/scitransmed/5/203/203ra127.full</a> <a href="http://stm.sciencemag.org/content/scitransmed/5/211/211ra156.full">http://stm.sciencemag.org/content/scitransmed/5/211/211ra156.full</a>
REFERENCES	This article cites 35 articles, 5 of which you can access for free <a href="http://stm.sciencemag.org/content/3/88/88ra54#B1B1">http://stm.sciencemag.org/content/3/88/88ra54#B1B1</a>

Use of this article is subject to the Terms of Service

*Science Translational Medicine* (ISSN 1946-6242) is published by the American Association for the Advancement of Science, 1200 New York Avenue NW, Washington, DC 20005. 2017 © The Authors, some rights reserved; exclusive licensee American Association for the Advancement of Science. No claim to original U.S. Government Works. The title *Science Translational Medicine* is a registered trademark of AAAS.

PERMISSIONS

<http://www.sciencemag.org/help/reprints-and-permissions>

Downloaded from <http://stm.sciencemag.org/> by guest on March 11, 2019

Use of this article is subject to the Terms of Service

---

*Science Translational Medicine* (ISSN 1946-6242) is published by the American Association for the Advancement of Science, 1200 New York Avenue NW, Washington, DC 20005. 2017 © The Authors, some rights reserved; exclusive licensee American Association for the Advancement of Science. No claim to original U.S. Government Works. The title *Science Translational Medicine* is a registered trademark of AAAS.

EX. C

# AAV9 Targets Cone Photoreceptors in the Nonhuman Primate Retina

Luk H. Vandenberghe<sup>1\*</sup>, Peter Bell<sup>1</sup>, Albert M. Maguire<sup>2</sup>, Ru Xiao<sup>1,2a</sup>, Tim B. Hopkins<sup>2,2ab</sup>, Rebecca Grant<sup>1</sup>, Jean Bennett<sup>2</sup>, James M. Wilson<sup>1\*</sup>

**1** Gene Therapy Program, Department of Pathology and Laboratory Medicine, University of Pennsylvania, Philadelphia, Pennsylvania, United States of America, **2** F. M. Kirby Center for Molecular Ophthalmology, Scheie Eye Institute, University of Pennsylvania, Philadelphia, Pennsylvania, United States of America

## Abstract

Transduction of retinal pigment epithelial cells with an adeno-associated viral vector (AAV) based on serotype 2 has partially corrected retinal blindness in Leber congenital amaurosis type 2. However, many applications of gene therapy for retinal blindness rely on the efficient transduction of rod and cone photoreceptor which is difficult to achieve with first generation vector technology. To address this translational need, we evaluated rod and cone photoreceptor targeting of 4 novel AAV capsids (AAV7, AAV9, rh.64R1 and rh.8R) versus AAV2 and AAV8 in a foveated retina. Eyes of 20 nonhuman primates were injected subretinally in the proximity of the fovea. While numerous vectors efficiently transduced rods, only AAV9 targeted cones both centrally and peripherally efficiently at low doses, likely due to the abundance of galactosylated glycans, the primary receptor for AAV9, on cone photoreceptors. We conclude AAV9 is an ideal candidate for strategies that require restoration of cone photoreceptor function.

**Citation:** Vandenberghe LH, Bell P, Maguire AM, Xiao R, Hopkins TB, et al. (2013) AAV9 Targets Cone Photoreceptors in the Nonhuman Primate Retina. *PLoS ONE* 8(1): e53463. doi:10.1371/journal.pone.0053463

**Editor:** Xiao Xiao, UNC Eshelman School of Pharmacy, United States of America

**Received:** October 2, 2012; **Accepted:** November 22, 2012; **Published:** January 30, 2013

**Copyright:** © 2013 Vandenberghe et al. This is an open-access article distributed under the terms of the Creative Commons Attribution License, which permits unrestricted use, distribution, and reproduction in any medium, provided the original author and source are credited.

**Funding:** The authors would like to acknowledge the support of GlaxoSmithKline for a research grant and NIH P30 DK47757 (JMW). This work was also supported by the Foundation Fighting Blindness (LHV, JB), its CHOP-PENN Pediatric Center for Retinal Degenerations (JB), Transdisciplinary Award Program in Translational Medicine and Therapeutics (TAPITMAT) from the University of Pennsylvania (LHV, JB), Research to Prevent Blindness, the Paul and Evanina Mackall Foundation Trust at Scheie Eye Institute, and the F. M. Kirby Foundation (JB). The funders had no role in study design, data collection and analysis, decision to publish, or preparation of the manuscript.

**Competing Interests:** The authors have the following interests. LHV is co-inventor on patents describing several of the AAV serotypes described in this manuscript as well as related technologies. These patents have been licensed to various pharmaceutical and biotechnological enterprises, and further details are available on request. LHV and JB are co-founders of GenSight Biologics which pursues ocular gene therapy approaches using AAV. JB and AMM are co-inventors of a patent for a method to treat or slow the development of blindness (US patent 424/93.2), but both waived any financial interest in this technology in 2002. JMW is a consultant to ReGenX Holdings, and is a founder of, holds equity in, and receives a grant from affiliates of ReGenX Holdings; in addition, he is an inventor on patents licensed to various biopharmaceutical companies, including affiliates of ReGenX Holdings. Further details are available on request. This study was partly supported by GlaxoSmithKline. There are no further patents, products in development or marketed products to declare. This does not alter the authors' adherence to all the PLOS ONE policies on sharing data and materials, as detailed online in the guide for authors.

\* E-mail: wilsonjm@mail.med.upenn.edu (JMW); luk\_vandenberghe@mei.harvard.edu (LHV)

† These authors contributed equally to this work.

<sup>2a</sup> Current address: Massachusetts Eye and Ear Infirmary and Schepens Eye Research Institute, Harvard Medical School, Boston, Massachusetts, United States of America

<sup>2b</sup> Current address: F. Edward Hebert School of Medicine, Uniformed Services University of the Health Sciences, Bethesda, Maryland, United States of America

## Introduction

The normal human retina contains two main classes of light-sensing neurons: rod photoreceptors (PR), which are sensitive to dim light, and cone PR, which respond to bright light stimuli. Gene mutations hinder the function of either or both of these sets of cells, and lead to their degeneration and subsequent loss of vision. Over 200 different genes/loci are implicated in these types of blinding disorders (<http://www.sph.uth.tmc.edu/retnet/disease.htm>). Retinitis pigmentosa (RP) primarily affects rod PR but can result in secondary abnormalities of cones [1]. Cone and cone-rod dystrophies such as Stargardt's disease are characterized by a primary cone involvement, with possibly concomitant loss of rods [2]. Achromatopsia is associated with reduced or minimal cone function, and the complete form of this disorder is autosomal recessive in inheritance [3]. Age-related macular degeneration affects rods and cones centrally in the retina due to atrophy of the retinal pigment epithelium (RPE).

The normal arrangement and ratios of cone and rod photoreceptors across the retina are important variables affecting disease presentation. Only primates have a cone-rich macula and cone-only fovea; this region provides humans (and other primates) with fine visual resolution and color discrimination. Besides its involvement in retinal degenerative disease, the macula is vulnerable to damage from other genetic and environmental insults (e.g., age-related macular degeneration and diabetic retinopathy). While some non-primate retinas have regions of increased cone density (e.g., canine area centralis), none reflect the organization, set of color pigments, or high cone density as in primates. Cones are particularly sparse in rodent models of human retinal disease.

Multiple gene therapy strategies for inherited retinal degeneration are actively considered and have been tested in animal models, including: a) gene augmentation, in which a correct cDNA of the disease gene is introduced in the native cell type; b) ocular

Table 1. Design, surgical and ophthalmoscopic observations.

ID	animal	weight (kg)	duration (days)	dose 10 <sup>4</sup>	RIGHT				LEFT										
					SR (%)	IV (%)	notes	GFP Score	OD	dose 10 <sup>4</sup>	SR (%)	IV (%)	notes	GFP Score	OD				
								1w	1mo	3mo				1w	1mo	3mo	4mo		
<b>AAV7</b>	C21332	2.30	127.00	10	100	0	0	3	4	+	9	100	0	2x	0	2	2	-	
	C21410	2.60	127.00	10	100	0	A,F	0	4+	+	9	90	10		0	1	2+	-	
	C21418	3.35	128.00	9	100	0	JF	0	2-	-	10	100	0	JF	0	3+	4	+	
	C21427	2.45	135.00	10	50	0	F	0	4	+	9	100	0	F	0	0	3-	-	
	C21429	2.25	135.00	9	0	100	IV	0	0	+	10	100	0	F	0	2+	2F	-	
<b>AAV9</b>	C21361	2.30	146.00	10	100	0	F	0	4	+	9	100	0	F	0	1	2-	-	
	C21382	2.35	146.00	10	100	0	B,F	0	4-	+	9	15	0	SRPE,M	0	0	2+	-	
	C21387	2.50	147.00	10	30	70	IV	0	4	+	9	100	0		0	2+	2-	-	
	C21388	2.75	147.00	10	100	0		0	3	+	9	100	0		0	2	3	-	
	C21390	2.35	149.00	10	100	0	A,F	0	4	+	9	10	60	SRPE	0	0	0	-	
<b>rh64R1</b>	C21366	2.35	153.00	10	100	0	F	0	4	4F	NA	9	100	0	JF	0	2	2	-
	C21369	2.30	153.00	10	50	50	F	0	1-	3+	+	9	60	0	SRPE,F	0	2	0	-
	C21376	2.10	154.00	10	100	0	F	0	4	+	9	100	0	F	0	2+	2	-	
	C21379	2.30	154.00	10	100	0	B,F	4	3	+	9	50	50		0	0	3	-	
	C21380	3.30	156.00	10	100	0	2x,6M,F	0	3-	+	10	100	0	F	0	4	4	+	
<b>rh8R</b>	C21336	2.30	118.00	10	100	0	2x	0	4	4+	+	9	100	0	2x	0	2-	3-	-
	C21339	3.35	118.00	10	100	0		2	4-	3+	+	9	100	0		0	3	2-	-
	C21342	2.30	119.00	10	100	0		2	4	4+	+	9	100	0		0	2	2+	-
	C21355	2.25	119.00	10	100	0		0	4	4+	+	9	100	0		0	2	3+	+
	C21360	2.40	121.00	10	100	0		1	4	4+	+	9	100	0		1	2+	3+	+

Cells with italicized font are excluded from the quantitative post mortem analysis shown in Fig. 1 due to injection issues as highlighted in the notes column; % SR and IV reflect estimates of vector deposit in subretinal and vitreal spaces respectively; GFP Score ranges from 0 (no visible expression) to 4 (broad and intense GFP) and reflects a subjective composite of both intensity and area of transduction as observed by indirect ophthalmoscopy; F: foveal; B: blood; A: viable air bubble; 2x: injection procedure was interrupted following sclerotomy and restarted making use of the initial sclerotomy a second time due to technical concerns; SRPE: subRPE or choroidal injection; JF: juxtatapeal; M: macular hole; SR: subretinal; IV: intravitreal; ID: identification number; GFP: green fluorescent protein; OD: optic disc.

doi:10.1371/journal.pone.0055463.t001



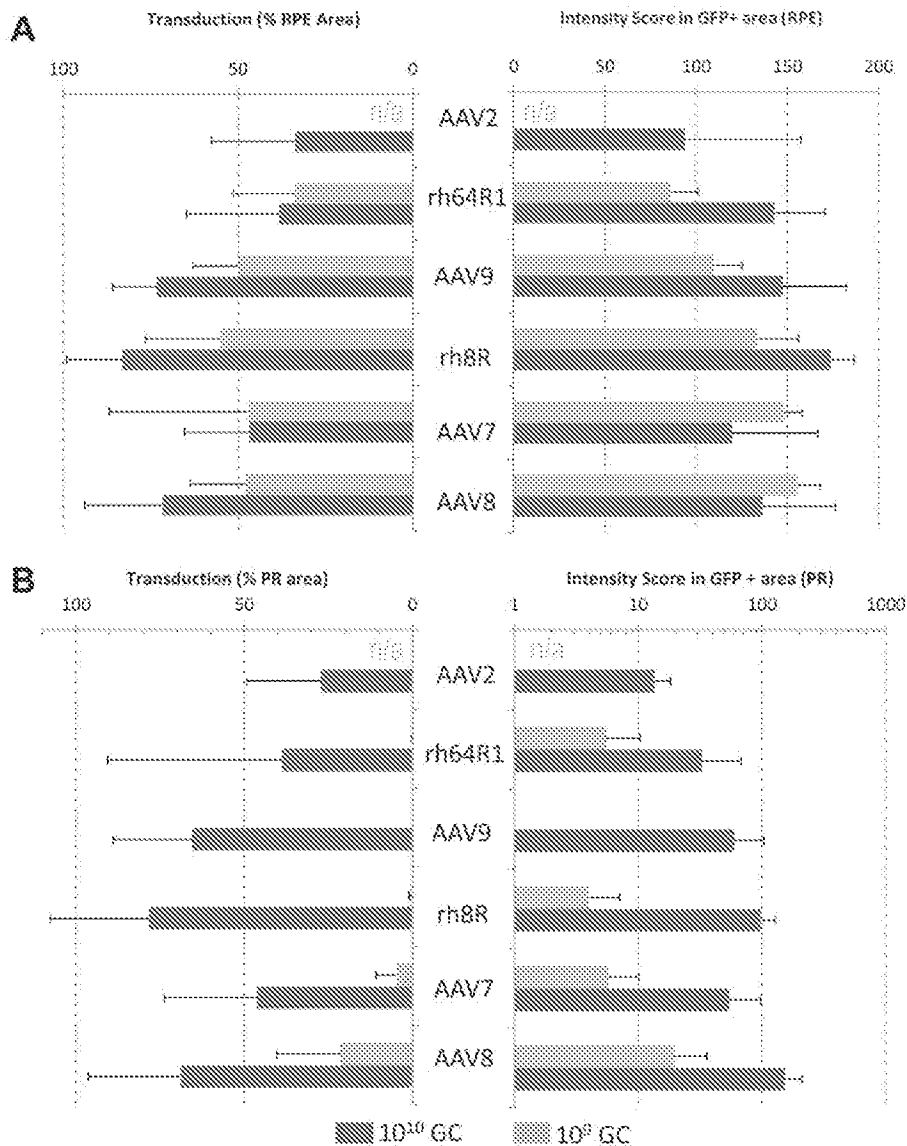


**Figure 1. Quantitative analysis of tropism and transgene expression levels in the NHP eye.** Cynomolgus macaques were injected with AAVs expressing  $10^9$  or  $10^{10}$  GC per eye. Following necropsy at 4–5 month post injection, retinas were sectioned and analyzed for direct fluorescence. Data from a morphometric analysis in the RPE (A) and PR (B) layers is presented with the relative area of transduction on the left and an intensity scoring on the right. AAV2 and AAV8 data are historical data from an analogous, previously reported study [6] [a  $10^9$  GC injection was not performed for AAV2 (n/a)]. Eyes for which the injection failed as noted in Table 1 were excluded from this analysis. Data is presented as average and standard deviation.

doi:10.1371/journal.pone.0053463.g001

expression of a trophic factor geared to stall disease progression; c) gene knock-down of a toxic gene product in combination with gene augmentation; and d) re-sensitization of the remaining retinal cells to light [4]. In one promising method of re-sensitization of the retina, genetic reactivation of atrophic cones can be achieved by cone-targeted expression of halorhodopsin, a light-activated chloride pump isolated from *Archaea* [5].

Vectors based on AAV have shown distinct promise for *in vivo* applications of retinal gene therapy for PR degenerative disease. Vectors coated with different AAV capsid structures such as those derived from naturally occurring serotypes demonstrate dose-related tropism following subretinal injection [6]. All human applications of AAV gene transfer to the retina, and most other target organs, have utilized vectors based on serotype 2 (AAV2) [7,8,9]. Small and large animal studies demonstrate that AAV2

primarily targets the RPE following subretinal injection. AAV2-mediated transduction of RPE has achieved partial reconstitution of function in three different clinical trials for a severe, early onset form of RP termed Leber congenital amaurosis caused by a defect in RPE65. Whereas these trials rely on gene augmentation in the RPE, the majority of the other gene defects that can lead to blindness will require targeting of PR including rods and/or cones [10]. PR transduction is feasible with high-dose AAV2 vectors in canine, feline and primate animal models where it targets rods more efficiently than cones [6,11,12]. AAV5 targets PR more readily, but analogous to AAV2 also preferentially targets rods [13], though some level of cone and rod transduction was observed with the use of the human rhodopsin kinase promoter [14]. Indeed, studies using AAV5 with cone-specific promoters and at high dose did achieve functional rescue of achromatopsia (rod

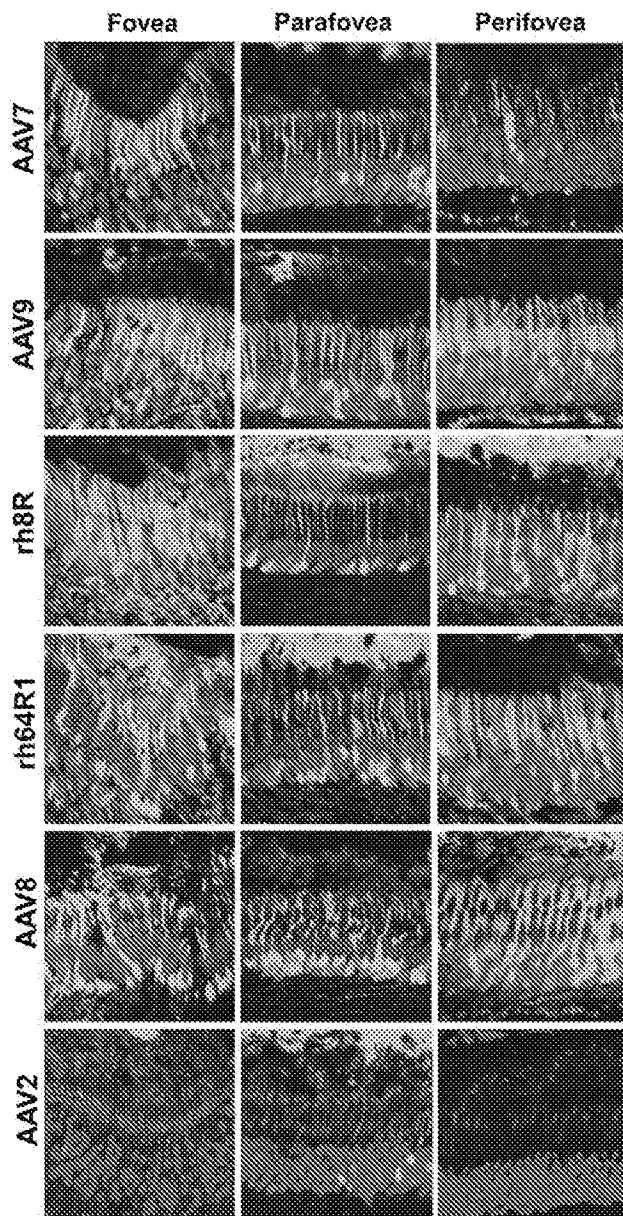


**Figure 2. AAV cell targeting in the fovea, parafovea and perifovea.** Histological sections were stained with DAPI (blue) and peanut agglutinin (red), a lectin specific for terminal galactose residues prevalent on cone PR, and finally visualized for GFP (green) by direct fluorescence. The foveal, parafoveal and perifoveal regions were identified based on topology and cone density. Perifoveal areas were chosen in a region between 1.3 and 1.9 mm from the fovea. Within the subretinal injection area, cone transduction in the peripheral retina was similar in efficiency to that in the perifovea. doi:10.1371/journal.pone.0053463.g002

monochromacy) in a dog [15] and dichromatism (red-green color blindness) in an NHP model [16]. AAV7 and AAV8 are more effective than AAV5 in PR targeting in mouse [17,18]. In dogs, subretinally injected AAV8 demonstrated significant transduction of the neuroretina including PRs [19]. AAV8 pig studies reflect similar findings with some but limited cone transduction [20]. Data from our previous NHP study demonstrated that AAV8 was markedly more efficient at targeting rod PR than AAV2 at all

doses studied. Partial cone transduction was achieved but only at elevated doses of  $10^{11}$  GC [6].

What determines the tropism and pharmacology of AAV serotypes in the retina remains largely unknown, although studies in other therapeutic target organs noted that serotypes interact differentially with entry and post-entry cellular determinants of transduction. AAV9 was recently found to use terminal galactose on cell-surface bound glycans as its receptor *in vitro* and *in vivo* [21]. AAV2 is known to utilize heparin sulfate proteoglycans as its primary receptor for cellular recognition [22]. Viral entry of AAV1, 4, 5, and 6 is initiated by sialylated glycoproteins [23,24].

The distinct properties of AAV serotypes in terms of tropism and dosage thresholds in the retina and other organs motivated us to explore other natural AAV variants derived from novel viral clades identified in a biopanning effort in our laboratory from human and NHP tissues [25,26]. In this study, six promising capsids representing different clades were selected for evaluation in NHP including AAV2, AAV7, AAV8, AAV9, rh.8R and rh.64R1 in order to quantitatively assess RPE, rod and cone transduction.

## Results

Cynomolgus macaques, 2–3 years of age, were injected subretinally with  $10^9$  or  $10^{10}$  GC of AAV.CMV.eGFP packaged with the respective capsids. A total of 40 eyes from 20 animals were injected with vector and subjected to experimental analysis. Informative doses to evaluate vector tropism were established in previous AAV dose-ranging studies with AAV2 and AAV8 [6]. Injections were generally superior-temporal the details of which are summarized in **Table 1**. In some eyes, the subretinal exposure area extended over the fovea. Most injections were uneventful, however in eight eyes, surgical complications were noted (**Table 1**). The most significant complications occurred with injections in the vicinity of the fovea. In two eyes, a fistula developed through the fovea and vector leaked through the macular hole. In addition to the retinal complications, hyphema (anterior chamber blood) developed prior to injection at the time of paracentesis in another two eyes, although these did not obscure the retina during the injection procedure. The other complications involved unintentional deposition of vector in areas outside the subretinal space. Of note, the surgical procedure in the animal studies described here is not the same used in humans, where standard 3 port pars plana vitrectomy (without paracentesis) is performed. The NHP injection procedure is modified to take into account the unique surgical anatomy of these smaller animals and the desire to reduce anesthesia time.

Animals were followed for general well-being and retinal health throughout the study. The breadth, intensity and onset of the retinal GFP expression were monitored by indirect ophthalmoscopy (**Table 1**). Clinicopathologic correlates were evaluated for 4–5 months following injection after which animals were euthanized and tissue was harvested for extensive and detailed histological analysis.

Indirect ophthalmoscopy assessed intensity and distribution of retinal GFP expression during the in-life phase of the study. The composite score, which incorporated intensity and area of transduction, ranged from a low of 0 to a high of 4. Expression peaked at 1 month and was stable for the duration of the study. More than 50% of eyes had detectable GFP in the optic disc at the high dose. Remarkably, only two eyes in the low dose presented GFP in the optic disc and both were rh.8R-transduced (**Table 1**). Histological sections from several relevant retinal regions of each eye were analyzed including the injection area, the fovea and optic disc. The retina is organized into regions circumferential to the

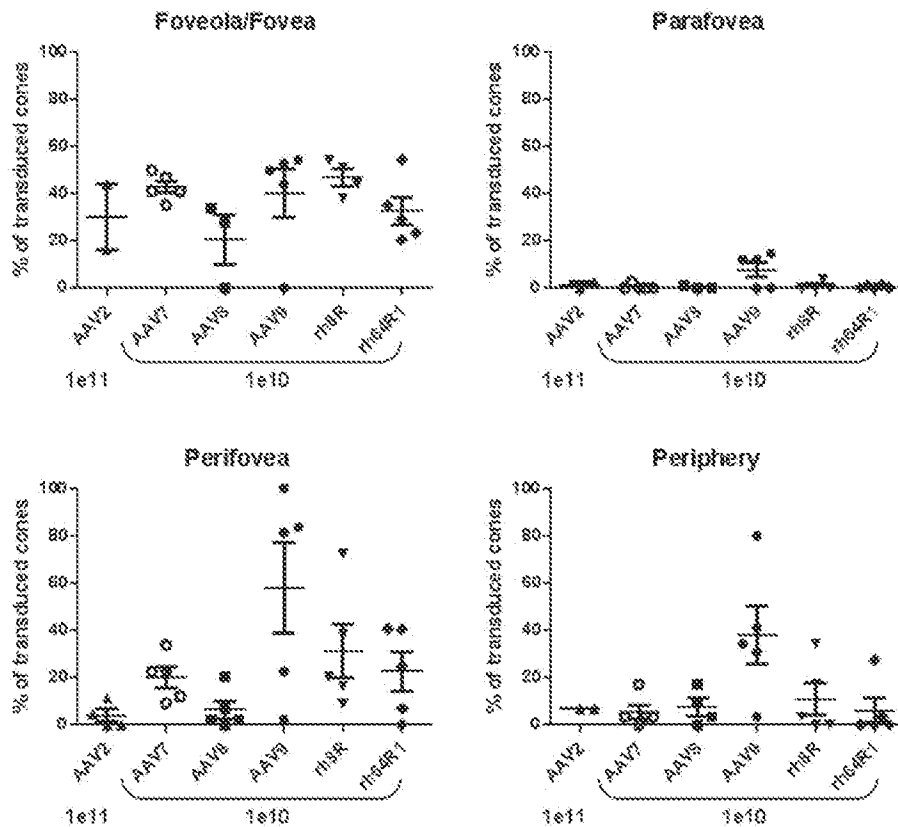


**Figure 3. Quantitative assessment of cone photoreceptor transduction across the nonhuman primate retina.** For each eye and for each of the foveal, parafoveal, perifoveal and peripheral retina regions, GFP positive cones were counted on histological sections. Shown is the percentage of the average number of GFP-positive cones relative to the average total cone number for each eye and region. Each eye for which viable sections were available was included in this analysis, including those for which the injection was suboptimal or problematic and the bleb may not have extended across the fovea/parafovea. doi:10.1371/journal.pone.0053463.g003

foveola/fovea including the parafovea, perifovea, and the periphery (Figure S1). To quantitatively assess vector targeting, morphometric analysis for GFP in PR (without rod/cone differentiation) and RPE was performed in the most distal regions from the fovea including the perifovea and periphery. Figure 1 summarizes these data for the 4 candidate capsids and includes those from similarly designed studies with AAV2 and AAV8 [6] in terms of the relative area of transduction and GFP intensity in transduced areas. RPE transduction was found to be variable yet efficient with all experimental serotypes at either dose suggesting that transduction of RPE by AAV at these doses is not determined by dose or capsid (Figure 1A). At the high dose, PRs were broadly and intensely transduced with most AAV types, though some serotype-dependency was noted. Due to the abundance of rods in the regions evaluated here, data in Figure 1B largely captures rod transduction with cones contributing only marginally. Substantially lower transduction was observed at the  $10^9$  GC dose, with a clear serotype-dependent permissivity of PRs. Whereas AAV9, rh.64R1 and rh.8R achieve very limited rod PR transduction at  $10^9$  GC, AAV7 or AAV8 result in GFP expression in 5% and 22% of rod PR within the region exposed to vector, respectively, at levels of expression similar to AAV2 at a 10-fold higher dose (Figure 1B).

To study in greater detail the relative targeting of rods and cones, we expanded the analyses to include the cone-only foveola, and the concentric ring around the foveola named the parafovea, as well as the surrounding cone-enriched perifovea, and the retinal

periphery (Figure S1). Histological analysis provided in Figure 2, illustrates that across serotypes, foveal cones are more readily transduced as compared to extrafoveal cones. High dose of AAV9 ( $10^{10}$  GC) however appeared to achieve higher levels of cone transduction in the fovea and the perifovea (Figure 2) than other vectors, including AAV2 and 8 at the even higher dose of  $10^{11}$  GC [6]. A surprising observation with all AAVs tested, including AAV9, was that only limited cone transduction was observed in the parafoveal region, even in the presence of RPE and rod PR transduction (Figure 2).

A quantitative assessment of cone transduction of all vectors at a moderate dose of  $10^{10}$  GC compared to AAV2 at a 10-fold higher dose illustrated similar levels of transduction in the fovea for all serotypes ranging from 20% for AAV8 and approximately 40% for AAV9 and rh.8R (Figure 3). In some eyes, no foveal cone transduction was found, indicating that vector was likely not able to reach this retinal region following injection. Conversely, some injections were not noted to include the fovea however transduction in this area was noted, due to either diffusion beyond the bleb or, more likely, expansion of the bleb following surgery and monitoring after the animal became mobile after anesthesia (Table 1). As evidenced from the histological data in Figure 2, parafoveal transduction is minimal with AAV9 however still superior to all other AAVs tested. In the perifoveal macular region and beyond in the peripheral retina, cone transduction was achieved robustly by AAV9, and to a lesser extent rh.8R and rh.64R1. AAV7 is fairly weak in its ability to target cone PR but

still outperforms AAV8 and AAV2 in this respect. In ideal conditions of vector delivery to the subretinal space, AAV9 was able to target over 80% of cones in the perifoveal macula (Figure 3).

## Discussion

In summary, we show that AAV9 uniquely targets cone PRs at high efficiency. This property may be due to the abundance of terminal galactose, the cognate receptor for AAV9 [21,27], on cone PR in vertebrates including humans [28], as we confirmed by the specific and high level of the lectin peanut agglutinin (PNA) [28] staining of cone PR in our studies (Figure 2). The findings here in which a dose-related, quantitative assessment of vector targeting is made for all cells lining the subretinal space provide a first step toward understanding the pharmacodynamics of AAV in this setting. It is apparent from our data and others that most AAVs efficiently transduce the RPE at low to moderate doses. However, where rod PR transduction is highly efficient with AAV7 and particularly AAV8 at lower doses, AAV9, rh.8R and rh.64R1 do not perform quite as well (Figure 1B). Conversely, cone targeting with AAV9, rh.8R and rh.64R1 is superior to that of AAV7 and particularly AAV8 (Figure 2 and 3). We speculate that these findings are due to an intricate combination of differential receptor usage, saturation of vector binding sites on the surface of the cell type of interest and particle trapping in the glycan matrix within the subretinal space. Our observation that transducing parafoveal cones is challenging, even with a highly efficient cone targeting vector such as AAV9, may be a function of some of these factors. Future studies will have to be designed to determine whether injection procedure and/or dose may be able to overcome this hurdle. Ultimately these data will contribute to a deeper pharmacological understanding of the use of AAV in the emerging clinical field of gene therapy treatments for inherited and acquired forms of blindness.

Our comprehensive analysis of a number of AAV vectors based on different capsid structures in NHP retinas provides directly useful information for treating a large spectrum of inherited retinopathies following subretinal injection. Virtually any AAV capsid including that from serotype 2 efficiently targets RPE which would be sufficient in a limited number of diseases, the most celebrated being LCA due to RPE65. A majority of the remaining disorders require high level transduction of rod PR such as X-linked RP due to RPGR mutations; RP due to PDE6B mutations or rhodopsin mutations; and LCA due to lebercilin mutations. Our studies suggest that AAV8 is best suited for these diseases based on efficiency of rod transduction in NHP retina. However, AAV9 may be best suited for strategies targeting cones with endocrine survival factors, functional rescue of central vision using optogenetic restoration of vision in cones, or for gene augmentation for inherited retinopathies which require transduction of cones, such as achromatopsia and Stargardt disease.

## Experimental Procedures

### Animals, Injection and Follow-up

Cynomolgus macaques were treated and cared for at the Nonhuman Primate Research Program facility of the Gene Therapy Program of the University of Pennsylvania (Philadelphia, PA) during the study. Anterior chamber fluid was tapped prior to injection to relieve intraocular pressure. The studies were performed in accordance with study protocols approved by the Environmental Health and Radiation Safety Office, the Institutional Biosafety Committee, and the Institutional Animal Care and

Use Committee of the University of Pennsylvania. At the time of enrollment, all animals in the study had serum neutralizing antibody titer to AAV of less than 1/20. Injections were complicated by hyphemas caused by the anterior segment tap in a few eyes (Table 1). The study length was between 119 and 156 days at which time the eyes were collected and fixed for histology (Table 1). Injection procedure, clinical and ophthalmoscopic follow-up are as previously described [6]. Fundus photos were taken with a hand-held Kowa fundus camera.

### Vectors

AAV vectors were manufactured and purified from cell lysates by PennVector (<http://www.med.upenn.edu/gtp/vectorcore/>) by triple transfection in HEK293 cells as previously described [29]. The transgene plasmid encoded an early cytomegalovirus promoter (CMV), the enhanced green fluorescent protein and a woodchuck hepatitis virus post-transcriptional regulatory element, and the bovine growth hormone poly-adenylation (bGH) signal. Vector preparations were assayed for quality by multiple assays including TaqMan quantitative PCR with primers and probes directed towards bGH for genome (GC) titration (which is repeated independently 3 times for NHP studies), whole protein analysis by SDS-PAGE for purity, and endotoxin determination with <20 EU/ml as a lot release criterion.

### Histology and Morphometry

Histological sectioning was performed analogously as described for the previously published AAV2 and AAV8 study [6]. GFP morphometry in RPE and ONL was performed with ImageJ software (Rasband 1997–2006; National Institutes of Health, Bethesda, MD, <http://rsb.info.nih.gov/ij/>) on only those NHP eyes injected with the entire dose and without concerns related to the injection (Table 1). For 5 representative sections of each injected eye, two separate measuring lines were drawn through the RPE and the outer nuclear layer. Images and the brightness in the green channel were quantified per pixel as a value between 0 and 255. Background levels were established per pixel from a section from an uninjected retina. Percent of transduced area was determined as an average per eye and per group by determining the relative number of pixels above background as compared to the total number of pixels within the injected area. Intensity was established by averaging per eye and per group the intensity score of the RPE and ONL per section. Intensity scoring per positive area was performed in the NHP to represent level of relative expression of positively transduced areas and calculated per eye by averaging intensity values only when GFP signal exceeded background level.

Determination of percentage of GFP-positive cones was performed by GFP-positive cone counts per retina region (foveola/fovea, para-, perifovea, periphery). Images were taken from sections corresponding to the plane shown in Figure S1 at identical exposure time but variable gain setting to visualize both strong and weak GFP expression. Typically two and sometimes three images were recorded per region, for the foveola only one picture could be taken due to the small size of this structure. The images were recorded so that the retina was in a horizontal position within the image and its length equivalent to 235  $\mu\text{m}$ . Cones were considered positive for GFP expression if they were visually clearly recognizable as both GFP-positive and as cone PR and if they had a minimum intensity value at least 3-fold over the background as measured in an untransduced area (usually within the choroidea) within the same image. The intensities were determined with ImageJ software. For every serotype and region the average number of GFP-positive cones per 235  $\mu\text{m}$  section was

calculated. The eyes evaluated were injected at a dose of  $10^{10}$  vector genome copies except for AAV2 with  $10^{11}$  genome copies ( $10^{10}$  gave too low expression levels to be comparable with other serotypes). One eye (C21366 OD) was excluded due to lack of expression, likely due to the fact that the injection area was not included in the injection. In some eyes (18173 ODR, 18204 ODR, 18144 ODR, 18168 ODR, C21360 ODR) the section containing the fovea could not be exactly determined, in this case cone transduction in the fovea and parafovea was not evaluated but a section parallel to the fovea section was used to count transduced cones in the perifovea and periphery. Total cone numbers per section for each region were determined by counts from sections stained with rhodamin-labeled peanut agglutinin (PNA), a cone-specific stain. To this end images were taken for every region from PNA-stained sections obtained from five to eleven eyes and the number of all cones was counted per 235  $\mu$ m section and averaged per region. The percentage of GFP-positive cones was then determined by calculating the ratio of GFP+ cones to total cone counts per section for each region.

## References

- Milam AH, Li ZY, Fariss RN (1998) Histopathology of the human retina in retinitis pigmentosa. *Prog Retin Eye Res* 17: 175–205.
- Hamel CP (2007) Cone rod dystrophies. *Orphanet J Rare Dis* 2: 7.
- Pang JJ, Alexander J, Lei B, Deng W, Zhang K, et al. (2010) Achromatopsia as a potential candidate for gene therapy. *Adv Exp Med Biol* 664: 639–646.
- Jacobson SG, Cideciyan AV (2010) Treatment possibilities for retinitis pigmentosa. *N Engl J Med* 363: 1669–1671.
- Buskamp V, Duebel J, Balya D, Fradot M, Viney TJ, et al. (2010) Genetic reactivation of cone photoreceptors restores visual responses in retinitis pigmentosa. *Science* 329: 413–417.
- Vandenbergh LH, Bell P, Maguire AM, Cearley CN, Xiao R, et al. (2011) Dosage thresholds for AAV2 and AAV8 photoreceptor gene therapy in monkey. *Sci Transl Med* 3(88): 88ra54.
- Bainbridge JW, Smith AJ, Barker SS, Robbie S, Henderson R, et al. (2008) Effect of gene therapy on visual function in Leber's congenital amaurosis. *N Engl J Med* 358: 2231–2239.
- Hauswirth WW, Aleman TS, Kaushal S, Cideciyan AV, Schwartz SB, et al. (2008) Treatment of Leber congenital amaurosis due to RPE65 mutations by ocular subretinal injection of adeno-associated virus gene vector: short-term results of a phase I trial. *Hum Gene Ther* 19: 979–990.
- Maguire AM, Simonelli F, Pierce EA, Pugh EN Jr, Mingozzi F, et al. (2008) Safety and efficacy of gene transfer for Leber's congenital amaurosis. *N Engl J Med* 358: 2240–2248.
- den Hollander AI, Black A, Beaudet J, Cremers FP (2010) Lighting a candle in the dark: advances in genetics and gene therapy of recessive retinal dystrophies. *J Clin Invest* 120: 3042–3053.
- Bennett J, Maguire AM, Cideciyan AV, Schnell M, Glover E, et al. (1999) Stable transgene expression in rod photoreceptors after recombinant adeno-associated virus-mediated gene transfer to monkey retina. *Proc Natl Acad Sci U S A* 96: 9920–9925.
- Bainbridge JW, Mistry A, Schlichtenbrede FC, Smith A, Broderick C, et al. (2003) Stable rAAV-mediated transduction of rod and cone photoreceptors in the canine retina. *Gene Ther* 10: 1336–1344.
- Beltran WA, Boye SL, Boye SE, Chiodo VA, Lewin AS, et al. (2010) rAAV2/5 gene-targeting to rods: dose-dependent efficiency and complications associated with different promoters. *Gene Ther* 17: 1162–1174.
- Boye SE, Alexander JJ, Boye SL, Witherspoon CD, Sandefer K, et al. (2012) The human rhodopsin kinase promoter in an AAV5 vector confers rod and cone specific expression in the primate retina. *Hum Gene Ther* 23: 1101–1115.
- Komaromy AM, Alexander JJ, Rowlan JS, Garcia MM, Chiodo VA, et al. (2010) Gene therapy rescues cone function in congenital achromatopsia. *Hum Mol Genet* 19: 2581–2593.
- Mancuso K, Hauswirth WW, Li Q, Connor TB, Kuchenbecker JA, et al. (2009) Gene therapy for red-green colour blindness in adult primates. *Nature* 461: 784–787.
- Allocca M, Mussolino C, Garcia-Hoyos M, Sanges D, Iodice C, et al. (2007) Novel adeno-associated virus serotypes efficiently transduce murine photoreceptors. *J Virol* 81: 11372–11380.
- Leibler C, Maguire A, Tang W, Bennett J, Wilson JM (2008) Novel AAV serotypes for improved ocular gene transfer. *J Gene Med* 10: 375–382.
- Strieger K, Colle MA, Dubreil L, Mendes-Madeira A, Weber M, et al. (2008) Subretinal delivery of recombinant AAV serotype 8 vector in dogs results in gene transfer to neurons in the brain. *Mol Ther* 16: 916–923.
- Mussolino C, della Corte M, Rossi S, Viola F, Di Vicino U, et al. (2011) AAV-mediated photoreceptor transduction of the pig cone-enriched retina. *Gene Ther* 18: 637–645.
- Bell CL, Vandenbergh LH, Bell P, Limberis MP, Gao GP, et al. (2011) The AAV9 receptor and its modification to improve in vivo lung gene transfer in mice. *J Clin Invest* 121: 2427–2435.
- Summerford C, Samulski RJ (1998) Membrane-associated heparan sulfate proteoglycan is a receptor for adeno-associated virus type 2 virions. *J Virol* 72: 1438–1445.
- Kaludov N, Brown KE, Walters RW, Zabner J, Chiorini JA (2001) Adeno-associated virus serotype 4 (AAV4) and AAV5 both require sialic acid binding for hemagglutination and efficient transduction but differ in sialic acid linkage specificity. *J Virol* 75: 6884–6893.
- Wu Z, Müller E, Agbandje-McKenna M, Samulski RJ (2006) Alpha2,3 and alpha2,6 N-linked sialic acids facilitate efficient binding and transduction by adeno-associated virus types 1 and 6. *J Virol* 80: 9093–9103.
- Vandenbergh LH, Breous E, Nam HJ, Gao G, Xiao R, et al. (2009) Naturally occurring singleton residues in AAV capsid impact vector performance and illustrate structural constraints. *Gene Ther* 16: 1416–1428.
- Gao G, Vandenbergh LH, Alvira MR, Lu Y, Calcedo R, et al. (2004) Clades of Adeno-associated viruses are widely disseminated in human tissues. *J Virol* 78: 6381–6389.
- Shen S, Bryant KD, Brown SM, Randell SH, Asokan A (2011) Terminal N-linked galactose is the primary receptor for adeno-associated virus 9. *J Biol Chem* 286: 13532–13540.
- Blanks JC, Johnson LV (1984) Specific binding of peanut lectin to a class of retinal photoreceptor cells. A species comparison. *Invest Ophthalmol Vis Sci* 25: 546–557.
- Vandenbergh LH, Xiao R, Lock M, Liu J, Korn M, et al. (2010) Efficient serotype-dependent release of functional vector into the culture medium during adeno-associated virus manufacturing. *Hum Gene Ther* 21: 1251–1257.

## Supporting Information

### Figure S1 Topology sampling for cone tropism study.

Mapping of the foveal, parafoveal and perifoveal regions was done based on measured distance from the fovea and morphological hallmarks. Specifically, the fovea and foveola are located along the slopes or in the foveal pit which has the highest cone density. The parafovea, at a distance of 350–500  $\mu$ m from the foveal center, is located on the foveal rim, i.e., the circular rim surrounding the fovea where the retina is thickest, largely due to a thicker retinal ganglion cell layer. The perifovea was located 1.3–1.9 mm from the fovea, and finally the peripheral retina, at 3.3–4.3 mm, which is part of the extrafoveal macula. D, optic disc; F, foveola/fovea; I, injection site. Images show cones in red (PNA stain) and nuclei in blue (DAPI). (PDF)

## Author Contributions

Conceived and designed the experiments: LHV JB JMW. Performed the experiments: LHV PB AMM RX TBH RG. Analyzed the data: LHV PB AMM JB JMW. Contributed reagents/materials/analysis tools: JMW. Wrote the paper: LHV PB JB JMW.

EX. D

# What Is Next for Retinal Gene Therapy?

Luk H. Vandenberghe

Ocular Genomics Institute, Grousbeck Gene Therapy Center, Schepens Eye Research Institute, Massachusetts Eye and Ear Infirmary, Harvard Medical School, Boston, Massachusetts 02114

Correspondence: luk\_vandenberghe@meei.harvard.edu

The field of gene therapy for retinal blinding disorders is experiencing incredible momentum, justified by hopeful results in early stage clinical trials for inherited retinal degenerations. The premise of the use of the gene as a drug has come a long way, and may have found its niche in the treatment of retinal disease. Indeed, with only limited treatment options available for retinal indications, gene therapy has been proven feasible, safe, and effective and may lead to durable effects following a single injection. Here, we aim at putting into context the promise and potential, the technical, clinical, and economic boundaries limiting its application and development, and speculate on a future in which gene therapy is an integral component of ophthalmic clinical care.

## PROMISE DELIVERED

Three critical components have to be defined and brought together for any therapeutic approach to be successful: target, intervention, and delivery. The target requires the identification of a cell type, tissue, or process relevant to the pathophysiology of the disease. The information on these targets can then be used to devise an intervention through which a disease process can be inhibited, circumvented, or interfered with. The bundling of this intervention with an approach to deliver it to the target within a therapeutic window in a manner that is feasible, safe, and efficient constitutes an attractive treatment paradigm. Over the past two or three decades, efforts of the vision and neuroscience research community have converged with those of the genetics and gene delivery field to lead to the definition of targets, the evalua-

tion of multiple intervention modalities, and the validation of a host of delivery systems.

The first incarnation of this approach was targeting a form of Leber congenital amaurosis (LCA), an early onset form of autosomal recessive retinal degeneration leading to progressive vision loss and nystagmus. *RPE65*, a gene encoding an enzyme pivotal in the recycling of the visual pigment chromophore 11-*cis*-retinal, was identified as one of the genes leading to LCA when mutated on both alleles (Marlbens et al. 1997). The addition of a correct copy of the *RPE65* gene led to the restoration of gene expression in this loss-of-function, single gene disorder (Acland et al. 2001). In parallel, the field of *in vivo* gene transfer was embarking on evaluating technologies for therapeutic applications, out of which the adeno-associated viral vector (AAV) emerged as a minimally immunogenic vector capable of stably transducing nondividing cells

---

Editors: Eric A. Pierce, Richard H. Masland, and Joan W. Miller  
Additional Perspectives on Retinal Disorders: Genetic Approaches to Diagnosis and Treatment available at  
www.perspectivesinmedicine.org

Copyright © 2015 Cold Spring Harbor Laboratory Press; all rights reserved; doi: 10.1101/cshperspect.a017442  
Cite this article as *Cold Spring Harb Perspect Med* 2015;5:a017442

(Ali et al. 1996). An unconventional surgical route of delivery that layered the gene therapy vector below the retina, adjacent to the therapeutic target cell type, that is, the retinal pigment epithelium (RPE), was proven to be essential for allowing AAV to come to its full potential in terms of gene transfer efficiency, specificity, and safety (Bennett et al. 1994; Ali et al. 1996). Bundled, these pivotal findings led to a demonstration, in a canine model of the disease, that subretinal injection of AAV encoding a promoter driven cDNA of *RPE65* restored objective and behavioral measures of vision (Acland et al. 2001). Validated by three independent groups, clinical trials along this premise yielded promising results with moderate improvements in visual function of patients (Bainbridge et al. 2008; Cideciyan et al. 2008, 2009; Maguire et al. 2008). A successful phase 2 trial (Bennett et al. 2012) justified initiation of a currently active phase 3 study which is aimed at licensure of the first effective gene therapy drug in the United States.

The cumulative research in this area that led to this sequence of events in less than two decades is a model in this era of translational medicine, and has generated an increased interest in gene therapy applications to target ophthalmic disease, particularly for indications in which no treatment options are available or current therapeutic paradigms are inadequate or sub-optimal. Moreover, these studies disrupted a prevalent school of thought that experimental treatments such as gene therapy could only be applied in fatal disorders for which no therapies were available.

#### CARBON COPY?

In 2012, The National Institutes of Health Office of Biotechnological Activities convened several stakeholders in gene therapy. At this meeting, it was suggested that future retinal degeneration therapies could be developed in a streamlined fashion by building on a delivery platform established in the *RPE65* studies (O'Reilly et al. 2013). The idea is to use an identical vector type, surgical procedure, and transgene cassette to deliver therapeutic genes for other retinal indi-

cations. Indeed, the example that these studies have set, provides a guide for the design and development of gene therapies for other forms of retinal blindness.

The need for streamlining the development of these innovative therapies is high. Treatment options for many retinal blinding disorders are limited to nonexisting yet numerous therapeutic approaches and targets are being pursued preclinically. This requires a multitude of therapies to be developed, for example, there are more than 200 genes causative of inherited retinal disorders when mutated (see <https://sph.uth.edu/RetNet/sum-dis.htm#A-genes>). Moreover, a variety of different interventions are considered, ranging from gene addition, neuroprotection, and optogenetics. This, added to the targets and intervening modalities in more complex retinal disease, such as age-related macular degeneration (AMD), amounts to a large translational need (Sahel and Roska 2013; Simonato et al. 2013). The time and cost of translating a pre-clinical proof-of-concept that brings together target, intervention, and delivery is extremely high, and any cost-saving or streamlining of this process would bring transformative therapies to the patient faster.

Since the publication, in 2008, of the results of the early phase studies on the *RPE65* gene therapy trials, extensive efforts have been underway to build on this momentum, and to deliver a second success built on this same mold. In 2014, promising data from a phase 1/2 clinical trial for gene augmentation therapy for choroideremia, an X-linked form of retinal degeneration caused by defects in the *REP-1* protein, was presented (MacLaren et al. 2014). These studies used the same vector (AAV2), delivery route (subretinal injection), and promoter (cytomegalovirus [CMV] enhanced chicken  $\beta$ -actin) as two of the *RPE65* studies, evidently building on, and adding to, the platform potential of this approach. It is important to highlight also the point of divergence in design of the gene therapy, and its translational path to clinical studies. First, certain design elements of the transgene were added, most notably the woodchuck hepatitis virus posttranscriptional response element (WPRE) known to increase





mRNA half-life and thereby lead to enhanced transgene expression. Second, the targeted area for treatment extended, much more than in the RPE65 studies into the macula, the area of the retina where in these patients' most target cells remained viable substrates for gene therapy. In terms of the body of evidence supporting the clinical translation for this second gene target, it appeared less exhaustive animal data was sufficient (Tolmachova et al. 2013). This is an important evolution as animal models of the retinal dystrophies are often lacking, not reflecting human disease, or only demonstrating a slow progressing or mild phenotype within the animal's lifespan (Chang et al. 2002). Also, to take advantage of the clinical validation AAV2 received in the prior studies, improved AAV serotypes that are thought to lead to a more robust expression in photoreceptor cells, next to RPE targets for the gene transfer (Boye et al. 2012; Vandenberghe and Auricchio 2012; Vandenberghe et al. 2011), were not pursued here, possibly limiting the efficacy potential of the study. This highlights an important decision point in the pursuit of developing a novel retinal gene therapy: Does one take advantage of a platform such as AAV2, risking subtherapeutic levels of expression in important target cells, or does one diverge from the validated platform at the risk of complicating the translational path of dealing with more unknowns and higher regulatory hurdles?

#### A PIPELINE OF PROGRESS

A cadre of clinical studies is currently ongoing, pending, or actively being developed at a pre-clinical stage (Boye et al. 2013). Many of these studies build on AAV2, but often also chose for a different vector including alternative AAV serotypes or lentiviral systems, either for improved targeting, or to overcome the limited transgene size capacity of AAV. Once results emerge from the clinic, these alternative vector systems may become novel platforms that can be built on. Specifically, trials are ongoing using a lentiviral vector encoding *ABCA4* and *MYO7A* for the treatment of Stargardt disease (Binley et al. 2013) and Usher Type 1B (Zalocchi et al.

2014), respectively. These cDNAs are too large to be packaged in AAV, yet can be accommodated by a lentiviral vector. A concern with this vector system has been the low transduction efficiency for photoreceptor cells, a primary therapeutic target for both these diseases (Auricchio et al. 2001; Bainbridge et al. 2001; Binley et al. 2013). Two clinical studies are underway with a gene therapy approach for durable expression of an antiangiogenic molecule in the treatment of exudative AMD (Maclachlan et al. 2011; Lai et al. 2012). Interestingly, the two trials use similar therapeutic molecules (sFlt1) and AAV2 as a vector, however differ in the surgical delivery of the gene therapy; a group out of Lions Eye Institute in Australia in collaboration with Avalanche Biosciences injects subretinally (Lai et al. 2012), whereas Genzyme/Sanofi is pursuing intravitreal injection (Maclachlan et al. 2011). The outcome of these approaches will inform us on another gene therapy modality: gene transfer for sustained delivery of a secreted therapeutic protein drug. Several gene augmentations approaches are underway clinically: all are AAV2-based, one building on the RPE65 results but directed at *MERTK* (NCT01482195), a disease-causing gene in retinitis pigmentosa, and another set of studies for Leber hereditary optic neuropathy (LHON) caused by mutations in the mitochondrial gene *ND4* (NCT02161380 and NCT02064569), which is expressed in the retinal ganglion cells that make up the optic nerve. Dozens of other preclinical programs are at various stages of development, for example, AAV5 mediated expression of *GUCY2D* for treatment of another form of LCA, which is soon expected to head to the clinic (Boye et al. 2013).

In short, following a pioneering era of first-in-human, a number of studies are bound to yield results, some building and solidifying the subretinal AAV2 approach, whereas others hopefully will expand the toolset and therapeutic reach for retinal degeneration gene therapies.

#### IMPROVING ON EFFICACY

In more than a dozen gene therapy clinical trials of several hundreds of subjects, safety endpoints



have been met in the absence of significant, drug-related adverse events (Simonato et al. 2013). No phase 3 studies have been completed, and efficacy in a randomized controlled trial has yet to be established for any of the ongoing approaches, although these results are anticipated in the near future for a phase 3 study for one of the RPE65 gene therapies. Reports on efficacy in retinal gene therapy, therefore, have been limited to the phase 1/2 RPE65 and choroideremia (CHM) studies. Data presented there has been promising and demonstrating increased light sensitivity by a variety of measures, and in some subjects improved navigation of a mobility course, indicating not only biological effect of the treatment, but also the potential for clinical benefit. However, based on the remarkable disease rescue observed in dog models following AAV2.RPE65 gene therapy, which appears not as robust as in humans, several hypotheses have been suggested to explain the apparent differences in treatment effect.

Cideciyan and colleagues (2013a) followed treated subjects and compared those to the natural disease progression in dogs and humans as well as the therapeutic effects seen in dogs over time. Using spectral domain optical coherence tomography (SD-OCT) and a novel methodology to model the decay of retinal structure, the investigators concluded that in humans, as opposed to canines, retinal degeneration starts earlier, and the optimal intervention for a gene therapy in this form of LCA is likely before birth (Cideciyan et al. 2013a). Their data suggests treated subjects show stable visual function in the context of ongoing retinal degeneration. To improve both visual function and structural preservation, the investigators propose a combination therapy in which neuroprotective treatment is combined with the gene addition. These results have extensively been argued, over its unorthodox modeling, the limited longitudinal data from patients (as opposed to dogs) following treatment, the small data set with several variables that are unaccounted for in the analysis, and its suggested solution to overcome this concern (Cepko and Vandenberghe 2013; Cideciyan et al. 2013b; Townes-Anderson 2013; Wojno et al. 2013). Moreover, only data from

one of the clinical studies was included, making it difficult to assess if the observations can be extended to the other trial designs.

Alternative hypotheses argue that the limitations of the current gene therapy formulations and surgical approaches can be improved on by targeting a larger area of the retina than a sub-retinal injection can reach, the level of transgene expression is limiting for full treatment effect, or the specificity of expression and stoichiometry of RPE65 in the context of the visual cycle is not in balance, arguing for more specific and regulated expression. These interventions may not have been required in the murine or canine models because of species-specific parameters such as the size of the globe, the procedural difference in terms of surgery, molecular kinetics of vector uptake, transduction, or promoter activity that are possibly distinct in canine versus human retina.

These discussions highlight, in our view, the need to continue to define the therapeutic window for each approach and indication, and to seek to improve the technology and biology of the treatment. Clinical, ethical, and pragmatic boundaries limit us in considering prenatal or neonatal (and before some of these studies, pediatric) gene therapy in ophthalmology, which, at least for now, determines the start of the potential therapeutic window for intervention. The field is in agreement that there is also a clear closing of the window when the therapeutic target cell (often RPE and/or photoreceptors) are atrophied. What is also agreed on, however less defined, is the threshold at which for many of these progressively degenerative diseases, degeneration cannot be stemmed in a cell autonomous fashion. Elucidation and diagnosis of that transition point is essential for identifying the appropriate therapeutic approach for each patient. Technological improvement to gene therapy that can restore gene function in a more physiological manner is likely also to prove important. The prospect of genome editing therapy in this respect is a fascinating one, because this technology may permit the adoption of endogenous regulation of gene expression. Albeit early, and faced with critical hurdles still, the recent advances in this field make this

approach compelling (Cong et al. 2013; Mali et al. 2013).

While this debate and detailed level of analysis is essential to progress, we cannot lose track of the fact that the noted clinical studies have concluded a biological effect in the absence of harm, with the potential of remarkable, clinically relevant, improvements of visual function. Absent of other treatment options for these patients, this first generation gene therapy is a milestone that can be used as a benchmark for future improvements. It is also important to note that these improvements often can only be validated in cautious, yet pivotal, human clinical studies. The careful translation of this experimental paradigm that has led to the first demonstration of efficacy in the context of safety for in vivo gene therapy is therefore a salute to the need for experimental clinical research to move these important questions forward.

#### WIDENING THE SPECTRUM

The compelling data from the early clinical trials, and the pipeline of preclinical studies moving to translation, has illustrated, for many, the transformative potential of gene therapy in ophthalmic care. It needs to be noted, however, that the current studies only address very small patient populations, and, at least in the short to mid-term, the prospect of gene therapy alleviating blinding disorders on a wider scale is limited. Several parameters determine this current limitation: (1) LCA, owing to mutations in *RPE65* and *CHM*, only affect few, and many other forms of inherited retinal degeneration will require a different treatment; (2) more common disorders, such as AMD, are currently only in clinical trials in populations at the very late stage of the disease, and even when proven safe and effective in current trials it remains to be seen how these results can be extended to a wider wet AMD population; (3) the therapeutic window for most of the approaches currently in trials is limited to those with remaining target cells and some level of vision; and (4) the prohibitive cost of clinical translation and trial costs for experimental biological therapies.

To broaden the potential of gene therapy for wider patient populations in ophthalmology, progress is made on several fronts. Not unlike the development of this first generation of therapies, the convergence of several fields including genetics, gene delivery, retinal biology, neuroscience, and cell therapy, is leading the charge in this effort. New targets are continuously being identified through gene discovery and studies into the pathophysiology of retinal disease; new disease genes in inherited retinal degenerations are being discovered, as are new targets in AMD and other common-complex retinal disorders. Novel and improved paradigms to intervene are now also more actively considered for vision restoration, in part, because of the traction and excitement spurred by the retinal gene therapy trial success. Specifically, the restoration of vision through gene transfer of an optogenetic switch that is accurately embedded within the neural circuitry of the retina is pursued by several groups and may lead to some level of visual perception in the blind, even in the absence of (endogenous) photoreceptors (Buskamp et al. 2012). Advances in neuroprotection through survival factors, antiapoptotic, or antioxidant agents will be beneficial to other gene therapy strategies, or may be delivered in a sustained fashion via gene transfer (Sahel and Roska 2013). The intersect of gene transfer and genome editing with cell-based transplantation approaches is highly promising to enable visual restoration even when retinal degeneration is extensive, and more traditional approaches of gene therapy are outside of consideration. Finally, progress in the field of gene delivery can further unlock further applications. The limitation on the size of the transgene imposed by the clinically used vector systems currently is not only preventing gene addition in the most common forms of LCA and RP (*CEP290* and *USH2A*, respectively), it also often prevents transgene cassettes to be designed with transcriptional or translational elements (e.g., cell-specific promoters or introns) that would be beneficial, or multiple genes to be transferred in a single vector (e.g., gene replacement combined with a neuroprotective gene). Novel vector technologies like nanoparticle approaches

(Conley and Naash 2010), or methods like genome editing to restore endogenous gene regulation, are expected to have an important impact. To further expand on the paradigm pursued by the pending AMD trials delivering an antiangiogenic protein by gene therapy to achieve long-lived and stable drug delivery to overcome repeat injections in a chronic disease, novel and improved methods to modulate transgene expression will become essential. Somewhat surprisingly, although several methods are available (Zoltick and Wilson 2001), few of them are actively pursued clinically in a gene therapy context, in part due to vector size limitations and the complexity related to translating these systems to human use. Last, efficient and safe targeting from the vitreous would overcome several shortcomings of the subretinal injection route and, certainly, make gene therapy a more routine clinical procedure (Dalkara et al. 2013; Kay et al. 2013).

#### MEASURING OUTCOME

Shared with other experimental therapeutic strategies in ophthalmology, the ability to measure outcome is pivotal for gene therapy to become a clinical modality in the care of patients. This is primarily of importance to convincingly establish the level of efficacy these therapies bring. Equally important is the quest for early endpoints to assess therapeutic effect to shorten the “bench to bedside and back” life-cycle of the gene therapy development of these cost-heavy trials in often slowly progressing diseases. Because of the advantages that the visual system has in terms of access, diagnosis, and imaging, the measures to establish a biological effect of a treatment are available, and several of those have been used by the different groups pursuing ophthalmic gene therapy clinically. Moving forward, to the extent possible, a standardization of these measures will be beneficial to accurately compare outcomes from different trials and the variables between those. A higher bar to meet is the demonstration of clinical benefit, in part, because of the fact that a sensitive measure of biological effect may not equate to an improvement in quality of life or clinical status. Another

aspect, however, is the regulatory definition of clinical benefit in ophthalmology that traditionally has been quite narrow. Because of the onslaught of novel therapeutic approaches for indications for which no treatments options are in current clinical use, disease organizations and clinical researchers continue a dialogue with regulators to establish new endpoint measures for clinical research, and ultimately market approval (Cellular, Tissue and Gene Therapies Advisory Committee 2011, see <http://www.fda.gov/downloads/advisor.../ucm259087.pdf>). While traditionally, visual acuity, and in limited cases visual field, has been acceptable, the RPE65 phase 3 study currently in progress uses a validated mobility assay as an endpoint (NCT 00999609). Validated surrogate measures such as those obtained via SD-OCT will likely also prove to be extremely valuable (Birch et al. 2013). The availability of a functionally validated biomarker to assess visual function, the stage of a disease process, or the activity of a therapeutic target is generally considered a “Holy Grail” for expediting and quantitation of therapeutic effect in humans. A key requirement for all endpoints, particularly in light of the fact that placebo controlled studies will remain difficult to design in gene therapy, is the availability of natural history studies to outline the disease course by that measure for that particular indication.

#### ECONOMIC FACTORS

With clinical proof-of-concept established, a delivery platform proposed, and a range of therapeutic targets and intervention of promise in the scientific literature, it may seem surprising and disappointing, particularly to patients and their families, that not more retinal gene therapies reached the clinic. As outlined above, several scientific, biological, and clinical limitations are at cause here. However, economic factors arguably play a primary role. The development of a single gene therapy is a time- and resource-demanding effort. Few centers have all the components under one roof to carry these efforts, and traditionally these have been pursued in academia with, until recently limited, interest from industry. The infrastructure



cost to establish a preclinical and particularly a translational gene therapy center is extremely high, and in a declining funding environment, difficult to justify by academic institutions. In the past two years, by the excitement that the first clinical results have generated, fortunately, significant private investment has entered the arena (see <http://www.forbes.com/sites/matthewherper/2014/03/26/once-seen-as-too-scary-editing-peoples-genes-with-viruses-makes-a-618-million-comeback/>). To sustain this momentum, novel regulatory and economic frameworks are being developed that are tailored to this novel therapeutic domain. One important aspect here is the pricing of a gene therapy drug once on the market, which is expected to determine the incentive for industry to pursue development of these therapies (Brennan and Wilson 2014). Particularly, for gene-specific therapies in rare disorders, these aspects will become vital for continued development as therapies with a larger market are likely more desirable to investors. This is ironic as this field was founded and catapulted to success by demonstrating its potential for very rare disorders. To alleviate this tension, policy and regulatory changes have made orphan drug development more attractive, including extended patent protection, and distinct regulatory paths. The idea to work toward a platform that through clinical experience gains a higher regulatory comfort level is an attractive one, as it is expected to lead to a reduced cost and time of development. To meet this ambition, standardization has to be sought for in vector manufacturing and quality control, clinical trial design, endpoint measures, and clinical follow up. While this is a challenge in an increasingly competitive arena, we argue it is beneficial for both academic and private pursuits in terms of cost-savings and the rate at which therapies can be brought to the patients.

#### A BRIGHT FUTURE

Gene addition therapy in two forms of inherited retinal degenerations has proven to improve visual function, in some subjects with remarkable success, in the context of a relatively safe procedure and formulation. These results have

validated an approach and a technology in a manner that it has the potential to alter the treatment of retinal disorders in the future. Although many aspects in this endeavor remain the subject of research, debate, policy and regulatory adjustments, a light at the end of the tunnel is a driving force for many in the field to pursue, mature, and create novel therapies for vision loss based on this paradigm. The extent to which gene therapy can broaden its impact beyond its current niche applications hinges on scientific and clinical advances, continued funding and investment, and balanced effort between competition and standardization of this promising field.

#### ACKNOWLEDGMENTS

We thank Livia Carvalho, Heikki Turunen, and Eric Pierce for discussion and manuscript comments. Support for this work was from National Institutes of Health (NIH) Grant DP1-OD008267, Curing Kids Fund, Foundation for Retina Research, Foundation Fighting Blindness, Research to Prevent Blindness, and the Grousbeck Family Foundation. LHV is an inventor on patents related to AAV gene therapy; has served as a consultant and is inventor on technologies licensed to biotechnology and pharmaceutical industry; and is cofounder and consultant to GenSight Biologics.

#### REFERENCES

- Acland GM, Aguirre GD, Ray J, Zhang Q, Aleman TS, Cideciyan AV, Pearce-Kelling SE, Anand V, Zeng Y, Maguire AM, et al. 2001. Gene therapy restores vision in a canine model of childhood blindness. *Nat Genet* **28**: 92–95.
- Ali RR, Reichel MB, Thrasher AJ, Levinsky RJ, Kinnon C, Kanuga N, Hunt DM, Bhattacharya SS. 1996. Gene transfer into the mouse retina mediated by an adeno-associated viral vector. *Hum Mol Genet* **5**: 591–594.
- Auricchio A, Kobinger G, Anand V, Hildinger M, O'Connor E, Maguire AM, Wilson JM, Bennett J. 2001. Exchange of surface proteins impacts on viral vector cellular specificity and transduction characteristics: The retina as a model. *Hum Mol Genet* **10**: 3075–3081.
- Bainbridge JW, Stephens C, Parsley K, Demaison C, Halfyard A, Thrasher AJ, Ali RR. 2001. In vivo gene transfer to the mouse eye using an HIV-based lentiviral vector; efficient long-term transduction of corneal endothelium



- and retinal pigment epithelium. *Gene Ther* **8**: 1665–1668.
- Bainbridge JW, Smith AJ, Barker SS, Robbie S, Henderson R, Balaggan K, Viswanathan A, Holder GE, Stockman A, Tyler N, et al. 2008. Effect of gene therapy on visual function in Leber's congenital amaurosis. *N Engl J Med* **358**: 2231–2239.
- Bennett J, Wilson J, Sun D, Forbes B, Maguire A. 1994. Adenovirus vector-mediated in vivo gene transfer into adult murine retina. *Invest Ophthalmol Vis Sci* **35**: 2535–2542.
- Bennett J, Ashtari M, Wellman J, Marshall KA, Cyckowski LL, Chung DC, McCague S, Pierce EA, Chen Y, Bencicelli JL, et al. 2012. AAV2 gene therapy readministration in three adults with congenital blindness. *Sci Transl Med* **4**: 120ra115.
- Binley K, Widdowson P, Loader J, Kelleher M, Iqbal S, Ferrige G, de Belin J, Carlucci M, Angell-Manning D, Hurst F, et al. 2013. Transduction of photoreceptors with equine infectious anemia virus lentiviral vectors: Safety and biodistribution of StarGen for Stargardt disease. *Invest Ophthalmol Vis Sci* **54**: 4061–4071.
- Birch DG, Locke KG, Wen Y, Locke KI, Hoffman DR, Hood DC. 2013. Spectral-domain optical coherence tomography measures of outer segment layer progression in patients with X-linked retinitis pigmentosa. *JAMA ophthalmol* **131**: 1143–1150.
- Boye SE, Alexander JJ, Boye SL, Witherspoon CD, Sandefer KJ, Conlon TJ, Erger K, Sun J, Ryals R, Chiodo VA, et al. 2012. The human rhodopsin kinase promoter in an AAV5 vector confers rod- and cone-specific expression in the primate retina. *Hum Gene Ther* **23**: 1101–1115.
- Boye SE, Boye SL, Lewin AS, Hauswirth WWA. 2013. A comprehensive review of retinal gene therapy. *Mol Ther* **21**: 509–519.
- Brennan TA, Wilson JM. 2014. The special case of gene therapy pricing. *Nat Biotechnol* **32**: 874–876.
- Busskamp V, Picaud S, Sahel JA, Roska B. 2012. Optogenetic therapy for retinitis pigmentosa. *Gene Ther* **19**: 169–175.
- Cepko CL, Vandenberghe LH. 2013. Retinal gene therapy coming of age. *Hum Gene Ther* **24**: 242–244.
- Chang B, Hawes NL, Hurd RE, Davisson MT, Nusinowitz S, Heckenlively JR. 2002. Retinal degeneration mutants in the mouse. *Vision Res* **42**: 517–525.
- Cideciyan AV, Aleman TS, Boye SL, Schwartz SB, Kaushal S, Roman AJ, Pang JJ, Sumaroka A, Windsor EA, Wilson JM, et al. 2008. Human gene therapy for RPE65 isomerase deficiency activates the retinoid cycle of vision but with slow rod kinetics. *Proc Natl Acad Sci* **105**: 15112–15117.
- Cideciyan AV, Hauswirth WW, Aleman TS, Kaushal S, Schwartz SB, Boye SL, Windsor EA, Conlon TJ, Sumaroka A, Roman AJ, et al. 2009. Vision 1 year after gene therapy for Leber's congenital amaurosis. *N Engl J Med* **361**: 725–727.
- Cideciyan AV, Jacobson SG, Beltran WA, Sumaroka A, Swider M, Iwabe S, Roman AJ, Olivares MB, Schwartz SB, Komáromy AM, et al. 2013a. Human retinal gene therapy for Leber congenital amaurosis shows advancing retinal degeneration despite enduring visual improvement. *Proc Natl Acad Sci* **110**: E517–E525.
- Cideciyan AV, Jacobson SG, Beltran WA, Hauswirth WW, Aguirre GD. 2013b. Reply to Townes-Anderson. RPE65 gene therapy does not alter the natural history of retinal degeneration. *Proc Natl Acad Sci* **110**: E1706.
- Cong L, Ran FA, Cox D, Lin S, Barretto R, Habib N, Hsu PD, Wu X, Jiang W, Marraffini LA, et al. 2013. Multiplex genome engineering using CRISPR/Cas systems. *Science* **339**: 819–823e.
- Conley SM, Naash MI. 2010. Nanoparticles for retinal gene therapy. *Prog Retin Eye Res* **29**: 376–397.
- Dalkara D, Byrne LC, Klimczak RR, Visel M, Yin L, Merigan WH, Flannery JG, Schaffer DV. 2013. In vivo-directed evolution of a new adeno-associated virus for therapeutic outer retinal gene delivery from the vitreous. *Sci Transl Med* **5**: 189ra176.
- Kay CN, Ryals RC, Aslanidi GV, Min SH, Ruan Q, Sun J, Dyka FM, Kasuga D, Ayala AE, Van Vliet K, et al. 2013. Targeting photoreceptors via intravitreal delivery using novel, capsid-mutated AAV vectors. *PLoS ONE* **8**: e62097.
- Lai CM, Estcourt MJ, Himbeck RP, Lee SY, Yew-San Yeo I, Luu C, Loh BK, Lee MW, Barathi A, Villano J, et al. 2012. Preclinical safety evaluation of subretinal AAV2-sFlt-1 in non-human primates. *Gene Ther* **19**: 999–1009.
- MacLachlan TK, Lukason M, Collins M, Munger R, Isenberger E, Rogers C, Malatos S, Dufresne E, Morris J, Calcedo R, et al. 2011. Preclinical safety evaluation of AAV2-sFLT01—A gene therapy for age-related macular degeneration. *Mol Ther* **19**: 326–334.
- MacLaren RE, Groppe M, Barnard AR, Cottrill CL, Tolmachova T, Seymour L, Clark KR, During MJ, Cremers FP, Black GC, et al. 2014. Retinal gene therapy in patients with choroideremia: Initial findings from a phase 1/2 clinical trial. *Lancet* **383**: 1129–1137.
- Maguire AM, Simonelli F, Pierce EA, Pugh EN Jr, Mingozzi F, Bencicelli J, Banfi S, Marshall KA, Testa F, Surace EM, et al. 2008. Safety and efficacy of gene transfer for Leber's congenital amaurosis. *N Engl J Med* **358**: 2240–2248.
- Mali P, Yang L, Esvelt KM, Aach J, Guell M, DiCarlo JE, Norville JE, Church GM. 2013. RNA-guided human genome engineering via Cas9. *Science* **339**: 823–826.
- Marlhens E, Bareil C, Griffioen JM, Zrenner E, Amalric P, Eliaou C, Liu SY, Harris E, Redmond TM, Arnaud B, et al. 1997. Mutations in RPE65 cause Leber's congenital amaurosis. *Nat Genet* **17**: 139–141.
- O'Reilly M, Kohn DB, Bartlett J, Benson J, Brooks PJ, Byrne BJ, Camozzi C, Cornetta K, Crystal RG, Fong Y, et al. 2013. Gene therapy for rare diseases: Summary of a National Institutes of Health workshop, September 13, 2012. *Hum Gene Ther* **24**: 355–362.
- Sahel JA, Roska B. 2013. Gene therapy for blindness. *Annu Rev Neurosci* **36**: 467–488.
- Simonato M, Bennett J, Boulis NM, Castro MG, Fink DJ, Goins WF, Gray SJ, Lowenstein PR, Vandenberghe LH, Wilson TJ, et al. 2013. Progress in gene therapy for neurological disorders. *Nat Rev Neurol* **9**: 277–291.
- Tolmachova T, Tolmachov OE, Barnard AR, de Silva SR, Lipinski DM, Walker NJ, MacLaren RE, Seabra MC. 2013. Functional expression of Rab escort protein 1 following AAV2-mediated gene delivery in the retina of cho-

- roideremia mice and human cells *ex vivo*. *J Mol Med (Berl)* **91**: 825–837.
- Townes-Anderson E. 2013. Increased levels of gene therapy may not be beneficial in retinal disease. *Proc Natl Acad Sci* **110**: E1705.
- Vandenberghe LH, Auricchio A. 2012. Novel adeno-associated viral vectors for retinal gene therapy. *Gene Ther* **19**: 162–168.
- Vandenberghe LH, Bell P, Maguire AM, Cearley CN, Xiao R, Calcedo R, Wang L, Castle MJ, Maguire AC, Grant R, et al. 2011. Dosage thresholds for AAV2 and AAV8 photoreceptor gene therapy in monkey. *Sci Transl Med* **3**: 88ra54.
- Wojno AR, Pierce EA, Bennett J. 2013. Seeing the light. *Sci Transl Med* **5**: 175fs178.
- Zalocchi M, Binley K, Lad Y, Ellis S, Widdowson R, Iqbal S, Scripps V, Kelleher M, Loader J, Miskin J, et al. 2014. ELAV-based retinal gene therapy in the *shaker1* mouse model for usher syndrome type 1B: Development of Ush-Stat. *PLoS ONE* **9**: e94272.
- Zoltick PW, Wilson JM. 2001. Regulated gene expression in gene therapy. *Ann NY Acad Sci* **953**: 53–63.

EX. E





Published in final edited form as:

*Ophthalmology*. 2016 August ; 123(8): 1751–1761. doi:10.1016/j.ophtha.2016.03.045.

## 5-Year Outcomes with Anti-VEGF Treatment of Neovascular Age-related Macular Degeneration (AMD): The Comparison of AMD Treatments Trials

Comparison of Age-related Macular Degeneration Treatments Trials (CATT) Research Group<sup>†</sup>

### Abstract

**Purpose**—To describe outcomes 5 years after initiation of treatment with bevacizumab or ranibizumab for neovascular age-related macular degeneration (AMD).

**Design**—Cohort study.

**Participants**—Patients enrolled in the Comparison of AMD Treatments Trials (CATT).

**Methods**—Patients were randomly assigned to ranibizumab or bevacizumab and to 1 of 3 dosing regimens. After 2 years, patients were released from the clinical trial protocol. At approximately 5 years, patients were recalled for examination.

**Main Outcome Measures**—Visual acuity (VA) and morphologic retinal features.

**Results**—VA was obtained for 647 (71%) of 914 living patients with average follow-up time 5.5 years. The mean number of examinations for AMD care after the clinical trial ended was 25.3, and the mean number of treatments in the study eye was 15.4. Most (60%) patients were treated  $\geq 1$  times with a drug other than their randomly assigned drug. At the 5-year visit, 50% of study eyes had VA 20/40 or better and 20% had VA 20/200 or worse. Mean change in VA was  $-3$  letters from baseline and  $-11$  letters from 2 years. Among 467 eyes with fluorescein angiography, mean total lesion area was 12.9 mm<sup>2</sup>, a mean of 4.8 mm<sup>2</sup> larger than at 2 years. Geographic atrophy was present in 213 (41%) of 515 gradable eyes and was subfoveal in 85 (17%). Among 555 eyes with

---

Corresponding Author: Maureen G. Maguire, PhD 215 615 1501 (V) 215 615 1520 (Fax) maguirem@mail.med.upenn.edu  
Department of Ophthalmology 3535 Market Street, Suite 700, Philadelphia PA 19104.

<sup>†</sup>The members of the Comparison of Age-related Macular Degeneration Treatments Trials (CATT) Research Group are listed in the Appendix.

Reprints requests to: Maureen Maguire, PhD, CATT Coordinating Center, University of Pennsylvania, 3535 Market Street, Suite 700, Philadelphia, PA 19104-3309

Part of this material is to be presented at the ARVO 2016 Annual Meeting.

ClinicalTrials.gov number NCT00593450

This article contains additional online-only material. The following should appear online-only: Tables 4 and 6, and Appendix.

**Conflict of Interest Disclosure:** Dr. Maguire reports personal fees from Roche/Genentech; Dr. Ying reports personal fees from Janssen R & D and Chengdu Kanghong Biotech Co; Dr. Jaffe reports personal fees from Alcon/Novartis, Neurotech, and Roche/Genentech; Dr. Toth grants from Genentech, Inc., personal fees from Alcon, Inc. and Thrombogenics, non-financial support from Bioptigen, and a patent unlicensed issued to Duke University.

**Publisher's Disclaimer:** This is a PDF file of an unedited manuscript that has been accepted for publication. As a service to our customers we are providing this early version of the manuscript. The manuscript will undergo copyediting, typesetting, and review of the resulting proof before it is published in its final citable form. Please note that during the production process errors may be discovered which could affect the content, and all legal disclaimers that apply to the journal pertain.

spectral domain optical coherence tomography, 83% had fluid (61% intraretinal, 38% subretinal, and 36% sub-retinal pigment epithelium). Mean foveal total thickness was 278  $\mu\text{m}$ ; a decrease of 182  $\mu\text{m}$  from baseline and 20  $\mu\text{m}$  from 2 years. An abnormally thin retina at the foveal center ( $<120 \mu\text{m}$ ) was present in 36%. Between 2 and 5 years, the group originally assigned to ranibizumab for 2 years lost more VA than the bevacizumab group ( $-4$  letters;  $p=0.008$ ). Otherwise, there were no statistically significant differences in VA or morphological outcomes between drug or regimen groups.

**Conclusion**—Vision gains during the first 2 years of the trial were not maintained at 5 years. However, 50% of eyes had VA 20/40 or better, confirming anti-VEGF therapy as a major long-term therapeutic advance for neovascular AMD.

---

Anti-vascular endothelial growth factor (VEGF) therapy has revolutionized the treatment of neovascular age-related macular degeneration (AMD). Currently, nearly all patients diagnosed with neovascular AMD are treated with intravitreal administration of drugs that target VEGF. In 2005 and 2006, results from Phase III randomized clinical trials showed dramatic improvements in visual acuity when eyes with neovascular AMD were treated with ranibizumab (Lucentis) compared to sham treatment or photodynamic therapy.<sup>1,2</sup> During the 1-year period between first presentation of results and approval of ranibizumab by the Food and Drug Administration, ophthalmologists began treating neovascular AMD patients with off-label bevacizumab (Avastin). Despite the absence of evidence of efficacy and safety from any randomized clinical trials, use of bevacizumab moved quickly from rescue therapy to first-line therapy.<sup>3–5</sup> Subsequently, large-scale, multicenter randomized clinical trials of ranibizumab and bevacizumab were initiated in the United States and 5 other countries to compare safety and effectiveness.<sup>6–14</sup> Results from these trials showed that visual acuity outcomes at 1 and 2 years were similar between ranibizumab and bevacizumab under several different dosing strategies. A recent meta-analysis of all comparative trials yielded essentially no difference between drugs in mean change in visual acuity at 1 year (bevacizumab-ranibizumab,  $-0.5$  letters, 95% confidence interval  $[-1.6, 0.6]$ ).<sup>15</sup> Results from later Phase III clinical trials showed that aflibercept (Eylea) injected every 8 weeks provided gains in visual acuity equivalent to those of ranibizumab injected every 4 weeks.<sup>16–17</sup>

Although clinical outcomes from the first 1 to 2 years of anti-VEGF treatment have been well documented by large-scale clinical trials, relatively few investigators have addressed outcomes after 4 or more years.<sup>18–24</sup> Longer term outcomes that have been reported vary considerably across studies. In addition, the annual number of treatments has been low in some reports and only patients who continued regular follow-up and treatment have been included in other reports. In this paper, we report the clinical outcomes of patients enrolled in the Comparison of AMD Treatments Trials (CATT) who returned at approximately 5 years after initiation of treatment with either ranibizumab or bevacizumab. The clinical trial ended after 2 years of follow-up when patients were released from the study protocol. All CATT patients who were alive at the end of the clinical trial were targeted for participation in the CATT Follow-up Study.

## METHODS

### Design of the CATT Clinical Trial

The design and methods for the clinical trial have been published; therefore, only the key features with bearing on this paper are provided.<sup>6,7,25,26</sup> Patients enrolled in CATT between February 20, 2008 and December 9, 2009. Eligible eyes (one study eye per patient) had active choroidal neovascularization secondary to AMD, no previous treatment, visual acuity between 20/25 and 20/320, and neovascularization, fluid, or hemorrhage under the foveal center. Patients were assigned randomly to 1 of 4 treatment groups defined by drug (ranibizumab or bevacizumab) and by dosing regimen (monthly or as-needed [PRN]). At one year, patients initially assigned to monthly treatment were re-assigned randomly to either monthly or PRN treatment ("switched regimen group"). A volume of 0.05 ml containing either 0.50 mg ranibizumab or 1.25 mg bevacizumab was used for intravitreal injection. Patients on the PRN dosing regimen were evaluated for treatment every 4 weeks and treated when fluid on optical coherence tomography (OCT), new or persistent hemorrhage, decreased visual acuity relative to the previous visit, or dye leakage on fluorescein angiography was present. All patients were scheduled for follow-up visits every 4 weeks through 104 weeks. Patients were released from their assigned treatment groups during the visit at 104 weeks; at that visit and thereafter, all treatments were administered according to best medical judgment. The study was registered (NCT00593450) on <http://www.clinicaltrials.gov>.

### Follow-up Methods

All patients who enrolled in the clinical trial, except for those known to be dead at 2 years, were targeted for participation in the Follow-up Study. Clinical coordinators attempted to contact patients and schedule an appointment for them to be seen in a CATT clinical center between March 14, 2014 and March 31, 2015. Patients completing a visit in a CATT clinical center signed a consent statement for the follow-up visit and signed a medical records release form if they had received care for AMD from outside the CATT clinical center. Patients were interviewed about treatment to either eye, visits to ophthalmologists, and serious medical events since their last visit in the clinical trial. Returning patients had a dilated eye examination, refraction and visual acuity measurement, spectral domain OCT, fundus color stereophotography and fluorescein angiography. All examinations were performed by study-certified personnel following the same protocols used during the clinical trial. Some patients who did not complete a visit in a CATT clinical center were willing to complete an interview about past care, treatment, and serious medical events and/or signed a medical records release form. Information on treatment, visual acuity, and imaging was requested from the outside ophthalmologists who provided AMD care for these patients. The institutional review board associated with each of the participating CATT centers reviewed and approved the Follow-Up study protocol and consent forms. The study was performed in compliance with the Health Insurance Portability and Accountability Act and adhered to the tenets of the Declaration of Helsinki.

When patients were unable or refused to participate, could not be contacted, or were identified as deceased, clinical coordinators submitted patient status forms to the CATT

Coordinating Center. After the end of the recruitment period, information on patients whose life status could not be verified and on patients reported as deceased, but without confirmation of the cause of death, was submitted to the National Death Index. When a match was identified ( $\geq 99\%$  chance of being correct), the date and cause of death were returned to the CATT Coordinating Center for use in data analysis.

### Ascertainment of History of Patient Care and Treatment

Medical records from the CATT clinical center were abstracted for the date of each visit for AMD care at the center after the clinical trial ended, dates of treatment for either eye, and type of treatment administered (bevacizumab, ranibizumab, aflibercept, pegaptanib (Macugen), triamcinolone, photodynamic therapy, thermal laser, and any other treatment). When patients reported care from outside of the CATT center and signed a medical records release form, the same information was requested from each ophthalmologist who provided AMD care for the patient.

### Data and Statistical Analysis

Only patients with a visual acuity measurement between 51 months (4.3 years) and 85 months (7.1 years) after the date of treatment assignment in the clinical trial were included in the data analyses, tables, and graphs on outcomes presented in this paper. The limits of the interval represent the minimum and maximum times between the enrollment period for the clinical trial and the enrollment period for the Follow-up Study. Differences in outcomes between drugs and among dosing regimens were assessed with analysis of variance for continuous outcome measures and chi-square tests for categorical outcome measures. Retinal thickness was classified as above ( $>212\mu$ ) or below ( $<120\mu$ ) 2 standard deviations from the mean of normal eyes.<sup>27</sup> Serious medical events were coded according to the *Medical Dictionary for Regulatory Activities (MedDRA)* system and further classified as arteriothrombotic and as previously associated with drugs affecting the VEGF pathway (arteriothrombotic events, systemic hemorrhage, congestive heart failure, venous thrombotic events, hypertension, vascular death).<sup>28–30</sup> Investigators from 3 of the 43 CATT clinical centers chose not to participate in the Follow-up Study; the 27 patients from these centers were considered non-participants and excluded from the analyses on serious medical events. Statistical computations were performed with SAS 9.4.

## RESULTS

### Patients

Among the 1117 patients alive at the end of the clinical trial (end of Year 2), 203 (18.2%) died before the end of the Follow-up Study. Of the remaining 914 patients, 647 (70.8%) had a visual acuity measurement in the required time interval of 51 months (4.3 years) to 85 months (7.1 years) after assignment of treatment in the clinical trial. The mean (SD) time interval between enrollment in the clinical trial and the Follow-up Study visit was 66.5 (6.7) months (5.5 years). The percentage of patients with a visual acuity measurement was similar across the 6 drug-dosing regimen groups, ranging from 68.3% to 75.0%. Most (85.5%) of the visual acuity information was obtained by examination at a CATT clinical center by a certified examiner. Three CATT centers responsible for 27 (3.0%) patients did not

participate in the Follow-up Study. Forty-one patients (4.5%) agreed to be interviewed but had no visual acuity information available, 102 (11.1%) declined participation, 93 (10.2%) could not be contacted, and 4 (0.4%) could not provide informed consent because of dementia or the absence of a consent statement in their native language.

The characteristics at baseline and at 2 years of the patients who participated in the Follow-up Study are displayed in Table 1, along with characteristics of those who did not participate and those who died after their 2-year visit. Non-participants had a mean age 2.3 years older ( $p<0.001$ ) and a mean baseline visual acuity score 3.1 letters worse than participants ( $p=0.001$ ). At 2 years, non-participants had a mean visual acuity 5.4 letters worse ( $p<0.001$ ) than participants. Among patients assigned treatment PRN for 2 years, non-participants had a mean 1.8 fewer injections ( $p=0.01$ ). Patients who died after 2 years were on average 5.6 years older than participants and had worse mean visual acuity both at baseline ( $-4.1$  letters) and 2 years ( $-7.9$  letters). Baseline ocular characteristics were similar among these 3 groups of patients.

### Care and Treatment after Release from the Clinical Trial Protocol

Most (591 [91.3%]) of the 647 Follow-up Study patients continued care at a CATT center after release from the clinical trial; however, 51 (7.9%) were seen also or seen exclusively by non-study ophthalmologists, and 5 (0.8%) received no eye care. Records were obtained for 49 (96%) of the 51 patients seen by non-study ophthalmologists. The mean (SD) number of visits for AMD care between the end of the clinical trial and the Follow-up Study visit was 25.3 (13.3); with 8.0 (4.0) in Year 3, 7.2 (4.0) in Year 4, and 6.5 (4.0) in Year 5. The mean (SD) number of treatments was 15.4 (12.5) with 4.8 (4.0) in Year 3, 4.5 (3.8) in Year 4, and 4.0 (3.6) in Year 5. The most recent treatment in the study eye before the Follow-up Study visit was within 3 months for 360 (55.6%) patients. There were 96 (14.8%) patients who had no treatments between the end of the clinical trial and the Follow-up Study visit, with a mean (SD) of 12.5 (8.4) visits. Among these 96 patients, 21 (48.8%) of 43 patients treated PRN in Year 2 of the clinical trial received no treatment during Year 2.

After release from the clinical trial protocol, more than half of the patients received a treatment other than the drug assigned to them in the clinical trial. Among the 328 patients assigned to ranibizumab, 46 (14.0%) had no treatments, 64 (19.5%) had treatments with only ranibizumab, and 218 (66.5%) had at least 1 other type of treatment (Table 2). Among the 319 patients assigned bevacizumab, 50 (15.7%) had no treatments, 99 (31.0%) had treatments with only bevacizumab, and 170 (53.3%) had at least 1 other type of treatment.

### Visual Acuity

Approximately half (321 [49.6%]) of the 647 Follow-up Study patients had visual acuity 20/40 or better at approximately 5 years (Table 3). The percentage of eyes with visual acuity 20/200 or worse was 5% to 6% at baseline through 2 years and increased to 20% by the Follow-up Study visit (Figure 1). The mean (SD) visual acuity score was 58.9 [20/63] (24.1) letters (Figure 2A). The mean (SD) change from Year 2 was  $-10.8$  (18.9) letters and the mean change from baseline was  $-3.3$  (22.3) letters. Mean visual acuity was similar among eyes assigned to ranibizumab (57.7 letters) and eyes assigned to bevacizumab (60.2 letters);

$p=0.19$ ) throughout the first 2 years in the clinical trial. Relative to the mean visual acuity at 2 years, eyes assigned to ranibizumab had lost more letters at the Follow-up Study visit ( $-12.7$ ) than eyes assigned to bevacizumab ( $-8.8$ ;  $p=0.008$ ) (Figure 2A). There were no statistically significant differences in these vision outcomes among eyes assigned to the different dosing regimens (Table 4 [available at <http://www.aaojournal.org>]; Figure 2B).

### Morphologic Outcomes from OCT

Spectral domain OCT scans were available for 555 (85.8%) of the Follow-up Study patients (Table 3). The mean (SD) total thickness at the foveal center was 278 (160)  $\mu\text{m}$  corresponding to a mean change from 2 years of  $-20$  (132)  $\mu\text{m}$  (Table 3) and a mean change of  $-182$  (209)  $\mu\text{m}$  from baseline (Figure 3A). Neurosensory retinal thickness was less than 120  $\mu\text{m}$  in 201 (36.2%) eyes, an increased percentage from 22% at 2 years (Figure 4). Retinal thickness was greater than 212  $\mu\text{m}$  in 62 (11.2%) eyes, similar to the percentage (14%) at 2 years. Intraretinal, subretinal, or sub-retinal pigment epithelium fluid was present in 458 (83.0%) of 552 gradable eyes (Figure 5). Although the percentages with subretinal fluid (37.7%) and sub-retinal pigment epithelium fluid (36.2%) at 5 years were similar to the percentages at Year 2, the percentage with intraretinal fluid (61.0%) was greater than at Year 2 (50%). There were no statistically significant differences in these spectral domain OCT features between eyes assigned to ranibizumab and bevacizumab in the clinical trial or among eyes assigned to the different dosing regimens (Table 3 and 4 [available at <http://www.aaojournal.org>], Figures 3A and 3B).

### Morphologic Outcomes from Fundus Photography and Angiography

Fundus photographs were available for 527 (81.4%) of the Follow-up Study patients and fluorescein angiograms were available for 467 (72.2%; Table 3). Fluorescein leakage was detected in 111 (24.5%) eyes. The mean area of the total neovascular lesion was 12.9 (11.4)  $\text{mm}^2$ , an increase of 4.8 (8.8)  $\text{mm}^2$  from 2 years. Geographic atrophy was present in 213 eyes (41.4%), and was subfoveal in 85 (16.5%). Fibrotic scar was present in the foveal center in 93 (19.6%) of eyes and non-fibrotic scar in an additional 26 (5.5%) among 474 gradable eyes. The mean area of the total neovascular lesion was 2  $\text{mm}^2$  greater in eyes assigned to ranibizumab in the clinical trial than in eyes assigned to bevacizumab (13.9 vs 11.9  $\text{mm}^2$ ); however, the difference was not statistically significant ( $p=0.06$ ). Percentages of eyes with fluorescein leakage and with geographic atrophy were similar between eyes assigned to ranibizumab and eyes assigned to bevacizumab. There were no statistically significant differences in these features on fundus photography and angiography among eyes assigned to the different dosing regimens (Table 4 [available at <http://www.aaojournal.org>]).

### Safety Data

Deaths and serious medical events occurring after 2 years are displayed in Table 5. There were 203 (18.6%) of 1090 patients who survived to 2 years but died before a Follow-up Study visit. Among 555 patients originally assigned to ranibizumab, 42 (7.6%) had an arteriothrombotic event compared with 24 (4.5%) of patients originally assigned to bevacizumab ( $p=0.04$ ). Otherwise, there were no statistically significant differences in the type of serious medical events between drug or dosing regimen groups (Table 6 [available at <http://www.aaojournal.org>]).

## DISCUSSION

The randomized clinical trials that established the efficacy of ranibizumab, bevacizumab, and aflibercept demonstrated that anti-VEGF therapy for neovascular AMD improved visual acuity on average by 1 to 2 lines through 2 years.<sup>1,2,6-14,16,17</sup> The CATT Follow-up Study provides long-term follow-up (mean 5.5 years) on 70.8% of survivors. Mean visual acuity declined to 3 letters worse than at baseline and 11 letters worse than at the 2 years. This decrease in vision was accompanied by expansion of the size of the total neovascular complex composed of neovascularization, scarring, and atrophy and by persistence of fluid on OCT. Despite these morphologic changes, 50% of CATT Follow-up Study patients had a visual acuity 20/40 or better, while only 20% had visual acuity 20/200 or worse. These results emphasize both the tremendous advances over the past 15 years in preserving vision for a large proportion of patients as well as the limitations of current treatment.

The characteristics of the CATT patients who returned for the Follow-up Study are important to interpret the 5-year results. Overall, 71% of living patients from the original clinical trial population returned. On average, these patients were 2 years younger, had visual acuity that was 3 letters better at baseline, and had visual acuity that was 5 letters better at 2 years than patients who did not return. Study eyes received an average of 15.4 injections after release from the clinical trial protocol and most received regular care by their CATT ophthalmologist, even if not receiving frequent treatment. Among the group not returning were patients who dropped out of the clinical trial, were too ill to participate, moved out of the area, or refused to return. Thus, the Follow-up Study results are likely better than would have been observed if 100% of CATT patients had returned. In addition, some of the Follow-up Study participants did not have an OCT scan (14%), color photographs (19%), or a fluorescein angiogram (28%), eroding the generalizability of the Follow-up Study results on morphological outcomes.

Similarly, the long-term outcomes of patients treated with anti-VEGF drugs reported from other studies (discussed below) are likely better than if all patients originally identified had been observed. The magnitude of the overestimation is related to the degree of selection of patients for study and the percentage of patients lost to follow-up. In the only other extended follow-up study of patients enrolled in a key randomized clinical trial for an anti-VEGF drug, participants were eligible for the HORIZON study only if their ophthalmologist believed that further treatment with ranibizumab beyond the 2-year clinical trial period would be beneficial.<sup>19</sup> Comparison of participants to non-participants in this cohort showed that visual acuity and lesion characteristics were better for participants, and only 388 (65%) of these selected 600 participants had 4-year follow-up. Several large-scale retrospective or registry studies have reported 4- and 5-year outcomes, but as demonstrated in a retrospective review of patients in Australia, patients who stop returning for care often do so soon after losing vision, so that patients with better vision are over-represented in these studies.<sup>18,20-24</sup>

The CATT Follow-up Study finding of 50% of patients with VA of 20/40 or better at 5 years and nearly 10% with VA 20/20 or better is remarkable when one considers the visual acuity outcomes in neovascular AMD prior to the development of anti-VEGF treatment. Two years after diagnosis, fewer than 10% of patients retained vision of 20/40 or better with no

treatment and fewer than 15% of patients treated with photodynamic therapy retained 20/40 or better.<sup>31-33</sup> Visual acuity decreased to 20/200 or worse at 2 years in 45% to 75% of patients with no treatment and in 30% to 40% with photodynamic therapy, compared to 20% at 5 years in the CATT Follow-up Study.

In CATT and all randomized clinical trials of anti-VEGF treatment for neovascular AMD, most of the improvement in mean visual acuity from baseline occurred within the first 3 to 6 months with little erosion of the benefit through 2 years when a fixed schedule of monthly (ranibizumab, bevacizumab, aflibercept) or bi-monthly (aflibercept) treatment was maintained.<sup>1,7,9,17,34</sup> In CATT, patients who switched at 1 year from a monthly to a PRN dosing regimen received 5 to 6 injections on average and experienced a mean visual acuity decrease of 2 to 3 letters over the second year.<sup>7</sup> During the 3.5 year period after release from the CATT protocol, patients received 4 to 5 injections per year on average and the mean visual acuity decreased an additional 11 letters to 59 letters (20/63). Similarly, in HORIZON, mean visual acuity declined by 7 letters to 20/80 with total 4 injections on average during the 2 years following exit from the formal clinical trials.<sup>19</sup> In the Australian retrospective review, the mean number of injections over 5 years was 25 with mean visual acuity decreasing to 20/63.<sup>20</sup> In contrast, the mean number of injections was 11 over 5 years in the Pan-American Study and the mean visual acuity at 5 years was 20/250.<sup>18</sup> Thus, more frequent treatment, both in the initial 2 years and in later years appears associated with better long-term outcomes, and many patients require treatment through 5 years and beyond. This observation is in distinct contrast to the experience of treating diabetic macular edema with anti-VEGF therapy where the majority of patients do not require treatment beyond 3 years. In Diabetic Retinopathy Clinical Research Network Protocol I clinical trial, a mean of 8 or 9 injections were given in Year 1, decreasing to 2 or 3 in Year 2, to 1 or 2 in Year 3, and to 0 or 1 in Year 4, depending on treatment assignment.<sup>35</sup>

The processes responsible for the decrease in vision in CATT and other studies are multiple but appear to be related to an increase in the proportion patients with an abnormally thin retina (<120 microns), an increase in prevalence of geographic atrophy, and a substantial increase in lesion size. We previously reported that retinal thinning to <120 microns was associated with worse VA outcomes at 1 and 2 years.<sup>36,37</sup> The proportion of eyes with an abnormally thin retina increased from 22% at the end of Year 2 to 36% at 5 years.<sup>37</sup> We also previously reported that the proportion of eyes with geographic atrophy was 20% at 2 years and this proportion increased to 41% at 5 years, with an increase in subfoveal geographic atrophy from 6% to 17%.<sup>7,37</sup> Worse VA outcomes have also been associated with increased lesion size, and in the Follow-up Study, mean lesion size increased more than 50% over the 3.5 year period (Table 3). These data highlight the need for agents that can prevent or minimize geographic atrophy and expansion of the total neovascular lesion.

The specific contribution of persistent fluid to long-term vision loss is unclear. The proportion of eyes with fluid decreased the most during the first year of treatment, but remained relatively unchanged throughout the remaining 4 years of follow up. More than 70% of eyes demonstrated intraretinal, subretinal, or sub-RPE fluid as determined by the OCT Reading Center throughout the study (Figure 5). Since the elimination of fluid is the primary goal at most treatment visits and almost no patients received treatment at every visit,



it is reasonable to assume that the amount of fluid was frequently small and not detected by the ophthalmologist or was tolerated because of stable vision. On a cross-sectional basis, the presence of intraretinal fluid is associated with worse visual acuity during anti-VEGF treatment while the presence of subretinal fluid is associated with better visual acuity.<sup>36–38</sup> Further studies to quantify the amount and location of residual fluid and to assess their impact on visual acuity are warranted.

During CATT, both the use of ranibizumab and monthly treatment were associated with an increased rate of development of geographic atrophy. At the end of Year 2, eyes treated with ranibizumab had a higher incidence (21%) of geographic atrophy than eyes treated with bevacizumab (17%;  $p=0.02$ ).<sup>7</sup> However, in the IVAN study, the incidence was similar in eyes treated with ranibizumab (28%) and with bevacizumab (31%;  $p=0.46$ ), decreasing the likelihood of a true effect of ranibizumab on development of geographic atrophy.<sup>9</sup> The association of monthly treatment with an increased rate of development of geographic atrophy was more consistent. At the end of Year 2 of CATT, eyes that received monthly treatment were more likely to have developed geographic atrophy than those treated with PRN therapy (24% vs 15%,  $p=0.003$ ).<sup>7</sup> In the IVAN study, 34% of eyes that received continuous (monthly) treatment developed geographic atrophy as compared with 26% in the discontinuous (PRN) group ( $p=0.03$ ).<sup>9</sup> In the HARBOR trial, eyes that received monthly ranibizumab had a higher incidence of geographic atrophy when compared with PRN treatment (HR, 1.3; 95% CI, 1.0–1.7).<sup>29</sup> After release from the clinical trial at 2 years, very few patients continued monthly treatment and most were treated with at least 1 additional anti-VEGF drug that was different from their original treatment assignment. When examining the 5-year data for evidence of a residual drug or dosing effect on the development of geographic atrophy, there was still a higher proportion (44%) of eyes originally assigned to ranibizumab with geographic atrophy than eyes assigned to bevacizumab (38%), and a higher proportion (47%) of eyes assigned to monthly treatment for 2 years with geographic atrophy than eyes assigned to PRN treatment (40%). However, these differences were not statistically significant.

Although few patients remained on their originally assigned drug and dosing regimen beyond the 2-year period of the clinical trial, our study does allow assessment as to whether or not the drugs and dosing regimens used during the first 2 years led to any detectable outcome differences at 5 years. At the end of 2 years of treatment in the clinical trial, mean VA was 70 letters (20/40) and there was no statistically significant difference in mean visual acuity between eyes originally assigned to ranibizumab and eyes originally assigned to bevacizumab. Over the next 3.5 years of follow-up, patients originally assigned to ranibizumab lost more vision (–13 letters) than those originally assigned to bevacizumab (–9 letters;  $p=0.008$ ; Figure 2A). The reasons for the decline are unclear, but it is clear that 2 years of initial therapy with bevacizumab and the accompanying lesser degree of reduction in fluid and retinal thickness did not compromise long-term visual acuity outcomes relative to ranibizumab, as some had speculated. There were no obvious differences in visual acuity outcomes at 5 years between patients who were treated monthly for 2 years versus those treated PRN for 2 years.

With most patients changing drugs over time, the ability to identify differential safety effects of the 2 drugs is compromised. During the period between the end of the clinical trial and the Follow-up Study visit, more patients originally assigned to ranibizumab had arteriothrombotic events than patients assigned to bevacizumab (7.6% versus 4.5%;  $p=0.04$ ). However, during the 2 years of the clinical trial, the proportion of patient with these events was nearly equal with 4.7% of ranibizumab-treated patients and 5.0% of bevacizumab-treated patients having an event ( $p=0.62$ ). Because of the absence of any difference when the history of drug exposure was certain we do not believe that the difference in events observed when a large portion of patients were not receiving ranibizumab are meaningful. Otherwise, we did not identify any statistically significant differences between groups based on the initially assigned drugs with respect to death or serious medical events. Overall concerns about the relative safety of bevacizumab and ranibizumab when treating patients with neovascular AMD have largely been assuaged by the results of 2 Cochrane comprehensive meta-analyses clinical trials comparing ranibizumab and bevacizumab.<sup>15,40</sup>

In summary, the CATT Follow-up Study provides the most complete follow up reported to date on the long-term outcomes for the treatment of neovascular AMD with anti-VEGF drugs. The original trial was designed to assess differences between ranibizumab and bevacizumab as well as differences between monthly and PRN dosing. Because very few patients remained on their originally assigned drug or dosing schedule between the end of year 2 and follow-up at approximately 5 years, the CATT Follow-up study results provide information primarily on overall treatment outcomes with anti-VEGF drugs and limited information on effects of different drugs and dosing regimens. Mean visual acuity at 5 years was 3 letters worse than baseline, highlighting an unmet need for further therapeutic advances. Still, 50% of patients were 20/40 or better and almost 10% were 20/20. These results would have been unimaginable in the era prior to the availability of anti-VEGF therapy.

## Supplementary Material

Refer to Web version on PubMed Central for supplementary material.

## Acknowledgments

Supported by cooperative agreements U10 EY017823, U10 EY017825, U10 EY017826, and U10 EY017828 from the National Eye Institute, National Institutes of Health, Department of Health and Human Services. The funding organization participated in the design and conduct of the study, data analysis and interpretation, and review of the manuscript.

## Writing Committee

---

Maurcen G. Maguire, PhD	{University of Pennsylvania, Department of Ophthalmology }
Daniel F. Martin, MD	{Cleveland Clinic, Cole Eye Institute }
Gui-shuang Ying, PhD	{University of Pennsylvania, Department of Ophthalmology }
Glenn J. Jaffe, MD	{Duke University, Department of Ophthalmology }
Ebenezer Daniel, MBBS, PhD	{University of Pennsylvania, Department of Ophthalmology }

Juan E. Grunwald, MD	{University of Pennsylvania, Department of Ophthalmology}
Cynthia A. Toth	{Duke University, Department of Ophthalmology}
Frederick L. Ferris, 3rd, MD;	{National Eye Institute}
Stuart L. Fine, MD	{University of Colorado-Denver, Department of Ophthalmology}

## Abbreviations and Acronyms

<b>AMD</b>	age-related macular degeneration
<b>CATT</b>	Comparison of Age-related Macular Degeneration Treatments Trials
<b>OCT</b>	optical coherence tomography
<b>VA</b>	visual acuity
<b>VEGF</b>	vascular endothelial growth factor

## References

1. Rosenfeld PJ, Brown DM, Heier JS, et al. Ranibizumab for neovascular age-related macular degeneration. *N Engl J Med.* 2006; 355:1419–31. [PubMed: 17021318]
2. Brown DM, Kaiser PK, Michels M, et al. Ranibizumab versus verteporfin for neovascular age-related macular degeneration. *N Engl J Med.* 2006; 355:1432–44. [PubMed: 17021319] Rosenfeld PJ, Moshfeghi AA, Puliafito CA. Optical coherence tomography after an intravitreal injection of bevacizumab (Avastin) for neovascular age-related macular degeneration. *Ophthalmic Surg Lasers Imaging.* 2005; 36:331–5. [PubMed: 16156152]
3. Avery RL, Pieramici DJ, Rabena MD, Castellarin AA, Nasir MA, Giust MJ. Intravitreal bevacizumab (Avastin) for neovascular age-related macular degeneration. *Ophthalmology.* 2006; 113:363–72. [PubMed: 16458968]
4. Curtis LH, Hammill BG, Schulman KA, Cousins SW. Risks of mortality, myocardial infarction, bleeding, and stroke associated with therapies for age-related macular degeneration. *Arch Ophthalmol.* 2010; 128:1273–1279. [PubMed: 20937996]
5. The CATT Research Group. Ranibizumab and bevacizumab for neovascular age-related macular degeneration. *N Engl J Med.* 2011; 364:1897–1908. Epub 2011 Apr 28. [PubMed: 21526923]
6. The CATT Research Group. Ranibizumab and bevacizumab for treatment of neovascular age-related macular degeneration: 2-year results. *Ophthalmology.* 2012; 119:1388–98. [PubMed: 22555112]
7. The IVAN Study Investigators. Ranibizumab versus bevacizumab to treat neovascular age-related macular degeneration. One-year findings from the IVAN randomized trial. *Ophthalmology.* 2012; 119:1399–1411. [PubMed: 22578446]
8. Chakravarthy U, Harding SP, Rogers CA, et al. Alternative treatments to inhibit VEGF in age-related choroidal neovascularisation: 2-year findings of the IVAN randomised controlled trial. *Lancet.* 2013; 382:1258–67. [PubMed: 23870813]
9. Kodjikian L, Souied EH, Mimoun G, et al. Ranibizumab versus bevacizumab for neovascular age-related macular degeneration: results from the GEFAL Noninferiority Randomized Trial. *Ophthalmology.* 2013; 120:2300–9. [PubMed: 23916488]
10. Krebs I, Schmetterer L, Boltz A, et al. A randomised double-masked trial comparing the visual outcome after treatment with ranibizumab or bevacizumab in patients with neovascular age-related macular degeneration. *Br J Ophthalmol.* 2013; 97:266–71. [PubMed: 23292928]
11. Berg K, Pederson TR, Sandvik L, Bragadottir R. Comparison of ranibizumab and bevacizumab for neovascular age-related macular degeneration according to LUCAS treat-and-extend protocol. *Ophthalmology.* 2015; 122:146–52. [PubMed: 25227499]

12. Berg K, Hadzalic E, Gjertsen I, et al. Ranibizumab or bevacizumab for neovascular age-related macular degeneration according to the Lucentis compared to Avastin study treat-and-extend protocol: Two-year results. *Ophthalmology*. 2016; 123:51–9. [PubMed: 26477842]
13. Schauwvlieghe A-SM, Dijkman G, Hooymans JM, et al. Comparing the effectiveness of bevacizumab to ranibizumab in patients with exudative age-related macular degeneration. *BRAMD. Invest Ophthalmol Vis Sci*. 2014; 55:ARVO E-Abstract 870.
14. Solomon SD, Lindsley KB, Krzystolik MG, Vedula SS, Hawkins BS. Intravitreal bevacizumab versus ranibizumab for treatment of neovascular age-related macular degeneration: Findings from a Cochrane Systematic Review. *Ophthalmology*. 2016; 123:70–7. [PubMed: 26477843]
15. Heier JS, Brown DM, Chong V, Korobelnik JF, et al. Intravitreal aflibercept (VEGF trap-eye) in wet age-related macular degeneration. *Ophthalmology*. 2012; 119:2537–48. [PubMed: 23084240]
16. Schmidt-Erfurth U, Kaiser PK, Korobelnik JF, et al. Intravitreal aflibercept injection for neovascular age-related macular degeneration: ninety-six-week results of the VIEW studies. *Ophthalmology*. 2014; 121:193–201. [PubMed: 24084500]
17. Arevalo JF, Lasave AF, Wu L, et al. Intravitreal bevacizumab for choroidal neovascularization in age-related macular degeneration: 5-year results of the Pan-American Collaborative Retina Study Group. *Retina*. 2015 Nov 2.
18. Singer MA, Awh CC, Sadda S, et al. HORIZON: An open-label extension trial of ranibizumab for choroidal neovascularization secondary to age-related macular degeneration. *Ophthalmology*. 2012; 119:1175–83. [PubMed: 22306121]
19. Gillies MC, Campain A, Barthelmes D, et al. Long-Term Outcomes of Treatment of Neovascular Age-Related Macular Degeneration. *Ophthalmology*. 2015; 122:1837–45. [PubMed: 26096346]
20. Peden MC, Suner IJ, Hammer ME, et al. Long-Term Outcomes in Eyes Receiving Fixed-Interval Dosing of Anti-Vascular Endothelial Growth Factor Agents for Wet Age-Related Macular Degeneration. *Ophthalmology*. 2015; 122:803–8. [PubMed: 25596618]
21. Rasmussen A, Bloch SB, Fuchs S, et al. A 4-Year Longitudinal Study of 555 Patients Treated with Ranibizumab for Neovascular Age-Related Macular Degeneration. *Ophthalmology*. 2013; 120:2630–36. [PubMed: 23830760]
22. Rofagha S, Bhisitkul RB, Boyer DS, et al. Seven-year outcomes in ranibizumab-treated patients in ANCHOR, MARINA, and HORIZON. A multicenter cohort study (SEVEN-UP). *Ophthalmology*. 2013; 120:2292–9. [PubMed: 23642856]
23. Zhu M, Chew JK, Broadhead GK, et al. Intravitreal Ranibizumab for neovascular Age-related macular degeneration in clinical practice: five-year treatment outcomes. *Arch Clin Exp Ophthalmol*. 2015; 253:1217–25.
24. Grunwald JE, Daniel E, Ying G-S, Pistilli M, Maguire MG, Alexander J, Whittock-Martin R, Parker CR, Sepielli K, Blodi BA, Martin DF, the CATT Research Group. Photographic assessment of baseline fundus morphologic features in the Comparison of Age-Related Macular Degeneration Treatments Trials. *Ophthalmology*. 2012; 119:1634–41. Epub 2012 Apr 17. [PubMed: 22512984]
25. DeCraos FC, Toth CA, Stinnett SS, Heydary CS, Burns R, Jaffe GJ, for the CATT Research Group. Optical coherence tomography grading reproducibility during the Comparison of Age-Related Macular Degeneration Treatments Trials. *Ophthalmology*. 2012; 119:2549–57. Epub 2012 Aug 28. [PubMed: 22939114]
26. Chan A, Duker JS, Ko TH, et al. Normal macular thickness measurements in healthy eyes using Stratus optical coherence tomography. *Arch Ophthalmol*. 2006; 124:193–8. [PubMed: 16476888]
27. Antiplatelet Trialists' Collaboration. Collaborative overview of randomized trials of antiplatelet therapy—I: Prevention of death, myocardial infarction, and stroke by prolonged antiplatelet therapy in various categories of patients. *BMJ*. 1994; 308:81–106. [PubMed: 8298418]
28. Chen HX, Cleck JN. Adverse effects of anticancer agents that target the VEGF pathway. *Nat Rev Clin Oncol*. 2009; 6:465–77. [PubMed: 19581909]
29. Nalluri SR, Chu D, Keresztes R, Zhu X, Wu S. Risk of venous thromboembolism with the angiogenesis inhibitor bevacizumab in cancer patients: a meta-analysis. *JAMA*. 2008; 300:2277–85. [PubMed: 19017914]

30. Macular Photocoagulation Study Group. Laser photocoagulation of subfoveal neovascular lesions of age related macular degeneration: updated findings from two clinical trials. *Arch Ophthalmol.* 1993; 111:1200–9. [PubMed: 7689827]
31. Treatment of Age-related Macular Degeneration With Photodynamic Therapy (TAP) Study Group. Photodynamic therapy of subfoveal choroidal neovascularization in age-related macular degeneration with verteporfin: two-year results of 2 randomized clinical trials- TAP Report #2. *Arch Ophthalmol.* 2001; 119:198–207. [PubMed: 11176980]
32. Verteporfin in Photodynamic Therapy Study Group. Verteporfin therapy of subfoveal choroidal neovascularization in age-related macular degeneration: Two-year results of a randomized clinical trial including lesions with occult with no classic choroidal neovascularization-Verteporfin in Photodynamic Therapy Report 2. *Am J Ophthalmol.* 2001; 131:541–560. [PubMed: 11336929]
33. Brown DM, Michels M, Kaiser PK, et al. ANCHOR Study Group. Ranibizumab versus verteporfin photodynamic therapy for neovascular age-related macular degeneration: two- year results of the ANCHOR Study. *Ophthalmology.* 2009; 116:57–65. [PubMed: 19118696]
34. Elman MJ, Ayala A, Bressler NM, et al. Intravitreal ranibizumab for diabetic macular edema with prompt versus deferred laser treatment: 5-year randomized trial results. *Ophthalmology.* 2015; 122:375–381. [PubMed: 25439614]
35. Jaffe GJ, Martin DF, Toth CA, et al. Macular morphology and visual acuity in the Comparison of Age-related Macular Degeneration Treatments Trials (CATT). *Ophthalmology.* 2013; 120:1860–70. [PubMed: 23642377]
36. Sharma S, Toth CA, Daniel E, Grunwald JE, Maguire MG, Ying G-S, Huang J, Martin DF, Jaffe GJ, the CATT Research Group. Macular morphology and visual acuity in the second year of the Comparison of Age-related Macular Degeneration Treatments Trials (CATT). *Ophthalmology.* 2016 Jan 9.
37. Schmidt-Erfurth U, Waldstein SM, Deak G-G, Kundi M, Simader C. Pigment epithelial detachment followed by retinal cystoid degeneration leads to vision loss int treatment of neovascular age-related macular degeneration. *Ophthalmology.* 2015; 122:822–832. [PubMed: 25578255]
38. Holz FG, Tuomi L, Ding B, Hopkins JJ. Development of atrophy in neovascular AMD treated with ranibizumab in the HARBOR study. *Invest Ophthalmol Vis Sci.* 2015; 56:ARVO E- Abstract 890.
39. Moja L, Lucenteforte E, Kwag K, et al. Systemic safety of bevacizumab versus ranibizumab for neovascular age-related macular degeneration. *Cochrane Database Syst Rev.* 2014 Sep 15.9:CD011230. [PubMed: 25220133]

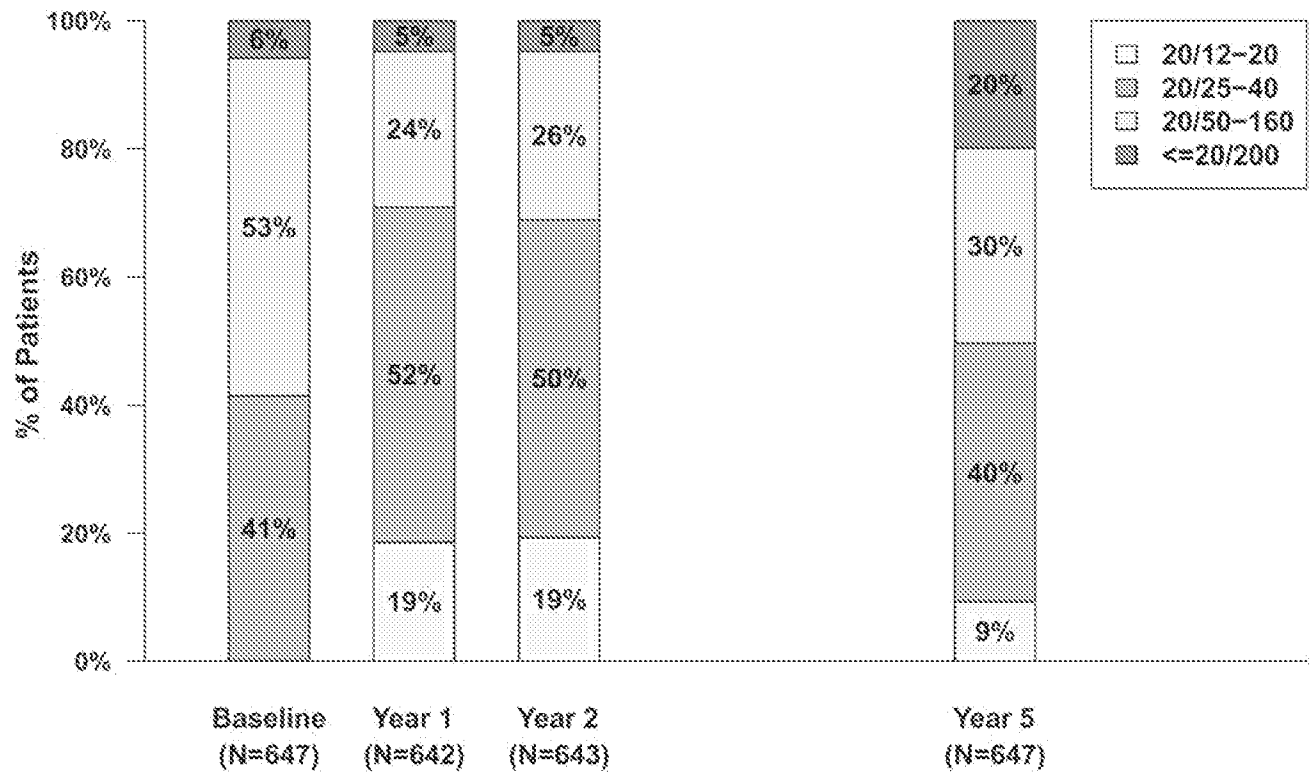


Figure 1.  
Distribution of visual acuity over time for 647 patients in the Follow-up Study.

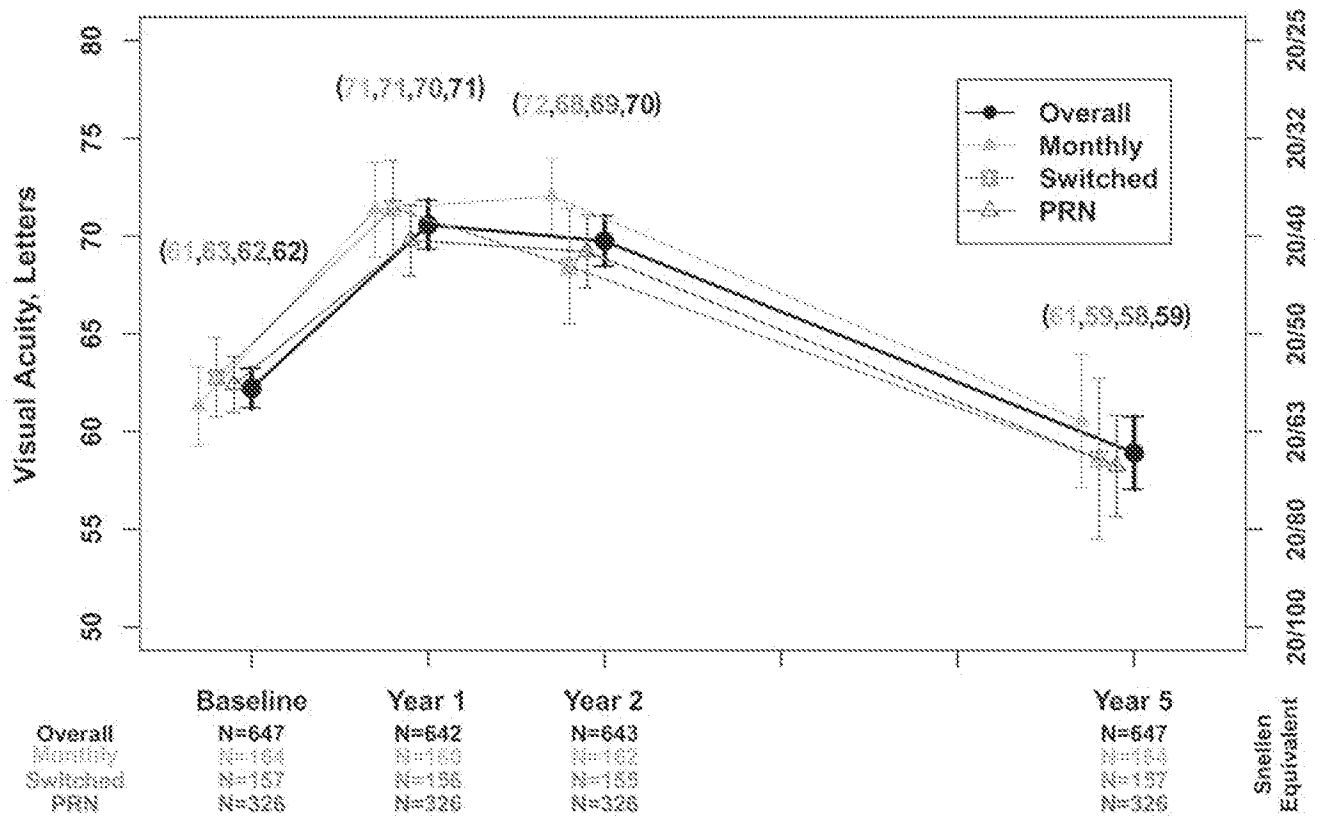
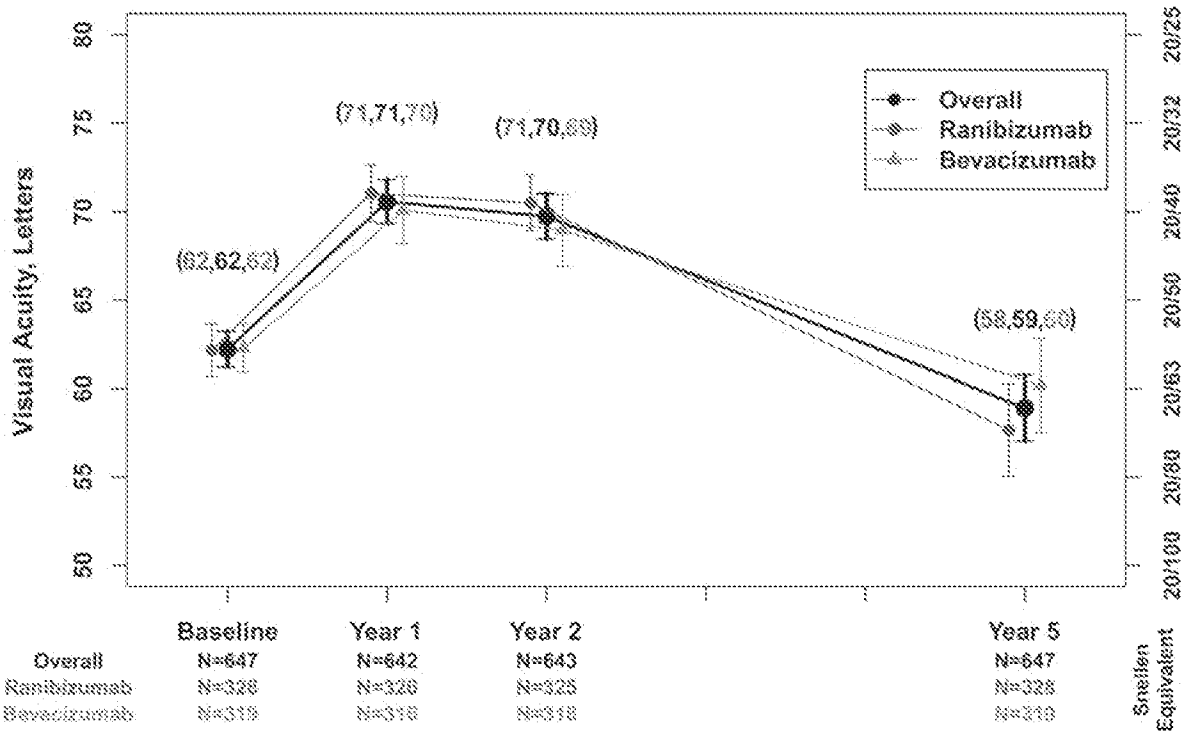


Figure 2.

Mean visual acuity and 95% confidence interval for 647 patients in the Follow-up Study. A. Overall and by drug assigned in the clinical trial; B. Overall and by dosing regimen assigned in the clinical trial.

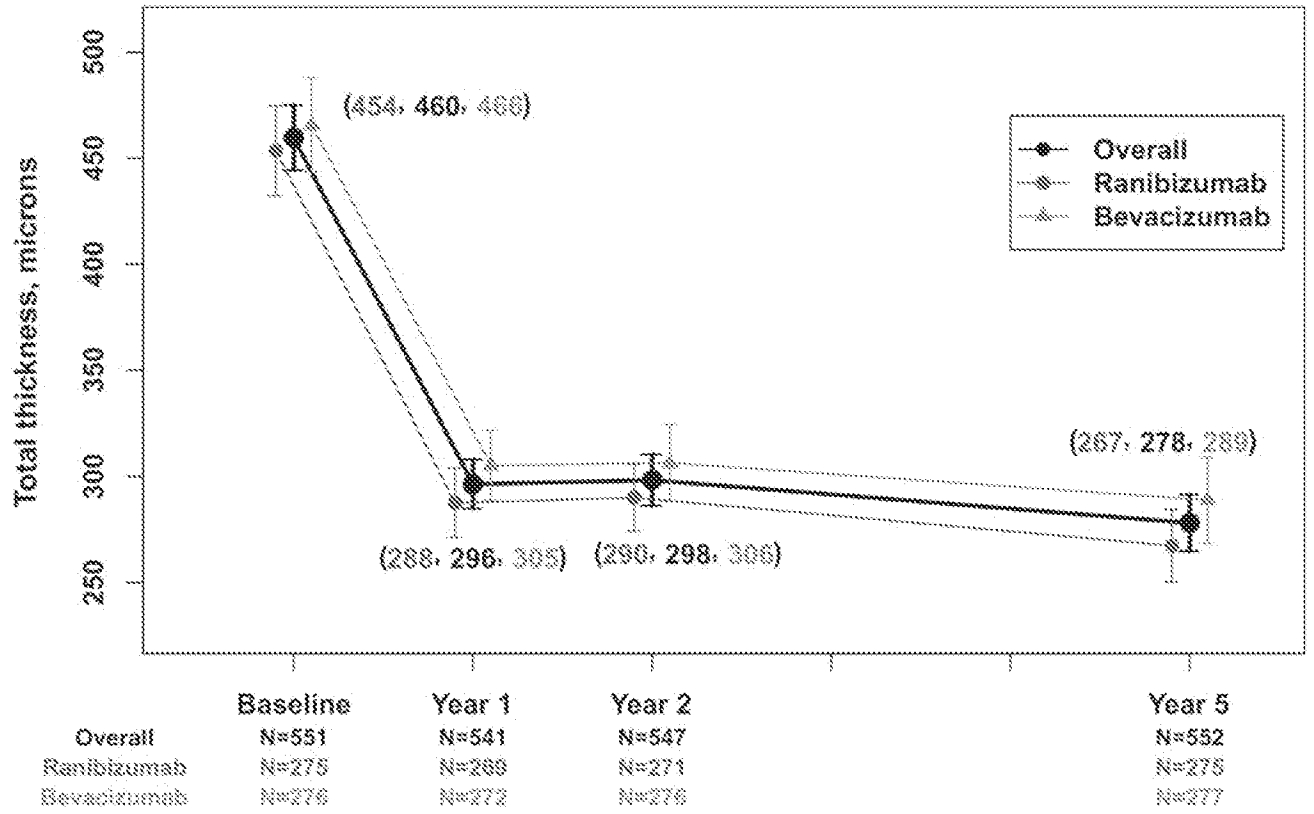
Author Manuscript

Author Manuscript

Author Manuscript

Author Manuscript





Author Manuscript

Author Manuscript

Author Manuscript

Author Manuscript

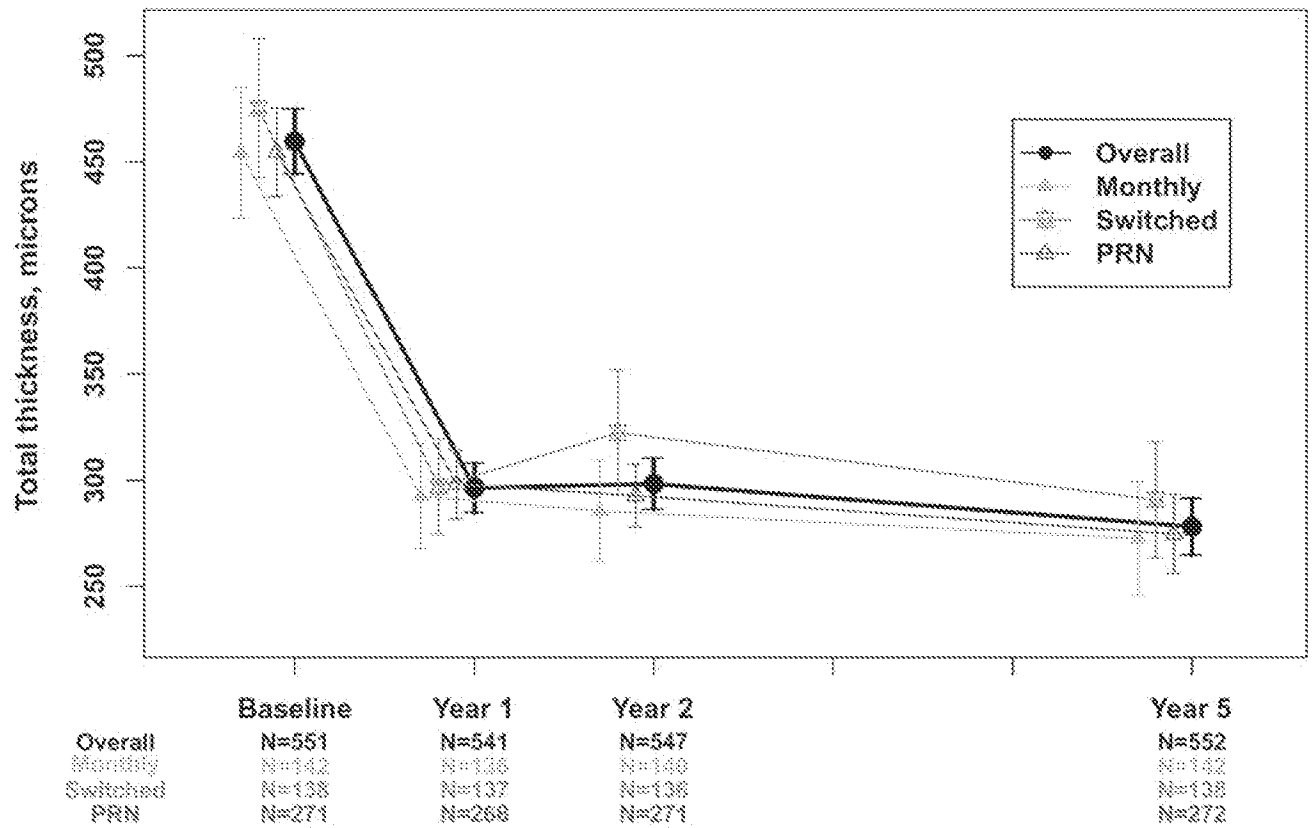


**Figure 3.** Mean total thickness at the foveal center and 95% confidence interval for 552 patients in the Follow-up Study with values available from optical coherent tomography. A. Overall and by drug assigned in the clinical trial; Overall and by dosing regimen assigned in the clinical trial.

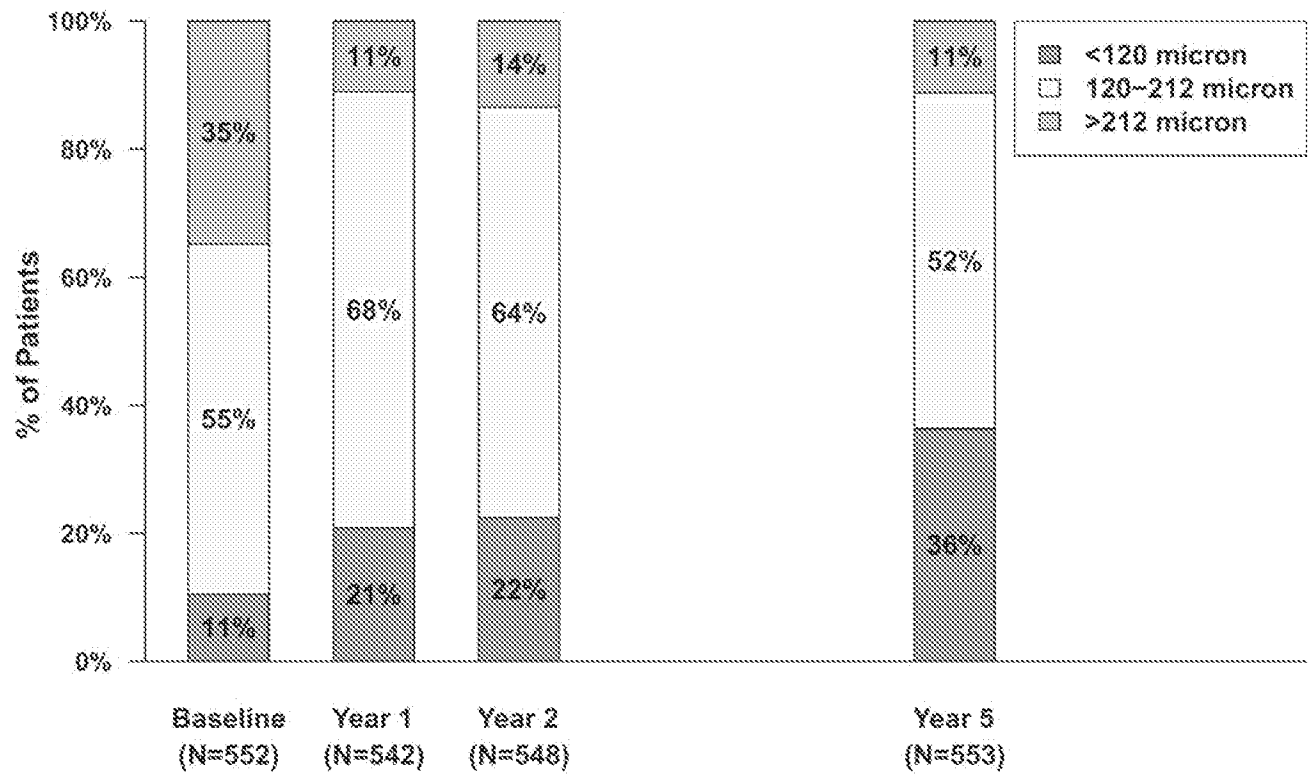


Figure 4.  
Retinal thickness at the foveal center in 553 patients with values available from optical coherent tomography, by category over time.

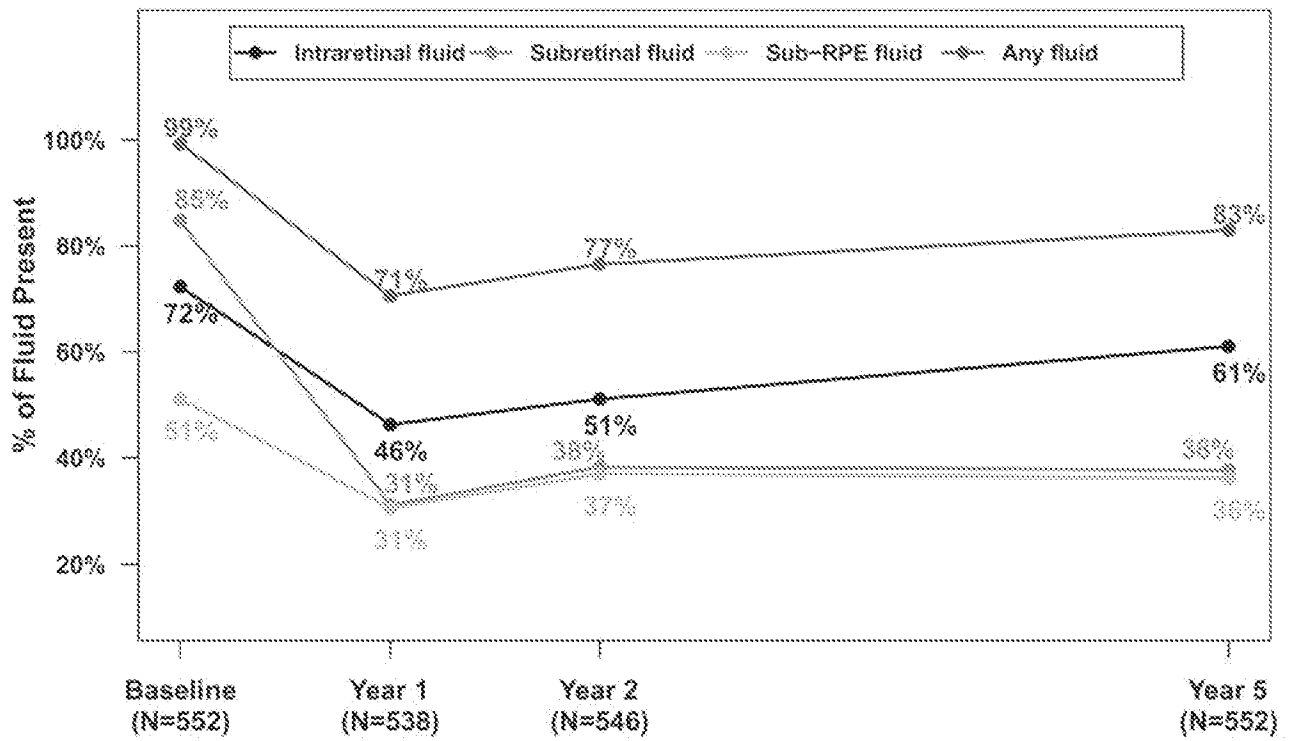


Figure 5.  
Percentage of eyes with fluid for 552 eyes in the Follow-up Study with values available from optical coherent tomography, over time.

Table 1

Characteristics at Baseline and 2 Years by Participation in the Follow-up Study

Characteristics at Baseline	Participants (N=647)	Non-participants (N=267)	P-value *	Died after Clinical Trial (N=203)
Age (yrs); mean (SD)	77.5 (7.3)	79.8 (7.8)	<0.001	83.0 (6.1)
Female gender; no. (%)	419 (64.8%)	166 (62.2%)	0.46	112 (55.2%)
White race; no. (%)	637 (98.5%)	261 (97.8%)	0.63	202 (99.5%)
Never cigarette smoking; no. (%)	274 (42.3%)	136 (50.9%)	0.06	80 (39.4%)
Definite hypertension; no. (%)	438 (67.7%)	187 (69.7%)	0.73	152 (74.9%)
Visual acuity score, letters; mean (SD)	62.2 (13.1)	59.1 (13.6)	0.002	58.0 (13.5)
Total area of neovascular lesion (mm <sup>2</sup> );	6.4 (6.6)	6.1 (5.7)	0.60	6.3 (7.0)
Geographic atrophy; no. (%)	47 (7.3%)	17 (6.4%)	0.64	13 (6.4%)
Total retinal thickness; mean (SD)	464 (185)	469 (212)	0.73	447 (168)
<b>Characteristics at 2 Years</b>				
Completed Year 2 visit	643	221		170
Visual acuity score, letters; mean (SD)	69.7 (16.6)	64.3 (19.5)	<0.001	61.9 (21.0)
Total area of neovascular lesion (mm <sup>2</sup> )	8.1 (7.9)	8.3 (7.6)	0.80	8.9 (8.6)
Geographic atrophy; no. (%)	127 (19.9%)	52 (24.9%)	0.13	37 (22.4%)
Scarring; no. (%)	280 (44.2%)	78 (37.7%)	0.10	69 (41.8%)
Total retinal thickness; mean (SD)	301 (145)	292 (149)	0.45	280 (123)
Number of injections – eyes				
assigned as-needed dosing yrs; mean (SD) for 2	13.3 (6.8)	11.5 (7.1)	0.01	12.7 (6.7)
N	326	134		98

\* P-values are for the comparison of participants to non-participants

Table 2

## Drugs Used to Treat the Study Eye after the End of the Clinical Trial

Drugs Used	Drug Assigned in the Clinical Trial	
	Ranibizumab (N=328)	Bevacizumab (N=319)
None	46 (14.0%)	50 (15.7%)
Bevacizumab only	77 (23.5%)	99 (31.0%)
Ranibizumab only	64 (19.5%)	37 (11.6%)
Aflibercept only	8 (2.4%)	4 (1.3%)
Bevacizumab and ranibizumab	41 (12.5%)	31 (9.7%)
Bevacizumab and aflibercept	28 (8.5%)	35 (11.0%)
Ranibizumab and aflibercept	36 (11.0%)	28 (8.8%)
Bevacizumab, ranibizumab and aflibercept	28 (8.5%)	33 (10.3%)
Other treatment	0 (0.0%)	2 (0.6%)

Author Manuscript

Author Manuscript

Author Manuscript

Author Manuscript

**Table 3**  
**Vision and Morphological Outcomes for All Eyes and by Drug Assigned in the Clinical Trial**

Outcome	Drug Assigned in the Clinical Trial			P-value
	All (N=647)	Ranibizumab (N=328)	Bevacizumab (N= 319)	
Visual acuity score, letters				
Snellen equivalent, no. (%)				
83-97, 20/12-20	60 (9.3)	24 (7.3)	36 (11.3)	
68-82, 20/25-40	261 (40.3)	129 (39.3)	132 (41.4)	
53-67, 20/50-80	132 (20.4)	68 (20.7)	64 (20.1)	
38-52, 20/100-160	65 (10.0)	36 (11.0)	29 (9.1)	
57-18, 20/200-400	73 (11.3)	42 (12.8)	31 (9.7)	
≤17, ≤20/400	56 (8.7)	29 (8.8)	27 (8.5)	
Mean letters (SD)	58.9 (24.1)	57.7 (42.1)	60.2 (24.1)	0.19
Change in visual acuity score, from baseline, letters, no. (%)				
≥15 increase	114 (17.6)	49 (14.9)	65 (20.4)	
5-14 increase	156 (24.2)	76 (23.2)	80 (25.0)	
≤4 change	142 (21.9)	76 (23.2)	66 (20.7)	
5-14 decrease	82 (12.7)	48 (14.6)	34 (10.7)	
15-29 decrease	71 (11.0)	37 (11.3)	34 (10.7)	
≥30 decrease	82 (12.7)	42 (12.8)	40 (12.5)	
Mean (SD)	-3.3 (22.3)	-4.5 (22.3)	-2.1 (22.3)	0.17
Change in visual acuity score, from 2 years, letters, no. (%) <sup>§</sup>				
≥15 increase	17 (2.6)	5 (1.5)	12 (3.8)	
5-14 increase	60 (9.3)	28 (8.6)	32 (10.0)	
≤4 change	215 (33.4)	101 (31.1)	114 (35.8)	
5-14 decrease	167 (26.0)	90 (27.7)	77 (24.2)	
15-29 decrease	101 (15.7)	48 (14.8)	53 (16.7)	
≥30 decrease	83 (12.9)	53 (16.3)	30 (9.4)	
Mean (SD)	-10.8 (18.9)	-12.7 (19.4)	-8.8 (18.2)	0.008

Outcome	Drug Assigned in the Clinical Trial				P-value
	AH (N=647) (N=555)	Ranibizumab (N=328) (N=277)	Bevacizumab (N=319) (N=278)		
Total thickness at fovea, $\mu\text{m}$					
Mean (SD) *	278 (160)	267 (145)	289 (174)		0.11
Mean Change(SD) from 2 years ***	-20 (132)	-23 (129)	-17 (136)		0.63
Fluid on optical coherence tomography					
None	94 (17.0)	42 (15.3)	52 (18.8)		0.27
Present	458 (83.0)	233 (84.7)	225 (81.2)		
Unknown/missing	3	2	1		
Dye leakage on angiogram (N <sup>§§</sup> =527/467)	(N <sup>§§</sup> =265/228)	(N <sup>§§</sup> =265/228)	(N <sup>§§</sup> =262/239)		
None	342 (75.5)	167 (75.6)	175 (75.4)		0.97
Present	111 (24.5)	54 (24.4)	57 (24.6)		
Unknown/missing	74	44	30		
Area of lesion, mm <sup>2</sup>					
Mean (SD) <sup>§</sup>	12.9 (11.4)	13.9 (11.7)	11.9 (11.0)		0.06
Mean Change (SD) from 2years <sup>§§</sup>	4.8 (8.8)	5.6 (9.9)	4.2 (7.6)		0.10
Geographic atrophy, no. (%)					
None	302 (58.6)	145 (55.8)	157 (61.6)		0.34
Non-foveal	128 (24.9)	67 (25.8)	61 (23.9)		
Foveal	85 (16.5)	48 (18.5)	37 (14.5)		
Unknown/missing	12	5	7		

<sup>§</sup> 4 Year 2 visual acuity scores missing, 3 in ranibizumab and 1 in bevacizumab group

\* 3 missing in total thickness at Year 5, 2 in ranibizumab and 1 in bevacizumab

\*\* Number with color photographs/fluorescein angiograms

\*\*\* 8 missing in change of total thickness from Year 2, 6 in ranibizumab and 2 in bevacizumab group

<sup>§</sup> 34 with lesion area ungradable at Year 5, 15 ranibizumab and 19 in bevacizumab group

<sup>§§</sup> 53 with missing in change of area of lesion due to ungradable images at Year 2 or Year 5, 29 in ranibizumab and 24 in bevacizumab group



**Table 5**  
 Serious Medical Events between Year 2 and the Follow-up Study Visit by Drug Assigned in the Clinical Trial

Serious Medical Event	Drug Assigned in the Clinical Trial						P <sup>§</sup>
	All (N=1090)		Ranibizumab (N=555)		Bevacizumab (N=535)		
	n	(%)	n	(%)	n	(%)	
Death-all causes	203	(18.6)	101	(18.2)	102	(19.1)	0.76
Arteriothrombotic events	66	(6.1)	42	(7.6)	24	(4.5)	0.04
Venous thrombotic events	9	(0.8)	4	(0.7)	5	(0.9)	0.75
Hypertension	27	(2.5)	13	(2.3)	14	(2.6)	0.85
One or more serious medical events	533	(48.9)	273	(49.2)	260	(48.6)	0.86
Previously associated with anti-VEGF treatment <sup>‡</sup>	177	(16.2)	90	(16.2)	77	(14.4)	0.15
MedDRA <sup>‡</sup> system organ class**							
Cardiac disorders	120	(11.0)	62	(11.2)	58	(10.8)	0.92
Infections	75	(6.9)	32	(5.8)	43	(8.0)	0.15
Nervous system disorders	82	(7.5)	44	(7.9)	38	(7.1)	0.65
Injury and procedural complications	57	(5.2)	33	(5.9)	24	(4.5)	0.34
Neoplasms benign and malignant	97	(8.9)	48	(8.6)	49	(9.2)	0.83
Gastrointestinal disorders	36	(3.3)	20	(3.6)	16	(3.0)	0.61

<sup>§</sup>Fisher's exact test

<sup>‡</sup>Arteriothrombotic events, systemic hemorrhage, congestive heart failure, venous thrombotic events, hypertension, vascular death

<sup>‡</sup>Medical Dictionary for Regulatory Activities

EX. F



Trial record **1 of 1** for: NCT00109499


[Previous Study](#) | [Return to List](#) | [Next Study](#)

## Study of AdGVPEDF.11D in Neovascular Age-related Macular Degeneration (AMD)




The safety and scientific validity of this study is the responsibility of the study sponsor and investigators. Listing a study does not mean it has been evaluated by the U.S. Federal Government. Read our [disclaimer](#) for details.

ClinicalTrials.gov Identifier: NCT00109499

**Recruitment Status**  : Completed

**First Posted**  : April 29, 2005

**Last Update Posted**  : May 12, 2011

### Sponsor:

GenVec

### Information provided by:

GenVec

[Study Details](#)

[Tabular View](#)

[No Results Posted](#)

[Disclaimer](#)

[How to Read a Study Record](#)

### Tracking Information

**First Submitted Date** ICMJE

April 28, 2005

**First Posted Date** ICMJE

April 29, 2005

**Last Update Posted Date**

May 12, 2011
<b>Study Start Date</b> <small>ICMJE</small>
<i>Not Provided</i>
<b>Primary Completion Date</b>
<i>Not Provided</i>
<b>Current Primary Outcome Measures</b> <small>ICMJE</small>
<i>Not Provided</i>
<b>Original Primary Outcome Measures</b> <small>ICMJE</small>
<i>Not Provided</i>
<b>Change History</b>
<u>Complete list of historical versions of study NCT00109499 on ClinicalTrials.gov Archive Site</u>
<b>Current Secondary Outcome Measures</b> <small>ICMJE</small>
<i>Not Provided</i>
<b>Original Secondary Outcome Measures</b> <small>ICMJE</small>
<i>Not Provided</i>
<b>Current Other Pre-specified Outcome Measures</b>
<i>Not Provided</i>
<b>Original Other Pre-specified Outcome Measures</b>
<i>Not Provided</i>
<b>Descriptive Information</b>
<b>Brief Title</b> <small>ICMJE</small>
Study of AdGVPEDF.11D in Neovascular Age-related Macular Degeneration (AMD)
<b>Official Title</b> <small>ICMJE</small>
An Open-label, Phase I, Single Administration, Dose- Escalation Study of AdGVPEDF.11D in Neovascular Age-related Macular Degeneration (AMD)
<b>Brief Summary</b>

The primary purpose of this study is to assess the safety of AdGVPEDF.11D when given to patients with "wet" age-related macular degeneration (AMD). AdGVPEDF.11D is a replication deficient (E1, E3 and E4 deleted) adenovirus vector containing the gene for the PEDF (pigment epithelium-derived factor) protein. PEDF is a protein that naturally exists in the human eye, but whose levels are altered in diseases characterized by ocular neovascularization like AMD. The PEDF protein is known to have anti-angiogenic effects or, in other words, it has the ability to inhibit growth of new blood vessels.

AdGVPEDF.11D will be delivered once via intravitreal injection into one eye. The injected eye will be the eye with the worst visual acuity.

#### Detailed Description

*Not Provided*

#### Study Type ICMJE

Interventional

#### Study Phase ICMJE

Phase 1

#### Study Design ICMJE

Masking: None (Open Label)

Primary Purpose: Treatment

#### Condition ICMJE

Macular Degeneration

#### Intervention ICMJE

Drug: AdGVPEDF.11D

#### Study Arms ICMJE

*Not Provided*

#### Publications \*

*Not Provided*

\* Includes publications given by the data provider as well as publications identified by ClinicalTrials.gov Identifier (NCT Number) in Medline.

#### Recruitment Information

<b>Recruitment Status</b> <small>ICMJE</small>
Completed
<b>Enrollment</b> <small>ICMJE</small>
<i>Not Provided</i>
<b>Original Enrollment</b> <small>ICMJE</small>
<i>Not Provided</i>
<b>Study Completion Date</b> <small>ICMJE</small>
<i>Not Provided</i>
<b>Primary Completion Date</b>
<i>Not Provided</i>
<b>Eligibility Criteria</b> <small>ICMJE</small>
<p>Inclusion Criteria:</p> <ul style="list-style-type: none"> <li>• Age greater than or equal to 50 years;</li> <li>• Severe neovascular AMD in at least one eye responsible for a best corrected vision of 20/200 or worse in the study eye (if both eyes have neovascular AMD and equal visual acuity scores, the study eye will be determined by the investigator);</li> <li>• Best corrected visual acuity in the fellow eye must be equal to or better than the study eye;</li> <li>• Fluorescein angiography of the study eye must show evidence of a leaking subfoveal choroidal neovascular lesion. The subfoveal component must consist of CNV (choroidal neovascularization), blood or fibrosis. The total size of the lesion must be <math>\leq 12</math> MPS disc areas. The presence of a leaking subfoveal choroidal neovascular lesion will be evaluated by the investigator at the clinical site to determine patients' eligibility.</li> <li>• Must not be candidates for (including patients who have had treatment with either modality in the past and are no longer candidates) or must have refused treatment with subfoveal laser photocoagulation or PDT (photodynamic therapy);</li> <li>• Informed consent;</li> <li>• Able to comply with protocol requirements including follow-up visits.</li> </ul> <p>Exclusion Criteria:</p> <ul style="list-style-type: none"> <li>• Liver enzymes <math>&gt; 2 \times</math> ULN (ALT, AST, bilirubin);</li> <li>• Clinical evidence of active infection of any type, including adenovirus, hepatitis A, B, or C virus or HIV virus;</li> <li>• Other treatment for AMD in the study eye within the last twelve weeks prior to Day 1;</li> </ul>

- Other experimental medications within the last four weeks prior to Day 1;
- Significant retinal disease other than neovascular AMD, such as diabetic retinopathy or retinal vascular occlusion;
- Significant non-retinal disease such as ocular atrophy;
- Cataract or other significant media opacity that might compromise examination and photography of the posterior segment;
- Other causes of choroidal neovascularization such as pathologic myopia (> 8 diopters), ocular histoplasmosis or angioid streaks;
- Evidence of inflammation (grade 1 or higher) in the anterior and/or posterior chambers;
- Cataract surgery or submacular surgery within 3 months;
- Prior ocular treatment with radiation;
- Known allergy to fluorescein;
- Abnormal prothrombin or partial thromboplastin time (> 1.5 X ULN) or anticoagulant therapy that cannot be withheld for treatment.

**Sex/Gender** ICMJE**Sexes Eligible for Study:**

All

**Ages** ICMJE

50 Years and older (Adult, Older Adult)

**Accepts Healthy Volunteers** ICMJE

No

**Contacts** ICMJE*Contact information is only displayed when the study is recruiting subjects***Listed Location Countries** ICMJE

United States

**Removed Location Countries****Administrative Information****NCT Number** ICMJE

NCT00109499
<b>Other Study ID Numbers</b> <small>ICMJE</small>
GV-003.001
<b>Has Data Monitoring Committee</b>
<i>Not Provided</i>
<b>U.S. FDA-regulated Product</b>
<i>Not Provided</i>
<b>IPD Sharing Statement</b> <small>ICMJE</small>
<i>Not Provided</i>
<b>Responsible Party</b>
Paul Fischer, PhD, GenVec
<b>Study Sponsor</b> <small>ICMJE</small>
GenVec
<b>Collaborators</b> <small>ICMJE</small>
<i>Not Provided</i>
<b>Investigators</b> <small>ICMJE</small>
<i>Not Provided</i>
<b>PRS Account</b>
GenVec
<b>Verification Date</b>
May 2011
<small>ICMJE</small> <b>Data element required by the <u>International Committee of Medical Journal Editors</u> and the <u>World Health Organization ICTRP</u></b>



EX. G



Trial record **1 of 1** for: NCT01024998


[Previous Study](#) | [Return to List](#) | [Next Study](#)

## Safety and Tolerability Study of AAV2-sFLT01 in Patients With Neovascular Age-Related Macular Degeneration (AMD)



The safety and scientific validity of this study is the responsibility of the study sponsor and investigators. Listing a study does not mean it has been evaluated by the U.S. Federal Government. Read our [disclaimer](#) for details.

ClinicalTrials.gov Identifier: NCT01024998

Recruitment Status  : Completed

First Posted  : December 3, 2009

Last Update Posted  : August 22, 2018

### Sponsor:

Genzyme, a Sanofi Company

### Information provided by (Responsible Party):

Sanofi ( Genzyme, a Sanofi Company )

[Study Details](#)

[Tabular View](#)

[No Results Posted](#)

[Disclaimer](#)

[How to Read a Study Record](#)

### Tracking Information

**First Submitted Date** ICMJE

December 2, 2009

**First Posted Date** ICMJE

December 3, 2009

**Last Update Posted Date**

August 22, 2018

**Actual Study Start Date** <sup>ICMJE</sup>

January 11, 2010

**Actual Primary Completion Date**

July 2014 (Final data collection date for primary outcome measure)

**Current Primary Outcome Measures** <sup>ICMJE</sup>

(submitted: April 5, 2011)

- Maximum tolerated dose of a single unocular intravitreal injection of AAV2-sFLT01 [ Time Frame: Time of treatment through Week 52 (referred to as the "core" study) ]
- Number of Treatment Emergent Adverse Events [ Time Frame: Time of treatment through Week 52 (referred to as the "core" study) ]
- Number of Treatment Emergent Adverse Events [ Time Frame: Up to 4 years after the "core" study (referred to as the "Extended Follow-up" period) ]

**Original Primary Outcome Measures** <sup>ICMJE</sup>

(submitted: December 2, 2009)

Maximum tolerated dose of a single unocular intravitreal injection of AAV2-sFLT01 [ Time Frame: Time of treatment through Week 52 ]

**Change History**[Complete list of historical versions of study NCT01024998 on ClinicalTrials.gov Archive Site](#)**Current Secondary Outcome Measures** <sup>ICMJE</sup>

(submitted: April 5, 2011)

- Decreased retinal thickness [ Time Frame: Time of treatment through Week 52 (referred to as the "core" study) ]
- Decreased retinal thickness [ Time Frame: Up to 4 years after the "core" study (referred to as the "Extended Follow-up" period) ]

**Original Secondary Outcome Measures** <sup>ICMJE</sup>

(submitted: December 2, 2009)

Decreased retinal thickness [ Time Frame: Time of treatment through Week 52 ]

**Current Other Pre-specified Outcome Measures***Not Provided*

**Original Other Pre-specified Outcome Measures**

*Not Provided*

**Descriptive Information****Brief Title** ICMJE

Safety and Tolerability Study of AAV2-sFLT01 in Patients With Neovascular Age-Related Macular Degeneration (AMD)

**Official Title** ICMJE

A Phase 1, Open-Label, Multi-Center, Dose-Escalating, Safety and Tolerability Study of a Single Intravitreal Injection of AAV2-sFLT01 in Patients With Neovascular Age-Related Macular Degeneration

**Brief Summary**

This Phase 1 clinical research study will examine the safety and tolerability of an experimental gene transfer agent, AAV2-sFLT01, in patients with Neovascular Age-Related Macular Degeneration (AMD).

**Detailed Description**

A new treatment for neovascular age-related macular degeneration (AMD) is being investigated. Neovascular AMD is sometimes referred to as the "wet" form of AMD. The purpose of this Phase 1 clinical research study is to examine the safety and ability of an experimental study drug to treat a complication of the disease which leads to vision loss. The name of the study drug is "AAV2-sFLT01." This experimental study drug uses a virus to transfer a gene (genetic code) into cells within the eye. The gene codes for a protein that is intended to diminish the growth of abnormal blood vessels under the retina. The duration of the gene's effect is currently unknown, but might last for years.

This clinical research study will look at the safety of a single administration of AAV2-sFLT01 injected directly into the eye. There are 2 parts to this study, but patients will take part in only one of them. In the first part of the study, 4 different doses of the study drug will be studied in 4 separate groups of patients. Patients in the first part of the study will not be randomized. In the second part of the study, the highest dose that was safe and well tolerated will be studied in 10 more patients. Patients in this part of the study may have a ranibizumab (Lucentis®) injection 26 weeks after their AAV2-sFLT01 injection to verify their responsiveness to anti-VEGF therapy, if they have not demonstrated a response to AAV2-sFLT01. The initial two parts of this protocol are expected to be completed in July, 2013.

All patients injected with AAV2-sFLT01 will be asked to participate in an Extended Follow-Up (EFU) program for up to an additional 4 years. Participation is voluntary but strongly encouraged as it allows for the long term collection of safety information as well as information about the potential long term effects of the study drug. Study visits will take place at the site every 6 months.

Up to thirty-four (34) patients at multiple centers will take part in this study in the United States.

**Study Type** ICMJE

Interventional

**Study Phase** ICMJE

Phase 1

**Study Design** ICMJE

Allocation: Non-Randomized

Intervention Model: Parallel Assignment

Masking: None (Open Label)

Primary Purpose: Treatment

**Condition** ICMJE

- Macular Degeneration
- Age-Related Maculopathies
- Age-Related Maculopathy
- Maculopathies, Age-Related
- Maculopathy, Age-Related
- Retinal Degeneration
- Retinal Neovascularization
- Gene Therapy
- Therapy, Gene
- Eye Diseases

**Intervention** ICMJE

- Biological: AAV2-sFLT01  
2 x 10<sup>8</sup> vector genomes (vg) AAV2-sFLT01. Single intravitreal injection to a single eye, using a fixed volume of 100 µL.
- Biological: AAV2-sFLT01  
2 x 10<sup>9</sup> vector genomes (vg) AAV2-sFLT01. Single intravitreal injection to a single eye, using a fixed volume of 100 µL.
- Biological: AAV2-sFLT01  
6 x 10<sup>9</sup> vector genomes (vg) AAV2-sFLT01. Single intravitreal injection to a single eye, using a fixed volume of 100 µL.

- **Biological: AAV2-sFLT01**

2 x 10<sup>10</sup> vector genomes (vg) AAV2-sFLT01. Single intravitreal injection to a single eye, using a fixed volume of 100 µL.

### Study Arms ICMJE

- **Experimental: 2 x 10<sup>8</sup> vector genomes (vg) AAV2-sFLT01**  
Intervention: Biological: AAV2-sFLT01
- **Experimental: 2 x 10<sup>9</sup> vector genomes (vg) AAV2-sFLT01**  
Intervention: Biological: AAV2-sFLT01
- **Experimental: 6 x 10<sup>9</sup> vector genomes (vg) AAV2-sFLT01**  
Intervention: Biological: AAV2-sFLT01
- **Experimental: 2 x 10<sup>10</sup> vector genomes (vg) AAV2-sFLT01**  
Intervention: Biological: AAV2-sFLT01

### Publications \*

Heier JS, Kherani S, Desai S, Dugel P, Kaushal S, Cheng SH, Delacono C, Purvis A, Richards S, Le-Halpere A, Connolly J, Wadsworth SC, Varona R, Buggage R, Scaria A, Campochiaro PA. Intravitreal injection of AAV2-sFLT01 in patients with advanced neovascular age-related macular degeneration: a phase 1, open-label trial. Lancet. 2017 Jul 1;390(10089):50-61. doi: 10.1016/S0140-6736(17)30979-0. Epub 2017 May 17. Erratum in: Lancet. 2017 Jul 1;390(10089):28.

\* Includes publications given by the data provider as well as publications identified by ClinicalTrials.gov Identifier (NCT Number) in Medline.

### Recruitment Information

#### Recruitment Status ICMJE

Completed

#### Actual Enrollment ICMJE

(submitted: October 26, 2015)

19

#### Original Estimated Enrollment ICMJE

(submitted: December 2, 2009)

34

**Actual Study Completion Date** <sup>ICMJE</sup>

July 2018

**Actual Primary Completion Date**

July 2014 (Final data collection date for primary outcome measure)

**Eligibility Criteria** <sup>ICMJE</sup>

## Inclusion Criteria:

- Choroidal neovascular membrane (CNV) secondary to AMD, as confirmed by the patient's medical history and a documented diagnosis of CNV.
- Distance BCVA of 20/100 or worse in the study eye.
- The fellow eye must have distance BCVA of 20/400 or better.
- The study eye, i.e., the eye that receives investigational product, has the worst CVA (As compared to the fellow eye).
- Subfoveal disciform scarring in the study eye for the first part of the study (the dose-escalation part). Patients may or may not have macular scarring in the study eye for the second part of the study (MTD phase). In addition, patients enrolled in the second part of the study must have demonstrated responsiveness to an anti-VEGF therapy within 12 months prior to screening and after the patient's most recent treatment of anti-VEGF therapy.
- Noted presence of intra- or sub-retinal fluid.
- Adequate dilation of pupils to permit thorough ocular examination and testing.
- Must be willing to have samples of anterior chamber fluid collected from the study eye.

## Exclusion Criteria:

- CNV in the study eye due to any reason other than AMD.
- History of conditions in the study eye during Screening which might alter visual acuity or interfere with study testing.
- Active uncontrolled glaucoma.
- Had any intraocular surgeries in the study eye within 3 months of enrollment or are known or likely candidates for intraocular surgery (including cataract surgery) in the study eye within 1 year of treatment.
- Acute or chronic infection in the study eye.
- History of inflammation in the study eye or ongoing inflammation in either eye.
- Any contraindication to intravitreal injection.
- Received Photo Dynamic Therapy in the study eye within 60 days, or laser photocoagulation within 14 days prior to Screening.

- Currently using or have used ranibizumab (Lucentis®), bevacizumab (Avastin™), or pegaptanib sodium (Macugen®) within 1 month prior to Screening.
- Currently using or have used Aflibercept (Eylea®) within 4 months prior to Screening.
- Currently using any periocular (study eye), intravitreal (study eye), or systemic (oral or intravenous) steroids within 3 months prior to Screening.
- Any active herpetic infection, in particular active lesions in the eye or on the face.
- Any significant poorly controlled illness that would preclude study compliance and follow-up.
- Current or prior use of any medication known to be toxic to the retina or optic nerve.
- Previous treatment with any ocular or systemic gene transfer product.
- Received any investigational product within 120 days prior to Screening.

**Sex/Gender** ICMJE**Sexes Eligible for Study:**

All

**Ages** ICMJE

50 Years and older (Adult, Older Adult)

**Accepts Healthy Volunteers** ICMJE

No

**Contacts** ICMJE*Contact information is only displayed when the study is recruiting subjects***Listed Location Countries** ICMJE

United States

**Removed Location Countries****Administrative Information****NCT Number** ICMJE

NCT01024998

**Other Study ID Numbers** ICMJE



sFLT01-AMD-00106 0810-948 ( Other Identifier: NIH Office of Biotechnology Activities ) MSC12870 ( Other Identifier: Sanofi )
<b>Has Data Monitoring Committee</b>
Yes
<b>U.S. FDA-regulated Product</b>
<i>Not Provided</i>
<b>IPD Sharing Statement</b> <sup>ICMJE</sup>
<i>Not Provided</i>
<b>Responsible Party</b>
Sanofi ( Genzyme, a Sanofi Company )
<b>Study Sponsor</b> <sup>ICMJE</sup>
Genzyme, a Sanofi Company
<b>Collaborators</b> <sup>ICMJE</sup>
<i>Not Provided</i>
<b>Investigators</b> <sup>ICMJE</sup>
<b>Study Director:</b> Medical Monitor Genzyme, a Sanofi Company
<b>PRS Account</b>
Sanofi
<b>Verification Date</b>
August 2018
<sup>ICMJE</sup> <b>Data element required by the <u>International Committee of Medical Journal Editors</u> and the <u>World Health Organization</u> <u>ICTRP</u></b>

EX. H



Trial record **1 of 1** for: NCT01494805


[Previous Study](#) | [Return to List](#) | [Next Study](#)

## Safety and Efficacy Study of rAAV.sFlt-1 in Patients With Exudative Age-Related Macular Degeneration (AMD)



The safety and scientific validity of this study is the responsibility of the study sponsor and investigators. Listing a study does not mean it has been evaluated by the U.S. Federal Government. Read our [disclaimer](#) for details.

ClinicalTrials.gov Identifier: NCT01494805

[Recruitment Status](#)  : Completed

[First Posted](#)  : December 19, 2011

[Last Update Posted](#)  : September 1, 2017

### Sponsor:

Lions Eye Institute, Perth, Western Australia

### Collaborator:

Adverum Biotechnologies, Inc.

### Information provided by (Responsible Party):

Prof. P. Elizabeth Rakoczy, Lions Eye Institute, Perth, Western Australia

[Study Details](#)

[Tabular View](#)

[No Results Posted](#)

[Disclaimer](#)

[How to Read a Study Record](#)

### Tracking Information

**First Submitted Date** ICMJE

December 14, 2011

**First Posted Date** ICMJE

December 19, 2011

**Last Update Posted Date**

September 1, 2017

**Actual Study Start Date** ICMJE

December 2011

**Actual Primary Completion Date**

May 2017 (Final data collection date for primary outcome measure)

**Current Primary Outcome Measures** ICMJE

(submitted: December 15, 2011)

No sign of unresolved ophthalmic complications, toxicity or systemic complications as measured by laboratory tests from 1 month post injection [ Time Frame: Primary endpoint at 1 month ]

## 1. Ocular examination:

- Ocular inflammation
- Intraocular pressure
- Visual acuity
- Retinal bleeding

## 2. Abnormal laboratory data

**Original Primary Outcome Measures** ICMJE*Same as current***Change History**

[Complete list of historical versions of study NCT01494805 on ClinicalTrials.gov Archive Site](#)

**Current Secondary Outcome Measures** ICMJE

(submitted: December 15, 2011)

Maintenance or improvement of vision without the necessity of ranibizumab re-injections [ Time Frame: Up to 3 years ]

1. Best-corrected visual acuity
2. CNV lesion
3. Foveal thickness

**Original Secondary Outcome Measures** ICMJE

Same as current

**Current Other Pre-specified Outcome Measures**

Not Provided

**Original Other Pre-specified Outcome Measures**

Not Provided

**Descriptive Information****Brief Title** ICMJE

Safety and Efficacy Study of rAAV.sFlt-1 in Patients With Exudative Age-Related Macular Degeneration

**Official Title** ICMJE

A Phase I/II Controlled Dose-escalating Trial to Establish the Baseline Safety and Efficacy of a Single Subretinal Injection of rAAV.sFlt-1 Into Eyes of Patients With Exudative Age-related Macular Degeneration (AMD)

**Brief Summary**

The study will involve approximately 40 subjects aged 55 or above who have exudative age-related macular degeneration (wet AMD). Patients will be randomized to receive one of two doses of rAAV.sFlt-1 or assigned to the control group.

**Detailed Description**

A new treatment for exudative age-related macular degeneration (wet AMD) is being investigated. The purpose of this Phase I/II clinical research study is to examine the baseline safety and efficacy of an experimental study drug to treat a complication of the disease which leads to vision loss. The name of the study drug is rAAV.sFlt-1.

This experimental study uses a non-pathogenic virus to express a therapeutic protein within the eye. The therapeutic diminishes the growth of abnormal blood vessels under the retina. The duration of effect is thought to be long-term (years) following a single administration.

The clinical research study will look at the baseline safety and efficacy of a single injection of rAAV.sFlt-1 injected directly into the eye.

Approximately forty (40) subjects will participate in Australia. The primary endpoint of the study is at one month, with extended follow up for 3 years.

**Study Type** ICMJE

Interventional

**Study Phase** ICMJE

Phase 1

Phase 2

**Study Design** ICMJE

Allocation: Randomized

Intervention Model: Parallel Assignment

Masking: Single (Outcomes Assessor)

Primary Purpose: Treatment

**Condition** ICMJE

- Macular Degeneration
- Age-related Maculopathies
- Age-related Maculopathy
- Maculopathies, Age-related
- Maculopathy, Age-related
- Retinal Degeneration
- Retinal Neovascularization
- Eye Diseases

**Intervention** ICMJE

- Biological: rAAV.sFlt-1  
1 x 10<sup>10</sup> vector genomes (vg) rAAV.sFlt-1, delivered by subretinal injection
- Biological: rAAV.sFlt-1  
1 x 10<sup>11</sup> vector genomes (vg) rAAV.sFlt-1, delivered by subretinal injection
- Other: Control (ranibizumab alone)  
Patients will not receive rAAV.sFlt-1, but will be eligible for retreatment with ranibizumab (Lucentis).

**Study Arms** ICMJE

- Experimental: Low Dose rAAV.sFlt-1  
Intervention: Biological: rAAV.sFlt-1
- Experimental: High Dose rAAV.sFlt-1  
Intervention: Biological: rAAV.sFlt-1
- Active Comparator: Control - ranibizumab only

Intervention: Other: Control (ranibizumab alone)

#### Publications \*

- [Constable IJ, Pierce CM, Lai CM, Magno AL, Degli-Esposti MA, French MA, McAllister IL, Butler S, Barone SB, Schwartz SD, Blumenkranz MS, Rakoczy EP. Phase 2a Randomized Clinical Trial: Safety and Post Hoc Analysis of Subretinal rAAV.sFLT-1 for Wet Age-related Macular Degeneration. EBioMedicine. 2016 Dec;14:168-175. doi: 10.1016/j.ebiom.2016.11.016. Epub 2016 Nov 10.](#)
- [Rakoczy EP, Lai CM, Magno AL, Wikstrom ME, French MA, Pierce CM, Schwartz SD, Blumenkranz MS, Chalberg TW, Degli-Esposti MA, Constable IJ. Gene therapy with recombinant adeno-associated vectors for neovascular age-related macular degeneration: 1 year follow-up of a phase 1 randomised clinical trial. Lancet. 2015 Dec 12;386\(10011\):2395-403. doi: 10.1016/S0140-6736\(15\)00345-1. Epub 2015 Sep 30.](#)

\* Includes publications given by the data provider as well as publications identified by ClinicalTrials.gov Identifier (NCT Number) in Medline.

#### Recruitment Information

**Recruitment Status** ICMJE

Completed

**Actual Enrollment** ICMJE

(submitted: March 17, 2014)

40

**Original Estimated Enrollment** ICMJE

(submitted: December 15, 2011)

24

**Actual Study Completion Date** ICMJE

August 2017

**Actual Primary Completion Date**

May 2017 (Final data collection date for primary outcome measure)

**Eligibility Criteria** ICMJE

Inclusion Criteria:

- Age greater than or equal to 55 years;
- Subfoveal CNV secondary to AMD and with best corrected visual acuity of 3/60 - 6/9 with 6/60 or better in the other eye;
- Fluorescein angiogram of the study eye must show evidence of a leaking subfoveal choroidal neovascular lesion, or CNV currently under active management with anti-VEGF therapy;
- Must be a candidate for anti-VEGF intravitreal injections;
- No previous retinal treatment of photodynamic therapy or laser;
- Able to provide informed consent;
- Able to comply with protocol requirements, including follow-up visits.

#### Exclusion Criteria:

- Liver enzymes > 2 X upper limit of normal;
- Any prior treatment for AMD in the study / control eye, excluding anti-VEGF injections;
- Extensive sub-foveal scarring, extensive geographic atrophy, or thick subretinal blood in the study eye as determined by the investigator;
- Significant retinal disease other than sub-foveal CNV AMD;

#### Sex/Gender ICMJE

#### Sexes Eligible for Study:

All

#### Ages ICMJE

55 Years and older (Adult, Older Adult)

#### Accepts Healthy Volunteers ICMJE

No

#### Contacts ICMJE

*Contact information is only displayed when the study is recruiting subjects*

#### Listed Location Countries ICMJE

Australia

#### Removed Location Countries

#### Administrative Information



<b>NCT Number</b> <small>ICMJE</small>
NCT01494805
<b>Other Study ID Numbers</b> <small>ICMJE</small>
2008-135
<b>Has Data Monitoring Committee</b>
Yes
<b>U.S. FDA-regulated Product</b>
<i>Not Provided</i>
<b>IPD Sharing Statement</b> <small>ICMJE</small>
<i>Not Provided</i>
<b>Responsible Party</b>
Prof. P. Elizabeth Rakoczy, Lions Eye Institute, Perth, Western Australia
<b>Study Sponsor</b> <small>ICMJE</small>
Lions Eye Institute, Perth, Western Australia
<b>Collaborators</b> <small>ICMJE</small>
Adverum Biotechnologies, Inc.
<b>Investigators</b> <small>ICMJE</small>
<b>Principal Investigator:</b> Ian Constable, Professor Lions Eye Institute
<b>PRS Account</b>
Lions Eye Institute, Perth, Western Australia
<b>Verification Date</b>
August 2017
<small>ICMJE</small> <b>Data element required by the <u>International Committee of Medical Journal Editors</u> and the <u>World Health Organization</u> <u>ICTRP</u></b>

EX. I



Trial record **1 of 1** for: NCT01301443


[Previous Study](#) | [Return to List](#) | [Next Study](#)


## Phase I Dose Escalation Safety Study of RetinoStat in Advanced Age-Related Macular Degeneration (AMD) (GEM)



The safety and scientific validity of this study is the responsibility of the study sponsor and investigators. Listing a study does not mean it has been evaluated by the U.S. Federal Government. Read our [disclaimer](#) for details.

ClinicalTrials.gov Identifier: NCT01301443

[Recruitment Status](#)  : Completed

[First Posted](#)  : February 23, 2011

[Last Update Posted](#)  : April 5, 2017

### Sponsor:

Oxford BioMedica

### Information provided by (Responsible Party):

Oxford BioMedica

[Study Details](#)

[Tabular View](#)

[No Results Posted](#)

[Disclaimer](#)

[How to Read a Study Record](#)

### Tracking Information

**First Submitted Date** ICMJE

February 21, 2011

**First Posted Date** ICMJE

February 23, 2011

**Last Update Posted Date**

April 5, 2017

**Study Start Date** ICMJE

February 2011

**Actual Primary Completion Date**

September 2014 (Final data collection date for primary outcome measure)

**Current Primary Outcome Measures** ICMJE

(submitted: February 22, 2011)

The incidence of adverse events [ Time Frame: 24 weeks ]

The number and percentage of patients with treatment emergent adverse events.

**Original Primary Outcome Measures** ICMJE*Same as current***Change History**[Complete list of historical versions of study NCT01301443 on ClinicalTrials.gov Archive Site](#)**Current Secondary Outcome Measures** ICMJE

(submitted: February 22, 2011)

Change from baseline in subretinal and intraretinal fluid as measured by OCT [ Time Frame: 24 weeks ]

The change from baseline in the amount of subretinal and intraretinal fluid measured by Optical Coherence tomography

**Original Secondary Outcome Measures** ICMJE*Same as current***Current Other Pre-specified Outcome Measures***Not Provided***Original Other Pre-specified Outcome Measures***Not Provided***Descriptive Information****Brief Title** ICMJE

Phase I Dose Escalation Safety Study of RetinoStat in Advanced Age-Related Macular Degeneration (AMD)

<b>Official Title</b> <small>ICMJE</small>
A Phase I Dose Escalation Safety Study of Subretinally Injected RetinoStat, a Lentiviral Vector Expressing Endostatin and Angiostatin, in Patients With Advanced Neovascular Age-Related Macular Degeneration
<b>Brief Summary</b>
The purpose of this first in man study is to examine the safety of an experimental gene transfer agent, RetinoStat, designed to treat neovascular age-related macular degeneration.
<b>Detailed Description</b>
There are two parts to the study. A dose-escalation phase looking at three doses of RetinoStat starting with the lowest dose, three patients will be recruited at each dose level. The escalation phase will be followed by a dose confirmation phase where the highest dose that is safe and well tolerated will be examined in 9 patients.
<b>Study Type</b> <small>ICMJE</small>
Interventional
<b>Study Phase</b> <small>ICMJE</small>
Phase 1
<b>Study Design</b> <small>ICMJE</small>
Intervention Model: Single Group Assignment Masking: None (Open Label) Primary Purpose: Treatment
<b>Condition</b> <small>ICMJE</small>
Age Related Macular Degeneration
<b>Intervention</b> <small>ICMJE</small>
Drug: Subretinally injected RetinoStat Single subretinal injections, with increasing doses. 9 patients with 3 patients at each dose followed, by 12 patients at maximum tolerated dose. Other Name: OXB-201
<b>Study Arms</b> <small>ICMJE</small>
Experimental: Subretinally Injected RetinoStat Subretinally injected RetinoStat Intervention: Drug: Subretinally injected RetinoStat
<b>Publications *</b>

Campochiaro PA, Lauer AK, Sohn EH, Mir TA, Naylor S, Anderton MC, Kelleher M, Harrop R, Ellis S, Mitrophanous KA. Lentiviral Vector Gene Transfer of Endostatin/Angiostatin for Macular Degeneration (GEM) Study. Hum Gene Ther. 2017 Jan;28(1):99-111. doi: 10.1089/hum.2016.117. Epub 2016 Sep 26.

\* Includes publications given by the data provider as well as publications identified by ClinicalTrials.gov Identifier (NCT Number) in Medline.

## Recruitment Information

**Recruitment Status** ICMJE

Completed

**Actual Enrollment** ICMJE  
(submitted: October 21, 2014)

21

**Original Estimated Enrollment** ICMJE  
(submitted: February 22, 2011)

18

**Actual Study Completion Date** ICMJE

May 2015

**Actual Primary Completion Date**

September 2014 (Final data collection date for primary outcome measure)

**Eligibility Criteria** ICMJE

Inclusion Criteria:

- Clinical diagnosis of AMD with active CNV that shows evidence of leakage.
- BCVA less than or equal to 20/200 in the study eye for dose escalation phase.
- BCVA less than or equal to 20/80 in the study eye for maximum tolerated dose phase.

Exclusion Criteria:

- Significant ocular abnormalities that prevent retinal assessment.
- Treatment with steroids within three months of screening.
- Treatment with anti-VEGF therapy to either eye within one month of screening.
- Clinically significant intercurrent illnesses, laboratory, ECG or chest XRay abnormalities.

**Sex/Gender** ICMJE**Sexes Eligible for Study:**

All

**Ages** ICMJE

50 Years and older (Adult, Older Adult)

**Accepts Healthy Volunteers** ICMJE

No

**Contacts** ICMJE*Contact information is only displayed when the study is recruiting subjects***Listed Location Countries** ICMJE

United States

**Removed Location Countries****Administrative Information****NCT Number** ICMJE

NCT01301443

**Other Study ID Numbers** ICMJE

RS1/001/10

**Has Data Monitoring Committee**

Yes

**U.S. FDA-regulated Product****Studies a U.S. FDA-regulated Device Product:**

No

**IPD Sharing Statement** ICMJE**Plan to Share IPD:**

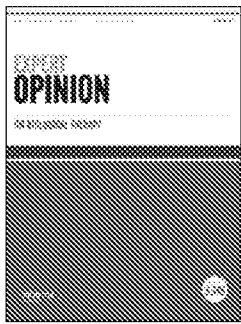
Undecided

**Responsible Party**

Oxford BioMedica
<b>Study Sponsor</b> <small>ICMJE</small>
Oxford BioMedica
<b>Collaborators</b> <small>ICMJE</small>
<i>Not Provided</i>
<b>Investigators</b> <small>ICMJE</small>
<b>Principal Investigator:</b> Peter A Campochiaro, MD Johns Hopkins University Hospital
<b>PRS Account</b>
Oxford BioMedica
<b>Verification Date</b>
April 2017
<small>ICMJE</small> <b>Data element required by the <u>International Committee of Medical Journal Editors</u> and the <u>World Health Organization ICTRP</u></b>



EX. J



## Gene therapy for age-related macular degeneration

Nicholas A. Moore, Peter Bracha, Rehan M. Hussain, Nuria Morral & Thomas A. Ciulla

To cite this article: Nicholas A. Moore, Peter Bracha, Rehan M. Hussain, Nuria Morral & Thomas A. Ciulla (2017) Gene therapy for age-related macular degeneration, *Expert Opinion on Biological Therapy*, 17:10, 1235-1244, DOI: [10.1080/14712598.2017.1356817](https://doi.org/10.1080/14712598.2017.1356817)

To link to this article: <https://doi.org/10.1080/14712598.2017.1356817>



Published online: 20 Jul 2017.



Submit your article to this journal [↗](#)



Article views: 894



View related articles [↗](#)



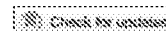
View Crossmark data [↗](#)



Citing articles: 6 View citing articles [↗](#)

---

REVIEW



## Gene therapy for age-related macular degeneration

Nicholas A. Moore<sup>a</sup>, Peter Bracha<sup>a</sup>, Rehan M. Hussain<sup>a</sup>, Nuria Morral<sup>c</sup> and Thomas A. Ciulla<sup>a,b</sup>

<sup>a</sup>Department of Ophthalmology, Indiana University School of Medicine, Indianapolis, IN, USA; <sup>b</sup>Retina Service, Midwest Eye Institute, Indianapolis, IN, USA; <sup>c</sup>Department of Medical and Molecular Genetics, Indiana University School of Medicine, Indianapolis, IN, USA

### ABSTRACT

**Introduction:** In neovascular age related macular degeneration (nAMD), gene therapy to chronically express anti-vascular endothelial growth factor (VEGF) proteins could ameliorate the treatment burden of chronic intravitreal therapy and improve limited visual outcomes associated with 'real world' undertreatment.

**Areas covered:** In this review, the authors assess the evolution of gene therapy for AMD. Adeno-associated virus (AAV) vectors can transduce retinal pigment epithelium; one such early application was a phase I trial of AAV2-delivered pigment epithelium derived factor gene in advanced nAMD. Subsequently, gene therapy for AMD shifted to the investigation of soluble fms-like tyrosine kinase-1 (sFLT-1), an endogenously expressed VEGF inhibitor, binding and neutralizing VEGF-A. After some disappointing results, research has centered on novel vectors, including optimized AAV2, AAV8 and lentivirus, as well as genes encoding other anti-angiogenic proteins, including ranibizumab, aflibercept, angiostatin and endostatin. Also, gene therapy targeting the complement system is being investigated for geographic atrophy due to non-neovascular AMD.

**Expert opinion:** The success of gene therapy for AMD will depend on the selection of the most appropriate therapeutic protein and its level of chronic expression. Future investigations will center on optimizing vector, promoter and delivery methods, and evaluating the risks of the chronic expression of anti-angiogenic or anti-complement proteins.

### ARTICLE HISTORY

Received 2 June 2017  
Accepted 14 July 2017

### KEYWORDS

Adeno-associated virus; age-related macular degeneration; gene therapy; retina; vascular endothelial growth factor

## 1. Introduction

### 1.1. Overview of age-related macular degeneration

Age-related macular degeneration (AMD) is one of the leading causes of blindness worldwide. By the year 2020, an estimated 196 million people will have AMD and 11 million will have significant vision loss [1]. AMD can broadly be categorized into non-neovascular and neovascular (nAMD) forms. Non-neovascular AMD is characterized by the development of drusen and retinal pigment epithelial (RPE) changes early in the disease course, and with loss of RPE and associated severe vision loss in advanced disease (Figure 1). Neovascular AMD is characterized by choroidal neovascularization (CNV) causing central vision loss from macular exudation (Figure 2); subsequently, despite treatment, fibrosis and/or RPE atrophy develop in nearly half of patients by 2 years, resulting in severe permanent central vision loss [2]. Anti-vascular endothelial growth factor (anti-VEGF) therapy is currently the standard of care for nAMD. The original ANCHOR and MARINA trials of monthly ranibizumab, respectively, yielded 11.3 and 7.2 Early Treatment of Diabetic Retinopathy Study (ETDRS) letters of improvement at one year [3,4]. Subsequent longer-term trials and 'real-world' studies revealed a visual acuity decline over the ensuing years, likely due to a combination of undertreatment, incomplete treatment effectiveness, and progression of fibrotic scarring and/or geographic atrophy (GA) [5–10]. These

therapeutic limitations, in addition to the treatment burden of monthly injections, demonstrate the unmet need for more effective therapy.

Genetic therapy has been investigated in inherited retinal diseases such as Leber's congenital amaurosis (LCA), choroideremia, retinitis pigmentosa (RP), Usher's disease, Stargardt's disease, Leber's hereditary optic neuropathy, achromatopsia, and X-linked retinoschisis [11]. The early success of gene therapy in the treatment of LCA has created enthusiasm in translating the therapy to AMD, which has a significantly greater prevalence and societal burden. In particular, one-time gene therapy in AMD to transduce RPE cells has the potential to chronically produce anti-angiogenic and other therapeutic proteins [12].

### 1.2. Introduction to viral vectors

A variety of viral and nonviral gene delivery methods have been developed over the past couple of decades. The viral vectors most extensively used include the adenovirus, adeno-associated virus (AAV), gamma-retrovirus, and lentivirus. The choice of viral vector is specific to each application, and depends on a combination of factors such as tissue tropism, cloning capacity of the vector (which determines the size of the expression cassette that can be accommodated in the genome of the virus), and safety concerns (inflammatory

## Article highlights

- In neovascular age related macular degeneration (nAMD), gene therapy could ameliorate the treatment burden associated with chronic intravitreal therapy and has the potential to improve poor visual outcomes associated with 'real world' anti-vascular endothelial growth factor (anti-VEGF) undertreatment.
- To date, the most common viral vector utilized in retinal genetic therapy is the adeno-associated virus (AAV). The AAV vector has many features making it an excellent vector choice in retinal diseases, including non-integrating nature, low inflammatory potential, low retinal toxicity at appropriate doses, non-pathogenic nature, ability to transduce non-dividing cells, and excellent track record of safety in human trials.
- Vector delivery to the target retinal tissue involves two potential methods: intravitreal injection or pars plana vitrectomy (PPV) followed by subretinal injection.
- In neovascular AMD (nAMD), gene therapy is being assessed to chronically express anti-angiogenic proteins such as pigment epithelium derived factor (PEDF), fms-like tyrosine kinase-1 (sFLT-1), as well as ranibizumab, aflibercept, angiostatin and endostatin.
- In geographic atrophy (GA), gene therapy is being assessed to target the complement system.
- The risks of chronic and extensive inhibition of the VEGF pathway are incompletely known and require further assessment.

This box summarizes key points contained in the article.

responses, and genotoxicity/insertional oncogenesis). Adenovirus vectors, particularly the third-generation or helper-dependent vectors, have a high cloning capacity

(~35 kb), and can transduce a wide range of cell types, including quiescent tissues. The genome of the adenoviral vector largely remains in the nucleus as an episome and rarely integrates. However, use of first-generation vectors has been limited by the activation of inflammatory responses [13,14]. Second-generation vectors are less immunogenic, while helper-dependent adenoviral vectors are by far the safest [15,16]. AAV vectors display, in general, low immunogenicity, making this vector system an attractive tool for gene therapy of many human diseases. Like adenoviral vectors, AAV vectors transduce quiescent tissues, and their genome is mostly maintained as an episome [17]. An added feature is the availability of multiple serotypes, each of them displaying enhanced tropism for a specific set of tissues. For example, AAV2, transduces skeletal muscle, liver, central nervous system (CNS) and retina, while AAV8 transduces liver, retina, CNS, pancreas, and heart [18]. Lentiviral vectors are derived from the human immunodeficiency virus 1 (HIV1) or the equine infectious anemia virus (EIAV) [19], and have a cloning capacity of up to 10 kb [20]. Lentiviral vectors are used in applications requiring vector genome integration into the host genome, and have been extensively used for transduction of hematopoietic stem cells [21]. Lentiviruses have recently become a popular choice because they can transduce quiescent tissues, in addition to dividing cells, and have improved safety features relative to gamma retroviruses, as the vector genome does not preferentially integrate in the proximity of oncogenes [22].

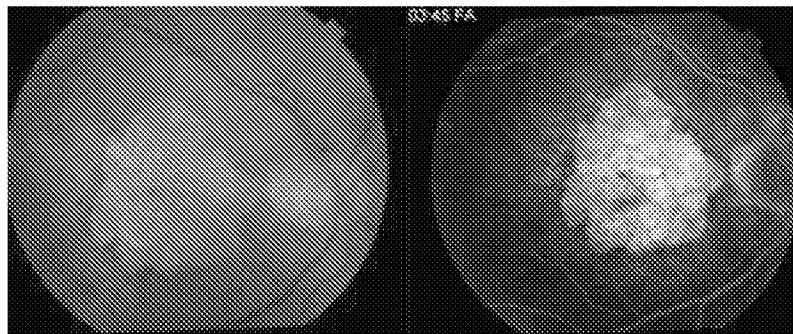


Figure 1. Left: Fundus photo of geographic atrophy in advanced non-exudative age-related macular degeneration. Note the confluent loss of retinal pigment epithelium centrally, which results in the geographic lesion, and causes a central scotoma. Right: The corresponding fluorescein angiogram demonstrates hyperfluorescence of the lesion due to a 'window defect' through the atrophic retina to the underlying choroidal vasculature.

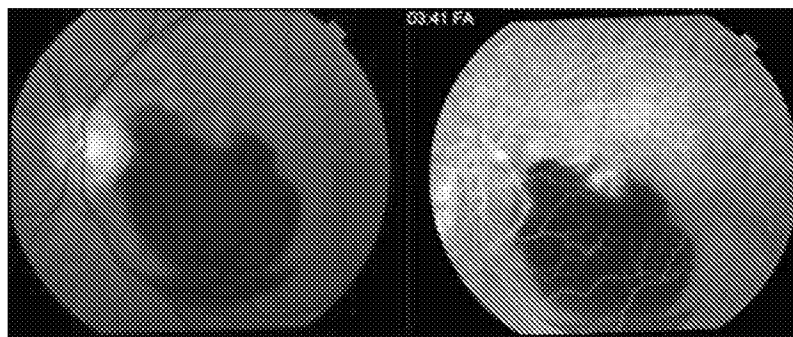


Figure 2. Left: Fundus photo of severe subretinal hemorrhage in neovascular age-related macular degeneration. The subretinal hemorrhage extends from the temporal edge of the optic disc through the central and inferior macula. Such hemorrhages typically lead to central retinal scarring and associated central scotoma. Right: The corresponding fluorescein angiogram demonstrates hypofluorescence of the lesion due to a blockage by the deep subretinal hemorrhage. Note the hyperfluorescent focus in the central macula, which represents leakage by the central portion of the underlying choroidal neovascularization not obscured by the hemorrhage.

Furthermore, nonintegrating lentiviral vectors have recently been developed, which significantly reduce the possibility of genotoxic effects [23].

To date, the most common viral vector utilized in retinal genetic therapy is the adeno-associated virus. The AAV vector has many features making it an excellent vector choice in retinal diseases, including nonintegrating nature, low inflammatory potential, low retinal toxicity at appropriate doses, nonpathogenic nature, ability to transduce nondividing cells, and excellent track record of safety in human trials [24,25]. AAV vectors do have limitations, which include having a restricted transgene capacity (4.5–5.0 kb) and the risk of being rapidly eliminated by the humoral immune response in patients who have previously been exposed to the virus [26]. However, the risk for immunogenicity with AAV vectors is low when targeting relatively immune-privileged tissues such as the retina [27].

### 1.3. Methods of introducing viral vectors to the eye

The eye provides an excellent model for investigating gene therapy for AMD because the ocular relative immune-privilege limits an immune response to the implanted genetic material and the tight blood-ocular barrier limits the systemic dissemination of the introduced genetic material. Additional advantages include ease of accessibility for delivery of the genetic material directly to the target cells of interest, the noninvasive ability to monitor for disease progression and response to therapy, and use of the contralateral eye as an excellent *in vivo* control [28].

Vector delivery to the target retinal tissue has not been standardized. Currently, vector delivery involves two potential methods. The most commonly investigated method involves pars plana vitrectomy (PPV) followed by a retinotomy and injection of the viral vector with genetic material into the subretinal space (Figure 3). This more invasive method creates a temporary retinal detachment, but allows for direct delivery to the cells of interest. The virus then ‘infects’ the RPE cells or photoreceptors, causing the host cells to transcribe and translate the virally transferred genetic material into therapeutic protein. The location and number of retinotomies through which to deliver vector has not been optimized.

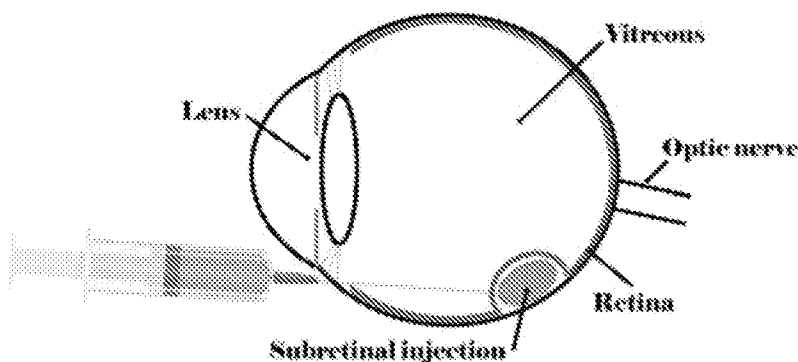


Figure 3. Subretinal injection: This figure demonstrates the location of a subretinal injection of therapeutic viral vectors, a procedure that is performed in an outpatient surgical setting. After pars plana vitrectomy to remove vitreous, a small retinotomy is created and the neurosensory retina is detached to create a small bleb. The vectors are then delivered directly into this atrogenic space, between the photoreceptors and the retinal pigment epithelium. The volume and dose of viral vector, precise retinal location within the eye, and the number of retinotomies through which to deliver has yet to be optimized.

Alternatively, injection of the vector into the vitreous cavity has been attempted, and although this method may be less invasive and potentially have fewer procedure-related complications, the penetration of viral vector to the target tissue is perceived to be inferior to that of subretinal injections (Figure 4) [29,30]. In this review, the pathophysiologic mechanisms contributing to AMD are explored along with the recent gene therapy trials targeting this degenerative process (Table 1).

### 1.4. Genetic therapy for nAMD

nAMD pathogenesis is complex and involves multiple pathways that contribute to pathologic endothelial proliferation, particularly the imbalance of pro-angiogenesis and antiangiogenesis factors. Several well-characterized factors include the overexpression of vascular endothelial growth factor (VEGF), a relative deficiency of pigment epithelium-derived factor (PEDF), and an underexpression of secreted extracellular domain of VEGF receptor 1, soluble fms-like tyrosine kinase-1 (sFLT-1) [31]. Numerous other factors are known to be

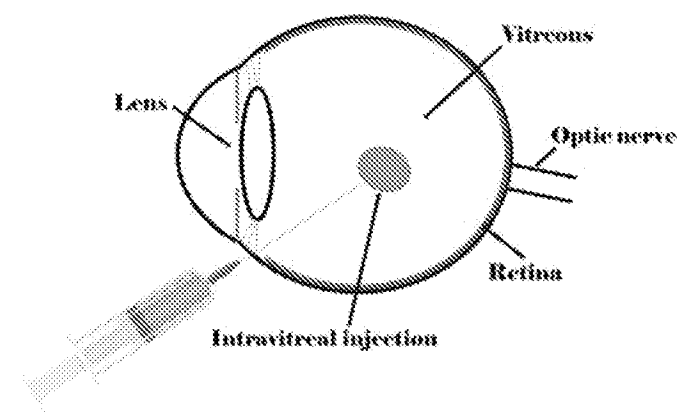


Figure 4. Intravitreal injection: This figure represents the location of an intravitreal injection of therapeutic viral vectors, a brief office-based procedure. Following local anesthesia and application of betadine to reduce the risk of infection, a small-gauge needle is inserted through the pars plana into the vitreous. The vector is injected directly into the vitreous humor and must traverse posteriorly through the vitreous and inner retinal layers in order to transduce the retinal pigment epithelium and photoreceptors.

Table 3. List of ongoing or recently completed human gene therapy trials for age-related macular degeneration.

Therapy and delivery method	Mechanism of gene therapy	Targeted disease	Clinical trials, gov Number	Sponsor	Study phase
Intravitreal AdGVPEDF.11D	PEDF expression with antiangiogenesis	nAMD	NCT00109499	GenVec	Phase I
Subretinal rAAV. sFLT-1	Cellular expression of VEGF binding receptor FLT1	nAMD	NCT01494805	Lions Eye Institute Avalanche Biotechnologies, Inc.	Phase I Phase II
Intravitreal AAV2-sFLT01	Cellular expression of VEGF binding receptor FLT1	nAMD	NCT01024998	Sanofi Genzyme	Phase I
Subretinal AAV-8-based anti-VEGF (RGX-314)	Monoclonal antibody binds VEGF	nAMD	NCT03066258	Regenxbio Inc.	Phase I
Subretinal lentiviral vector expressing endostatin and angiostatin (RetinoStat)	Angiogenesis inhibition	nAMD	NCT01301443 NCT01678872	Oxford BioMedica	Phase I
Intravitreal AAVCAGsCD59	Inhibition of the membrane attack complex (MAC) formation through CD59 expression	Non-Neovascular AMD	NCT03144999	Hemera Biosciences	Phase I

involved in AMD pathogenesis such as antiangiogenic endostatin and angiostatin.

#### 1.4.1. Pigment epithelial-derived growth factor

One of the earliest human applications of intraocular gene therapy for AMD was a phase I trial of AAV-delivered PEDF gene in advanced nAMD, which was published in 2006 (NCT00109499) [32]. PEDF is a naturally occurring antiangiogenic peptide that was proven effective at preventing and regressing neovascularization in murine AMD models prior to human studies [33,34]. Campochiaro et al. evaluated the delivery of a single intravitreal injection of an E1-, partial E3-, E4-deleted adenoviral vector (a second-generation and less cytotoxic and immunogenic vector) expressing human PEDF (AdPEDF.11) in 28 patients with advanced nAMD. There were no serious adverse events related to AdGVPEDF.11, but they did report transient intraocular inflammation in 25% of patients. No conclusion could be made regarding visual outcomes due to a lack of a control group and small sample size; however, patients receiving less than  $10^8$  particle units were reported to have a decrease in visual acuity and increase in the size of the CNV lesion, in contrast to patients receiving  $10^9$  or greater particle units who largely remained stable, suggesting a possible dose-escalation response [32].

#### 1.4.2. Anti-VEGFs

The primary focus of gene therapy in AMD research subsequently shifted to the investigation of sFLT-1, an endogenously expressed VEGF inhibitor that binds to and neutralizes VEGF-A, preventing the normal binding of VEGF with its endothelial receptors [35–37]. Preclinical rodent and primate models demonstrated the proof of mechanism of subretinally administered recombinant AAV (rAAV) with sFLT-1 in preventing CNV formation [38–41]. Authors hypothesized that local vector entry into the RPE cells and photoreceptors enables the uptake and transduction of the viral vectors, with expression of sFLT-1 through the normal protein-producing mechanisms of the host cells.

Avalanche Biotechnologies in collaboration with the Australian Lions Eye Institute (NCT01494805) investigated the safety profile and effectiveness of subretinal injections of rAAV sFLT-1 in human clinical trials. The phase I results were published in 2015, with 3-year outcomes published in 2017

[12,42]. Their techniques included performing PPV followed by the subretinal injection of a low-dose ( $1 \times 10^{10}$  vector genomes (vg)) or high-dose ( $1 \times 10^{11}$  vg) vector at a location adjacent to the vascular arcades, superior and temporal to the fovea and contiguous with disease-associated subretinal fluid. All patients received ranibizumab injections at baseline and week 4, and as needed thereafter according to prespecified criteria for active nAMD based on ETDRS best corrected visual acuity (BCVA), optical coherence tomography (OCT), and fluorescein angiography (FA) findings. At 3-years follow-up, they reported no proliferation of RPE cells, scarring, or chorioretinal atrophy in the area of subretinal injection [12]. Some of the ocular adverse events recorded in the treatment groups included subconjunctival hemorrhage, retinal hemorrhage, and cataract progression, which were expected sequelae from PPV [12]. Due to the small sample size, statistical analysis could not be performed on visual or anatomic outcomes. However, patients with the higher dose of viral vector required fewer intravitreal anti-VEGF injections than the low dose and control groups. The tolerable safety concerns of this phase I trial led to further investigation.

Similar to this prior study, patients in the phase IIa clinical trial were randomized to either subretinal rAAV.sFLT-1 gene therapy ( $n = 21$ ) or to the control group ( $n = 11$ ). Patients in the gene therapy group received subretinal rAAV.sFLT-1 ( $1 \times 10^{11}$  vg) following PPV. All patients received ranibizumab injections at baseline, week 4, and as needed thereafter following the prespecified criteria for subretinal fluid indicative of active nAMD; ophthalmic and systemic endpoints were assessed at 12 months. A press release of preliminary data in June 2015 from Avalanche Biotechnologies reported the high dose rAAV.sFLT-1 group gained a mean change of BCVA of only 2.2 letters, while the control group fared even worse (compared to phase 1 results) by losing 9.3 letters compared with baseline [43]. Additional results were recently published in December of 2016. Similar to the phase 1 results, there were no systemic side effects and no serious ocular adverse events associated with rAAV.sFLT-1 administration. Importantly, there were only two cases (10%) of transient intraocular inflammation as compared to the 25% rate in the aforementioned PEDF study, possibly related to the subretinal versus intravitreal administration of virus vector. Three of the patients treated with rAAV seroconverted following injections, suggesting a

systemic immune response to the viral particles. However, the implications of this finding are not clear, as patients did not experience an ocular inflammatory response or related systemic symptoms. As would be anticipated following PPV, 11 patients developed a cataract in the therapeutic arm [44].

In the rAAV.sFLT-1 group, BCVA improved by a median of 1.0 (interquartile range, IQR: -3.0 to 9.0) ETDRS letter from baseline compared to a median of -5.0 (IQR: -17.5 to 1.0) ETDRS letters change in the control group. This loss in the control group was largely related to 3 of 11 patients who lost in excess of 20 ETDRS letters caused by complications of the natural history of nAMD [44]. When these 3 patients were removed from the analysis, there was no statistically significant difference in BCVA improvement between the gene therapy and the control groups. The median number of ranibizumab retreatments was 2.0 (IQR: 1.0 to 6.0) for the gene therapy group compared to 4.0 (IQR: 3.5 to 4.0) for the control group [44]. The retina and investment communities viewed the trial as a failure, as both the control and treatment groups meaningfully underperformed compared to the 11.3 and 7.2 ETDRS letter improvement in the landmark MARINA and ANCHOR trials.

Based on the disappointing results from this phase IIa trial, the company reorganized; Avalanche Biotechnologies merged with Annapurna Therapeutics to become Adverum Biotechnologies. Their next-generation gene therapy products for AMD, ADVM-022, and ADVM-032, utilize an AAV vector that has been optimized for intravitreal injection of vectors carrying anti-VEGF cDNA, leading to the expression of aflibercept and ranibizumab, respectively. These therapies are in the pre-clinical research phase [45]. According to publicly disclosed corporate materials, both ADVM-022 and ADVM-032 inhibit laser-induced CNV in a primate model at day 28, comparable in extent to intravitreal injections of aflibercept and ranibizumab respectively. ADVM-022 has been selected to advance, with ongoing preclinical studies to assess for anti-VEGF protein expression beyond 20 weeks [46].

Another company, Sanofi Genzyme investigated intravitreal delivery of AAV2-sFLT01 (NCT01024998). The sFLT1 produced by this company is similar to that used in the Avalanche studies, except that it is a fusion protein of the sFLT-1 domain 2 with the Fc domain of IgG1. The chicken- $\beta$ -actin (CBA) promoter, a fusion of the chicken-actin promoter and cytomegalovirus (CMV) immediate-early enhancer, was used, which leads to high levels of expression in Müller and ganglion cells in macaques after intravitreal injection [47]. In a phase 1, dose-escalation trial, 19 patients with advanced nAMD were treated with a single 100- $\mu$ L intravitreal injection of AAV2-sFLT01 according to four dose-ranging cohorts (cohort 1:  $2 \times 10^8$  vg; cohort 2:  $2 \times 10^9$  vg; cohort 3:  $6 \times 10^9$  vg; and cohort 4:  $2 \times 10^{10}$  vg,  $n = 3$  per cohort) and one maximum tolerated dose cohort (cohort 5:  $2 \times 10^{10}$  vg,  $n = 7$ ). The results of this trial were recently published in May 2017 [48]. Two patients who received  $2 \times 10^{10}$  vg experienced adverse events deemed to be related to the study drug. One patient had pyrexia that resolved within 3 h. The second patient developed intraocular inflammation 1 month after injection and was successfully treated over 5 weeks with a topical steroid. There were ten adverse events reported in five patients including retinal

hemorrhage, retinal tear, and one death of a 91-year-old patient 1 year after study completion and 2 years after vector injection; no event was thought to be related to the vector administration. There was no reported systemic detection of the AAV2-sFLT01 vector or immunogenicity to the vector. None of the patients in cohorts 1–3 had detectable concentrations of sFLT01 in aqueous humor (AH), but five of ten patients in cohorts 4 and 5 had concentrations of sFLT01 above the limit of quantification at one or more times during the study period suggesting a dose related effect. At week 52, four of 19 patients (2 from cohorts 1–3 and 2 from cohorts 4/5) showed sustained reductions of central subfield thickness (CST) on OCT. BCVA assessments were difficult to assess in this study due to the variability in baseline fluid and retinal scarring among the participants of each cohort. The authors point out that there may be a relationship between the baseline presence of serum antibodies directed against AAV2 and a reduction in transgene expression. They found that five of ten patients injected with the highest dose of AAV2-sFLT01 had no detectable anti-AAV2 serum antibodies and four of those five patients had detectable sFLT01 in AH after injection. The five patients injected with  $2 \times 10^{10}$  vg who failed to show detectable sFLT01 in AH had detectable baseline anti-AAV2 titers of 0, 1:400, 1:400, 1:3200, and 1:3200. The fact that one patient who received the highest dose and showed no sFLT01 in AH despite undetectable anti-AAV2 antibodies indicates that antibody titers and vector dose cannot be the only factors influencing transgene expression [48,49]. The company has not expressed any plans to continue development of this therapy.

Another company, Regenxbio is developing a novel AAV8 vector, RGX-314, which expresses a soluble anti-VEGF monoclonal antibody fragment in transduced retinal cells. The company suggests that their proprietary gene delivery platform (NAV Technology Platform) may yield higher levels of anti-VEGF expression than earlier generation AAV vectors. According to publicly disclosed corporate materials, maximal expression of therapeutic protein in the anterior chamber of primate eyes treated with RGX-314 measured 4,992 ng/ml, compared to at most 528 ng/ml and 0.217 ng/ml for the Genzyme and Avalanche therapies respectively [38,50,51]. RGX-314 is to be delivered via subretinal injection during vitrectomy and a phase I, open-label dose-escalation trial will commence in 2017 (NCT03066258) [52]. Three doses will be assessed in 18 subjects with previously treated nAMD. The primary end point involves safety assessments at 26 weeks. Secondary end points, assessed at 106 weeks, include change in BCVA, change in central retinal thickness, mean number of rescue anti-VEGF injections, and mean change in the area of CNV and leakage.

#### 1.4.3. Angiostatin and endostatin

Oxford Biomedica is evaluating the efficacy of simultaneous expression of angiostatin and endostatin by subretinal injection of equine infectious anemia lentivirus (EIAV-LV) (RetinoStat, NCT01301443). A bicistronic expression cassette leads to production of both molecules from one lentivirus vector. This approach derives from preclinical work by Lai et al. demonstrating that direct intravitreal injections of either

AAV-endostatin, AAV-angiostatin, or lentiviral vector-angiostatin significantly inhibited a neonatal murine model of proliferative retinopathy [53,54]. The phase I trial enrolled 21 patients with advanced, recalcitrant nAMD and subjects received one of three viral doses subretinally following PPV ( $2.4 \times 10^4$  ( $n = 3$ ),  $2.4 \times 10^5$  ( $n = 3$ ), or  $8.0 \times 10^5$  transduction units (TU;  $n = 15$ )). During the surgery, one patient developed macular hole and two developed retinal tears; all complications were managed intraoperatively without sequelae. There were no adverse effects related to the lentivirus vector. Treated eyes sustained high levels of angiostatin and endostatin expression throughout the study, as determined by direct sampling of the anterior chamber. A reduction in leakage on FA occurred in 71% of patients, but only one patient showed a significant reduction in intraretinal/subretinal fluid compared to baseline [55]. These results were not particularly promising, but eyes with end-stage disease were enrolled in this trial, likely limiting any potential benefit.

### 1.5. Genetic therapy for non-neovascular AMD via complement inhibition

Currently no effective treatment exists for GA, the advanced form of non-neovascular AMD. The pathogenesis of GA is complex and involves numerous etiologies, one of which is the complement pathway. Complement was first implicated in the pathogenesis of AMD in 2005. Complement factor H (CFH) gene was noted to be strongly associated with AMD, with individuals homozygous for the allele possessing a 7.4-fold increased risk [56,57]; several other genetic variants in complement genes have since been associated with AMD [58–60]. C5b, a key terminal component of the complement cascade, is involved in the formation of the membrane attack complex (MAC: C5b-9), which causes cell death through disruption of the cell membrane. In humans, deposition of MAC in Bruch's membrane and choriocapillaris increases significantly with aging and with AMD [61]. When choroidal endothelial cells are exposed to MAC, cell lysis occurs and the surviving cells express VEGF and matrix metalloproteinases; thus, MAC deposition in the choriocapillaris may play a role in atrophic and nAMD [62]. CD59 is a naturally occurring membrane bound inhibitor of MAC formation, and functions by binding the terminal complement protein complex, thereby preventing the incorporation of C9 molecules required to complete the formation of a pore in the cell membrane [63].

Preclinical effectiveness at attenuating murine MAC formation has led Hemera Biosciences to create an AAV2-CD59 (HMR59) gene therapy for the treatment of GA due to non-neovascular AMD in humans [64]. It is to be delivered intravitreally, transducing normal retinal cells to increase the expression of a soluble form of CD59 (sCD59). As of March 2017, a phase I open-label dose-escalation clinical trial (NCT03144999) is enrolling GA patients for a one-time intravitreal injection of HMR59 [65]. Three doses will be assessed in 25 subjects at 26 weeks followed by an additional 18-month safety evaluation. The primary end point involves safety assessments, and secondary end points include change in area of GA, growth of GA, incidence of conversion to nAMD, change in drusen volume, and prevention of loss of  $\geq 15$  ETDRS letters. Another

company targeting the complement cascade is MeiraGTx, who is currently sponsoring preclinical studies and has not elaborated in detail on their efforts [66].

Even if these approaches show promise in treating GA, the ideal timing for intervention would be unknown, as the risks of treatment must be balanced against the benefit of delayed progression, which may be heterogeneous. However, improved efficacy and surgical techniques would favor earlier intervention.

## 2. Future gene therapies for AMD

MeiraGTx has developed a single-administration gene therapy product using antibodies to both VEGFR2 and PDGFR-Beta, and is planning preclinical evaluation of this approach to treat nAMD [66]. Applied Genetic Technologies Corporation (AGTC) has developed a proof-of-concept and is evaluating different genetic targets for the treatment of AMD [67]. Also, Gensight has developed GS030, an optogenetic technology that renders cells responsive to light by using an AAV vector to introduce a DNA sequence that encodes a photosensitive protein belonging to the subfamily of channelrhodopsins, which function as sensory photoreceptors in green algae. Once this protein is expressed, it confers a photoreceptor-like function to the target cell, hence enabling restoration of vision in patients with extremely reduced vision or total blindness due to retinitis pigmentosa (RP). They plan to investigate if GS030 can be used to restore visual perception within the atrophic zone of the central retina in AMD once completed with the ongoing RP clinical trial [68]. Similarly, RetroSense Therapeutics is investigating RST-001, a channelrhodopsin-2 photosensitivity gene, to create new photosensors in retinal cells and restore vision in RP (NCT02556736) with a plan to investigate its utility in advanced dry-AMD [69].

Using a completely different approach, Askou and colleagues have developed an AAV2/8 vector to express short hairpin RNAs (shRNAs) that target the VEGF mRNA by way of RNA interference (RNAi). ShRNAs have similar structure to cellular noncoding small RNAs known as microRNAs (miRNAs), and are processed by the same pathway, generating short-interfering RNAs (siRNAs) [70]. The guide strand binds to its target mRNA, which is then cleaved by the RNA-induced silencing complex [70,71]. Investigators have demonstrated CNV reduction in a mouse model through the introduction of a viral vector encoding shRNAs [72].

Alterations in miRNA expression have been implicated as a contributor of AMD progression. Plasma and vitreous samples have yielded evidence that particular miRNAs are upregulated while others are downregulated in patients with AMD. In addition, variations in miRNAs also exist between individuals with dry and nAMD [73]. Further characterization of these differences in miRNA regulation could lead to new targets in AMD therapeutics research.

## 3. Considerations with chronic VEGF inhibition

With improving techniques and technology in gene therapy, as demonstrated by many of the aforementioned studies, chronic and extensive inhibition of the VEGF pathway may



be possible. However, inhibition of this normally physiologic, but at times pathophysiologic, pathway may have negative effects on multiple levels of the neurosensory retina and RPE. There are seven different members of the VEGF family including VEGF-A, PlGF (placental growth factor), VEGF-B, VEGF-C, VEGF-D, VEGF-E, and snake venom VEGF. VEGF-A is a well-known signal for endothelial cell survival and proliferation, mediating vascular permeability and angiogenesis. The actions of VEGF family members are mediated by the activation of tyrosine kinase receptors [74]. The VEGF receptors have seven immunoglobulin-like loops in their extracellular domain and a kinase insert region in the intracellular domain. VEGF-A acts at VEGF receptors (VEGFR) 1 and 2. VEGFR1 (fms-like tyrosine kinase-1) has both positive and negative angiogenic effects; VEGFR2 (fetal liver kinase-1 and kinase insert domain-containing receptor) is the primary mediator of the mitogenic, angiogenic and vascular permeability effects of VEGF-A [75]. VEGF mediates angiogenesis by promoting endothelial cell migration, proliferation, and survival.

In addition to playing a key role in vascular permeability and angiogenesis, there is growing evidence suggesting that VEGF has neurotrophic and neuroprotective effects on neuronal and glial cells [76]. There are several *in vitro* studies showing that VEGF maintains RPE and choriocapillaris and there are several papers suggest that anti-VEGF therapy could promote RPE atrophy. In one study, VEGF neutralization increased RPE apoptosis *in vitro*. ARPE-19 cells, an immortalized human RPE cell line, cultured on membranes for 4 weeks were treated with the anti-VEGF agent bevacizumab, or an IgG control. Terminal deoxynucleotidyl transferase (TdT) dUTP Nick-End Labeling (TUNEL) assay was used to detect apoptotic cells. The bevacizumab treated cells showed greater apoptosis [77]. Another *in vitro* study employed a mouse model to corroborate a vital supportive role for VEGF in the maintenance of RPE and choriocapillaris. In mice, RPE normally produces the more soluble VEGF isoforms, VEGF<sub>120</sub> and VEGF<sub>164</sub>, but virtually no VEGF<sub>188</sub>, reflecting the fact that molecules secreted by the RPE must diffuse across Bruch's membrane to reach the choriocapillaris. Transgenic mice that produce only VEGF<sub>188</sub> show severe abnormalities of RPE and choroid at 8 months [78]. This suggests that VEGF is necessary for the maintenance of RPE and choriocapillaris, and that withdrawal of VEGF leads to loss of RPE and vacuolization of the choriocapillaris. Clinically, several clinical trials of anti-VEGF therapy in nAMD suggest that anti-VEGF therapy can contribute to RPE loss. Specifically, both CATT & IVAN showed that monthly anti-VEGF therapy increased the risk of RPE atrophy compared to as-needed treatment, and similar results were found in the HARBOR and IVAN *post hoc* analyses [79–81].

As with RPE cells, anti-VEGF therapy has been thought to lead to loss of ganglion cells, which contributes to glaucomatous change. Specifically, VEGF is thought to be neuroprotective through the molecular interaction with VEGFR2, and Neuropilin-1, a non-tyrosine kinase transmembrane molecule [82,83]. Consistent with these findings, VEGF-A has been demonstrated to have a protective effect on retinal ganglion cells in animal models. Nishijima et al. demonstrated that exogenously administered VEGF-A served as an antiapoptotic agent for retinal neurons and that VEGF-A administration

reduced ischemia-induced alterations to the cellular architecture of the ganglion cells and inner plexiform and inner nuclear retinal layers. They also reported a dose-dependent decrease in ganglion neurons after VEGF depletion with anti-VEGF agents. They recognized that anti-VEGF agents may be beneficial at reducing the edema, inflammation, hemorrhage, and neovascularization associated with retinal vascular diseases, but that depressed VEGF-A levels could also reduce ganglion cell survival [84].

With the potential for chronic and extensive VEGF inhibition through gene therapy, clinical trials of this gene therapy for nAMD may observe development or progression of GA as well as glaucomatous optic neuropathy. With this in mind, evolving gene regulation technology may enable small orally administered molecules to regulate a transgene, turning protein production on and off as needed. This, in turn, could theoretically facilitate expression of large amounts of anti-VEGF protein during an initial induction phase followed by a chronic lower level of expression during a maintenance phase, which could improve the long-term safety profile [85–88]. This strategy could also potentially increase expression of a therapeutic protein to treat nAMD exacerbations.

#### 4. Conclusion

With the development of safer and more efficacious viral vectors, improvements in tropism to make vectors more cell-specific, improvements in transgene expression through promoter regulation, and advances in the surgical delivery of genetic treatments to minimize cell loss, the future of gene therapy shows great promise, especially in retinal disease [89,90]. The eye is an optimal organ for gene therapy, given its immune-privileged status that may limit an immune response, as well as ease of accessibility for delivery of the genetic material directly to the target cells of interest. Gene therapy to chronically express therapeutic proteins holds the promise of a one-time therapy in nAMD that could ameliorate treatment burden associated with chronic intravitreal therapy, and potentially improve poor visual outcomes associated with current undertreatment. Gene therapy may also have applications in GA.

#### 5. Expert opinion

Intravitreal anti-VEGF injections have revolutionized the treatment of nAMD. However, patients are required to receive monthly injections, often over years, which places significant burdens on patients, family members, ophthalmology clinics, as well as cost to the healthcare system. Gene therapy to chronically express therapeutic proteins for nAMD holds the promise of a one-time therapy that could ameliorate treatment burden associated with chronic intravitreal therapy, and potentially improve poor visual outcomes associated with current undertreatment. Additionally, no effective treatment exists for advanced GA in non-neovascular AMD, and consequently gene therapy to target the complement system, or other pathophysiologic pathways, holds great potential.

The early success of gene therapy in the treatment of LCA has created enthusiasm in translating the therapy to AMD, which has a significantly greater prevalence and societal burden. Gene therapy for AMD differs from inherited retinal disease, in that the aim so far has been to express antiangiogenic or anti-complement proteins, as opposed to replacing defective or unexpressed proteins. However, AMD pathogenesis is complex and involves the amalgamation of normal aging, pathologic inflammation and excessive oxidative stress among other factors. Replacing a defective gene in a monogenic disorder such as LCA may hold more promise than in a complex disease process such as AMD.

To date, the main target tissue has been the RPE and the main target protein has been sFLT-1 with the goal of inhibiting the VEGF pathway. As reviewed here, early human studies of AAV vectors carrying the sFLT-1 gene inserted subretinally has suggested an acceptable safety profile and consequently, larger studies are currently underway to evaluate the efficacy of this therapy.

The success of gene therapy for the treatment of AMD will depend on the selection of the most appropriate therapeutic protein and its level of chronic expression, although some data suggest that patient heterogeneity may also be important [48]. In the future, the major issues to address include optimizing surgical delivery of vector, the potential risks of chronic expression of antiangiogenic or anti-complement proteins, as well as the unknown long-term tolerability and efficacy of gene therapy in the eye. Specifically, key factors that influence the level of expression include the route of administration (intravitreal vs. subretinal) and the type of virus vector and serotype (which determine the percentage of cells that are transduced), as well as the promoter used to drive expression of the transgene. In order to minimize surgical complications, intravitreal delivery of viral vectors is being evaluated, but this approach has the potential for lower penetration to the target RPE. Subretinal delivery would likely foster greater transduction over intravitreal delivery, but less invasive intravitreal delivery holds the potential for widespread adoption, if effective. Alternative investigational genes and viral vectors are being designed that can potentially overcome some of these problems. For example, lentiviruses have the advantage of being able to carry larger transgene expression cassettes than AAV, which is restricted to approximately 5.0 kb. Also, as mentioned previously, evolving gene regulation technology may enable small molecules to regulate a transgene, turning protein production on and off as needed, which could improve the long-term safety profile. Gene therapy for AMD holds great potential given the improvements in viral vector safety, more specific targeting to cell types/tissues, better candidate genes, and improved surgical approaches for gene delivery.

### Funding

This manuscript has not been funded.

### Declaration of interest

TA Ciulla has an employment relationship with the Ophthotech Corporation. The authors have no other relevant affiliations or financial involvement with any organization or entity with a financial interest in or

financial conflict with the subject matter or materials discussed in the manuscript apart from those disclosed.

### References

Papers of special note have been highlighted as either of interest (\*) or of considerable interest (\*\*\*) to readers.

1. Wong WL, Su X, Li X, et al. Global prevalence of age-related macular degeneration and disease burden projection for 2020 and 2040: a systematic review and meta-analysis. *Lancet Glob Health*. 2014;2(2):106–116.
2. Martin DF, Maguire MG, Fine SL, et al. Ranibizumab and bevacizumab for treatment of neovascular age-related macular degeneration: two-year results. *Ophthalmology*. 2012;119(7):1388–1398.
3. Brown DM, Kaiser PK, Michel M, et al. Ranibizumab versus verteporfin for neovascular age-related macular degeneration. *N Engl J Med*. 2006;355(14):1432–1444.
4. Rosenfeld PJ, Brown DM, Heier JS, et al. Ranibizumab for neovascular age-related macular degeneration. *N Engl J Med*. 2006;355(14):1419–1431.
5. Singer MA, Awh CC, Sadda S, et al. HORIZON: an open-label extension trial of ranibizumab for choroidal neovascularization secondary to age-related macular degeneration. *Ophthalmology*. 2012;119(6):1175–1183.
6. Maguire MG, Martin DF, Ying GS, et al. Five-year outcomes with anti-vascular endothelial growth factor treatment of neovascular age-related macular degeneration: the comparison of age-related macular degeneration treatments trials. *Ophthalmology*. 2016;123(8):1751–1761.
7. Holz FG, Tadayoni R, Beatty S, et al. Multi-country real-life experience of anti-vascular endothelial growth factor therapy for wet age-related macular degeneration. *Br J Ophthalmol*. 2015;99(2):220–226.
8. Kruger Falk M, Kemp H, Sorenson TL. Four-year treatment results of neovascular age-related macular degeneration with ranibizumab and causes for discontinuation of treatment. *Am J Ophthalmol*. 2013;155(1):89–95.
9. Rakic JM, Leys A, Brie H, et al. Real-world variability in ranibizumab treatment and associated clinical, quality of life, and safety outcomes over 24 months in patients with neovascular age-related macular degeneration: the HELIOS study. *Clin Ophthalmol*. 2013;7:1849–1858.
10. Arevalo JF, Lasave AF, Lu L, et al. Intravitreal bevacizumab for choroidal neovascularization in age-related macular degeneration: 5-year results of the pan-American Collaborative Retina Study Group. *Retina*. 2016;36(5):859–867.
11. Sengillo JD, Justus S, Tsai YT, et al. Gene and cell-based therapies for inherited retinal disorders: an update. *Am J Med Genet C Semin Med Genet*. 2016;172(4):349–366.
12. Constable IJ, Lai CM, Magno AL, et al. Gene therapy in neovascular age-related macular degeneration: three year follow-up of a phase 1 randomised dose escalation trial. *Am J Ophthalmol*. 2017;177:150–158.
13. Morral N, O'Neal W, Zhou H, et al. Immune responses to reporter proteins and high viral dose limit duration of expression with adenoviral vectors: comparison of E2a wild type and E2a deleted vectors. *Hum Gene Ther*. 1997;8(10):1275–1286.
14. Gao GP, Tang Y, Wilson JM. Biology of adenovirus vectors with E1 and E4 deletions for liver-directed gene therapy. *J Virol*. 1996;70(12):8934–8943.
15. Morral N, O'Neal W, Rice K, et al. Administration of helper-dependent adenoviral vectors and sequential delivery of different vector serotype for long-term liver-directed gene transfer in baboons. *Proc Natl Acad Sci USA*. 1999;96(22):12816–12821.
16. Morral N, Parks RJ, Zhou H, et al. High doses of a helper-dependent adenoviral vector yield supraphysiological levels of alpha1-antitrypsin with negligible toxicity. *Hum Gene Ther*. 1998;9(18):2709–2716.
17. Kay MA, Nakai H. Looking into the safety of AAV vectors. *Nature*. 2003;424(6946):251.

18. Lisowski L, Tay SS, Alexander IE. Adeno-associated virus serotypes for gene therapeutics. *Curr Opin Pharmacol*. 2015;24:59–67.
19. Everson EM, Trobridge GD. Retroviral vector interactions with hematopoietic cells. *Curr Opin Virol*. 2016;21:41–46.
20. Kumar M, Keller B, Makalou N, et al. Systematic determination of the packaging limit of lentiviral vectors. *Hum Gene Ther*. 2001;12(15):1893–1905.
21. Booth C, Gaspar HB, Thrasher HJ. Treating immunodeficiency through HSC gene therapy. *Trends Mol Med*. 2016;22(4):317–327.
22. Zufferey R, Dull T, Manel RJ, et al. Self-inactivating lentivirus vector for safe and efficient in vivo gene delivery. *J Virol*. 1998;72:9873–9880.
23. Shaw A, Cornetta K. Design and potential of non-integrating lentiviral vectors. *Biomedicines*. 2014;2:14–35.
24. Daya S, Berns KI. Gene therapy using adeno-associated virus vectors. *Clin Microbiol Rev*. 2008;21(4):583–593.
25. Stieger K, Cronin T, Bennett J, et al. Adeno-associated virus mediated gene therapy for retinal degenerative diseases. *Methods Mol Biol*. 2011;807:179–218.
26. Surace EM, Auricchio A. Versatility of AAV vectors for retinal gene transfer. *Vision Res*. 2008;48(3):353–359.
27. Hareendran S, Balakrishnan B, Sen D, et al. Adeno-associated virus (AAV) vectors in gene therapy: immune challenges and strategies to circumvent them. *Rev Med Virol*. 2013;23(6):399–413.
28. Streiflein JW. Ocular immune privilege: therapeutic opportunities from an experiment of nature. *Nat Rev Immunol*. 2003;3(11):879–889.
29. Yu-Wai-Man P. Genetic manipulation for inherited neurodegenerative diseases: myth or reality? *Br J Ophthalmol*. 2016;100(10):1322–1331.
30. Cheng L, Toyoguchi M, Looney DJ, et al. Efficient gene transfer to retinal pigment epithelium cells with long-term expression. *Retina*. 2005;25(2):193–201.
31. Campochiaro PA. Gene transfer for ocular neovascularization and macular edema. *Gene Ther*. 2012;19(2):121–126.
32. Campochiaro PA, Nguyen QD, Shah SM, et al. Adenoviral vector-delivered pigment epithelium-derived factor for neovascular age-related macular degeneration: results of a phase I clinical trial. *Hum Gene Ther*. 2006;17(2):167–176.
- **This is one of the earliest gene therapy clinical trials using PEDF for gene therapy in nAMD**
33. Mori K, Duh E, Gehlbach P, et al. Pigment epithelium-derived factor inhibits retinal and choroidal neovascularization. *J Cell Physiol*. 2001;188(2):253–263.
34. Mori K, Gehlbach P, Ando A, et al. Regression of ocular neovascularization in response to increased expression of pigment epithelium-derived factor. *Invest Ophthalmol Vis Sci*. 2002;43(7):2428–2434.
35. Bouck N. PEDF: anti-angiogenic guardian of ocular function. *Trends Mol Med*. 2002;8(7):330–334.
36. Ohno-Matsui K, Morita I, Tombran-Tink J, et al. Novel mechanism for age-related macular degeneration: an equilibrium shift between the angiogenesis factors VEGF and PEDF. *J Cell Physiol*. 2001;189(3):323–333.
37. Luo L, Uehara H, Zhang X, et al. Photoreceptor avascular privilege is shielded by soluble VEGF receptor-1. *Elife*. 2013;2:e00324.
38. Lai CM, Estcourt MJ, Himbeck RP, et al. Preclinical safety evaluation of subretinal AAV2.sFlt-1 in non-human primates. *Gene Ther*. 2012;19(10):999–1009.
39. Lai CM, Brankov M, Zaknich T, et al. Inhibition of angiogenesis by adenovirus-mediated sFlt-1 expression in a rat model of corneal neovascularization. *Hum Gene Ther*. 2001;12(10):1299–1310.
40. Lai CM, Estcourt MJ, Wikstrom M, et al. rAAV.sFlt-1 gene therapy achieves lasting reversal of retinal neovascularization in the absence of a strong immune response to the viral vector. *Invest Ophthalmol Vis Sci*. 2009;50(9):4279–4287.
41. Lai YK, Sharma S, Lai CM, et al. Virus-mediated secretion gene therapy—a potential treatment for ocular neovascularization. *Adv Exp Med Biol*. 2003;533:447–453.
42. Rakoczy EP, Lai CM, Magno AL, et al. Gene therapy with recombinant adeno-associated vectors for neovascular age-related macular degeneration: 1 year follow-up of a phase I randomised clinical trial. *Lancet*. 2015;386(10011):2395–2403.
43. Avalanche biotechnologies, inc. Announces positive top-line phase 2a results for ava-101 in wet age-related macular degeneration. Available at: <http://investors.adverum.com/news-releases/news-release-details/avalanche-biotechnologies-inc-announces-positive-top-line-phase>. [Last accessed 14 July 2017].
44. Constable IJ, Pierce CM, Lai CM, et al. Phase 2a randomized clinical trial: safety and post hoc analysis of subretinal rAAV.sFLT-1 for wet age-related macular degeneration. *EBioMedicine*. 2016;14:168–175.
- **This article reveals the results from a trial investigating sub-retinal rAAV.sFLT1 treatments for nAMD**
45. Avalanche biotechnologies (aavl) will not initiate phase 2b ava-101 trial in second half of 2015. Available at: [https://www.streetinsider.com/Corporate+News/Avalanche+Biotechnologies+\(AAVL\)+Will+Not+initiate+Phase+2b+AVA-101+Trial+in+Second+Half+of+2015/10813292.html](https://www.streetinsider.com/Corporate+News/Avalanche+Biotechnologies+(AAVL)+Will+Not+initiate+Phase+2b+AVA-101+Trial+in+Second+Half+of+2015/10813292.html). [Last accessed 14 July 2017].
46. Avalanche biotechnologies, inc. Corporate Presentation. May 2017. Available at: <http://adverum.com/science/>. [Last accessed 14 July 2017].
47. Yin L, Greenberg K, Hunter JJ, et al. Intravitreal injection of AAV2 transduces macaque inner retina. *Invest Ophthalmol Vis Sci*. 2011;52(5):2775–2783.
48. Heier JS, Kherani S, Desai S, et al. Intravitreal injection of AAV2-sFLT01 in patients with advanced neovascular age-related macular degeneration: a phase 1, open-label trial. *Lancet*. 2017. [Epub ahead of print]. DOI:10.1016/S0140-6736(17)30979-0.
- **This article highlights the results from AAV2-sFLT01 gene therapy in the treatment of nAMD using an intravitreal approach**
49. Scaria AL, LaHalpère A, Purvis A, et al. Preliminary results of a phase 1, open-label, safety and tolerability study of a single intravitreal injection of AAV2-sFLT01 in patients with neovascular age-related macular degeneration. *Mol Ther*. 2016;24(Supplement 1):S98.
50. Regenxbio, Corporate Presentation. May 2017. Available at: <http://ir.regenxbio.com/phoenix.zhtml?c=254175&p=irol-IRHome>. [Last accessed 14 July 2017].
51. MacLachlan TK, Lukason M, Collins M, et al. Preclinical safety evaluation of AAV2-sFLT01—a gene therapy for age-related macular degeneration. *Mol Ther*. 2011;19(2):326–334.
52. Regenxbio programs. Available at: <http://www.regenxbio.com/pages/programs/index.htm?panel=5>. [Last accessed 14 July 2017].
53. Lai LJ, Xiao X, Wu JH. Inhibition of corneal neovascularization with endostatin delivered by adeno-associated viral (AAV) vector in a mouse corneal injury model. *J Biomed Sci*. 2007;14(3):313–322.
54. Igarashi T, Miyake K, Kato K. Lentivirus-mediated expression of angiostatin efficiently inhibits neovascularization in a murine proliferative retinopathy model. *Gene Ther*. 2003;10(3):219–226.
55. Campochiaro PA, Lauer AK, Sohn EH, et al. Lentiviral vector gene transfer of endostatin/angiostatin for macular degeneration (GEM) study. *Hum Gene Ther*. 2017;28(1):99–111.
56. Klein RJ, Zeiss C, Chew EY, et al. Complement factor H polymorphism in age-related macular degeneration. *Science*. 2005;308(5720):385–389.
57. Haines JL, Hauser MA, Schmidt S, et al. Complement factor H variant increases the risk of age-related macular degeneration. *Science*. 2005;308(5720):419–421.
58. Ambati J, Atkinson JP, Galfand BD. Immunology of age-related macular degeneration. *Nat Rev Immunol*. 2013;13(6):438–451.
59. Khandhadia S, Cipriani V, Yates JR, et al. Age-related macular degeneration and the complement system. *Immunobiology*. 2012;217(2):127–146.
60. van Lookeren Campagne M, LeCouter J, Yaspan BL, et al. Mechanisms of age-related macular degeneration and therapeutic opportunities. *J Pathol*. 2014;232(2):151–164.
61. Mullins RF, Schoo DP, Sohn EH, et al. The membrane attack complex in aging human choriocapillaris: relationship to macular degeneration and choroidal thinning. *Am J Pathol*. 2014;184(11):3142–3153.
62. Benzaquen LR, Nicholson-Weller A, Halperin JA. Terminal complement proteins C5b-9 release basic fibroblast growth factor and platelet-derived growth factor from endothelial cells. *J Exp Med*. 1994;179(3):985–992.

63. Rollins SA, Sims PJ. The complement-inhibitory activity of CD59 resides in its capacity to block incorporation of C9 into membrane C5b-9. *Immunol.* 1990;144:3478–3483.
64. Cashman SM, Ramo K, Kumar-Singh R. A non membrane-targeted human soluble CD59 attenuates choroidal neovascularization in a model of age related macular degeneration. *PLoS One.* 2011;6(4):e19078.
65. Hemera Biosciences. Available at: <http://www.hemerabiosciences.com/>. [Last accessed 14 July 2017]
- **This website highlights Hemera Biosciences involvement in an active clinical trial targeting the complement system in the treatment of non-exudative AMD**
66. MeiraGTx. Available at: <http://meiragtx.com/pipeline/>. [Last accessed 14 July 2017]
67. Applied Genetic Technologies Corporation (AGTC). Available at: <https://www.agtc.com/products/macular-degeneration>. [Last accessed 14 July 2017]
68. Geographic Atrophy in Dry-AMD. Gensight. Available at: <http://www.gensight-biologics.com/index.php?page=amd> [Last accessed 14 July 2017].
- **This website describes future targets for gene therapy utilizing optogenetics in the treatment of geographic atrophy**
69. RetroSense Therapeutics. RST-001. 2017. Available at: <http://retrosense.com/development.html#rst>. [Last accessed 14 July 2017].
70. Hutvagner G, Zamore PD. A microRNA in a multiple-turnover RNAi enzyme complex. *Science.* 2002;297:2056–2060.
71. Ruiz R, Witting SR, Saxena R, et al. Robust hepatic gene silencing for functional studies using helper-dependent adenoviral vectors. *Hum Gene Ther.* 2009;20(1):87–94.
72. Askou AL, Pournaras JA, Pihlmann M, et al. Reduction of choroidal neovascularization in mice by adeno-associated virus-delivered anti-vascular endothelial growth factor shorthairpin RNA. *J Gene Med.* 2012;14:632–641.
73. Menard C, Rezende FA, Miloudi K, et al. MicroRNA signatures in vitreous humour and plasma of patients with exudative AMD. *Oncotarget.* 2016;7:19171–19184.
74. Takahashi H, Shibuya M. The vascular endothelial growth factor (VEGF)/VEGF receptor system and its role under physiological and pathological conditions. *Clinical Science.* 2005;109(3):227–241.
75. Ferrara N, Gerber HP, Lecouter J. The biology of VEGF and its receptors. *Nat Med.* 2003;9(6):669–676.
76. Zachary I. Neuroprotective role of vascular endothelial growth factor: signalling mechanisms, biological function, and therapeutic potential. *Neuro-Signals.* 2005;14(5):207–221.
77. Ford KM, Saint-Geniez M, Walshe T, et al. Expression and role of VEGF in the adult retinal pigment epithelium. *Invest Ophthalmol Vis Sci.* 2011;52(13):9478–9487.
78. Saint-Geniez M, Kurihara T, Sekiyama E, et al. An essential role for RPE-derived soluble VEGF in the maintenance of the choriocapillaris. *Proc Natl Acad Sci USA.* 2009;106(44):18751–18756.
79. Grunwald JE, Daniel E, Huang J, et al. Risk of geographic atrophy in the comparison of age-related macular degeneration treatments trials. *Ophthalmology.* 2014;121(1):150–161.
80. Ho AC, Busbee BJ, Regillo CD, et al. Twenty-four-month efficacy and safety of 0.5 mg or 2.0 mg ranibizumab in patients with subfoveal neovascular age-related macular degeneration. *Ophthalmology.* 2014;121(11):2181–2192.
81. Chakravarthy U, Harding SP, Rogers CA, et al. Alternative treatments to inhibit VEGF in age-related choroidal neovascularisation: 2-year findings of the IVAN randomised controlled trial. *Lancet.* 2013;382(9900):1258–1267.
82. Zachary I, Gliki G. Signaling transduction mechanisms mediating biological actions of the vascular endothelial growth factor family. *Cardiovasc Res.* 2001;49(3):568–581.
83. Neufeld G, Cohen T, Shraga N, et al. The neuropilins: multifunctional semaphorin and VEGF receptors that modulate axon guidance and angiogenesis. *Trends Cardiovasc Med.* 2002;12(1):13–19.
84. Nishijima K, Ng YS, Zhong L, et al. Vascular endothelial growth factor-A is a survival factor for retinal neurons and a critical neuro-protectant during the adaptive response to ischemic injury. *Am J Pathol.* 2007;171:53–67.
85. Sochor MA, Vasireddy V, Drivas TG, et al. An autogenously regulated expression system for gene therapeutic ocular applications. *Sci Rep.* 2015;5:17105.
86. Le Guiner C, Stieger K, Toromanoff A, et al. Transgene regulation using the tetracycline-inducible TetR-KRAB system after AAV-mediated gene transfer in rodents and nonhuman primates. *PLoS One.* 2014;9(9):e102538.
87. Stieger K, Le Meur G, Lasne F, et al. Long-term doxycycline-regulated transgene expression in the retina of nonhuman primates following subretinal injection of recombinant AAV vectors. *Mol Ther.* 2006;13(5):967–975.
- **This article describes future targets for gene therapy using a transgene to help regulate the long-term gene expression**
88. O'Callaghan J, Crosbie DE, Cassidy PS, et al. Therapeutic potential of AAV-mediated MMP-3 secretion from corneal endothelium in treating glaucoma. *Hum Mol Genet.* 2017;26(7):1230–1246.
89. Gao G, Vandenbergh LH, Wilson JM. New recombinant serotypes of AAV vectors. *Curr Gene Ther.* 2005;5(3):285–297.
90. Mitchell AM, Nicolson SC, Warischaik JK, et al. AAV's anatomy: roadmap for optimizing vectors for translational success. *Curr Gene Ther.* 2010;10(5):319–340.

EX. K



ORIGINAL ARTICLE

# Novel anti-VEGF chimeric molecules delivered by AAV vectors for inhibition of retinal neovascularization

P Pechan<sup>1</sup>, H Rubin<sup>1</sup>, M Lukason<sup>1</sup>, J Ardinger<sup>1</sup>, E DuFresne<sup>1</sup>, WW Hauswirth<sup>2</sup>, SC Wadsworth<sup>1</sup> and A Scaria<sup>1</sup>

<sup>1</sup>Department of Molecular Biology, Genzyme Corporation, Framingham, MA, USA and <sup>2</sup>Department of Ophthalmology, University of Florida, Gainesville, FL, USA

Vascular endothelial growth factor (VEGF) is important in pathological neovascularization, which is a key component of diseases such as the wet form of age-related macular degeneration, proliferative diabetic retinopathy and cancer. One of the most potent naturally occurring VEGF binders is VEGF receptor Flt-1. We have generated two novel chimeric VEGF-binding molecules, sFLT01 and sFLT02, which consist of the second immunoglobulin (IgG)-like domain of Flt-1 fused either to a human IgG1 Fc or solely to the CH3 domain of IgG1 Fc through a polyglycine linker 9Gly. *In vitro* analysis showed that these novel molecules are high-affinity VEGF binders. We

have demonstrated that adeno-associated virus serotype 2 (AAV2)-mediated intravitreal gene delivery of sFLT01 efficiently inhibits angiogenesis in the mouse oxygen-induced retinopathy model. There were no histological observations of toxicity upon persistent ocular expression of sFLT01 for up to 12 months following intravitreal AAV2-based delivery in the rodent eye. Our data suggest that AAV2-mediated intravitreal gene delivery of our novel molecules may be a safe and effective treatment for retinal neovascularization.

Gene Therapy (2009) 16, 10–16; doi:10.1038/gt.2008.115; published online 17 July 2008

**Keywords:** VEGF; VEGFR1; Flt-1; Fc fragment; retinal neovascularization; adeno-associated virus 2

## Introduction

Vascular endothelial growth factor (VEGF) is not only an important regulator of physiological angiogenesis but also involved in pathological neovascularization.<sup>1</sup> Formation of new blood vessels caused by the overproduction of growth factors such as VEGF is a key component of diseases such as wet age-related macular degeneration (AMD), proliferative diabetic retinopathy (PDR) and tumor growth.<sup>2–4</sup> Blocking of VEGF with antibodies, soluble VEGF receptors (sVEGFR) or inhibition of VEGF receptor (VEGFR) tyrosine kinase activity are useful strategies that have shown promising preclinical and clinical results.<sup>4–6</sup> Ranibizumab, an anti-VEGF drug given intravitreally to wet-AMD patients results in substantially improved visual acuity.<sup>7</sup> Intraocular gene delivery of VEGF antagonists could have theoretical advantages over the current treatment, which requires monthly intravitreal injections (for years) by a retinal specialist.

The angiogenic effect of VEGF is mediated predominantly by its binding to VEGFR KDR.<sup>8</sup> Another high-affinity VEGFR, Flt-1, binds VEGF about 10 times stronger than KDR, however Flt-1 activation does not significantly stimulate angiogenesis.<sup>9,10</sup> Both receptors,

Flt-1 and KDR, have similar structure with extracellular regions consisting of seven domains, 1–7.<sup>10,11</sup> There exists another naturally occurring soluble form of Flt-1 (sFlt-1) that contains only the extracellular domains and has the same VEGF-binding affinity as full-length Flt-1.<sup>11,12</sup> The VEGF-binding function of Flt-1 has been mapped to the second domain.<sup>13–16</sup> There have been previous studies with two truncated soluble receptor hybrids, Flt(1–3)-IgG and Flt(1–7)-IgG, consisting of either the first three domains or all seven domains fused to human IgG1-Fc region.<sup>13</sup> The molecule Flt(1–3)-IgG was reported to have the same VEGF-binding affinity as Flt(1–7)-IgG, however Flt(2)-IgG that contains only second domain was not capable of inhibiting VEGF.<sup>15,17</sup> Another molecule called VEGF-Trap, generated by the second domain of Flt-1 fused to the third domain of KDR and human IgG1-Fc region, has been shown to be a very potent VEGF binder.<sup>18</sup>

Adeno-associated virus (AAV) vectors offer an attractive tool for intraocular gene delivery because of their nonpathogenic nature, low toxicity, minimal immunogenicity and long-term persistence.<sup>19–22</sup> Intravitreal administration of AAV serotype 2 (AAV2) vector in mice results mostly in transduction of ganglion cells and few cells in the inner nuclear layer.<sup>21</sup> Subretinal delivery of AAV2 vector encoding full-length sFlt-1 (transduction of photoreceptors and retinal pigmented epithelium) prevented development of laser-induced choroidal neovascularization in all treated monkeys.<sup>22</sup>

In this study we have designed and constructed small novel soluble hybrid molecules that have strong anti-VEGF activity *in vitro*, incorporated these molecules

Correspondence: Dr A Scaria, Department of Molecular Biology, Genzyme Corporation, 49 New York Avenue, Room 4615, Framingham, MA 01701, USA.

E-mail: abraham.scaria@genzyme.com

Received 7 February 2008; revised 27 May 2008; accepted 3 June 2008; published online 17 July 2008

into AAV2 vectors and then tested *in vivo* persistence of expression and efficacy and safety following intravitreal delivery of these AAV2-based vectors in the oxygen-induced retinopathy of prematurity (OIR) mouse model.

## Results

### sFLT01 molecule inhibits VEGF-mediated cell proliferation

We first constructed molecules D1-3, sFLT01 and D2-Fc (Figure 1a). The molecule D1-3 has served a positive control for VEGF binding and contains first three Flt-1 domains. The second molecule, sFLT01, contains only one Flt-1 domain 2 linked by 9Gly to the human IgG1 heavy-chain Fc region that resulted in the generation of a forced homodimer. The formation of sFLT01 dimers was confirmed by western blot analysis (Figure 2b). The third molecule, D2-Fc, is identical to sFLT01, except it does not contain 9Gly linker. Plasmids encoding these molecules under control of a cytomegalovirus (CMV) promoter were used for transfection of 293 cells and the conditioned media (CM) were evaluated for their ability to block VEGF-stimulated human umbilical vein endothelial cells (HUVECs) proliferation (Figure 1b). The molecule D2-Fc was not able to neutralize VEGF and inhibit HUVECs proliferation whereas sFLT01 demonstrated an efficient inhibition of VEGF-dependent HUVECs proliferation (Figure 1b).

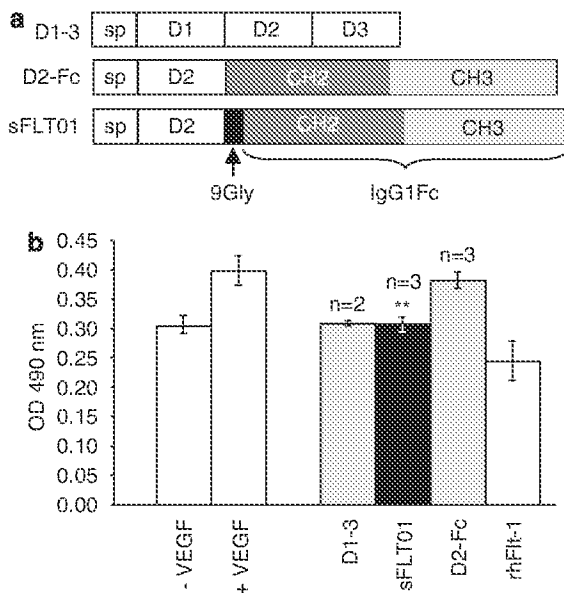


**Figure 1** Generation of novel soluble vascular endothelial growth factor (VEGF) receptor hybrid molecules. (a) Schematics of molecules D1-3, D2-Fc and sFLT01. The white blocks indicate signal peptides (sp) and Flt-1 domains (D1, D2, D3); black block represents 9Gly linker; grey blocks represent domains CH2 of human IgG1-Fc region. (b) Inhibitory effect of conditioned media containing molecules D1-3, D2-Fc and sFLT01 on VEGF-induced human umbilical vein endothelial cells (HUVECs) proliferation. Recombinant full-size rhFlt-1 protein (50 ng ml<sup>-1</sup>) was used as a positive control. The same lot of HUVECs was used in this set of assays. Data are expressed as mean ± s.d. where 'n' represents the number of independent proliferation experiments (for sFLT01 and D2-Fc, n=3; for D1-3, n=2). Student's non-paired *t*-test; \*\**P*<0.005 for difference between '+VEGF control' and 'VEGF binder'; D1-3 (n=2) was not included in statistics.

### IgG1 CH3 domain and peptide linker are important in VEGF binding

Using the sFLT01 as a parental molecule, we generated several mutant derivatives with various deletions along the IgG1-Fc region. When comparing several constructs with various deletions either in CH2 or in CH3 domains of IgG1, we have observed that the CH3 domain is involved in preserving the VEGF-binding function (data not shown). The molecule sFLT02, where the second domain of Flt-1 was linked to the IgG1 CH3 domain through 9Gly (Figures 2a and b), retained the VEGF-binding function (Figure 2c). This set of proliferation assays was performed using a different lot of HUVECs (not the same lot as used in Figure 1b) and it demonstrates that sFLT01 has comparable VEGF block-

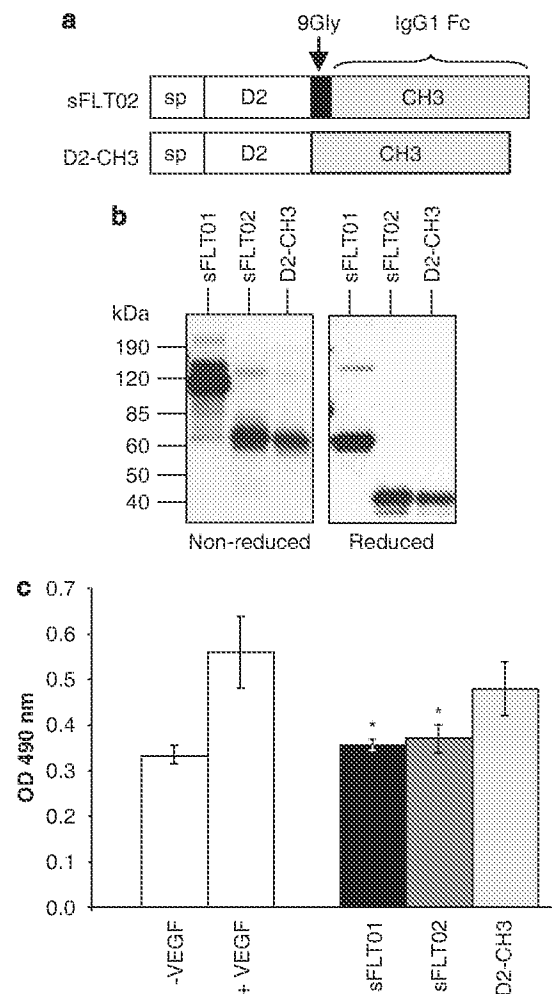


**Figure 2** Novel hybrid receptor molecules containing the human IgG1 CH3 domain. (a) Schematics of molecules sFLT02 and D2-CH3 as compared to sFLT01. The white blocks indicate signal peptides (sp) and Flt-1 domain 2 (D2); black block represents 9Gly linker; shaded blocks represent domain CH3 of human IgG1-Fc region. (b) Western Blot comparing migration of sFLT01, sFLT02 and D2-CH3 (c) Inhibitory effect of molecules sFLT01 and sFLT02 on human umbilical vein endothelial cells (HUVECs) proliferation. A different lot of HUVECs was used for this set of proliferation assays. Data are expressed as mean ± s.d. of three independent proliferation experiments (n=3). Student's non-paired *t*-test; \**P*<0.05 for difference between '+VEGF control' and 'VEGF binder'.

ing potency as in the first set of proliferation assays. The molecule sFLT02 was similar to the parental molecule sFLT01 in neutralizing VEGF (Figure 2c). On the other hand, the molecule D2-CH3 (Figures 2a and b) without 9Gly linker appeared to be a very weak inhibitor of VEGF-induced HUVECs proliferation (Figure 2c), even though VEGFR1 (Flt-1) enzyme-linked immunosorbent assay (ELISA) assay of CM from transfected 293 cells showed high concentrations of D2-CH3 protein ( $\sim 150 \text{ ng ml}^{-1}$ ) compared to sFLT02 ( $70\text{--}90 \text{ ng ml}^{-1}$ ). Hence we conclude that the presence of both the CH3 domain and the peptide linker facilitates VEGF binding. Western blot analyses of sFLT02 and D2-CH3 (Figure 2b) show a prevalence of the dimeric forms for both proteins under nonreducing conditions ruling out the possibility that the lack of efficacy of D2-CH3 is due to its inability to dimerize.

For the next construct we used another type of linker, the 15-mer  $(\text{Gly}_4\text{Ser})_3$ .<sup>23</sup> D2- $(\text{Gly}_4\text{Ser})_3$ -Fc protein was generated and it contained Flt-1 domain 2,  $(\text{Gly}_4\text{Ser})_3$  linker and the IgG1 Fc. The molecule D2- $(\text{Gly}_4\text{Ser})_3$ -Fc was further characterized in HUVECs proliferation assay. Biological activity of D2- $(\text{Gly}_4\text{Ser})_3$ -Fc as measured by inhibition of HUVEC proliferation was similar to that of sFLT01 (data not shown).

#### sFLT01 binds VEGF better than the other novel constructs

The relative binding affinity between VEGF and our novel molecules was determined using a cell-free assay system. CM containing known concentrations of sVEGFR (ranging from 0.29 to 150 pM) were serially diluted and mixed with VEGF (10 pM final concentration). The amount of unbound VEGF was then measured by a human VEGF-specific ELISA. sFLT01 binds VEGF with higher affinity than D1-3, sFLT02 and D2-CH3, where the latter showed a minimal VEGF-binding affinity (Figure 3). These data are in agreement with our HUVECs proliferation assays shown in Figures 1 and 2.

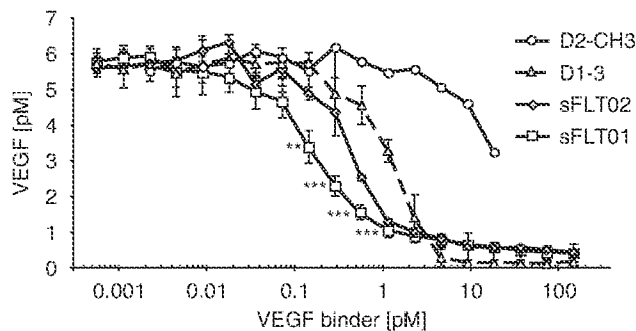


**Figure 3** Vascular endothelial growth factor (VEGF)-binding affinities of VEGF soluble receptors. Conditioned media from independent transfections of 293 cells were used in this cell-free binding assay. Increasing concentrations of soluble VEGF receptors molecules (x axis) were incubated overnight with 10 pM of human VEGF165. The amount of unbound VEGF (y axis) was measured by a human VEGF-specific enzyme-linked immunosorbent assay (ELISA) in triplicate. The number of independent transfections (*n*) for each molecule are: sFLT01 (*n* = 5), D1-3 (*n* = 3), sFLT02 (*n* = 2) and D2-CH3 (*n* = 1). Data are expressed as mean  $\pm$  s.d.; Student's non-paired *t*-test; \*\*\**P* < 0.0001, \*\**P* < 0.001 for differences between sFLT01 and D1-3. LOQ, limit of quantitation = 0.371 pM.

#### AAV2.sFLT01 transgene and mRNA localization

AAV2-based vectors were constructed encoding sFLT01 and adult C57BL/6 mice were intravitreally injected with  $2.2 \times 10^9$  drps (DNase resistant particles) of AAV2.sFLT01. The animals were killed 28 days following injection and the eyes were processed for histological sectioning. The presence of sFLT01 protein and mRNA was confirmed by immunofluorescence and by *in situ* hybridization. sFLT01 protein was predominantly observed in the retinal ganglion cells of mouse retinas (Figure 4a). Infrequently, cells deeper in the retina (presumably Müller cells) were also shown to contain the sFLT01 protein. Another set of retinas was examined using *in situ* hybridization to detect the mRNA of the sFLT01 transgene. The retinal ganglion cells were the predominant cell type transduced in the mouse retina (Figure 4c). No sFLT01 protein was detected in the uninjected control eyes. No sFLT01 mRNA message was detected in the AAV2.sFLT01 injected eyes when sense probe was used.

#### Longevity of transgene expression

Adult C57BL/6 mice were intravitreally injected with  $1 \times 10^9$  drps of AAV2.sFLT01. Animals were killed at predetermined time points and the level of sFLT01 was measured in individual eyes (homogenates of retina and vitreous humor) by ELISA against human Flt-1. The samples from each time point were assayed separately for animals treated with AAV2.sFLT01 (Figure 5). The data suggest that AAV2-mediated delivery of sFLT01 results in long-term stable protein expression in the murine eye with no transgene-related toxicities observed. The apparent rise in sFLT01 in the 12-month AAV2.sFLT01 cohort was due to a change in the tissue homogenization protocol.

#### AAV2.sFLT01 intravitreal delivery inhibits angiogenesis in OIR model

The efficacy of AAV2.sFLT01 was examined *in vivo* using OIR mouse model.<sup>24</sup> AAV2.sFLT01 was intravitreally administered into left eyes of neonatal C57BL/6 mice in a dose of  $1 \times 10^9$  drps per animal. Data shown in Figure 6 were expressed as percentage of neovascularization of untreated eyes in the AAV2.sFLT01 group (*n* = 43), or between left and right eyes in the control group (*n* = 26). The occurrence of neovascularization was significantly reduced to  $54 \pm 47\%$  in AAV2.sFLT01-treated eyes (AAV1.sFLT01 group) as compared to  $102 \pm 66\%$  between left and right eyes in the control group (mean  $\pm$  s.d.). Treatment with AAV2.sFLT01 significantly reduced ocular neovascularization (Student's *t*-test; *P* < 0.0009) compared to the untreated contralateral eyes.

## Discussion

Many reports from preclinical and clinical studies demonstrate that antagonizing VEGF is a potentially useful strategy for treatment of pathological neovascularization which is a key component of ocular diseases like wet-AMD or PDR. In this study, we have developed several novel hybrid molecules that inhibit VEGF *in vitro* and are capable of inhibiting ocular neovascularization *in vivo*. It has been reported that domain 2 of VEGFR Flt-1 requires the presence of flanking sequences from



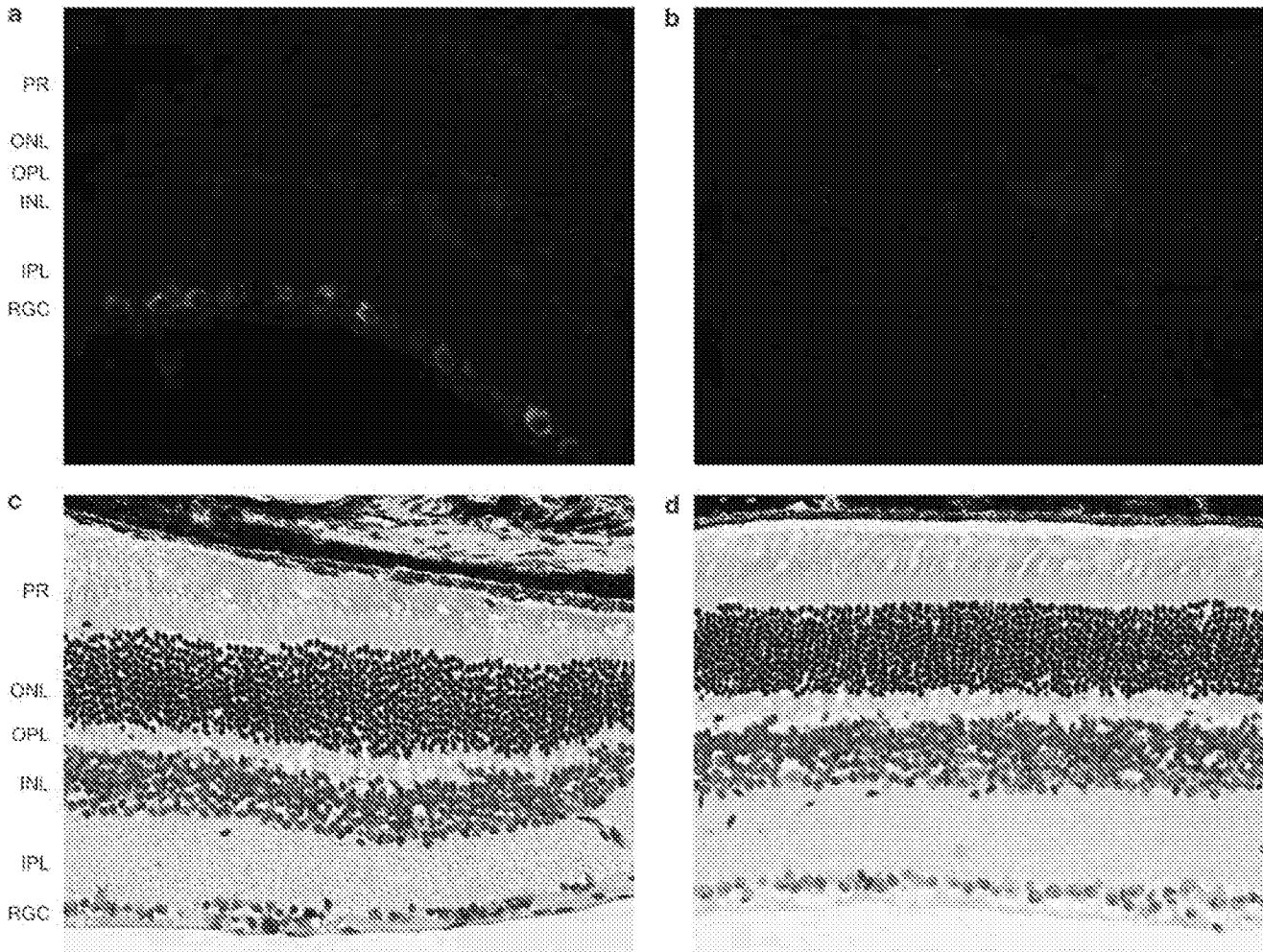


**Figure 4** Detection of sFLT01 protein and mRNA in the retina. sFLT01 was detected in retina 28 day after intravitreal injection with  $2.2 \times 10^9$  drps of AAV2.sFLT01 as (a) a protein by immunofluorescence or (c) as mRNA by *in situ* hybridization. Control in (b) represents the uninjected control eyes. Control in (d) represents the AAV2.sFLT01 injected eyes hybridized with sense probe. RGC: retinal ganglion cells; IPL, OPL: inner and outer plexiform layers; INL, ONL: inner and outer nuclear layers; PR: photoreceptors.

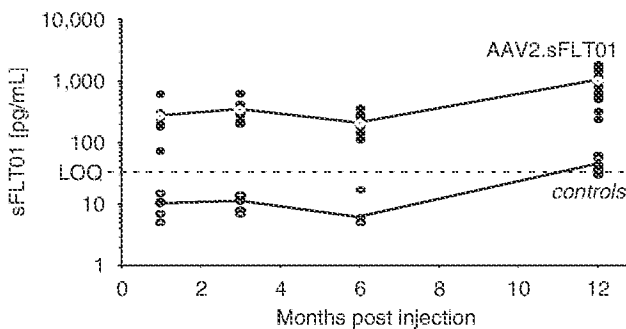


**Figure 5** Longevity of sFLT01 expression. Persistent transgene expression in excess of 1 year was observed in adult C57BL/6 mice treated with a single intravitreal injection of AAV2.sFLT01 ( $1 \times 10^9$  drps). The amount of sFLT01 was quantified in individual retinal homogenates by enzyme-linked immunosorbent assay (ELISA) against human Flt-1. LOQ, limit of quantitation.

Flt-1 or other VEGFR domains for efficient ligand binding and neutralization.<sup>12,17</sup> Our results show that domains other than second domain of Flt-1 were not necessary to preserve VEGFR/ligand binding. To obtain

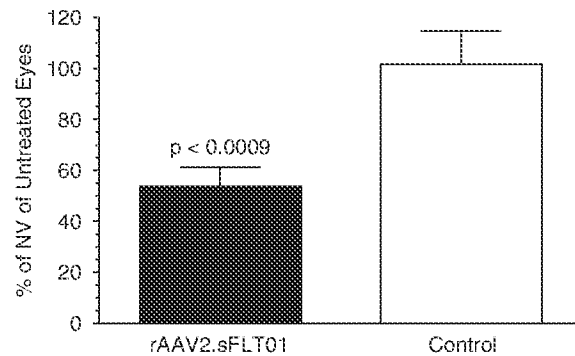


**Figure 6** Adeno-associated virus (AAV)-mediated delivery of sFLT01 inhibits retinal neovascularization in the murine oxygen-induced retinopathy (OIR) model. The eyes of newborn mice were treated with a single intravitreal injection of  $1.1 \times 10^9$  drps of AAV2.sFLT01 vector into the left eye. The number of endothelial cell nuclei internal to the inner limiting membrane in the treated (left) eye was compared to the contralateral (right) eye. Data in both groups, AAV.sFLT01 ( $n = 43$ ) and control ( $n = 26$ ), are expressed as percentage of neovascularization of untreated (right) eyes (mean  $\pm$  s.d.). The difference was found to be statistically significant by Student's *t*-test ( $P < 0.0009$ ; as compared to the untreated contralateral eye).

dimerization of the soluble receptor, we constructed Flt-1 domain 2 linked directly to IgG1-Fc fragment (molecule D2-Fc), but such a strategy did not enhance its binding to VEGF, in agreement with Davis-Smyth *et al.*<sup>13</sup> We then have linked the second domain of Flt-1 to Fc through a 9Gly linker, and thus generated a novel molecule, sFLT01, with potent VEGF binding. Our results show, for the first time, that Flt-1 domain 2 does not require presence of other VEGFR domains for high-affinity VEGF binding. Several other constructs where 9Gly was replaced with other short linkers like 15-mer (Gly<sub>4</sub>Ser)<sub>3</sub>, polyglycine pentamer (5Gly) or other random linkers showed VEGF binding comparable to sFLT01.

We also have constructed several other hybrid proteins by deleting selected regions of IgG1 Fc. Although deletion of the entire Fc CH2 domain did not have a significant impact, we find that the CH3 domain is important for VEGF binding of our molecules. The molecule sFLT02, which retains VEGF binding, was generated by the complete deletion of the Fc CH2 domain, such that Flt-1 domain 2 is linked directly to the Fc CH3 domain through the 9Gly linker.

From the variety of gene therapy vectors currently available we first decided to use the AAV vector because of its versatility, safety and long-term *in vivo* persistence.<sup>25,26</sup> There are several routes to deliver gene therapy vectors into the eye, however the most common ones are intravitreal and subretinal.<sup>19,21</sup> We first decided to investigate an intravitreal route of delivery because of its potential ease of use in the retinal clinic. The AAV2.sFLT01 vector predominantly transduced retinal ganglion cells in agreement with previous observation by other investigators.<sup>21</sup> Subretinal delivery of AAV2 encoding full-length sFlt-1 gene has been successfully tested in mouse and in primate models of ocular neovascularization.<sup>22,27,28</sup> An adenoviral vector encoding full-length sFlt-1, injected both intravitreally or periorbitally suppressed choroidal neovascularization at rupture sites in Bruch's membrane.<sup>29</sup> Our AAV2.sFLT01 vector administered intravitreally to neonatal mice significantly reduced the occurrence of neovascularization in the OIR model. To our knowledge this is the first demonstration of long-term persistent expression of a secreted protein following intravitreal delivery of AAV2 to retinal ganglion cells. There were no gross histological observations of AAV2.sFLT01-related toxicity for the duration of this study (1 year). These results have significant implications for a potential human therapeutic that could be very infrequently administered by a simple intravitreal injection.

## Materials and methods

### *Soluble VEGF receptor hybrids construction*

DNAs encoding hybrid sVEGFR molecules were synthesized by DNA 2.0 Inc. (Menlo Park, CA, USA). The construct D1-3 contains the Flt-1 signal peptide sequence and the first three domains of human Flt-1. In all other constructs, the Flt-1 signal peptide sequence was fused directly to Flt-1 domain 2. In molecules D2-Fc, the Flt-1 domain 2 is fused directly to human IgG1-Fc region. The molecule sFLT01 has Flt-1 domain 2 fused to human IgG1-Fc region through the polyglycine 9-mer (9Gly) linker. In molecules sFLT02 and D2-CH3, a shorter

fragment of IgG1, domain CH3, was used instead of using the full size of IgG1-Fc region. For initial testing, all hybrid molecules were produced by plasmid transfection of 293 cells followed by harvesting of CM, where the transgenes were under control of the CMV promoter.

### *HUVEC proliferation assay*

Pooled HUVECs were purchased from Cambrex—Lonza (East Rutherford, NJ, USA) and expanded through four passages in EGM-2-MV media (EGM basal media supplemented with bovine brain extract, hEGF, hydrocortisone, gentamicin, amphotericin-B, 5% fetal bovine serum (FBS), VEGF, hFGF-B, R3-IGF-1 and ascorbic acid) according to the manufacturer's instructions. For proliferation assays, HUVECs were seeded at  $2 \times 10^3$  cells per well in a 96-well culture plate and incubated overnight in M199 starvation media (M199, 5% FBS). The following day, fresh M199 media supplemented with  $10 \text{ ng ml}^{-1}$  recombinant human VEGF (R&D Systems, Minneapolis, MN, USA) and CM (5  $\mu\text{l}$ , approximately  $1 \text{ ng ml}^{-1}$  of each) from transfected 293 cells containing sVEGFR molecules were added. HUVECs were incubated 3–4 days followed by the addition of the MTS reagent CellTiter 96 Aqueous One Solution (Promega, Madison, WI, USA) and incubated for another 2–4 h. Absorbance was measured at OD490 on a VersaMax plate reader using SOFTmax PRO v4.5 (Molecular Devices, Sunnyvale, CA, USA). Data represent the means of independent proliferation experiments (mean  $\pm$  s.d.) each assayed in triplicate. Each independent proliferation experiment used supernatants from an independent transfection.

### *Western blot analysis*

CM from transfected 293 cells (15  $\mu\text{l}$ ), containing proteins of hybrid sVEGFR molecules were analyzed by western blot under nonreduced and reduced conditions. Briefly, samples were separated by SDS-electrophoresis and transferred to polyvinylidene difluoride membrane. Blots were then probed with goat anti-human VEGFR1 horseradish peroxidase antibody conjugate (R&D Systems) followed by detection using ECL Western Blotting Detection Reagent (GE Healthcare Biosciences, Piscataway, NJ, USA).

### *VEGF-binding assay*

Human VEGF (R&D Systems) adjusted to 20 pM in phosphate-buffered saline was mixed with an equal volume of increasing concentrations of sVEGFR molecules (0.001–10 000 pM; final VEGF concentration = 10 pM) overnight at room temperature with gentle shaking. To determine relative binding affinities, samples were assayed for residual unbound VEGF using the Human Quantikine VEGF ELISA kit (R&D Systems), which detects only unbound (noncomplexed) VEGF. VEGF concentration (pM) was plotted as a function of increasing sVEGFR concentration (pM).

### *AAV vector*

Synthetic sFLT01 chimeric transgene was cloned into a plasmid pCBA(2)-int-BGH, obtained from Mark Sands (Washington University Medical School, St Louis, MO, USA), which contains hybrid chicken  $\beta$ -actin (CBA) promoter and bovine growth hormone polyadenylation signal sequence (BGH poly A).<sup>30</sup> The whole sFLT01

expression cassette was then cloned into a previral plasmid vector pAAVSP70 containing AAV2 inverted terminal repeats (ITRs).<sup>31</sup> Total size of the resulting AAV genome in plasmid sp70.BR/sFLT01 including the region flanked by ITR was 4.6 kb.

The recombinant vector AAV2.sFLT01 was produced by triple transfection of 293 cells protocol using helper plasmids p5rep-Δ-CMVcap and pHelper (Stratagene, La Jolla, CA, USA), and purified according to the protocol using an iodixanol step gradient and HiTrap Heparin column (GE Healthcare Life Sciences, Piscataway, NJ, USA) on an AKTA FPLC system (GE Healthcare Life Sciences, Piscataway, NJ).<sup>32,33</sup> The AAV2.sFLT01 viral preparation had a titer of  $2.2 \times 10^{12}$  drps (DNase resistant particles) per ml. Viral titers were determined using a real-time TaqMan PCR assay (ABI Prism 7700; Applied Biosystems, Foster City, CA, USA) with primers that were specific for the BGH poly A sequence.

### Animals

Adult C57BL/6 mice were purchased from the Jackson Laboratory (Bar Harbor, ME, USA). The animals were maintained in Genzyme's AAALAC-accredited vivarium and given free access to food and water throughout the study. All procedures were performed under a protocol approved by the Institutional Animal Care and Use Committee.

### Intravitreal injection and OIR model

For the longevity experiment, 9-week-old C57BL/6 mice were intravitreally injected with 1  $\mu$ l of AAV2.sFLT01 containing  $1 \times 10^9$  drps of vector and killed 12 months later. For the immunofluorescence and *in situ* hybridization experiments, adult C57BL/6 mice were intravitreally injected with 1  $\mu$ l of AAV2.sFLT01 containing  $2.2 \times 10^9$  drps of AAV2.sFLT01 and killed 28 days later. For the OIR model, neonatal C57BL/6 mouse pups were intravitreally injected on the day of birth (0) with 0.5  $\mu$ l of AAV2.sFLT01 containing  $1.1 \times 10^9$  drps of AAV2.sFLT01. The pups and their nursing dam were placed in an isobaric chamber and were exposed to a hyperoxic environment (75% oxygen) from day 7 to 12.<sup>26</sup> The animals from the OIR model were killed on day 17. The eyes of all animals were processed for paraffin embedding and were serially sectioned. A single 5- $\mu$ m section was taken at each 100- $\mu$ m level through the entire eye resulting in 10–20 sections to evaluate per eye. The sections were stained with hematoxylin and eosin and the degree of neovascularization was determined by counting the number of endothelial cell nuclei internal to and contiguous with the inner limiting membrane ignoring the region of the regressing hyaloid vessels. The number of nuclei in the treated eye was compared to the number of nuclei in the contralateral control eye and the data were expressed as percentage of neovascularization of untreated eyes (mean  $\pm$  s.d.).

### Detection of transgene by immunofluorescence

The sFLT01 transgene was detected in eyes that were fixed in 10% neutral buffered formalin and embedded in paraffin. Tissue sections (5  $\mu$ m) were prepared and sFLT01 was detected using a goat anti-VEGFR1 primary antibody (R&D Systems) and a fluorescein isothiocyanate-conjugated rabbit anti-goat immunoglobulin G (IgG)

secondary antibody (Invitrogen Corp., Carlsbad, CA, USA).

### Detection of sFLT01 mRNA by *in situ* hybridization

The sFLT01 mRNA was detected in paraffin-embedded tissue sections by overnight hybridization of a DIG-labeled RNA probe specific for sFLT01. Signal was detected using peroxidase-labeled anti-DIG (Roche Applied Science, Indianapolis, IN, USA) and amplified using both biotinyl tyramide (Dako North America Inc., Carpinteria, CA) and alkaline phosphatase-labeled anti-biotin (Alpha Diagnostics International Inc., San Antonio, TX, USA). Fast Red (Dako North America Inc.) was then used to detect the complex, and the sections were counterstained using Mayer's hematoxylin (Dako North America Inc.).

### Acknowledgements

We thank Sirkka Kyostio-Moore and for helpful discussions; Michelle Deng for valuable comments on the paper; Shelley Nass and Denise Woodcock for virus production and Bob Brown for support with illustrations.

### References

- Ferrara N, Henzel WJ. Pituitary follicular cells secrete a novel heparin-binding growth factor specific for vascular endothelial cells. *Biochem Biophys Res Commun* 1989; **161**: 851–858.
- Kvanta A, Algvare PV, Berglin L, Seregard S. Subfoveal fibrovascular membranes in age-related macular degeneration express vascular endothelial growth factor. *Invest Ophthalmol Visual Sci* 1996; **37**: 1929–1934.
- Adamis AP, Miller JW, Bernal MT, D'Amico DJ, Folkman J, Yeo TK *et al*. Increased vascular endothelial growth factor levels in the vitreous of eyes with proliferative diabetic retinopathy. *Am J Ophthalmol* 1994; **118**: 445–450.
- Ferrara N. Vascular endothelial growth factor: basic science and clinical progress. *Endocr Rev* 2004; **25**: 581–611.
- Aiello LP, Pierce EA, Foley ED, Takagi H, Chen H, Riddle L *et al*. Suppression of retinal neovascularization *in vivo* by inhibition of vascular endothelial growth factor (VEGF) using soluble VEGF-receptor chimeric proteins. *Proc Natl Acad Sci USA* 1995; **92**: 10457–10461.
- Williet CG, Boucher Y, di Tomaso E, Duda DG, Munn LL, Tong RT *et al*. Direct evidence that the VEGF-specific antibody bevacizumab has antivascular effects in human rectal cancer. *Nat Med* 2004; **10**: 145–147.
- Rosenfeld PJ, Brown DM, Heier JS, Boyer DS, Kaiser PK, Chung CY *et al*. Ranibizumab for neovascular age-related macular degeneration. *N Engl J Med* 2006; **355**: 1419–1431.
- Terman BI, Dougher-Vermazen M, Carrion ME, Dimitrov D, Armellino DC, Gospodarowicz D *et al*. Identification of the KDR tyrosine kinase as a receptor for vascular endothelial cell growth factor. *Biochem Biophys Res Commun* 1992; **187**: 1579–1586.
- de Vries C, Escobedo JA, Ueno H, Houck K, Ferrara N, Williams LT. The fms-like tyrosine kinase a receptor for vascular endothelial growth factor. *Science* 1992; **255**: 989–991.
- Quinn TP, Peters KG, De Vries C, Ferrara N, Williams LT. Fetal liver kinase 1 is a receptor for vascular endothelial growth factor and is selectively expressed in vascular endothelium. *Proc Natl Acad Sci USA* 1993; **90**: 7533–7537.
- Shibuya M, Yamaguchi S, Yamane A, Ikeda T, Tojo A, Matsushima H *et al*. Nucleotide sequence and expression of a novel human receptor-type tyrosine kinase gene (flt) closely related to the fms family. *Oncogene* 1990; **5**: 519–524.

- 12 Kendall RL, Thomas KA. Inhibition of vascular endothelial cell growth factor activity by an endogenously encoded soluble receptor. *Proc Natl Acad Sci USA* 1993; **90**: 10705–10709.
- 13 Davis-Smyth T, Chen H, Park J, Presta LG, Ferrara N. The second immunoglobulin-like domain of the VEGF tyrosine kinase receptor Flt-1 determines ligand binding and may initiate a signal transduction cascade. *EMBO J* 1996; **15**: 4919–4927.
- 14 Barleon B, Totzke F, Herzog C, Blanke S, Kremmer E, Siemeister G *et al*. Mapping of the sites for ligand binding and receptor dimerization at the extracellular domain of the vascular endothelial growth factor receptor Flt-1. *J Biol Chem* 1997; **272**: 10382–10388.
- 15 Wiesmann C, Fuh G, Christinger HW, Eigenbrot C, Wells JA, de Vos AM. Crystal structure at 1.7 Å resolution of VEGF in complex with domain 2 of the Flt-1 receptor. *Cell* 1997; **91**: 695–704.
- 16 Davis-Smyth T, Presta LG, Ferrara N. Mapping the charged residues in the second immunoglobulin-like domain of the vascular endothelial growth factor/placenta growth factor receptor Flt-1 required for binding and structural stability. *J Biol Chem* 1998; **273**: 3216–3222.
- 17 Cunningham SA, Stephan CC, Arrate MP, Ayer KG, Brock TA. Identification of the extracellular domains of Flt-1 that mediate ligand interactions. *Biochem Biophys Res Commun* 1997; **231**: 596–599.
- 18 Hoiash J, Davis S, Papadopoulos N, Croll SD, Ho L, Russell M *et al*. VEGF-Trap: a VEGF blocker with potent antitumor effects. *Proc Natl Acad Sci USA* 2002; **99**: 11393–11398.
- 19 Ali RR, Reichel MB, Thrasher AJ, Levinsky RJ, Kimmon C, Kanuga N *et al*. Gene transfer into the mouse retina mediated by an adeno-associated viral vector. *Hum Mol Genet* 1996; **5**: 591–594.
- 20 Ali RR, Reichel MB, Hunt DM, Bhattacharya SS. Gene therapy for inherited retinal degeneration. *Br J Ophthalmol* 1997; **81**: 795–801.
- 21 Ali RR, Reichel MB, De Alwis M, Kanuga N, Kimmon C, Levinsky RJ *et al*. Adeno-associated virus gene transfer to mouse retina. *Hum Gene Ther* 1998; **9**: 81–86.
- 22 Lai CM, Shen WY, Brankov M, Lai YK, Barnett NL, Lee SY *et al*. Long-term evaluation of AAV-mediated sFlt-1 gene therapy for ocular neovascularization in mice and monkeys. *Mol Ther* 2005; **12**: 659–668.
- 23 Huston JS, Levinson D, Mudgett-Hunter M, Tai MS, Novotny J, Margolies MN *et al*. Protein engineering of antibody binding sites: recovery of specific activity in an anti-digoxin single-chain Fv analogue produced in *Escherichia coli*. *Proc Natl Acad Sci USA* 1988; **85**: 5879–5883.
- 24 Smith LE, Wesolowski E, McLellan A, Kostyk SK, D'Amato R, Sullivan R *et al*. Oxygen-induced retinopathy in the mouse. *Invest Ophthalmol Vis Sci* 1994; **35**: 101–111.
- 25 Bennett J. Commentary: an aye for eye gene therapy. *Hum Gene Ther* 2006; **17**: 177–179.
- 26 Jacobson SG, Acland GM, Aguirre GD, Aleman TS, Schwartz SB, Cideciyan AV *et al*. Safety of recombinant adeno-associated virus type 2-RPE65 vector delivered by ocular subretinal injection. *Mol Ther* 2006; **13**: 1074–1084.
- 27 Bainbridge JW, Mistry A, De Alwis M, Paleolog E, Baker A, Thrasher AJ *et al*. Inhibition of retinal neovascularisation by gene transfer of soluble VEGF receptor sFlt-1. *Gene Therapy* 2002; **9**: 320–326.
- 28 Lai YK, Shen WY, Brankov M, Lai CM, Constable IJ, Rakoczy PE. Potential long-term inhibition of ocular neovascularisation by recombinant adeno-associated virus-mediated secretion gene therapy. *Gene Therapy* 2002; **9**: 804–813.
- 29 Gehlbach P, Demetriades AM, Yamamoto S, Deering T, Xiao WH, Duh EJ *et al*. Periocular gene transfer of sFlt-1 suppresses ocular neovascularization and vascular endothelial growth factor-induced breakdown of the blood–retinal barrier. *Hum Gene Ther* 2003; **14**: 129–141.
- 30 Xu L, Daly T, Gao C, Flotte TR, Song S, Byrne BJ *et al*. CMV-beta-actin promoter directs higher expression from an adeno-associated viral vector in the liver than the cytomegalovirus or elongation factor 1 alpha promoter and results in therapeutic levels of human factor X in mice. *Hum Gene Ther* 2001; **12**: 563–573.
- 31 Ziegler RJ, Lonning SM, Armentano D, Li C, Souza DW, Cherry M *et al*. AAV2 vector harboring a liver-restricted promoter facilitates sustained expression of therapeutic levels of alpha-galactosidase A and the induction of immune tolerance in Fabry mice. *Mol Ther* 2004; **9**: 231–240.
- 32 Vincent KA, Piraino ST, Wadsworth SC. Analysis of recombinant adeno-associated virus packaging and requirements for rep and cap gene products. *J Virol* 1997; **71**: 1897–1905.
- 33 Zolotukhin S, Potter M, Zolotukhin I, Sakai Y, Loiler S, Fraites TJ *et al*. Production and purification of serotype 1, 2, and 5 recombinant adeno-associated viral vectors. *Methods* 2002; **28**: 158–167.

EX. L

# Persistent Suppression of Ocular Neovascularization with Intravitreal Administration of AAVrh.10 Coding for Bevacizumab

Yanxiong Mao,<sup>1,2,\*</sup> Szilard Kiss,<sup>3,\*</sup> Julie L. Boyer,<sup>2,†</sup> Neil R. Hackett,<sup>2</sup> Jianping Qiu,<sup>2</sup> Andrew Carbone,<sup>2</sup>  
Jason G. Mezey,<sup>2,4</sup> Stephen M. Kaminsky,<sup>2</sup> Donald J. D'Amico,<sup>3</sup> and Ronald G. Crystal<sup>2</sup>

## Abstract

Vascular endothelial growth factor (VEGF) plays an important role in the pathogenesis of neovascular age-related macular degeneration and diabetic retinopathy. Bevacizumab, an anti-VEGF monoclonal antibody, is efficacious for these disorders, but requires monthly intravitreal administration, with associated discomfort, cost, and adverse event risk. We hypothesized that a single intravitreal administration of adeno-associated virus (AAV) vector expressing bevacizumab would result in persistent eye expression of bevacizumab and suppress VEGF-induced retinal neovascularization. We constructed an AAV rhesus serotype rh.10 vector to deliver bevacizumab (AAVrh.10BevMab) and assessed its ability to suppress neovascularization in transgenic mice overexpressing human VEGF165 in photoreceptors. Intravitreal AAVrh.10BevMab directed long-term bevacizumab expression in the retinal pigmented epithelium. Treated homozygous mice had reduced levels of neovascularization, with  $90 \pm 4\%$  reduction 168 days following treatment. Thus, a single administration of AAVrh.10BevMab provides long-term suppression of neovascularization without the costs and risks associated with the multiple administrations required for the current conventional bevacizumab monoclonal drug delivery.

## Introduction

**P**ATHOLOGICAL OCULAR NEOVASCULARIZATION is the hallmark of age-related macular degeneration (AMD) and diabetic retinopathy (DR), two of the leading causes of blindness in the industrialized world (Elman *et al.*, 2010; Folk and Stone, 2010). The prevalence of AMD in the United States is expected to increase to nearly 3 million by 2020, whereas the prevalence of DR is projected to triple to 16 million by 2050 (Friedman *et al.*, 2004; Saaddine *et al.*, 2008). Local up-regulation of the expression of vascular endothelial growth factor (VEGF) plays a central role in the pathogenesis of both disorders (Aiello *et al.*, 1994; Ferrara, 2010). The clinical use of intravitreal anti-VEGF agents has been shown to slow the progression of vision loss and improve visual acuity in patients with AMD and DR (Avery *et al.*, 2006; Rosenfeld *et al.*, 2006; Elman *et al.*, 2010; Gulkilik *et al.*, 2010). A widely used anti-VEGF ocular therapy is bevacizumab (Avastin; Genen-

tech, South San Francisco, CA), a humanized monoclonal antibody (mAb) specific for human VEGF (Ferrara *et al.*, 2004; Avery *et al.*, 2006). Numerous clinical studies have established that intravitreal administration of bevacizumab inhibits VEGF-dependent neovascularization and vascular permeability, improves visual outcomes, and decreases vision loss in patients with DR and AMD. Since their introduction, intravitreal injections of bevacizumab and its Fab fragment ranibizumab have become the standard of care for treatment of AMD and are becoming the standard for DR, especially diabetic macular edema (Avery *et al.*, 2006; Gulkilik *et al.*, 2010; Nicholson and Schachat, 2010; Arevalo *et al.*, 2011; Montero *et al.*, 2011; Ozturk *et al.*, 2011; Salam *et al.*, 2011; Witkin and Brown, 2011). However, the positive effect on visual acuity is often of limited duration, with the need for repeated, most often monthly, injections to achieve optimal visual outcome (Regillo *et al.*, 2008; Elman *et al.*, 2010; Gulkilik *et al.*, 2010; Mitchell *et al.*, 2010; Schmidt-Erfurth *et al.*, 2010).

<sup>1</sup>Department of Respiratory Medicine, West China Hospital, Sichuan University, Sichuan 610041, China.

<sup>2</sup>Department of Genetic Medicine, Weill Cornell Medical College, New York, NY 10065.

<sup>3</sup>Department of Ophthalmology, Weill Cornell Medical College, New York, NY 10065.

<sup>4</sup>Department of Biological Statistics and Computational Biology, Cornell University, Ithaca, NY 14853.

\*These two authors contributed equally to the study.

†Current address: Yale School of Medicine, Yale University, New Haven, CT 06520.

In addition to the burden on the patient and the economic burden on the health-care system, repeated intravitreal administrations pose a risk of visually devastating ocular complications. The most serious adverse event is infectious endophthalmitis. Although the per-injection rate of endophthalmitis has a reported incidence ranging between 0.03% and 0.16%, after 1–2 years of repeated injections, the per-eye infection rate approaches 1.0% (Jager *et al.*, 2004; Brown *et al.*, 2006; Rosenfeld *et al.*, 2006; Elman *et al.*, 2010). More frequent (up to 5%), although less devastating, ocular adverse events associated with repeated intravitreal administrations include vitreous hemorrhage, retinal detachment, traumatic cataract, corneal abrasion, subconjunctival hemorrhage, and eyelid swelling (Jager *et al.*, 2004; Brown *et al.*, 2006; Rosenfeld *et al.*, 2006; Elman *et al.*, 2010; Folk and Stone, 2010). In the context of these issues, an intraocular therapy with a prolonged duration of anti-VEGF action following a single intravitreal administration would decrease the treatment burden of repeated intraocular injections and reduce the cost of chronic therapy, resulting in a profound impact on the treatment of both AMD and DR.

Adeno-associated viral (AAV) vectors are attractive for ocular gene therapy, as they can direct long-term transgene expression with low toxicity and immunogenicity, with established expression in a variety of retinal cell types (Bainbridge *et al.*, 2008; Buch *et al.*, 2008; Roy *et al.*, 2010; Simonelli *et al.*, 2010; Lukason *et al.*, 2011). There are currently six human clinical trials using intraocular administration of AAV vectors: five directed toward the treatment of Leber's congenital amaurosis (with RPE165 as the gene product), and one anti-VEGF therapy for the treatment of AMD (with soluble receptor to VEGF, sFLT01 as the gene product) (ClinicalTrials.gov, 2011). Knowing that intravitreal administration of bevacizumab is highly effective in treating AMD and DR (Avery *et al.*, 2006; Gulkilik *et al.*, 2010) and that of AAV gene-transfer vectors can be safely administered intraocularly to humans with persistent expression of a therapeutic transgene (Bainbridge *et al.*, 2008; Buch *et al.*, 2008; Roy *et al.*, 2010; Simonelli *et al.*, 2010; MacLachlan *et al.*, 2011), we hypothesized that a single intravitreal administration of an AAV vector expressing bevacizumab would result in sustained intraocular expression of bevacizumab at levels sufficient for long-term suppression of ocular neovascularization. Based on AAVrh.10, a clade E, nonhuman primate (rhesus macaque)-derived gene-transfer vector that we are using in human clinical trials for gene therapy for CNS hereditary disease (Sondhi *et al.*, 2007), we designed AAVrh.10BevMab, coding for the heavy and light chains of bevacizumab. The efficacy of AAVrh.10BevMab was tested for its ability to inhibit ocular neovascularization in the transgenic rho/VEGF mouse model that constitutively expresses the human VEGF165 isoform in photoreceptors under the rhodopsin promoter (Okamoto *et al.*, 1997). Unlike bevacizumab itself, which is effective in this model for 14 days (Miki *et al.*, 2009), the data demonstrate that a single administration of AAVrh.10BevMab is effective in suppressing ocular neovascularization in this murine model for at least 168 days, the longest time point evaluated.

## Materials and Methods

### Gene-therapy vectors

The AAVrh.10BevMab vector is based on the nonhuman primate-derived rh.10 capsid pseudotyped with AAV2 in-

verted terminal repeats surrounding the expression cassette consisting of cytomegalovirus (CMV)-enhancer chicken  $\beta$ -actin promoter (Niwa *et al.*, 1991; Daly *et al.*, 1999; Sondhi *et al.*, 2007), the bevacizumab anti-human VEGF heavy-chain and light-chain sequence separated by a furin 2A self-cleavage site (Fang *et al.*, 2005), and the rabbit  $\alpha$ -globin polyadenylation signal (see Fig. 1A). Nucleotide sequences for the antibody heavy- and light-chain variable domains were derived from the protein sequence for human kappa Fab-12, the original humanized version of the murine mAb corresponding to bevacizumab (Chen *et al.*, 1999). The coding sequences for the human IgG1 constant domain were added to the variable domain by overlap PCR.

AAVrh.10BevMab was produced by cotransfection of 293orf6 cells with three plasmids: (1) an expression cassette plasmid (pAAVrh.10BevMab) carrying the humanized anti-human VEGF antibody cDNA; (2) a packaging plasmid (pAAV44.2) that contains the AAV2 *rep* gene and AAVrh.10 *cap* necessary for vector replication and capsid production; and (3) pAdDF6, an adenovirus helper plasmid (Xiao *et al.*, 1998; Sondhi *et al.*, 2007). For AAVrh.10 vector production, pAAVrh.10BevMab (600  $\mu$ g), pAAV44.2 (600  $\mu$ g), and pAdDF6 (1.2 mg) were cotransfected into 293orf6 cells, a human embryonic kidney cell line expressing adenovirus E1 and E4 genes (Gao *et al.*, 2002; Sondhi *et al.*, 2007), using Polyfect (Qiagen, Valencia, CA). At 72 hr post transfection, the cells were harvested, and a crude viral lysate was prepared using four cycles of freeze/thaw and clarified by centrifugation. AAVrh.10BevMab was purified by iodixanol gradient and QHP anion-exchange chromatography. The purified AAVrh.10BevMab was concentrated using an Amicon Ultra-15 100K centrifugal filter device (Millipore, Billerica, MA) and stored in PBS, pH 7.4, at  $-80^{\circ}\text{C}$ . The negative control vectors AAVrh.10LacZ encodes  $\beta$ -galactosidase (Wang *et al.*, 2010), AAVrh.10GFP encodes green fluorescent protein (GFP) (Sondhi *et al.*, 2007), and AAVrh.10 $\alpha$ V encodes an unrelated antibody against *Y. pestis* V antigen, which replaces the bevacizumab coding region of the AAVrh.10BevMab vector. Vector genome titers were determined by quantitative TaqMan real-time PCR analysis using a chicken  $\beta$ -actin promoter-specific primer-probe set (Applied Biosystems, Foster City, CA).

### Assessment of AAVrh.10BevMab in vitro

Expression and specificity of the AAVrh.10BevMab-expressed bevacizumab from infected cells were assessed using western analysis. For expression, 293orf6 cells were infected with AAVrh.10BevMab [ $2 \times 10^5$  genome copies (gc)/cell], and infected cell supernatants were harvested 72 hr after infection. Supernatants were concentrated by passage through Ultracel YM-10 centrifugal filters (Millipore) and evaluated by western analysis, using a peroxidase-conjugated goat anti-human kappa light chain antibody (Sigma, St. Louis, MO) under nonreducing conditions or reducing conditions with the addition of peroxidase-conjugated goat anti-human IgG antibody (Santa Cruz Biotechnology, Santa Cruz, CA). Detection was by enhanced chemiluminescence reagent (GE Healthcare Life Sciences, Piscataway, NJ). The specificity of the AAVrh.10-expressed bevacizumab was determined by western analysis against human VEGF-165 and mouse VEGF-164 (Watanabe *et al.*, 2008). AAVrh.10BevMab-infected

cell supernatants were used as the primary antibody, followed by a peroxidase-conjugated goat anti-human kappa light-chain antibody and enhanced chemiluminescence reagent.

#### *Bevacizumab levels after in vivo administration of AAVrh.10BevMab*

Male C57BL/6 mice, 6–8 weeks of age, obtained from The Jackson Laboratory (Bar Harbor, ME), were housed under pathogen-free conditions. AAVrh.10BevMab ( $10^{11}$  gc) or AAVrh.10LacZ ( $10^{11}$  gc) in  $100 \mu\text{l}$  of PBS was administered by the intravenous route to C57BL/6 mice through the tail vein. At various times 0–24 weeks after vector administration, blood was collected through the tail vein, allowed to clot for 60 min, and centrifuged at 13,000 rpm for 10 min. Bevacizumab levels in serum were assessed by enzyme-linked immunosorbent assay (ELISA) using flat-bottomed 96-well EIA/RIA plates (Corning Life Sciences, Lowell, MA) coated overnight at  $4^{\circ}\text{C}$  with  $0.2 \mu\text{g}$  of human VEGF-165 per well in a total volume of  $100 \mu\text{l}$  of  $0.05 \text{ M}$  carbonate buffer and 0.01% thimerosal. The plates were washed three times with PBS and blocked with 5% dry milk in PBS for 60 min. The plates were washed three times with PBS containing 0.05% Tween 20. Serial serum dilutions in PBS containing 1% dry milk were added to each well and incubated for 60 min. The positive control standard was  $25 \mu\text{g}/\mu\text{l}$  bevacizumab (Genentech). The plates were washed three times with PBS containing 0.05% Tween 20 followed by  $100 \mu\text{l}/\text{well}$  1:5,000 diluted peroxidase-conjugated goat anti-human kappa light-chain antibody in PBS containing 1% dry milk for 60 min. The plates were washed four times with PBS containing 0.05% Tween 20 and once with PBS. Peroxidase substrate ( $100 \mu\text{l}/\text{well}$ ; Bio-Rad, Hercules, CA) was added, and the reaction was stopped at 15 min by addition of 2% oxalic acid ( $100 \mu\text{l}/\text{well}$ ). Absorbance at 415 nm was measured. Antibody titers were calculated with a log (OD)–log (dilution) interpolation model with cutoff value equal to twofold the absorbance of background (Watanabe *et al.*, 2008). The titers were converted to a bevacizumab concentration using results from the bevacizumab standard data curve.

AAVrh.10BevMab ( $10^{10}$  gc) and AAVrh.10 $\alpha$ V ( $10^{10}$  gc) in  $1 \mu\text{l}$  of PBS were administered by intravitreal injection to the left and right eyes, respectively, of C57BL/6 male mice. Intravitreal injection was done under a dissecting microscope with a 32-gauge needle (Hamilton Company, Reno, NV). After 0–24 weeks, mice were killed with  $\text{CO}_2$ ; eyes were collected, homogenized by sonication in  $100 \mu\text{l}$  of T-PER tissue protein extraction reagent (Thermo Scientific, Rockford, IL), and centrifuged at 13,000 rpm for 5 min; and supernatant was collected. Bevacizumab levels in supernatant were assessed by a human VEGF-specific ELISA as described above. Bevacizumab levels were standardized to total protein levels, which were assayed by the bicinchoninic protein assay (Thermo Scientific, Waltham, MA). The expression of bevacizumab in the eye at 12 weeks post intravitreal injection was evaluated by Western analysis as described above.

#### *Localization of bevacizumab expression by immunofluorescence*

To assess the intraocular site of bevacizumab expression, male C57BL/6 mice were injected with AAVrh.10BevMab

and AAVrh.10 $\alpha$ V, as described above, or left uninjected. Treated and control virus-injected eyes were enucleated 5 weeks after intravitreal injection, fixed in formalin, embedded in paraffin wax, sectioned, deparaffinized, and treated sequentially with biotin-conjugated donkey anti-human IgG(H+L) (dilution 1:100; Jackson ImmunoResearch, West Grove, PA) and Cy3-conjugated streptavidin (dilution 1:1,000; Jackson ImmunoResearch). Nuclei were stained with 4'-diamidino-2-phenylindole (DAPI; dilution 1:2,000; Invitrogen, Carlsbad, CA). The sections were embedded (Histoserv, Germantown, MD) and examined with a fluorescence microscope.

#### *AAVrh.10BevMab-mediated suppression of neovascularization*

Rho/VEGF mice (a gift of Peter Campochiaro, Department of Ophthalmology and Neuroscience, The Johns Hopkins School of Medicine, Baltimore, MD) (Okamoto *et al.*, 1997) were housed and bred under pathogen-free conditions. At postnatal day 14, homozygous rho/VEGF mice were injected intravitreally with  $1 \mu\text{l}$  of PBS to one eye and  $10^{10}$  gc of AAVrh.10BevMab in  $1 \mu\text{l}$  to the other eye. At 2, 14, 28, 84, and 168 days post therapy, mice were anesthetized and perfused with 2 ml of 25 mg/ml fluorescein-labeled dextran ( $2 \times 10^6$  average molecular weight; Sigma, St. Louis, MO) in PBS. The eyes were removed and fixed for 1 hr in 4% paraformaldehyde/PBS. The cornea and lens were removed, and the entire retina was carefully dissected from the eyecup, radially cut from the edge of the retina to the equator in all four quadrants, and flat-mounted in Prolong Gold antifade reagent (Invitrogen). The retinas were examined by fluorescence microscopy at  $200\times$ , providing a narrow depth of field to enable subretinal focus for neovascular buds on the outer surface of the retina. AxioVision LE (Carl Zeiss, Oberkochen, Germany) digital image analysis software was used by three investigators blinded to treatment group for quantifying subretinal neovascular growth area per retina.

#### *Statistical analysis*

All data are presented as the means or geometric means  $\pm$  standard error. Assessment of significant effects of treatment and variability due to observer or mouse was performed using a two-factor (treatment, observer) and three-factor (treatment, observer, mouse) ANOVA model fit separately at each time point (2, 14, 28, 84, and 168 weeks). As the data were nonnormal, a nonparametric approach was used to assess significance of each factor by implementing a permutation analysis. This was conducted by fitting the ANOVA model to the data and calculating  $p$  values associated with each factor using standard parametric statistics. The data were then permuted 10,000 times and, for each permutation, the ANOVA models were fit to the permuted data and  $p$  values calculated for each of the factors. For each factor, the rank of the data  $p$  values were then determined within the ordered list of permutation  $p$  values, where the rank of the data was used to determine the nonparametric  $p$  value. Overall, for the three-factor ANOVA, we conducted three tests at each of the five time points to produce 15 independent tests, whereas the two-factor ANOVA produced 10 tests that were highly nonindependent of the three-factor ANOVA tests. We therefore considered cases where  $p < 0.05/$



15=0.0033 to be significant after a multiple test correction, *e.g.*, we consider  $p > 0.0033$  as providing no evidence of significant effect of treatment or variability in a factor.

## Results

### Characterization of AAVrh.10BevMab

The AAVrh.10BevMab vector was tested for *in vitro* expression of human heavy and light chain by infection of 293orf6 cells (Fig. 1). Cell culture supernatant at 72 hr post infection, assessed by Western analysis under nonreducing and reducing conditions, established expression of the intact heavy and light chains and their ability to form the intact antibody (Fig. 1B and C). Infection with the control AAVrh.10GFP vector under identical conditions had no detectable bands, reduced or nonreduced, for human antibody. The supernatant from AAVrh.10BevMab-infected cells was tested for the capacity to specifically recognize human VEGF by probing a western against human VEGF165 and mouse VEGF164 (Fig. 1D). Only the human form of VEGF was recognized as expected from the known specificity of bevacizumab. In contrast, supernatants from AAVrh.10GFP-infected cells did not recognize either protein. To assess the ability of the AAVrh.10BevMab vector to direct persistent expression of bevacizumab *in vivo*, serum antibody levels of

human VEGF were assessed by ELISA at 0–24 weeks after intravenous administration of  $10^{11}$  gc of the AAVrh.10BevMab. Antibody levels peaked at about 12 weeks and were sustained through the 24 weeks (Fig. 1E), the last time point examined. No antibody was detected in serum of mice that received similar intravenous injection of AAVrh.10LacZ (control vector expressing  $\beta$ -galactosidase).

### Intravitreal administration of AAVrh.10BevMab

To evaluate the expression profile of AAVrh.10BevMab by local administration, antibody levels in the supernatant of eye homogenate were assessed for 0–24 weeks after intravitreal administration of  $10^{10}$  gc of the vector. The data showed that the bevacizumab levels were above 100 pg/ $\mu$ g total protein at 2 weeks and remained at similar levels to the last time point evaluated at 24 weeks (Fig. 2A). No bevacizumab was detected in the eyes from mice that received intravitreal AAVrh.10 $\alpha$ V, a control vector. The expression of bevacizumab in the eye post intravitreal administration of AAVrh.10BevMab was confirmed by Western analysis. Soluble protein collected from the AAVrh.10BevMab-injected eyes was positive for the presence of human antibody heavy and light chains, whereas no human antibody was detected in eyes injected with AAVrh.10 $\alpha$ V, which expresses a mouse mAb, or uninjected naive eyes (Fig. 2B).

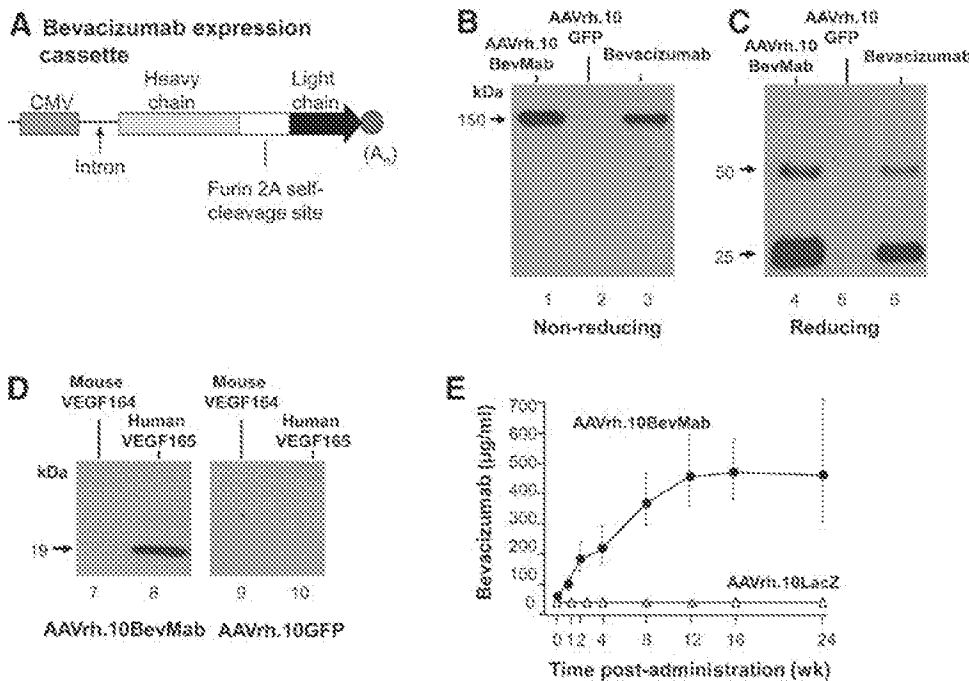
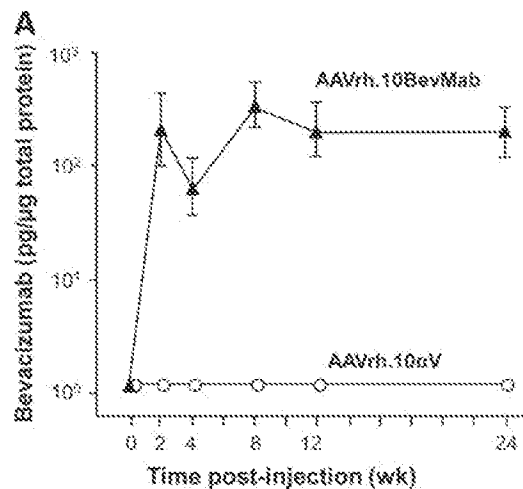


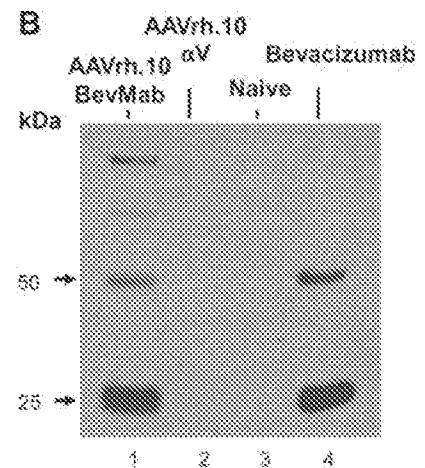
**FIG. 1.** Function of the AAVrh.10BevMab gene-transfer vector. (A) Schematic of the bevacizumab cDNA expression cassette. CMV, cytomegalovirus-chicken  $\beta$ -actin promoter. (B, C) AAVrh.10BevMab-directed expression of bevacizumab. 293orf6 cells were infected with AAVrh.10BevMab or AAVrh.10GFP at  $2 \times 10^5$  gc/cell. After 72 hr, infected cell supernatants were assessed for bevacizumab expression by western analysis with peroxidase-conjugated goat anti-human kappa light-chain antibody and peroxidase-conjugated goat anti-human IgG antibody. (B) Nonreducing western analysis. Lane 1, supernatant from AAVrh.10BevMab; lane 2, AAVrh.10GFP control; lane 3, bevacizumab alone. (C) Reducing western analysis. Lane 4, AAVrh.10BevMab; lane 5, AAVrh.10GFP; lane 6, bevacizumab control. Bevacizumab has a molecular mass of 150 kDa; the full-length heavy and light chains of bevacizumab are 50 and 25 kDa, respectively. (D) Specificity of human VEGF bevacizumab produced by AAVrh.10BevMab. 293orf6 cells were infected with AAVrh.10BevMab or AAVrh.10GFP at  $2 \times 10^5$  gc/cell. After 72 hr, supernatants were assessed for the ability to bind to human or mouse VEGF-A protein by Western analysis. *Left:* Supernatants from AAVrh.10BevMab-infected cells. Lane 7, specificity for mouse VEGF-164; lane 8, specificity for human VEGF-165. *Right:* Supernatants from AAVrh.10GFP-infected cells. Lane 9, specificity for mouse VEGF-164; lane 10, specificity for human VEGF-165. Human VEGF-165 has a molecular mass of 19 kDa. (E) Ability of AAVrh.10BevMab to direct persistent expression of bevacizumab *in vivo*. Shown are bevacizumab levels after systemic administration of the AAVrh.10BevMab vector. AAVrh.10BevMab ( $10^{11}$  gc) was administered to C57BL/6 mice by the intravenous route, using AAVrh.10LacZ ( $10^{11}$  gc) as a control. Over 24 weeks after vector administration, bevacizumab levels were measured by human VEGF-specific ELISA. Shown is the geometric mean  $\pm$  standard error from  $n = 5$  animals per group.

human VEGF were assessed by ELISA at 0–24 weeks after intravenous administration of  $10^{11}$  gc of the AAVrh.10BevMab. Antibody levels peaked at about 12 weeks and were sustained through the 24 weeks (Fig. 1E), the last time point examined. No antibody was detected in serum of mice that received similar intravenous injection of AAVrh.10LacZ (control vector expressing  $\beta$ -galactosidase).

FIG. 2. Ocular levels of bevacizumab after a single local administration of the AAVrh.10BevMab vector. AAVrh.10BevMab ( $10^{11}$  gc) was administered to C57BL/6 mice by the intravitreal route, with AAVrh.10 $\alpha$ V, an AAVrh.10 vector coding for an irrelevant IgG antibody, as a control. (A) Bevacizumab levels. Over 24 weeks after vector administration, bevacizumab levels in eye homogenate were measured by a human VEGF-specific ELISA. Data (geometric means  $\pm$  standard error) were obtained from  $n=6$  eyes for the AAVrh.10BevMab group



and  $n=4$  eyes for the AAVrh.10 $\alpha$ V group. (B) Western analysis. Twelve weeks after vector administration, bevacizumab levels in eye homogenate were assessed by Western analysis with peroxidase-conjugated goat anti-human kappa light-chain antibody and peroxidase-conjugated goat anti-human IgG antibody under reducing conditions. (Two primary antibodies are used to visualize both heavy and light chains with equal intensity.) Untreated control eyes of age-matched mice were evaluated in a similar fashion. Lane 1, homogenate from AAVrh.10BevMab-treated eyes; lane 2, homogenate from AAVrh.10 $\alpha$ V-treated eyes; lane 3, homogenate from naive eyes; lane 4, bevacizumab control. The heavy and light chains of the bevacizumab expressed by the AAV vector have molecular masses of 50 and 25 kDa, respectively.



The localization of bevacizumab within the eyes of mice administered intravitreal AAVrh.10BevMab was evaluated in paraffin-embedded and stained sections of eyes 35 days post injection. The bevacizumab was localized to the retinal pigment epithelium (RPE), whereas no bevacizumab staining was seen in uninjected eyes or eyes injected with the vector expressing the mouse mAb, AAVrh.10 $\alpha$ V (Fig. 3). Intravitreal administration of AAVrh.10 has previously been reported to efficiently transduce a wide range of retinal cells, including the RPE, the ganglion cell layer, the amacrine cells of the inner nuclear layer, the Müller and horizontal cells, as well as bipolar cells (Giove *et al.*, 2010). Therefore, we searched multiple immunohistochemical sections for staining of these cell types, but have observed no staining in any cell type other than RPE.

#### Efficacy of AAVrh.10BevMab

The efficacy of the AAVrh.10BevMab in the transgenic rho/VEGF mouse was assessed by evaluating the suppression of the development of neovascular buds following intravitreal injection to the eyes of 14-day-old homozygous rho/VEGF mice. As an internal control, the opposite eye received an intravitreal injection of PBS. Fluorescence microscopy of the retina from AAVrh.10BevMab- and PBS-injected eyes at 2, 14, 28, 84, and 168 days post injection was used to assess the phenotype (Fig. 4). In low-magnification views (Fig. 4A), multiple large areas of budding and vascular leak are evident in the PBS-treated eye of the mice at 168 days post injection; these areas were largely absent in the treated eye (Fig. 4B). By examining neovascular buds at higher power (Fig. 4C), the time-dependent increase in budding was seen. At 2 days post injection, AAVrh.10BevMab- and PBS-injected eyes appeared to have similar amounts of neovascular buds, but at longer time points, AAVrh.10BevMab-injected eyes had significantly fewer

subretinal neovascular buds than retinas from eyes injected with PBS.

The subretinal neovascular buds were quantified by three investigators blinded to treatment group. As an example of the individual data from each observer, at 84 days post injection, the data from each of the observers showed significant reduced area of subretinal neovascular buds in retinas of AAVrh.10BevMab-injected eyes compared with eyes injected with PBS (Fig. 5A). The interobserver variability in quantifying the neovascular buds was not significant at the multiple test correction threshold (Table 1). Data from the three observers was first averaged for each eye, and then the average and standard error for each condition and time point were plotted (Fig. 5B). Consistent with the fluorescence microscopy results, at 2 days post injection there was no significant reduction in the area of subretinal neovascular buds for AAVrh.10BevMab-injected eyes, but from 14 to 168 days after therapy, eyes injected with AAVrh.10BevMab had significantly less area of subretinal neovascular buds compared with retinas from eyes injected with PBS (Fig. 5B). The reduction ratio—calculated as [(mean neovascular bud area in PBS-injected eye at indicated time point) – (neovascular bud area in AAVrh.10BevMab-injected eye at indicated time point)] / (mean neovascular bud area in PBS-injected eye)—showed no reduction at 2 days post injection, but significant reduction at later time points: 14 days (49%) to 168 days (90%) (Fig. 5C). Thus, a single intravitreal administration of AAVrh.10BevMab can persistently suppress subretinal neovascularization in this model.

#### Discussion

Intraocular anti-VEGF therapy with bevacizumab or its Fab fragment ranibizumab, the standard worldwide therapy for the treatment of AMD and DR, requires monthly intravitreal administration to maintain optimal visual

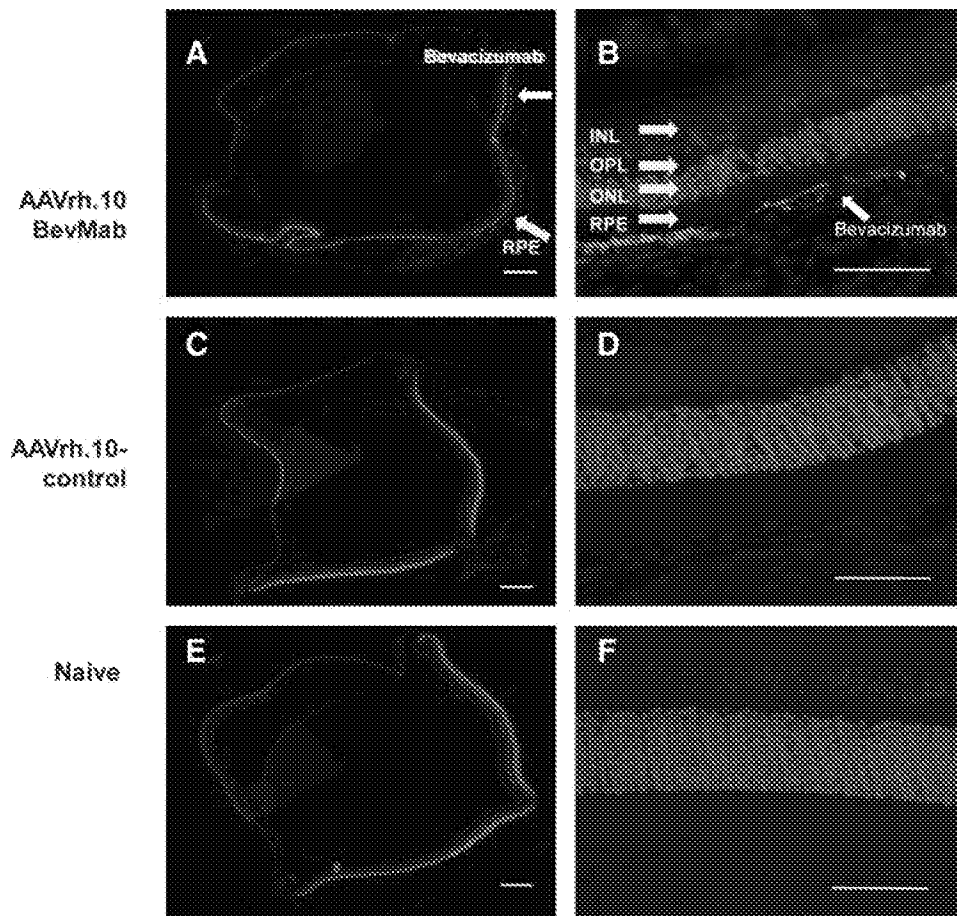


**FIG. 3.** Immunofluorescence localization of bevacizumab after local ocular administration of AAVrh.10BevMab. AAVrh.10BevMab ( $10^{10}$  gc) or the control vector AAVrh.10xV ( $10^{10}$  gc) in  $1\ \mu\text{l}$  of PBS was administered by the intravitreal route to C57BL/6 mice. Five weeks later, eyes were enucleated, and paraffin sections were stained using biotin-conjugated donkey anti-human IgG as primary antibody and Cy3-conjugated streptavidin as secondary antibody. Nuclei were stained with DAPI. Untreated control eyes were stained in the same way. Bevacizumab is indicated by red, and nucleus by blue. INL, inner nuclear layer; ONL, outer nuclear layer; OPL, outer plexiform layer; RPE, retinal pigment epithelium. Scale bars =  $200\ \mu\text{m}$  (A, C, E) and  $50\ \mu\text{m}$  (B, D, F). Note that A and E represent areas less central to the retina, so cell layers are thinner.

outcomes (Avery *et al.*, 2006; Brown *et al.*, 2006; Rosenfeld *et al.*, 2006; Regillo *et al.*, 2008; Elman *et al.*, 2010; Folk and Stone, 2010; Gulkilik *et al.*, 2010; Mitchell *et al.*, 2010; Nicholson and Schachat, 2010; Schmidt-Erfurth *et al.*, 2010; Waisbourd *et al.*, 2010). To circumvent the discomfort to the patient of monthly intravitreal injections, the economic burden of this expensive therapy, and the uncommon, but serious, ocular complication rate associated with repeated intravitreal administration, we have devised an AAV-mediated gene-therapy strategy to deliver persistent therapeutic levels of bevacizumab to the eye using a single administration. Using AAVrh.10BevMab, a rhesus-derived AAV coding for bevacizumab, the data demonstrate that AAVrh.10BevMab expresses intact functional bevacizumab that, with a single intravitreal administration, provides effective therapy in a murine model of VEGF-mediated ocular neovascularization for at least 24 weeks, the longest time point evaluated.

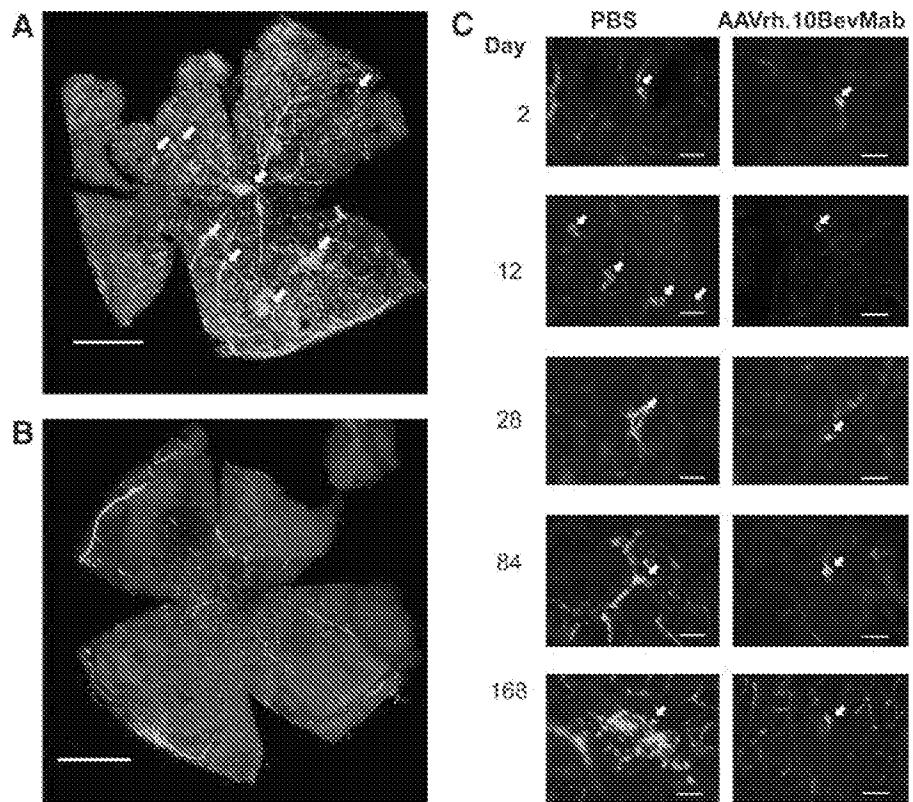
#### Anti-VEGF therapy for ocular neovascularization

DR, the primary cause of permanent blindness in adults aged 20–65 years, and AMD, the main cause of irreversible blindness in those over age 65, are predominantly VEGF-mediated pathological processes (Aiello *et al.*, 1994; Lu and Adamis, 2006; Ferrara, 2010). Up-regulation of VEGF within the eye leads to retinal neovascularization in DR and choroidal neovascularization in exudative AMD (Aiello *et al.*, 1994; Lu and Adamis, 2006; Ferrara, 2010). This pathological neovascularization results in increased vascular permeability producing

retina edema, vascular fragility leading to hemorrhage, and fibrovascular proliferation and scarring—all ultimately culminating in severe vision loss. Suppression of this VEGF-driven proangiogenic cycle has revolutionized the treatment of DR and AMD (Schlingemann and Witmer, 2009; Ferrara, 2010; Nicholson and Schachat, 2010; Waisbourd *et al.*, 2010). Numerous clinical trials have definitively demonstrated that, when compared with previously available therapies, intravitreal administration of anti-VEGF agents (either the full-length antibody bevacizumab or its Fab fragment ranibizumab) considerably improves visual outcome in these patients (Avery *et al.*, 2006; Brown *et al.*, 2006; Rosenfeld *et al.*, 2006; Regillo *et al.*, 2008; Schlingemann and Witmer, 2009; Elman *et al.*, 2010; Ferrara, 2010; Folk and Stone, 2010; Gulkilik *et al.*, 2010; Mitchell *et al.*, 2010; Nicholson and Schachat, 2010; Schmidt-Erfurth *et al.*, 2010; Waisbourd *et al.*, 2010). For example, in the two pivotal ranibizumab trials in patients with exudative AMD (ANCHOR and MARINIA), on average, all patients in the standard-of-care group lost vision at the 1- and 2-year time points. This is in dramatic contrast to those patients receiving monthly intraocular anti-VEGF injections, where 95% of patients maintained, and 30–40% improved, their vision at the 1- and 2-year time points (Brown *et al.*, 2006; Rosenfeld *et al.*, 2006; Mitchell *et al.*, 2010). Thus, anti-VEGF therapy has become the standard of care for these ocular disorders.

However, the relatively short half-life of intraocularly administered proteins (including bevacizumab and ranibizumab) necessitates frequent and repeated administration to maintain adequate therapeutic levels. When compared in AMD and DR

**FIG. 4.** Ability of AAVrh.10BevMab to suppress neovascularization in rho/VEGF transgenic mice with overexpression of VEGF in photoreceptors. At postnatal day 14, rho/VEGF mice were given an intravitreal injection of 1  $\mu$ l of PBS in one eye and 1  $\mu$ l containing  $10^{10}$  gc AAVrh.10BevMab in the other eye. At 2, 14, 28, 84, and 168 days post injection, the total area of subretinal neovascularization per eye was quantified from retinal flatmount. **(A)** Composite flatmount of whole retina from the untreated eye at 24 weeks post vector at low magnification (scale bar=1 mm). White arrows point to areas of extensive capillary leakage. **(B)** Composite flatmount of whole retina from the treated eye at 24 weeks post vector (scale bar=1 mm). For A and B, an overexposed image of the retina was taken using the red channel and then gray-scaled to demonstrate tissue morphology. This image was overlapped onto an image taken in the green channel (FITC-dextran), which is used to demonstrate vasculature. The histogram of the untreated control was then adjusted to show only the brightest fluorescing areas in the green channel. **(C)** Representative higher magnification images of fluorescence microscopy of retinal flatmounts at days 2–168 post therapy (scale bars=100  $\mu$ m).



clinical trials, patients treated less frequently (either quarterly or on an “as needed” basis) showed less pronounced benefit of visual outcomes (Regillo *et al.*, 2008; Mitchell *et al.*, 2010; Schmidt-Erfurth *et al.*, 2010). Patients switched from monthly therapy to an “as needed” anti-VEGF therapy regimen had, on average, greater visual decline compared with a monthly treatment regimen (Regillo *et al.*, 2008; Mitchell *et al.*, 2010; Schmidt-Erfurth *et al.*, 2010). Without prolonged VEGF blockage via repeated intravitreal injections of currently available anti-VEGF agents, the proangiogenic process is reactivated and visual outcome is compromised. However, these repeated injections come at the high cost of a cumulative risk of visually devastating complications, including intraocular hemorrhage, retinal detachment, and endophthalmitis (Jager *et al.*, 2004; Schmidt-Erfurth *et al.*, 2010). For example, when the anti-VEGF clinical trials are taken together, over a 1–2-year period of repeated intravitreal injections, the per-eye risk of intraocular infection approaches 1% (Brown *et al.*, 2006; Rosenfeld *et al.*, 2006; Elman *et al.*, 2010). With some patients potentially requiring decades-long VEGF suppression, the local complication rate becomes a significant impediment to the adequate treatment of pathological ocular neovascularization.

#### AAV-mediated anti-VEGF gene therapy

One rational approach to achieve a sustained therapeutic effect following a single intravitreal injection is that of AAV-mediated gene transfer. As a compartmentalized, self-contained, easily assessable, relatively small, immune privi-

leged organ, the eye is an ideal site for *in vivo* gene transfer (Bainbridge *et al.*, 2003). Ocular gene-transfer strategies have been developed for gene-augmentation therapy in recessively inherited disorders (*e.g.*, autosomal recessive and X-linked recessive retinitis pigmentosa, Usher syndrome, X-linked retinoschisis, Leber’s congenital amaurosis); for gene silencing in dominantly inherited disorders (*e.g.*, autosomal dominant retinitis pigmentosa, retinoblastoma); and for treatment of ocular pathologic processes (*e.g.*, DR and AMD) (Roy *et al.*, 2010). For example, the clinical trial of rAAV2-CB-hRPE65 in patients with Leber’s congenital amaurosis demonstrated the safety and efficacy of ocular gene therapy with clinically quantifiable improvements in visual function up to 1.5 years following a single injection, without any serious ocular or systemic side effects (Simonelli *et al.*, 2010). Given the accumulating evidence for the safety and efficacy of ocular gene therapy, our approach to the long-term suppression of ocular neovascularization in DR and AMD was that of AAV-mediated gene-transfer strategy.

Although all human studies on AAV gene transfer to the eye have involved serotype 2 (Hauswirth *et al.*, 2008; Simonelli *et al.*, 2010), there is ample evidence in animals that other AAV serotypes derived from nonhuman primates provide higher levels of transgene expression (Leberherz *et al.*, 2008). AAVrh.10 is derived from rhesus macaque and is extremely effective in gene transfer to pleura and brain (De *et al.*, 2006; Sondhi *et al.*, 2007). In a previous study, intravitreal injection into the eye of AAVrh.10 expressing enhanced GFP efficiently transduced several cell types of the retina, including cells of the outer

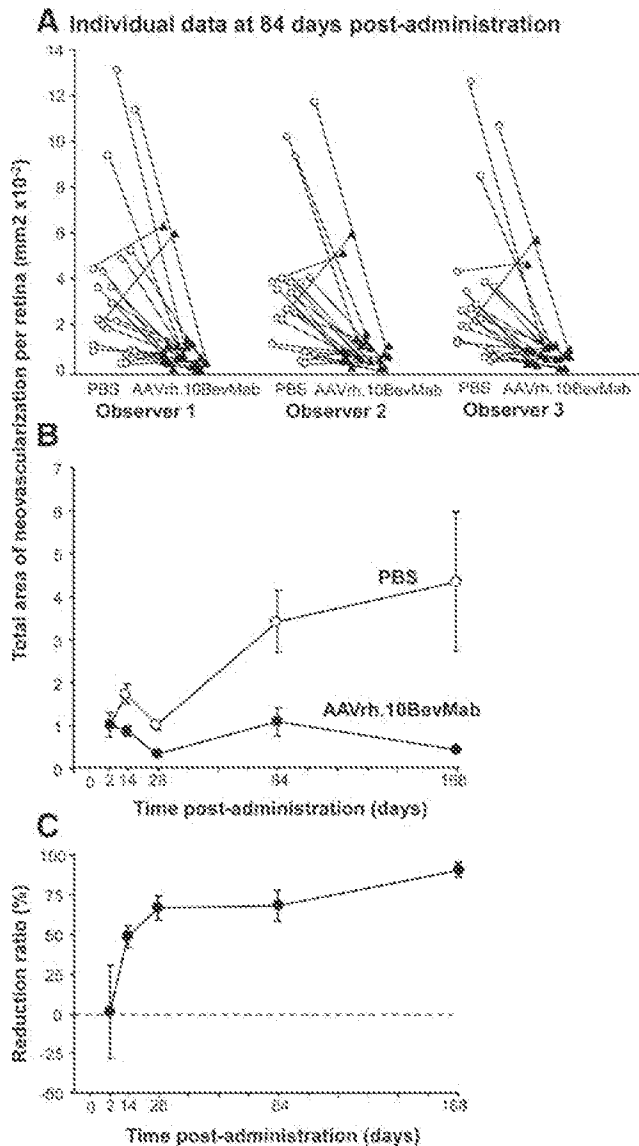


**FIG. 5.** AAVrh.10BevMab-mediated suppression of neovascularization compared with PBS. At postnatal day 14, homozygous rho/VEGF mice were injected intravitreally with 1  $\mu$ l of PBS to one eye and 10<sup>10</sup> gc of AAVrh.10BevMab in 1  $\mu$ l to the other eye. At 2, 14, 28, 84, and 168 days post therapy, the total area of subretinal neovascularization per eye was quantified by retinal flatmount. **(A)** Examples of data from three individual observers for individual mice. Shown are data at day 84 post administration. Lines connect the PBS versus AAVrh.10BevMab data for individual mice. **(B)** Average data for AAVrh.10BevMab versus PBS. **(C)** Percent reduction in total area of neovascularization per retina with AAVrh.10BevMab versus PBS, calculated as: [(mean neovascular bud area in PBS-injected eye at indicated time point) - (neovascular bud area in AAVrh.10BevMab-injected eye at indicated time point)] / (mean neovascular bud area in PBS-injected eye). A positive percentage represents a reduction in neovascularization. For A–C, see Table 1 for statistical assessment for intraobserver variability and statistics for all data at all time points.

plexiform layer, the ganglion cell layer, and the RPE (Grove *et al.*, 2010). In the present study, bevacizumab delivered by AAVrh.10 accumulated exclusively in the RPE. This apparent inconsistency may reflect several factors, including the use of an intracellular (GFP) versus a secreted transgene (bevacizumab) and mouse strain differences. In addition, the receptor for AAVrh.10 is unknown and the specific factors affecting tropism are not defined.

Other gene-therapy approaches for the treatment of pathologic ocular neovascularization have included viral vectors that encode various antiangiogenic agents, including endostatin, angiostatin, pigment epithelial-derived factor, and sFLT01 (Bainbridge *et al.*, 2003; Roy *et al.*, 2010). A phase 1 clinical trial using intravitreal AAV2-sFLT01 in patients with AMD has just recently been completed. Although no dose-limiting toxicities have been publicly reported in this trial, it is not known whether sFLT01 itself has sufficient antiangiogenic activity to provide similar visual outcomes to currently available anti-VEGF therapeutics. Anti-VEGF therapy with bevacizumab, on the other hand, is an existing, well-characterized, therapeutic agent with proven efficacy and an acceptable safety profile following repeated intravitreal injections in patients with DR and AMD (Avery *et al.*, 2006; Brown *et al.*, 2006; Rosenfeld *et al.*, 2006; Regillo *et al.*, 2008; Singerman *et al.*, 2008; Schlingemann and Witmer, 2009; Elman *et al.*, 2010; Ferrara, 2010; Folk and Stone, 2010; Gulkilik *et al.*, 2010; Mitchell *et al.*, 2010; Nicholson and Schachat, 2010; Schmidt-Erfurth *et al.*, 2010; Waisbourd *et al.*, 2010). Therefore, our approach was to use bevacizumab rather than another agent in the AAV-mediated intraocular antiangiogenesis gene therapy and improve the only known shortcoming of this therapy: persistence of action. Toward that end, we engineered an AAV vector that encodes the antibody heavy- and light-chain variable domains of the humanized version of the murine mAb corresponding to bevacizumab (AAVrh.10BevMab).

*In vitro* analysis of our AAVrh.10BevMab vector product showed it to have equivalent VEGF-binding properties to native bevacizumab used clinically. Following a single intravitreal injection, the vector was able to transfect the RPE cells and to produce bevacizumab. Intraocular bevacizumab levels were detected by day 14 and remained elevated up to 24 weeks, the last time point tested. *In vivo* efficacy of our AAVrh.10BevMab vector was tested in a well-characterized VEGF-mediated ocular neovascularization model that mimics critical features of neovascular AMD. A single intravitreal injection of bevacizumab in this model typically suppresses ocular neovascularization for 2 weeks. Using our AAVrh.10BevMab vector, we were able to meaningfully suppress ocular neovascularization following a single intravitreal injection for up to 24 weeks, the last time point tested.

Ocular gene-therapy strategies have used either intravitreal or subretinal approaches for intraocular delivery of the viral vector (Bainbridge *et al.*, 2003, 2008; Roy *et al.*, 2010; Lukason *et al.*, 2011). In current clinical practice, however, intravitreal injections are used for anti-VEGF treatment of AMD and DR. Intravitreal injections are less invasive than subretinal injections, have a considerably more favorable side-effect profile, and can be performed in an office setting. Subretinal injections, on the other hand, require the patient to undergo a surgical procedure. Hence, our approach for long-term suppression of ocular neovascularization was that of an

TABLE 1. INTEROBSERVER VARIABILITY

Observer	Treatment	Area of NV per retina ( $\text{mm}^2 \times 10^{-2}$ ; days)				
		2	14	28	84	168
1	PBS	0.90±0.23	1.64±0.20	1.02±0.11	3.61±0.79	4.29±1.60
	AAVrh.10BevMab	0.85±0.22	0.81±0.10	0.35±0.07	1.08±0.37	0.43±0.07
2	PBS	1.17±0.30	1.98±0.31	1.08±0.13	3.44±0.70	4.49±1.68
	AAVrh.10BevMab	1.22±0.35	1.03±0.16	0.33±0.08	1.15±0.33	0.45±0.06
3	PBS	1.01±0.28	1.59±0.21	0.94±0.11	3.21±0.73	4.28±1.60
	AAVrh.10BevMab	1.00±0.33	0.82±0.12	0.34±0.09	1.15±0.33	0.45±0.07
p value (2-way ANOVA)	For treatment	>0.96	<0.0001**	<0.0001**	<0.0001**	<0.0001**
	For observer	>0.52	>0.243	>0.76	>0.92	>0.99
p value (3-way ANOVA)	For treatment	>0.9	<0.0001**	<0.0001**	<0.0001**	<0.0001**
	For observer	>0.01*	>0.028	>0.49	>0.86	>0.98
	For mouse	<0.0001**	<0.0001**	<0.0001**	<0.0001**	<0.002**

Observer means and standard deviations were calculated after summing over mice. The effects of treatment, observer, and mouse were assessed using permutations after fitting a two-factor and three-factor ANOVA model.

NV, neovascularization.

\* $p < 0.05$ , but not significant after a multiple test correction.

\*\*Significant test results.

intravitreal injection route. This was the same strategy used for the AAV2-sFLT01 preclinical and phase 1 studies (ClinicalTrials.gov, 2011; Lukason *et al.*, 2011; MacLachlan *et al.*, 2011). Similar to the AAV2-sFLT01 data, the results of our approach include retinal cell transfection, localized transgene expression, and suppression of neovascularization.

One potential criticism of using AAVrh.10BevMab for ocular gene therapy for AMD and DR is the theoretical deleterious effect of prolonged ocular VEGF suppression. Although these warrant careful surveillance and further investigation, clinical experience with hundreds of thousands of patients who have received continued intraocular anti-VEGF therapy over many years (up to 3 years with the clinically available intraocular anti-VEGF therapies) have yet to show any detrimental consequences of prolonged VEGF blockage (Avery *et al.*, 2006; Brown *et al.*, 2006; Rosenfeld *et al.*, 2006; Regillo *et al.*, 2008; Singerman *et al.*, 2008; Schlingemann and Witmer, 2009; Elman *et al.*, 2010; Ferrara, 2010; Folk and Stone, 2010; Gulkilik *et al.*, 2010; Mitchell *et al.*, 2010; Nicholson and Schachat, 2010; Schmidt-Erfurth *et al.*, 2010; Waisbourd *et al.*, 2010). In fact, the opposite appears to be true, as patients who are not treated with anti-VEGF therapy ultimately end up with significantly worse visual function. Along the same lines, the most recent evidence on long-term ocular VEGF suppression in several animal models has shown no abnormalities of the choriocapillaris and no indication of retinal cell dysfunction (Singerman *et al.*, 2008; Ueno *et al.*, 2008). At this time, most experimental and all clinical evidence indicates that long-term VEGF suppression is preferred in patients with AMD and DM.

This study provides the first report of sustained suppression of ocular neovascularization using a well-characterized, existing therapeutic approach with proven clinical efficacy. With the goal of minimizing dosing intervals and maximizing clinical efficacy, a single administration of AAVrh.10-BevMab provides long-term expression of bevacizumab and suppression of VEGF-mediated ocular neovascularization. The results of this study warrant the further investigation of AAVrh.10BevMab as a long-term therapeutic approach for the treatment of AMD and DR.

## Acknowledgments

We thank Stacey Chen for help with the analysis and N. Mohamed for help in preparing the manuscript. These studies were supported, in part, by P50 HL084936, T32 HL094284, and UL1-RR024996, and Research to Prevent Blindness, New York, NY.

## Author Disclosure Statement

No competing financial interests exist.

## References

- Aiello, L.P., Avery, R.L., Arrigg, P.G., *et al.* (1994). Vascular endothelial growth factor in ocular fluid of patients with diabetic retinopathy and other retinal disorders. *N. Engl. J. Med.* 331, 1480–1487.
- Arevalo, J.F., Sanchez, J.G., Lasave, A.F., *et al.* (2011). Intravitreal bevacizumab (Avastin) for diabetic retinopathy: The 2010 GLADAOF Lecture. *J. Ophthalmol.* 2011, 584238.
- Avery, R.L., Pieramici, D.J., Rabena, M.D., *et al.* (2006). Intravitreal bevacizumab (Avastin) for neovascular age-related macular degeneration. *Ophthalmology* 113, 363–372.
- Bainbridge, J.W., Mistry, A.R., Thrasher, A.J., *et al.* (2003). Gene therapy for ocular angiogenesis. *Clin. Sci. (Lond.)* 104, 561–575.
- Bainbridge, J.W., Smith, A.J., Barker, S.S., *et al.* (2006). Effect of gene therapy on visual function in Leber's congenital amaurosis. *N. Engl. J. Med.* 358, 2231–2239.
- Brown, D.M., Kaiser, P.K., Michels, M., *et al.* (2006). Ranibizumab versus verteporfin for neovascular age-related macular degeneration. *N. Engl. J. Med.* 355, 1432–1444.
- Buch, P.K., Bainbridge, J.W., and Ali, R.R. (2008). AAV-mediated gene therapy for retinal disorders: from mouse to man. *Gene Ther.* 15, 849–857.
- Chen, Y., Wiesmann, C., Fuh, G., *et al.* (1999). Selection and analysis of an optimized anti-VEGF antibody: crystal structure of an affinity-matured Fab in complex with antigen. *J. Mol. Biol.* 293, 865–881.
- ClinicalTrials.gov (2011). Safety and tolerability study of AAV2-SFLT01 in patients with neovascular age-related macular

- degeneration (AMD). <http://clinicaltrials.gov/2011>. Reference type: electronic citation. ClinicalTrials.gov Identifier NCT01024998.
- Daly, T.M., Vogler, C., Levy, B., *et al.* (1999). Neonatal gene transfer leads to widespread correction of pathology in a murine model of lysosomal storage disease. *Proc. Natl. Acad. Sci. U.S.A.* 96, 2296–2300.
- De, B.P., Heguy, A., Hackett, N.R., *et al.* (2006). High levels of persistent expression of  $\alpha$ 1-antitrypsin mediated by the non-human primate serotype rh.10 adeno-associated virus despite preexisting immunity to common human adeno-associated viruses. *Mol. Ther.* 13, 67–76.
- Elman, M.J., Aiello, L.P., Beck, R.W., *et al.* (2010). Randomized trial evaluating ranibizumab plus prompt or deferred laser or triamcinolone plus prompt laser for diabetic macular edema. *Ophthalmology* 117, 1064–1077.
- Fang, J., Qian, J.J., Yi, S., *et al.* (2005). Stable antibody expression at therapeutic levels using the 2A peptide. *Nat. Biotechnol.* 23, 584–590.
- Ferrara, N. (2010). Vascular endothelial growth factor and age-related macular degeneration: from basic science to therapy. *Nat. Med.* 16, 1107–1111.
- Ferrara, N., Hillan, K.J., Gerber, H.P., *et al.* (2004). Discovery and development of bevacizumab, an anti-VEGF antibody for treating cancer. *Nat. Rev. Drug Discov.* 3, 391–400.
- Folk, J.C., and Stone, E.M. (2010). Ranibizumab therapy for neovascular age-related macular degeneration. *N. Engl. J. Med.* 363, 1648–1655.
- Friedman, D.S., O'Colmain, B.J., Munoz, B., *et al.* (2004). Prevalence of age-related macular degeneration in the United States. *Arch. Ophthalmol.* 122, 564–572.
- Gao, G.P., Alvira, M.R., Wang, L., *et al.* (2002). Novel adeno-associated viruses from rhesus monkeys as vectors for human gene therapy. *Proc. Natl. Acad. Sci. U.S.A.* 99, 11854–11859.
- Giove, T.J., Sena-Esteves, M., and Eldred, W.D. (2010). Transduction of the inner mouse retina using AAVrh8 and AAVrh10 via intravitreal injection. *Exp. Eye Res.* 91, 652–659.
- Gulkilik, G., Taskapili, M., Kocabora, S., *et al.* (2010). Intravitreal bevacizumab for persistent macular edema with proliferative diabetic retinopathy. *Int. Ophthalmol.* 30, 697–702.
- Hauswirth, W.W., Aleman, T.S., Kaushal, S., *et al.* (2008). Treatment of Leber congenital amaurosis due to RPE65 mutations by ocular subretinal injection of adeno-associated virus gene vector: short-term results of a phase I trial. *Hum. Gene Ther.* 19, 979–990.
- Jager, R.D., Aiello, L.P., Patel, S.C., *et al.* (2004). Risks of intravitreal injection: a comprehensive review. *Retina* 24, 676–698.
- Leberherz, C., Maguire, A., Tang, W., *et al.* (2008). Novel AAV serotypes for improved ocular gene transfer. *J. Gene Med.* 10, 375–382.
- Lu, M., and Adamis, A.P. (2006). Molecular biology of choroidal neovascularization. *Ophthalmol. Clin. North Am.* 19, 323–334.
- Lukason, M., Dufresne, E., Rubin, H., *et al.* (2011). Inhibition of choroidal neovascularization in a nonhuman primate model by intravitreal administration of an AAV2 vector expressing a novel anti-VEGF molecule. *Mol. Ther.* 19, 260–265.
- MacLachlan, T.K., Lukason, M., Collins, M., *et al.* (2011). Pre-clinical safety evaluation of AAV2-sFLT01—a gene therapy for age-related macular degeneration. *Mol. Ther.* 19, 326–334.
- Miki, K., Miki, A., Matsuoka, M., *et al.* (2009). Effects of intraocular ranibizumab and bevacizumab in transgenic mice expressing human vascular endothelial growth factor. *Ophthalmology* 116, 1748–1754.
- Mitchell, P., Korobelnik, J.F., Lanzetta, P., *et al.* (2010). Ranibizumab (Lucentis) in neovascular age-related macular degeneration: evidence from clinical trials. *Br. J. Ophthalmol.* 94, 2–13.
- Montero, J.A., Ruiz-Moreno, J.M., and Correa, M.E. (2011). Intravitreal anti-VEGF drugs as adjuvant therapy in diabetic retinopathy surgery. *Curr. Diabetes Rev.* 7, 176–184.
- Nicholson, B.P., and Schachat, A.P. (2010). A review of clinical trials of anti-VEGF agents for diabetic retinopathy. *Graefes Arch. Clin. Exp. Ophthalmol.* 248, 915–930.
- Niwa, H., Yamamura, K., and Miyazaki, J. (1991). Efficient selection for high-expression transfectants with a novel eukaryotic vector. *Gene* 108, 193–199.
- Okamoto, N., Tobe, T., Hackett, S.F., *et al.* (1997). Transgenic mice with increased expression of vascular endothelial growth factor in the retina: a new model of intraretinal and subretinal neovascularization. *Am. J. Pathol.* 151, 281–291.
- Ozturk, B.T., Kerimoglu, H., Bozkurt, B., and Okudan, S. (2011). Comparison of intravitreal bevacizumab and ranibizumab treatment for diabetic macular edema. *J. Ocul. Pharmacol. Ther.* 27, 373–377.
- Regillo, C.D., Brown, D.M., Abraham, P., *et al.* (2008). Randomized, double-masked, sham-controlled trial of ranibizumab for neovascular age-related macular degeneration: PIER Study year 1. *Am. J. Ophthalmol.* 145, 239–248.
- Rosenfeld, P.J., Brown, D.M., Heier, J.S., *et al.* (2006). Ranibizumab for neovascular age-related macular degeneration. *N. Engl. J. Med.* 355, 1419–1431.
- Roy, K., Stein, L., and Kaushal, S. (2010). Ocular gene therapy: an evaluation of recombinant adeno-associated virus-mediated gene therapy interventions for the treatment of ocular disease. *Hum. Gene Ther.* 21, 915–927.
- Saaddine, J.B., Honeycutt, A.A., Narayan, K.M., *et al.* (2008). Projection of diabetic retinopathy and other major eye diseases among people with diabetes mellitus: United States, 2005–2050. *Arch. Ophthalmol.* 126, 1740–1747.
- Salam, A., Mathew, R., and Sivaprasad, S. (2011). Treatment of proliferative diabetic retinopathy with anti-VEGF agents. *Acta Ophthalmol.* 89, 405–411.
- Schlingemann, R.O., and Witmer, A.N. (2009). Treatment of retinal diseases with VEGF antagonists. *Prog. Brain Res.* 175, 253–267.
- Schmidt-Erfurth, U., Eldem, B., Guymer, R., *et al.* (2010). Efficacy and safety of monthly versus quarterly ranibizumab treatment in neovascular age-related macular degeneration: The EXCITE Study. *Ophthalmology* 118, 831–839.
- Simonelli, F., Maguire, A.M., Testa, F., *et al.* (2010). Gene therapy for Leber's congenital amaurosis is safe and effective through 1.5 years after vector administration. *Mol. Ther.* 18, 643–650.
- Singerman, L.J., Masonson, H., Patel, M., *et al.* (2008). Pegaptanib sodium for neovascular age-related macular degeneration: third-year safety results of the VEGF Inhibition Study in Ocular Neovascularisation (VISION) trial. *Br. J. Ophthalmol.* 92, 1606–1611.
- Sondhi, D., Hackett, N.R., Peterson, D.A., *et al.* (2007). Enhanced survival of the LINCL mouse following CLN2 gene transfer using the rh.10 rhesus macaque-derived adeno-associated virus vector. *Mol. Ther.* 15, 481–491.
- Ueno, S., Pease, M.E., Wersinger, D.M., *et al.* (2008). Prolonged blockade of VEGF family members does not cause identifiable damage to retinal neurons or vessels. *J. Cell. Physiol.* 217, 13–22.
- Waisbourd, M., Goldstein, M., and Loewenstein, A. (2010). Treatment of diabetic retinopathy with anti-VEGF drugs. *Acta Ophthalmol.* 89, 203–207.
- Wang, G., Qiu, J., Wang, R., *et al.* (2010). Persistent expression of biologically active anti-HER2 antibody by AAVrh.10-mediated gene transfer. *Cancer Gene Ther.* 17, 559–570.

- Watanabe, M., Boyer, J.L., Hackett, N.R., *et al.* (2008). Genetic delivery of the murine equivalent of bevacizumab (Avastin), an anti-vascular endothelial growth factor monoclonal antibody, to suppress growth of human tumors in immunodeficient mice. *Hum. Gene Ther.* 19, 300–310.
- Witkin, A.J., and Brown, G.C. (2011). Update on nonsurgical therapy for diabetic macular edema. *Curr. Opin. Ophthalmol.* 22, 185–189.
- Xiao, X., Li, J., and Samulski, R.J. (1998). Production of high-titer recombinant adeno-associated virus vectors in the absence of helper adenovirus. *J. Virol.* 72, 2224–2232.

Address correspondence to:  
*Department of Genetic Medicine*  
*Medical College of Cornell University*  
*1300 York Avenue, Box 96*  
*New York, NY 10065*

*E-mail:* geneticmedicine@med.cornell.edu

Received for publication May 22, 2011;  
accepted after revision July 29, 2011.

Published online: July 29, 2011.



EX. M



US 20130090375A1

(19) **United States**

(12) **Patent Application Publication**

**Crystal et al.**

(10) **Pub. No.: US 2013/0090375 A1**

(43) **Pub. Date: Apr. 11, 2013**

(54) **VIRUS-MEDIATED DELIVERY OF BEVACIZUMAB FOR THERAPEUTIC APPLICATIONS**

**Related U.S. Application Data**

(60) Provisional application No. 61/544,210, filed on Oct. 6, 2011.

(75) Inventors: **Ronald G. Crystal**, New York, NY (US); **Stephen M. Kaminsky**, Bronx, NY (US); **Donald Joseph D'Amico**, New York, NY (US); **Julie Boyer**, Guilford, CT (US); **Sillard Kiss**, New York, NY (US)

**Publication Classification**

(51) **Int. Cl.**  
*A61K 31/7088* (2006.01)  
*A61P 9/00* (2006.01)  
*A61P 27/02* (2006.01)

(73) Assignee: **CORNELL UNIVERSITY**, Ithaca, NY (US)

(52) **U.S. CL.**  
USPC ..... **514/44 R**

(21) Appl. No.: **13/537,457**

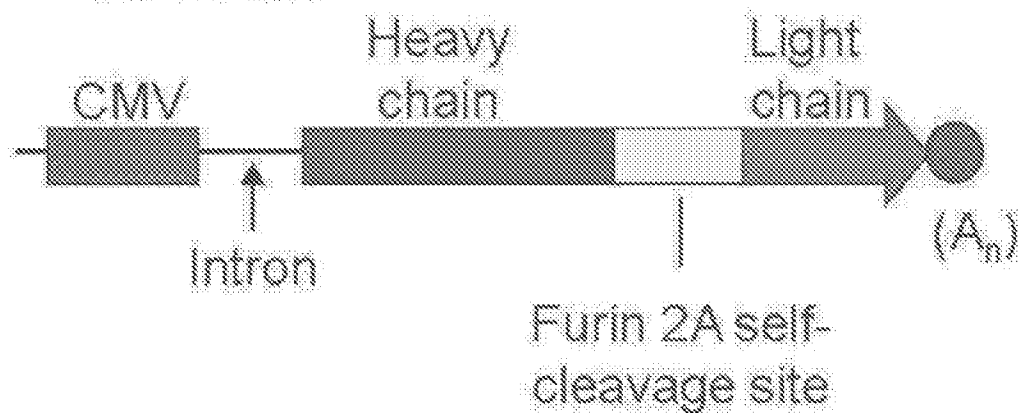
(57) **ABSTRACT**

(22) Filed: **Jan. 29, 2012**

The invention provides a method of inhibiting ocular neovascularization in a mammal by administering a composition comprising a bevacizumab-encoding adeno-associated virus (AAV) vector directly to the eye of the mammal.

FIG. 1

**Bevacizumab expression cassette**



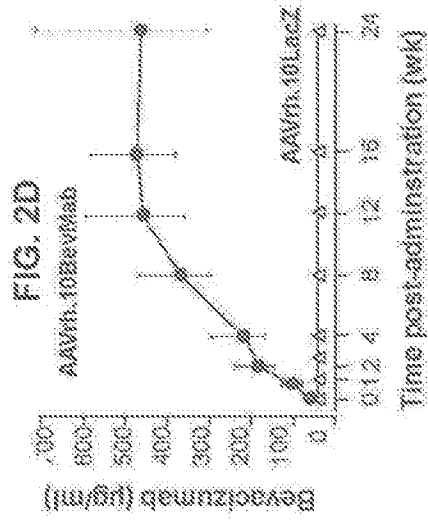
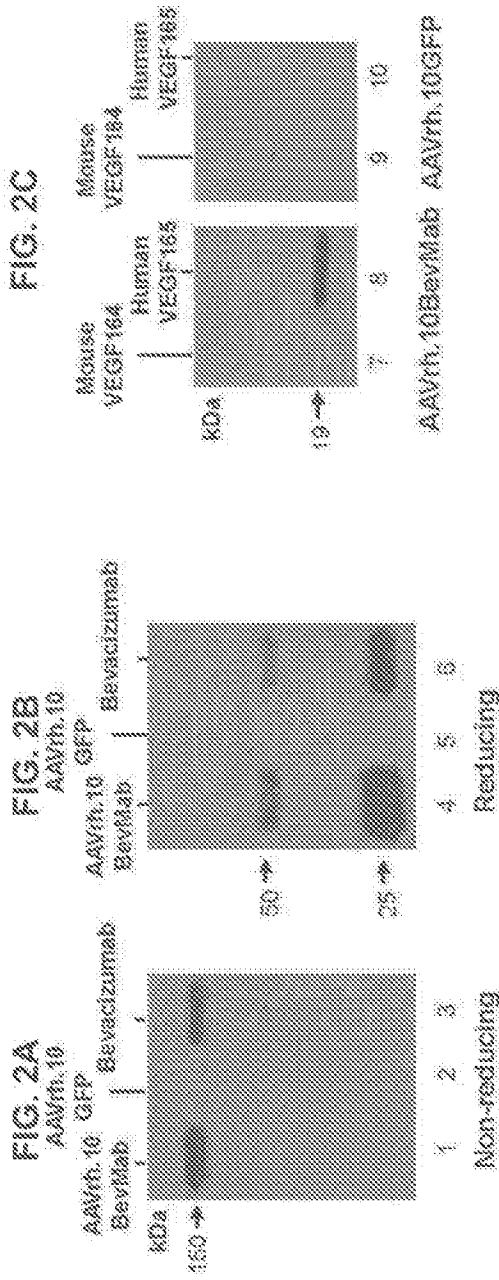


FIG. 3B

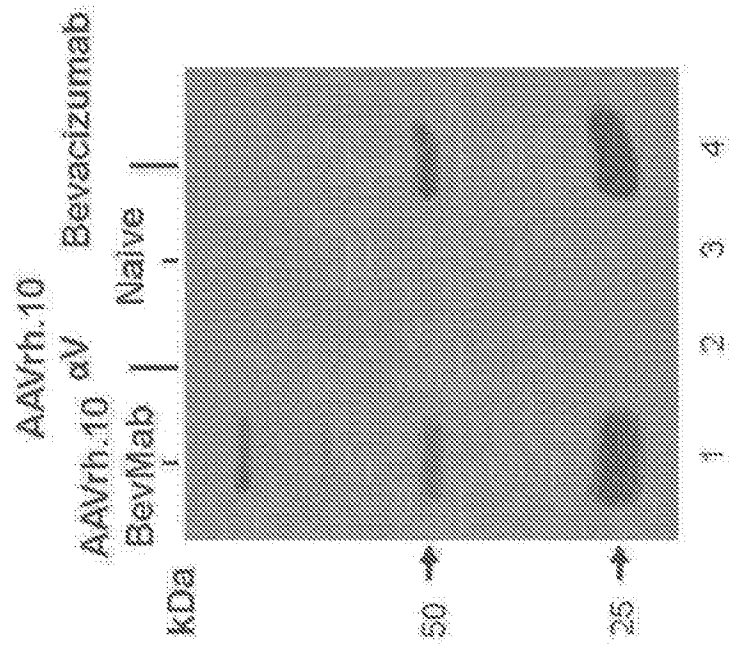


FIG. 3A

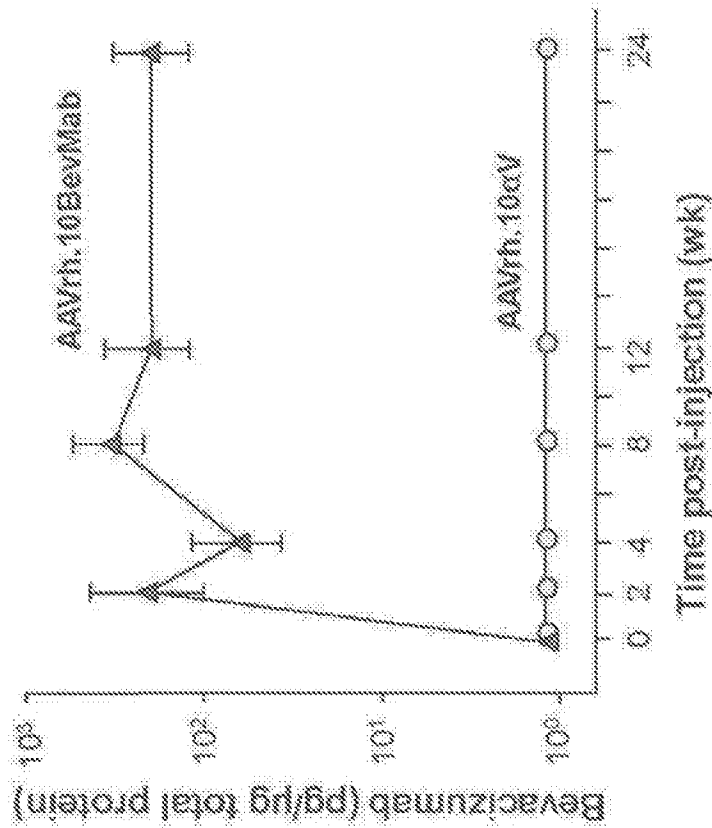


FIG. 4A

A. Individual data at 84 days post-administration

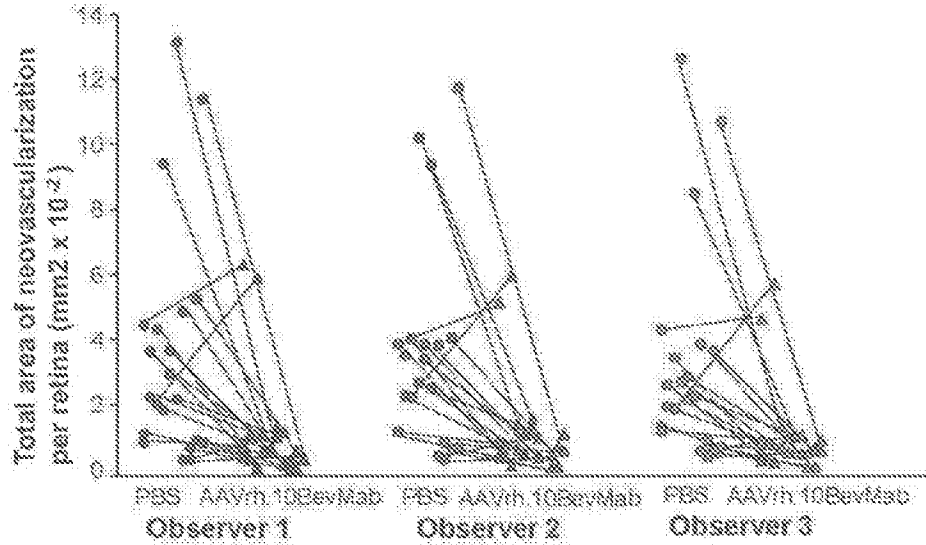


FIG. 4B

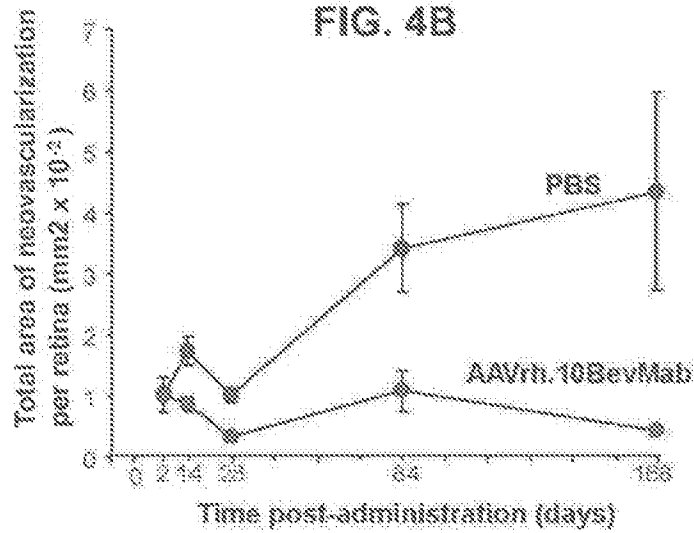
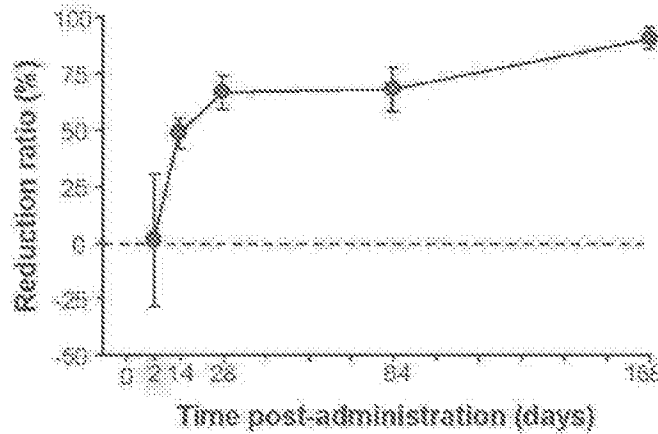


FIG. 4C



## VIRUS-MEDIATED DELIVERY OF BEVACIZUMAB FOR THERAPEUTIC APPLICATIONS

### INCORPORATION-BY-REFERENCE OF MATERIAL SUBMITTED ELECTRONICALLY

[0001] Incorporated by reference in its entirety herein is a computer-readable nucleotide/amino acid sequence listing submitted concurrently herewith and identified as follows: One 4,577 Byte ASCII (Text) file named "710331 ST25.TXT," created on Jun. 29, 2012.

### BACKGROUND OF THE INVENTION

[0002] Pathological ocular neovascularization is the hallmark of age-related macular degeneration (AMD) and diabetic retinopathy (DR), two of the leading causes of blindness in the industrialized world (see, e.g., Elman et al., *Ophthalmology*, 117: 1064-1077 (2010); and Folk and Stone, *N. Engl. J. Med.*, 363: 1648-1655 (2010)). The prevalence of AMD in the United States is expected to increase to nearly 3 million by 2020, whereas the prevalence of DR is projected to triple to 16 million by 2050 (see, e.g., Friedman et al., *Arch. Ophthalmol.*, 122: 564-572 (2004); and Saaddine et al., *Arch. Ophthalmol.*, 126: 1740-1747 (2008)). Local up-regulation of the expression of vascular endothelial growth factor (VEGF) plays a central role in the pathogenesis of both disorders (see, e.g., Aiello et al., *N. Engl. J. Med.*, 331: 1480-1487 (1994); and Ferrara et al., *Nat. Med.*, 16: 1107-1111 (2010)).

[0003] The clinical use of intravitreal anti-VEGF agents has been shown to slow the progression of vision loss and improve visual acuity in patients with AMD and DR (see, e.g., Avery et al., *Ophthalmology*, 113: 363-372 (2006); Rosenfeld et al., *N. Engl. J. Med.*, 355: 1419-1431 (2006); Elman et al., supra; and Gulkilik et al., *Int. Ophthalmol.*, 30: 697-702 (2010)). A widely used anti-VEGF ocular therapy is bevacizumab (AVASIN<sup>®</sup>; Genentech, Inc., South San Francisco, Calif.), which is a humanized monoclonal antibody (mAb) specific for human VEGF (see, e.g., Ferrara et al., *Nat. Rev. Drug Discov.*, 3: 391-400 (2004); Avery et al., supra, and U.S. Pat. No. 6,884,879). Numerous clinical studies have established that intravitreal administration of bevacizumab inhibits VEGF-dependent neovascularization and vascular permeability, improves visual outcomes, and decreases vision loss in patients with AMD and DR. Since their introduction, intravitreal injections of bevacizumab and its antigen-binding fragment (Fab) ranibizumab have become the standard of care for treatment of AMD and are becoming the standard of care for DR, especially diabetic macular edema (see, e.g., Avery et al., supra; Gulkilik et al., supra; Nicholson and Schachat, *Graefes Arch. Clin. Exp. Ophthalmol.*, 248: 915-930 (2010); Arevalo et al., *J. Ophthalmol.*, Article ID 584238 (2011); Montero et al., *Curr. Diabetes Rev.*, 7: 176-184 (2011); Öztürk et al., *J. Ocul. Pharmacol. Ther.*, 27: 373-377 (2011); Salam et al., *Acta Ophthalmol.*, 89: 405-411 (2011); and Witkin and Brown, *Curr. Opin. Ophthalmol.*, 22: 185-189 (2011)). However, the positive effect on visual acuity is often of limited duration, with the need for repeated (typically monthly) injections to achieve optimal visual outcome (see, e.g., Regillo et al., *Am J Ophthalmol.*, 145: 239-248 (2008); Elman et al., supra; Gulkilik et al., supra; Mitchell et al., *Br. J. Ophthalmol.*, 94: 2-13 (2010); and Schmidt-Erfurth et al., *Ophthalmology*, 118(5): 831-839 (2011) (Epub Dec. 13, 2010)).

[0004] Repeated intravitreal administrations pose significant burdens on the patient and the health care system, and also pose a risk of potentially devastating ocular complications. The most serious adverse event is infectious endophthalmitis. More frequent, although less devastating, adverse events associated with repeated intravitreal administrations include vitreous hemorrhage, retinal detachment, traumatic cataract, corneal abrasion, subconjunctival hemorrhage, and eyelid swelling (see, e.g., Jager et al., *Retina*, 24: 676-698 (2004); Brown et al., *N. Engl. J. Med.*, 355: 1432-1444 (2006); Rosenfeld et al., supra; Elman et al., supra; and Folk and Stone, supra).

[0005] Thus, there remains a need for improved methods for intraocular delivery of bevacizumab with reduced side effects. The invention provides such methods.

### BRIEF SUMMARY OF THE INVENTION

[0006] The invention provides a method of inhibiting ocular neovascularization in a mammal. The method comprises administering a composition comprising an adeno-associated virus (AAV) vector and a pharmaceutically acceptable carrier directly to the eye of a mammal, wherein the AAV vector comprises a nucleic acid sequence encoding bevacizumab, or an antigen-binding fragment thereof, whereupon the nucleic acid sequence is expressed in the eye and ocular neovascularization is inhibited in the mammal.

### BRIEF DESCRIPTION OF THE SEVERAL VIEWS OF THE DRAWING(S)

[0007] FIG. 1 is a diagram which schematically depicts the bevacizumab cDNA expression cassette described in Example 1. "CMV" denotes the cytomegalovirus-chicken  $\beta$ -actin promoter.

[0008] FIGS. 2A and 2B are images which depict experimental data from a Western blot to assay expression of bevacizumab from the AAV vector denoted AAVrh.10BevMab (see Example 2). FIG. 2A depicts a nonreducing Western analysis (lane 1—supernatant from AAVrh.10BevMab; lane 2—AAVrh.10GFP control; and lane 3—bevacizumab alone). FIG. 2B depicts a reducing Western analysis (lane 4—AAVrh.10BevMab; lane 5—AAVrh.10GFP; lane 6—bevacizumab control). The full-length heavy and light chains of bevacizumab have molecular masses of 50 and 25 kDa, respectively.

[0009] FIG. 2C is an image which depicts experimental data from a Western blot to assay the specificity of bevacizumab produced by AAVrh.10BevMab for human VEGF. The left panel depicts results using supernatants from AAVrh.10BevMab-infected cells (lane 7—specificity for mouse VEGF-164; lane 8—specificity for human VEGF-165). The right panel depicts results using supernatants from AAVrh.10GFP-infected cells (lane 9—specificity for mouse VEGF-164; lane 10—specificity for human VEGF-165). Human VEGF-165 has a molecular mass of 19 kDa.

[0010] FIG. 2D is a graph which depicts experimental data illustrating the ability of AAVrh.10BevMab to direct persistent expression of bevacizumab in vivo. Shown are bevacizumab levels after systemic administration of the AAVrh.10BevMab vector. AAVrh.10BevMab ( $10^{11}$  gc) was administered to C57BL/6 mice by the intravenous route, and AAVrh.10LacZ ( $10^{11}$  gc) served as a control. Over 24 weeks after vector administration, bevacizumab levels were mea-

sured by a human VEGF-specific ELISA. The data are shown as the geometric mean±standard error from n=5 animals per group.

[0011] FIG. 3A is a graph which depicts experimental data illustrating bevacizumab expression levels following intravitreal administration of AAVrh.10BevMab to C57BL/6 mice. Over 24 weeks after vector administration, bevacizumab levels in eye homogenate were measured by a human VEGF-specific ELISA. Data (geometric mean±standard error) were obtained from n=6 eyes for the AAVrh.10BevMab group and n=4 eyes for the AAVrh.10cV control group.

[0012] FIG. 3B is an image which depicts experimental data from a Western blot that was performed to confirm the expression of bevacizumab in the eye post intravitreal administration of AAVrh.10BevMab. Lane 1 contained a homogenate from AAVrh.10BevMab-treated eyes. Lane 2 contained a homogenate from AAVrh.10cV-injected eyes. Lane 3 contained a homogenate from naive eyes. Lane 4 contained bevacizumab as a control. The heavy and light chains of bevacizumab expressed by the AAV vector have molecular masses of 50 and 25 kDa, respectively.

[0013] FIG. 4A-4C are graphs which depict experimental data illustrating AAVrh.10BevMab-mediated suppression of ocular neovascularization quantified by three investigators blinded to the treatment group. FIG. 4A shows data at day 24 post administration of AAVrh.10BevMab. Lines connect data for PBS-injected mice versus AAVrh.10BevMab-injected mice individually. FIG. 4B shows the average data for PBS-injected mice versus AAVrh.10BevMab-injected mice. FIG. 4C shows the percent reduction in total area of neovascularization per retina for mice treated with AAVrh.10BevMab as compared to mice receiving PBS, calculated as indicated in Example 4. A positive percentage represents a reduction in neovascularization.

#### DETAILED DESCRIPTION OF THE INVENTION

[0014] The invention is predicated, at least in part, on the ability of adeno-associated virus (AAV) vectors to be safely administered intraocularly to humans and to provide persistent expression of a therapeutic transgene (see e.g., Bainbridge et al., *N. Engl. J. Med.* 358: 2231-2239 (2008); Buch et al., *Gene Ther.* 15: 849-857 (2008); Roy et al., *Hum. Gene Ther.* 21: 915-927 (2010); Simonelli et al., *Mol. Ther.* 18: 643-650 (2010); and MacLachlan et al., *Mol. Ther.* 19: 326-334 (2010)). A single intravitreal administration of an AAV vector expressing bevacizumab desirably results in sustained intraocular expression of bevacizumab at levels sufficient for long-term suppression of ocular neovascularization with minimal adverse events.

[0015] The invention provides a method of inhibiting ocular neovascularization in a mammal. The term "ocular neovascularization" as used herein, refers to any abnormal or inappropriate proliferation of blood vessels from preexisting blood vessels in the eye (also referred to as "ocular angiogenesis"). Ocular neovascularization can occur in any tissue of the eye, and is described in detail in, e.g., *Retinal and Choroidal Angiogenesis*, John S. Penn (ed.), Springer, Dordrecht, The Netherlands (2008). For example, ocular neovascularization can occur in the choroid. The choroid is a thin, vascular membrane located under the retina. Neovascularization of the choroid can result from a variety of disorders or injuries, including, for example, photocoagulation, anterior ischemic optic neuropathy, Best's disease, choroidal hemangioma, metallic intraocular foreign body, choroidal neovascularization,

choroidal osteomas, choroidal rupture, bacterial endocarditis, choroideremia, chronic retinal detachment, drusen, deposit of metabolic waste material, endogenous *Candida* endophthalmitis, neovascularization at ora serrata, operating microscope burn, punctate inner choroidopathy, radiation retinopathy, retinal cryoinjury, retinitis pigmentosa, retinochoroidal coloboma, rubella, subretinal fluid drainage, tilted disc syndrome, *Toxoplasma retinochoroiditis*, and tuberculosis.

[0016] Ocular neovascularization also can occur in the cornea, which is a projecting, transparent section of the fibrous tunic, i.e., the outer most layer of the eye. The outermost layer of the cornea contacts the conjunctiva, while the innermost layer comprises the endothelium of the anterior chamber. Neovascularization of the cornea can occur as a result of, for example, ocular injury, surgery, infection, improper wearing of contact lenses, and diseases such as, for example, corneal dystrophies.

[0017] Ocular neovascularization can occur in the retina. The retina is a delicate ocular membrane on which images are received. Near the center of the retina is the macula lutea, which is an oval area of retinal tissue where visual sense is most acute. Common causes of retinal neovascularization include ischemia, viral infection, and retinal damage. Retinal neovascularization also can be caused by ocular disorders including, for example, age-related macular degeneration (AMD) and diabetic retinopathy (DR). Neovascularization of the retina can lead to, for example, macular edema, subretinal discoloration, scarring, and hemorrhaging. As a result, vision often is impaired as blood fills the vitreous cavity without being efficiently removed. Not only is the passage of light impeded, but an inflammatory response to the excess blood and metabolites can cause further damage to ocular tissue. In addition, the new vessels form fibrous scar tissue, which, over time, will disturb the retina causing retinal tears and detachment.

[0018] In a preferred embodiment, the inventive method inhibits ocular neovascularization associated with age-related macular degeneration (AMD) or diabetic retinopathy (DR). Age-related macular degeneration (AMD) is a progressive, degenerative disorder of the eye that initially causes loss of visual acuity. Advanced age-related macular degeneration occurs in atrophic (or "dry") and exudative (or "wet") forms. The "dry" form of advanced AMD, also referred to as "central geographic atrophy," results from atrophy to the retinal pigment epithelial layer below the retina, which causes vision loss through loss of photoreceptors (rods and cones) in the central part of the eye. The "wet" form of advanced AMD (also referred to as "neovascular" or "exudative" AMD) causes vision loss due to abnormal blood vessel growth (i.e., choroidal neovascularization) in the choriocapillaris, through Bruch's membrane, ultimately leading to blood and protein leakage below the macula. Bleeding, leaking, and scarring from these blood vessels eventually cause irreversible damage to the photoreceptors and rapid vision loss if left untreated. About 10% of patients suffering from AMD have the "wet" form. The clinical features and physiology of AMD are reviewed in, for example, de Jong et al., *N. Engl. J. Med.*, 355: 1474-1485 (2006).

[0019] Diabetic retinopathy (DR) is a complication of diabetes that can eventually lead to blindness. DR can occur in Type I or Type II diabetes, and is subdivided into a nonproliferative stage and a proliferative stage. The nonproliferative stage typically develops first, while the proliferative stage is the more advanced and severe form of the disease. Vision loss



associated with nonproliferative diabetic retinopathy occurs as a result of retinal edema, in particular diabetic macular edema, which results from vascular leakage. Focal and diffuse vascular leakage occurs as a result of microvascular abnormalities, intraretinal microaneurysms, capillary closure, and retinal hemorrhages. Prolonged periods of vascular leakage ultimately lead to thickening of the basement membrane and formation of soft and hard exudates. Nonproliferative diabetic retinopathy also is characterized by loss of retinal pericytes. The proliferative stage of diabetic retinopathy is characterized by neovascularization and fibrovascular growth (i.e., scarring involving glial and fibrous elements) from the retina or optic nerve over the inner surface of the retina or disc or into the vitreous cavity. The pathology of diabetic retinopathy is described in detail in, e.g., Shah C. A., *Indian J. Med. Sci.*, 62(12): 500-19 (2008); Aiello et al., *Diabetes Care*, 21: 143-156 (1998); and Watkins, P. J., *British Medical Journal*, 326(7395): 924-926 (2003).

**[0020]** The inventive method comprises administering a composition comprising an adeno-associated virus (AAV) vector which comprises a nucleic acid sequence encoding bevacizumab, or an antigen-binding fragment thereof. Adeno-associated virus is a member of the Parvoviridae family and comprises a linear, single-stranded DNA genome of less than about 5,000 nucleotides. AAV requires co-infection with a helper virus (i.e., an adenovirus or a herpes virus), or expression of helper genes, for efficient replication. AAV vectors used for administration of therapeutic nucleic acids have approximately 96% of the parental genome deleted, such that only the terminal repeats (ITRs), which contain recognition signals for DNA replication and packaging, remain. This eliminates immunologic or toxic side effects due to expression of viral genes. In addition, delivering specific AAV proteins to producing cells enables integration of the AAV vector comprising AAV ITRs into a specific region of the cellular genome, if desired (see, e.g., U.S. Pat. Nos. 6,342,390 and 6,821,511). Host cells comprising an integrated AAV genome show no change in cell growth or morphology (see, for example, U.S. Pat. No. 4,797,368).

**[0021]** The AAV ITRs flank the unique coding nucleotide sequences for the non-structural replication (Rep) proteins and the structural capsid (Cap) proteins (also known as virion proteins (VPs)). The terminal 145 nucleotides are self-complementary and are organized so that an energetically stable intramolecular duplex forming a T-shaped hairpin may be formed. These hairpin structures function as an origin for viral DNA replication by serving as primers for the cellular DNA polymerase complex. The Rep genes encode the Rep proteins Rep78, Rep68, Rep52, and Rep40. Rep78 and Rep68 are transcribed from the p5 promoter, and Rep 52 and Rep40 are transcribed from the p19 promoter. The Rep78 and Rep68 proteins are multifunctional DNA binding proteins that perform helicase and nickase functions during productive replication to allow for the resolution of AAV termini (see, e.g., Im et al., *Cell*, 61: 447-57 (1990)). These proteins also regulate transcription from endogenous AAV promoters and promoters within helper viruses (see, e.g., Pereira et al., *J. Virol.*, 71: 1079-1088 (1997)). The other Rep proteins modify the function of Rep78 and Rep68. The cap genes encode the capsid proteins VP1, VP2, and VP3. The cap genes are transcribed from the p40 promoter.

**[0022]** The AAV vector used in the inventive method can be generated using any AAV serotype known in the art. Several AAV serotypes and over 100 AAV variants have been isolated

from adenovirus stocks or from human or nonhuman primate tissues (reviewed in, e.g., Wu et al., *Molecular Therapy*, 14(3): 316-327 (2006)). Generally, the AAV serotypes have genomic sequences of significant homology at the nucleic acid sequence and amino acid sequence levels, such that different serotypes have an identical set of genetic functions, produce virions which are essentially physically and functionally equivalent, and replicate and assemble by practically identical mechanisms. AAV serotypes 1-6 and 7-9 are defined as "true" serotypes, in that they do not efficiently cross-react with neutralizing sera specific for all other existing and characterized serotypes. In contrast, AAV serotypes 6, 10 (also referred to as Rh10), and 11 are considered "variant" serotypes as they do not adhere to the definition of a "true" serotype. AAV serotype 2 (AAV2) has been used extensively for gene therapy applications due to its lack of pathogenicity, wide range of infectivity, and ability to establish long-term transgene expression (see, e.g., Carter, B. J., *Hum. Gene Ther.*, 16: 541-550 (2005); and Wu et al., *supra*). Genome sequences of various AAV serotypes and comparisons thereof are disclosed in, for example, GenBank Accession numbers U89790, J01901, AF043303, and AF085716; Chiorini et al., *J. Virol.*, 71: 6823-33 (1997); Srivastava et al., *J. Virol.*, 45: 555-64 (1983); Chiorini et al., *J. Virol.*, 73: 1309-1319 (1999); Rutledge et al., *J. Virol.*, 72: 309-319 (1998); and Wu et al., *J. Virol.*, 74: 8635-47 (2000).

**[0023]** AAV rep and ITR sequences are particularly conserved across most AAV serotypes. For example, the Rep78 proteins of AAV2, AAV3A, AAV3B, AAV4, and AAV6 are reportedly about 89-93% identical (see Bantel-Schaal et al., *J. Virol.*, 73(2): 939-947 (1999)). It has been reported that AAV serotypes 2, 3A, 3B, and 6 share about 82% total nucleotide sequence identity at the genome level (Bantel-Schaal et al., *supra*). Moreover, the rep sequences and ITRs of many AAV serotypes are known to efficiently cross-complement (i.e., functionally substitute) corresponding sequences from other serotypes during production of AAV particles in mammalian cells.

**[0024]** Generally, the cap proteins, which determine the cellular tropicity of the AAV particle, and related cap protein-encoding sequences, are significantly less conserved than Rep genes across different AAV serotypes. In view of the ability Rep and ITR sequences to cross-complement corresponding sequences of other serotypes, the AAV vector can comprise a mixture of serotypes and thereby be a "chimeric" or "pseudotyped" AAV vector. A chimeric AAV vector typically comprises AAV capsid proteins derived from two or more (e.g., 2, 3, 4, etc.) different AAV serotypes. In contrast, a pseudotyped AAV vector comprises one or more ITRs of one AAV serotype packaged into a capsid of another AAV serotype. Chimeric and pseudotyped AAV vectors are further described in, for example, U.S. Pat. No. 6,723,551; Flotte, *Mol. Ther.*, 13(1): 1-2 (2006); Gao et al., *J. Virol.*, 78: 6381-6388 (2004); Gao et al., *Proc. Natl. Acad. Sci. USA*, 99: 11854-11859 (2002); De et al., *Mol. Ther.*, 13: 67-76 (2006); and Gao et al., *Mol. Ther.*, 13: 77-87 (2006).

**[0025]** In one embodiment, the AAV vector is generated using an AAV that infects humans (e.g., AAV2). Alternatively, the AAV vector is generated using an AAV that infects non-human primates, such as, for example, the great apes (e.g., chimpanzees), Old World monkeys (e.g., macaques), and New World monkeys (e.g., marmosets). Preferably, the AAV vector is generated using an AAV that infects a non-human primate pseudotyped with an AAV that infects

humans. Examples of such pseudotyped AAV vectors are disclosed in, e.g., Cearley et al., *Molecular Therapy*, 13: 528-537 (2006). In one embodiment, an AAV vector can be generated which comprises a capsid protein from an AAV that infects rhesus macaques pseudotyped with AAV2 inverted terminal repeats (ITRs). In a particularly preferred embodiment, the AAV vector of the inventive method comprises a capsid protein from AAV10 (also referred to as "AAVrh.10"), which infects rhesus macaques pseudotyped with AAV2 ITRs (see, e.g., Watanabe et al., *Gene Ther.*, 17(8): 1042-1051 (2010); and Mao et al., *Hum. Gene Therapy*, 22: 1525-1535 (2011)).

**[0026]** The AAV vector of the inventive method comprises a nucleic acid sequence encoding bevacizumab, or an antigen-binding fragment thereof. "Nucleic acid sequence" is intended to encompass a polymer of DNA or RNA, i.e., a polynucleotide, which can be single-stranded or double-stranded and which can contain non-natural or altered nucleotides. The terms "nucleic acid" and "polynucleotide" as used herein refer to a polymeric form of nucleotides of any length, either ribonucleotides (RNA) or deoxyribonucleotides (DNA). These terms refer to the primary structure of the molecule, and thus include double- and single-stranded DNA; and double- and single-stranded RNA. The terms include, as equivalents, analogs of either RNA or DNA made from nucleotide analogs and modified polynucleotides such as, though not limited to, methylated and/or capped polynucleotides.

**[0027]** Bevacizumab (AVASTIN™, Genentech, Inc., South San Francisco, Calif.) is a humanized monoclonal antibody that inhibits vascular endothelial growth factor A (VEGF-A) (Ferrara et al., *Nat. Rev. Drug Discov.*, 3(5): 391-400 (2004); Avery et al., *Ophthalmology*, 113: 363-372 (2006), and U.S. Pat. No. 6,884,879). Bevacizumab was first approved by the U.S. Food and Drug Administration (FDA) for use in combination with chemotherapy for the treatment of metastatic colon cancer. Bevacizumab has since been approved for the treatment of advanced nonsquamous non-small cell lung cancer (NSCLC), metastatic renal cancer, and glioblastoma (see AVASTIN™ prescribing information).

**[0028]** One of ordinary skill in the art will appreciate that an antibody consists of four polypeptides: two identical copies of a heavy (H) chain polypeptide and two copies of a light (L) chain polypeptide. Each of the heavy chains contains one N-terminal variable ( $V_H$ ) region and three C-terminal constant ( $C_H1$ ,  $C_H2$  and  $C_H3$ ) regions, and each light chain contains one N-terminal variable ( $V_L$ ) region and one C-terminal constant ( $C_L$ ) region. The variable regions of each pair of light and heavy chains form the antigen binding site of an antibody. The AAV vector of the inventive method can comprise one or more nucleic acid sequences, each of which encodes one or more of the heavy and/or light chain polypeptides of bevacizumab. In this respect, the AAV vector of the inventive method can comprise a single nucleic acid sequence that encodes the two heavy chain polypeptides and the two light chain polypeptides of bevacizumab. Alternatively, the AAV vector of the inventive method can comprise a first nucleic acid sequence that encodes both heavy chain polypeptides of bevacizumab, and a second nucleic acid sequence that encodes both light chain polypeptides of bevacizumab. In yet another embodiment, the AAV vector can comprise a first nucleic acid sequence encoding a first heavy chain polypeptide of bevacizumab, a second nucleic acid sequence encoding a second heavy chain polypeptide of bevacizumab, a third

nucleic acid sequence encoding a first light chain polypeptide of bevacizumab, and a fourth nucleic acid sequence encoding a second light chain polypeptide of bevacizumab.

**[0029]** The AAV vector of the inventive method can comprise a nucleic acid sequence encoding full-length heavy and light chain polypeptides of bevacizumab. Nucleic acid sequences encoding the full-length heavy and light chain polypeptides of bevacizumab are known in the art (see, e.g., Watanabe et al., *supra*; Mao et al., *supra*; and U.S. Pat. No. 6,884,879) and include, for example, SEQ ID NO: 1 and SEQ ID NO: 2, respectively. The AAV vector of the inventive method can comprise a nucleic acid sequence encoding a whole bevacizumab antibody, such as, for example, SEQ ID NO: 3. In another embodiment, the AAV vector can comprise a nucleic acid sequence that encodes an antigen-binding fragment (also referred to as an "antibody fragment") of bevacizumab. The term "antigen-binding fragment," refers to one or more fragments of an antibody that retain the ability to specifically bind to an antigen (e.g., VEGF) (see, generally, Holliger et al., *Nat. Biotech.*, 23(9): 1126-1129 (2005)). Examples of antigen-binding fragments include but are not limited to (i) a Fab fragment, which is a monovalent fragment consisting of the  $V_L$ ,  $V_H$ ,  $C_L$ , and  $C_H1$  domains; (ii) a  $F(ab')_2$  fragment, which is a bivalent fragment comprising two Fab fragments linked by a disulfide bridge at the hinge region; and (iii) a Fv fragment consisting of the  $V_L$  and  $V_H$  domains of a single arm of an antibody. In one embodiment, the AAV vector can comprise a nucleic acid sequence encoding a Fab fragment of bevacizumab. An example of a Fab fragment of bevacizumab is ranibizumab (LUCENTIS™, Genentech, Inc., South San Francisco, Calif.), which is derived from the same parent molecule of bevacizumab. Ranibizumab is approved by the FDA for the treatment of wet age-related macular degeneration. Nucleic acid sequences encoding Fab fragments of bevacizumab are known in the art and are disclosed in, for example, Chen et al., *Cancer Research*, 57: 4593-4599 (1997), and U.S. Pat. No. 6,884,879.

**[0030]** The nucleic acid sequence encoding bevacizumab, or an antigen-binding fragment thereof, can be generated using methods known in the art. For example, nucleic acid sequences, polypeptides, and proteins can be recombinantly produced using standard recombinant DNA methodology (see, e.g., Sambrook et al., *Molecular Cloning: A Laboratory Manual*, 3<sup>rd</sup> ed., Cold Spring Harbor Press, Cold Spring Harbor, N.Y., 2001; and Ausubel et al., *Current Protocols in Molecular Biology*, Greene Publishing Associates and John Wiley & Sons, NY, 1994). Further, a synthetically produced nucleic acid sequence encoding bevacizumab, or an antigen-binding fragment thereof, can be isolated and/or purified from a source, such as a bacterium, an insect, or a mammal, e.g., a rat, a human, etc. Methods of isolation and purification are well-known in the art. Alternatively, the nucleic acid sequences described herein can be commercially synthesized. In this respect, the nucleic acid sequence can be synthetic, recombinant, isolated, and/or purified.

**[0031]** In addition to the nucleic acid sequence encoding bevacizumab, or an antigen-binding fragment thereof, the AAV vector preferably comprises expression control sequences, such as promoters, enhancers, polyadenylation signals, transcription terminators, internal ribosome entry sites (IRES), and the like, that provide for the expression of the nucleic acid sequence in a host cell. Exemplary expression control sequences are known in the art and described in,

for example, Goeddel, *Gene Expression Technology: Methods in Enzymology*, Vol. 185, Academic Press, San Diego, Calif. (1990).

[0032] A large number of promoters, including constitutive, inducible, and repressible promoters, from a variety of different sources are well known in the art. Representative sources of promoters include for example, virus, mammal, insect, plant, yeast, and bacteria, and suitable promoters from these sources are readily available, or can be made synthetically, based on sequences publicly available, for example, from depositories such as the ATCC as well as other commercial or individual sources. Promoters can be unidirectional (i.e., initiate transcription in one direction) or bi-directional (i.e., initiate transcription in either a 3' or 5' direction). Non-limiting examples of promoters include, for example, the T7 bacterial expression system, pBAD (araA) bacterial expression system, the cytomegalovirus (CMV) promoter, the SV40 promoter, and the RSV promoter. Inducible promoters include, for example, the Tet system (U.S. Pat. Nos. 5,464,758 and 5,814,618), the Ecdysone inducible system (No et al., *Proc. Natl. Acad. Sci.*, 93: 3346-3351 (1996)), the T-REX™ system (Invitrogen, Carlsbad, Calif.), LACSWITCH™ System (Stratagene, San Diego, Calif.), and the Cre-ERT tamoxifen inducible recombinase system (Andra et al., *Nuc. Acid. Res.*, 27: 4324-4327 (1999); *Nuc. Acid. Res.*, 28: e99 (2000); U.S. Patent 7,112,715; and Kramer & Pussenegger, *Methods Mol. Biol.*, 308: 123-144 (2005)).

[0033] The term "enhancer" as used herein, refers to a DNA sequence that increases transcription of, for example, a nucleic acid sequence to which it is operably linked. Enhancers can be located many kilobases away from the coding region of the nucleic acid sequence and can mediate the binding of regulatory factors, patterns of DNA methylation, or changes in DNA structure. A large number of enhancers from a variety of different sources are well known in the art and are available as or within cloned polynucleotides (from, e.g., depositories such as the ATCC as well as other commercial or individual sources). A number of polynucleotides comprising promoters (such as the commonly-used CMV promoter) also comprise enhancer sequences. Enhancers can be located upstream, within, or downstream of coding sequences. Preferably, the nucleic acid sequence encoding bevacizumab, or an antigen-binding fragment thereof, is operably linked to a CMV enhancer/chicken 13-actin promoter (see, e.g., Niwa et al., *Gene*, 108: 193-199 (1991); Daly et al., *Proc. Natl. Acad. Sci. U.S.A.*, 96: 2296-2300 (1999); and Sondhi et al., *Mol. Ther.*, 15: 481-491 (2007)).

[0034] The inventive method comprises administering a composition comprising the above-described AAV vector and a pharmaceutically acceptable (e.g. physiologically acceptable) carrier. Any suitable carrier can be used within the context of the invention, and such carriers are well known in the art. The choice of carrier will be determined, in part, by the particular site to which the composition may be administered and the particular method used to administer the composition. The composition optionally can be sterile. The composition can be frozen or lyophilized for storage and reconstituted in a suitable sterile carrier prior to use. The compositions can be generated in accordance with conventional techniques described in, e.g., *Remington: The Science and Practice of Pharmacy, 21st Edition*, Lippincott Williams & Wilkins, Philadelphia, Pa. (2001).

[0035] The composition is administered directly to the eye of a mammal, such as, for example, a mouse, a rat, a non-

human primate, or a human. Any administration route is appropriate so long as the composition contacts an appropriate ocular cell. The composition can be appropriately formulated and administered in the form of an injection, eye lotion, ointment, implant, and the like. The composition can be administered, for example, topically, intracamerally, subconjunctivally, intracocularly, retrobulbarly, periorcularly (e.g., subtenon delivery), subretinally, or suprachoroidally. Topical formulations are well known in the art. Patches, corneal shields (see, e.g., U.S. Pat. No. 5,185,152), ophthalmic solutions (see, e.g., U.S. Pat. No. 5,710,182), and ointments also are known in the art and can be used in the context of the inventive method. The composition also can be administered non-invasively using a needleless injection device, such as the Biojector 2000 Needle-Free Injection Management System™ available from Bioject Medical Technologies Inc. (Tigard, Oreg.).

[0036] Alternatively, the composition can be administered using invasive procedures, such as, for instance, intravitreal injection or subretinal injection, optionally preceded by a vitrectomy, or periorcular (e.g., subtenon) delivery. The composition can be injected into different compartments of the eye, e.g., the vitreal cavity or anterior chamber. Preferably, the composition is administered intravitreally, most preferably by intravitreal injection.

[0037] In a preferred embodiment of the invention, the composition is administered once to the mammal. It is believed that a single administration of the composition will result in persistent expression of bevacizumab in the eye with minimal side effects. However, in certain cases, it may be appropriate to administer the composition multiple times during a therapeutic period and/or employ multiple administration routes, e.g., subretinal and intravitreal, to ensure sufficient exposure of ocular cells to the composition. For example, the composition may be administered directly to the eye of the mammal two or more times (e.g., 2, 3, 4, 5, 6, 8, 9, or 10 or more times) during a therapeutic period.

[0038] The composition can contact any suitable ocular cell. Ocular cells associated with age-related macular degeneration include, but are not limited to, cells of neural origin, cells of all layers of the retina, especially retinal pigment epithelial cells, glial cells, and pericytes. Other ocular cells that can be contacted as a result of the inventive method include, for example, endothelial cells, iris epithelial cells, corneal cells, ciliary epithelial cells, Mueller cells, astrocytes, muscle cells surrounding and attached to the eye (e.g., cells of the lateral rectus muscle), fibroblasts (e.g., fibroblasts associated with the episclera), orbital fat cells, cells of the sclera and episclera, connective tissue cells, muscle cells, and cells of the trabecular meshwork. Other cells linked to various ocular-related diseases include, for example, fibroblasts and vascular endothelial cells.

[0039] As a result of expression of the nucleic acid sequence encoding bevacizumab, or an antigen-binding fragment thereof, in the eye, ocular neovascularization is inhibited in the mammal. Ocular neovascularization is "inhibited" if the ocular neovascularization is reduced or alleviated in a mammal (e.g., a human). Improvement, alleviation, worsening, regression, or progression of ocular neovascularization may be determined by any objective or subjective measure known in the art. Neovascularization can be measured using any suitable assay known in the art, such as, for example, the mouse ear model of neovascularization, the rat hindlimb ischemia model, the in vivo/in vitro chick chorioallantoic

membrane (CAM) assay, and the *in vitro* cellular (proliferation, migration, tube formation) and organotypic (aortic ring) assays (see, e.g., Auerbach et al., *Clin. Chem.*, 49(1): 32-40 (2003)). The inventive method can achieve partial or complete inhibition of ocular neovascularization.

[0040] In one embodiment, the inventive method is used to treat an ocular disease, such as age-related macular degeneration (AMD) or diabetic retinopathy (DR) in a mammal, preferably a human. As used herein, the terms "treatment," "treating," and the like refer to obtaining a desired pharmacologic and/or physiologic effect. Preferably, the effect is therapeutic, i.e., the effect partially or completely cures a disease and/or adverse symptom attributable to the disease. To this end, the inventive method comprises administering a "therapeutically effective amount" of the composition comprising the bevacizumab-encoding (or bevacizumab fragment-encoding) AAV vector described herein. A "therapeutically effective amount" refers to an amount effective, at dosages and for periods of time necessary, to achieve a desired therapeutic result. The therapeutically effective amount may vary according to factors such as the disease state, age, sex, and weight of the individual, and the ability of the bevacizumab-encoding (or bevacizumab fragment-encoding) AAV vector to elicit a desired response in the individual. The dose of AAV vector in the composition required to achieve a particular therapeutic effect (i.e., inhibition of ocular neovascularization) typically is administered in units of vector genome copies per cell (gc/cell) or vector genome copies/per kilogram of body weight (gc/kg), and this dose will vary based on several factors including, but not limited to, the administration route of the composition, the level of gene expression required to achieve a therapeutic effect, the specific disease or disorder being treated, any host immune response to the AAV vector, and the stability of bevacizumab in the patient. One of ordinary skill in the art can readily determine an appropriate AAV vector dose range to treat a patient having a particular ocular disease or disorder based on these and other factors that are well known in the art.

[0041] Alternatively, the pharmacologic and/or physiologic effect may be prophylactic, i.e., the effect completely or partially prevents age-related macular degeneration (AMD) or diabetic retinopathy (DR) in a mammal, preferably a human. In this respect, the inventive method comprises administering a "prophylactically effective amount" of the composition comprising the bevacizumab-encoding (or bevacizumab fragment-encoding) AAV vector described herein to a human that is predisposed to, or otherwise at risk of developing, AMD or DR. A "prophylactically effective amount" refers to an amount effective, at dosages and for periods of time necessary, to achieve a desired prophylactic result (e.g., prevention of disease onset or prevention of disease flare-ups).

[0042] The inventive method may be performed in combination with other existing therapies for age related macular degeneration and diabetic retinopathy. For example, the inventive method can be performed in conjunction with the administration of other anti-angiogenic drugs (e.g., pegaptanib (MACUGEN™—Eyeteck, Inc., Cedar Knolls, N.J.) or aflibercept (EYLEA™—Regeneron Pharmaceuticals, Inc., Tarrytown, N.Y.)), photodynamic therapy, laser surgery (i.e., laser photocoagulation), and/or surgical removal of the vitreous gel (i.e., vitrectomy).

[0043] The following examples further illustrate the invention but, of course, should not be construed as in any way limiting its scope.

#### EXAMPLE 1

[0044] This example demonstrates the generation of an adeno-associated virus (AAV) vector comprising a nucleic acid sequence encoding bevacizumab.

[0045] AAVrh.10 is a clade E, nonhuman primate (rhesus macaque)-derived gene-transfer vector that has been used in human clinical trials for gene therapy for CNS hereditary disease (Sondhi et al., *supra*). A bevacizumab-encoding AAV vector, AAVrh.10BevMab, was designed based on the AAVrh.10 capsid pseudotyped with AAV2 inverted terminal repeats (ITRs). The ITRs flanked an expression cassette containing (i) the cytomegalovirus (CMV)-enhancer chicken  $\beta$ -actin promoter (Niwa et al., *Gene*, 108: 193-199 (1991); Daly et al., *Proc. Natl. Acad. Sci. U.S.A.*, 96: 2296-2300 (1999); and Sondhi et al., *supra*), (ii) nucleic acid sequences encoding the bevacizumab heavy and light chains separated by a furin 2A self cleavage site (Fang et al., *Nat. Biotechnol.*, 23: 584-590 (2005)), and (iii) the rabbit  $\alpha$ -globin polyadenylation signal. The bevacizumab cDNA expression cassette is depicted schematically in FIG. 1.

[0046] Specifically, nucleotide sequences encoding the bevacizumab heavy and light chain variable domains were derived from the protein sequence for human kappa Fab-12, which is the original humanized version of the murine monoclonal antibody (mAb) corresponding to bevacizumab (Chen et al., *J. Mol. Biol.*, 293: 865-881 (1999)). The coding sequences for the human IgG1 constant domain were added to the variable domain by overlapping PCR.

[0047] AAVrh.10BevMab was produced by cotransfection of 293orf6 cells with the following plasmids: (1) an expression cassette plasmid (pAAVrh.10BevMab) (600 pg) comprising cDNA encoding bevacizumab; (2) a packaging plasmid (pAAV44.2) (600 pg) comprising a nucleic acid sequence encoding the AAV2 rep protein and a nucleic acid sequence encoding the AAVrh.10 cap protein (which are necessary for AAV vector replication and capsid production); and (3) pAdDF6 (1.2 mg), an adenovirus helper plasmid (Xiao et al., *J. Virol.*, 72: 2224-2232 (1998); and Sondhi et al., *supra*). 293orf6 cells, which is a human embryonic kidney cell line expressing adenovirus E1 and E4 genes (see, e.g., Gao et al., *Proc. Natl. Acad. Sci. U.S.A.*, 99: 11854-11859 (2002); and Sondhi et al., *supra*), were cotransfected with the three plasmids using POLYFECT™ (Qiagen, Valencia, Calif.). At 72 hours post-transfection, the cells were harvested, and a crude viral lysate was prepared using four cycles of freeze/thaw and clarified by centrifugation.

[0048] AAVrh.10BevMab was purified by iodixanol gradient and QHP anion-exchange chromatography. The purified AAVrh.10BevMab vector was concentrated using an Amicon Ultra-15 100K centrifugal filter device (Millipore, Billerica, MA) and stored in PBS, pH 7.4, at  $-80^{\circ}$  C. Using similar methods, three negative control AAV vectors also were prepared: (1) AAVrh.10LacZ, which comprises a nucleic acid sequence encoding  $\beta$ -galactosidase (Wang et al., *Cancer Gene Ther.*, 17: 559-570 (2010)), (2) AAVrh.10GFP, which comprises a nucleic acid sequence encoding green fluorescent protein (GFP) (Sondhi et al., *supra*), and (3) AAVrh.10cV, which comprises a nucleic acid sequence encoding an unrelated antibody against *Y. pestis* V antigen. AAV vector genome titers were determined by quantitative TaqMan real-

time PCR analysis using a chicken  $\beta$ -actin promoter-specific primer-probe set (Applied Biosystems, Foster City, Calif.).

[0049] The results of this example confirm the production of an AAV vector comprising a nucleic acid sequence encoding bevacizumab in accordance with the invention.

#### EXAMPLE 2

[0050] This example demonstrates the expression and specificity of bevacizumab expressed from an AAV vector in vitro and in vivo.

[0051] The expression and specificity of bevacizumab encoded by AAVrh.10BeyMab (described in Example 1) in vitro were assessed using Western blot analysis. For expression analysis, 293orfl6 cells were infected with AAVrh.10BeyMab ( $2 \times 10^8$  genome copies (gc)/cell), and infected cell supernatants were harvested 72 hours after infection. Supernatants were concentrated by passage through Ultracel YM-10 centrifugal filters (Millipore, Billerica, Mass.) and evaluated by Western analysis using a peroxidase-conjugated goat anti-human kappa light chain antibody (Sigma, St. Louis, Mo.) under nonreducing conditions or reducing conditions with the addition of peroxidase-conjugated goat anti-human IgG antibody (Santa Cruz Biotechnology, Santa Cruz, Calif.). Detection was by enhanced chemiluminescence reagent (GE Healthcare Life Sciences, Piscataway, N.J.).

[0052] The results of the Western analysis are shown in FIGS. 2A and 2B, and established the expression of the intact heavy and light chains of bevacizumab in 293orfl6 cells and their ability to form the intact antibody. Infection with the control AAVrh.10GFP vector under identical reducing or nonreducing conditions gave no detectable bands for human antibody.

[0053] Bevacizumab specificity was determined by Western blot analysis against human VEGF-165 and mouse VEGF-164 (Watanabe et al., *Hum. Gene Ther.*, 19: 300-310 (2008)). AAVrh.10BeyMab cell supernatants were used as the primary antibody, followed by a peroxidase-conjugated goat anti-human kappa light-chain antibody and enhanced chemiluminescence reagent. The results of the Western analysis are shown in FIG. 2C. Only the human form of VEGF was recognized from the known specificity of bevacizumab. In contrast, supernatants from AAVrh.10GFP-infected cells did not recognize either VEGF protein.

[0054] The expression and specificity of bevacizumab in vivo were assessed after administering AAVrh.10BeyMab to mice. Specifically, male C57BL/6 mice, 6-8 weeks of age, were obtained from The Jackson Laboratory (Bar Harbor, Me.) and housed under pathogen-free conditions. AAVrh.10BeyMab ( $10^{11}$  gc) or negative control AAVrh.10LacZ ( $10^{11}$  gc) in 100  $\mu$ l of PBS was administered by the intravenous route to C57BL/6 mice through the tail vein.

[0055] At various timepoints 0-24 weeks after vector administration, blood was collected through the tail vein, allowed to clot for 60 minutes, and centrifuged at 13,000 rpm for 10 minutes. Bevacizumab levels in serum were assessed by enzyme linked immunosorbent assay (ELISA) using flat-bottomed 96-well EIA/RIA plates (Corning Life Sciences, Lowell, Mass.) coated overnight at 4 $^{\circ}$ C with 0.2  $\mu$ g of human VEGF-165 per well in a total volume of 100  $\mu$ l of 0.05 M carbonate buffer and 0.01% thimerosal. The plates were washed three times with PBS and blocked with 5% dry milk in PBS for 60 minutes. The plates were then washed three times with PBS containing 0.05% Tween 20. Serial serum dilutions in PBS containing 1% dry milk were added to each

well and incubated for 60 minutes. The positive control standard was 25  $\mu$ g/ $\mu$ l bevacizumab (Genentech, Inc., South San Francisco, Calif.). The plates were washed three times with PBS containing 0.05% Tween 20 followed by 100  $\mu$ l/well 1:5,000 diluted peroxidase-conjugated goat anti-human kappa light chain antibody in PBS containing 1% dry milk for 60 minutes. The plates were then washed four times with PBS containing 0.05% Tween 20 and once with PBS. Peroxidase substrate (100  $\mu$ l/well; Bio-Rad, Hercules, Calif.) was added, and the reaction was stopped at 15 minutes by addition of 2% oxalic acid (100  $\mu$ l/well). Absorbance at 415 nm was measured. Antibody titers were calculated using a log (OD)-log (dilution) interpolation model with a cutoff value equal to two-fold the absorbance of background (Watanabe et al., supra). The titers were converted to a bevacizumab concentration using results from the bevacizumab standard data curve.

[0056] The results of the ELISA assay are shown in FIG. 2D. Bevacizumab expression levels peaked at about 12 weeks post-administration and were sustained through the 24 week experimental period. Bevacizumab was not detected in the serum of mice that received intravenous injection of the control AAVrh.10LacZ vector.

[0057] The results of this example confirm that a nucleic acid sequence encoding bevacizumab is efficiently expressed in vitro and in vivo when delivered via an AAV vector.

#### EXAMPLE 3

[0058] This example demonstrates the expression and localization of bevacizumab following intravitreal administration of an AAV vector comprising a nucleic acid sequence encoding bevacizumab.

[0059] AAVrh.10BeyMab ( $10^{10}$  gc) (described in Example 1) and control vector AAVrh.10GFP ( $10^{10}$  gc) (described in Example 1) in 1  $\mu$ l of PBS were administered by intravitreal injection to the left and right eyes, respectively, of C57BL/6 male mice. Intravitreal injection was performed under a dissecting microscope with a 32-gauge needle (Hamilton Company, Reno, Nev.). At various timepoints 0-24 weeks after vector administration, mice were sacrificed with CO<sub>2</sub>. Eyes were collected, homogenized by sonication in 100  $\mu$ l of T-PER tissue protein extraction reagent (Thermo Scientific, Rockford, Ill.), and centrifuged at 13,000 rpm for five minutes, followed by supernatant collection.

[0060] Bevacizumab expression levels in the supernatant were assessed by a human VEGF-specific ELISA as described in Example 2. Bevacizumab levels were standardized to total protein levels, which were assayed by a bicinchoninic protein assay (Thermo Scientific, Waltham, Mass.). The expression of bevacizumab in the eye at 12 weeks post-intravitreal injection was evaluated by Western blot analysis as described in Example 2.

[0061] To identify the intraocular site of bevacizumab expression, male C57BL/6 mice were injected with AAVrh.10BeyMab and AAVrh.10GFP, as described above, or were left uninjected. Treated and control virus-injected eyes were enucleated five weeks after intravitreal injection, fixed in formalin, embedded in paraffin wax, sectioned, deparaffinized, and treated sequentially with biotin-conjugated donkey anti-human IgG(H+L) (dilution 1:100; Jackson ImmunoResearch, West Grove, Pa.) and Cy3-conjugated streptavidin (dilution 1:1,000; Jackson ImmunoResearch, West Grove, Pa.). Nuclei were stained with 4'-diamidino-2-phenylindole (DAPI; dilution 1:2,000; Life Technologies,

Carlsbad, Calif.). The sections were embedded (Histoserv, Germantown, Md.) and examined with a fluorescence microscope.

[0062] The results of the VEGF-specific ELISA are shown in FIG. 3A. Bevacizumab levels were above 100 pg/pg total protein at two weeks post vector administration and remained at similar levels up to the last time point evaluated at 24 weeks. Bevacizumab was not detected in the eyes from mice that received intravitreal administration of the control vector AAVrh.10cV. The expression of bevacizumab in the eye post-intravitreal administration of AAVrh.10BevMab was confirmed by Western blot analysis, the results of which are shown in FIG. 3B. Soluble protein collected from the AAVrh.10BevMab-injected eyes was positive for the presence of human antibody heavy and light chains, whereas no human antibody was detected in eyes injected with AAVrh.10cV, which expresses a mouse monoclonal antibody, or uninjected naive eyes.

[0063] Bevacizumab was localized to the retinal pigment epithelium (RPE), and bevacizumab staining was not observed in uninjected eyes or eyes injected with the control AAVrh.10cV vector. Intravitreal administration of AAVrh.10 has previously been reported to efficiently transduce a wide range of retinal cells, including the RPE, the ganglion cell layer, the amacrine cells of the inner nuclear layer, the Muller and horizontal cells, as well as bipolar cells (see, e.g., Giove et al., *Exp. Eye Res.*, 91: 652-659 (2010)). As such, multiple immunohistochemical sections were searched for staining of these cell types, but no staining was observed in any cell type other than RPE.

[0064] The results of this example confirm that bevacizumab is efficiently expressed in mice following intravitreal administration of an AAV vector comprising a nucleic acid sequence encoding bevacizumab, and that bevacizumab expression is localized to retinal pigment epithelium.

#### EXAMPLE 4

[0065] This example demonstrates a method of inhibiting ocular neovascularization in a mouse by administering directly to the eye of a mouse a composition comprising a bevacizumab-encoding AAV vector and a carrier.

[0066] The efficacy of bevacizumab expressed from the AAVrh.10BevMab vector was assessed in the transgenic rho/

VEGF mouse model. Rho/VEGF mice (Okamoto et al., *Am J Pathol.*, 151: 281-291 (1997)) were housed and bred under pathogen-free conditions. At postnatal day 14, homozygous rho/VEGF mice were injected intravitreally with 1  $\mu$ l of PBS to one eye and  $10^{10}$  gc of AAVrh.10BevMab in 1  $\mu$ l of PBS to the other eye. At 2, 14, 28, 84, and 168 days post-injection, mice were anesthetized and perfused with 2 ml of 25 mg/ml fluorescein-labeled dextran ( $2 \times 10^6$  average molecular weight; Sigma, St. Louis, Mo.) in PBS. Eyes were removed and fixed for 1 hr in 4% paraformaldehyde/PBS. The cornea and lens were removed, and the entire retina was carefully dissected from the eyecup, radially cut from the edge of the retina to the equator in all four quadrants, and flat-mounted in BRIGHT™ Gold antifade reagent (Life Technologies, Carlsbad, Calif.). The retinas were examined by fluorescence microscopy at 200x, providing a narrow depth of field to enable subretinal focus for neovascular buds on the outer surface of the retina. AxioVision LE (Carl Zeiss International, Oberkochen, Germany) digital image analysis software was used by three investigators blinded to treatment group for quantifying subretinal neovascular growth area per retina.

[0067] In low-magnification views, multiple large areas of budding and vascular leak were evident in the PBS-treated eye of the mice at 168 days post injection; however, these areas were largely absent in the treated eye. By examining neovascular buds at higher power, the time-dependent increase in budding was observed. At two days post-injection, AAVrh.10BevMab- and PBS-injected eyes appeared to exhibit similar amounts of neovascular buds, but at later time points AAVrh.10BevMab-injected eyes exhibited significantly fewer subretinal neovascular buds than retinas from eyes injected with PBS.

[0068] The subretinal neovascular buds were quantified by three investigators blinded to treatment group, and the results of this analysis are shown in FIGS. 4A-4C. As an example of the individual data from each observer, at 84 days post-injection, the data showed a significantly reduced area of subretinal neovascular buds in the retinas of AAVrh.10BevMab-injected eyes compared with eyes injected with PBS (see FIG. 4A). The inter-observer variability in quantifying the neovascular buds was not significant at the multiple test correction threshold, as shown in Table 1.

TABLE 1

Observer	Treatment	Area of NV per retina (mm <sup>2</sup> × 10 <sup>-2</sup> ) (days)					
		2	14	28	84	168	
1.	PBS	0.90 ± 0.23	1.84 ± 0.20	1.52 ± 0.11	3.61 ± 0.79	4.29 ± 1.09	
	AAVrh.10BevMab	0.85 ± 0.22	0.81 ± 0.10	0.35 ± 0.07	1.08 ± 0.37	0.43 ± 0.07	
2.	PBS	1.17 ± 0.30	1.98 ± 0.31	1.98 ± 0.13	3.44 ± 0.70	4.40 ± 1.08	
	AAVrh.10BevMab	1.22 ± 0.33	1.03 ± 0.18	0.33 ± 0.08	1.13 ± 0.33	0.45 ± 0.08	
3.	PBS	1.02 ± 0.28	1.89 ± 0.21	0.94 ± 0.11	3.21 ± 0.73	4.28 ± 1.00	
	AAVrh.10BevMab	1.00 ± 0.33	0.82 ± 0.12	0.34 ± 0.09	1.13 ± 0.33	0.45 ± 0.07	
p value	For treatment	>0.96	<0.0001**	<0.0001**	<0.0001**	<0.0001**	
	(2-way ANOVA)	For observer	>0.52	>0.243	>0.76	>0.92	>0.88
p value	For treatment	>0.9	<0.0001**	<0.0001**	<0.0001**	<0.0001**	
	(3-way ANOVA)	For observer	>0.01*	>0.028	>0.49	>0.86	>0.68
	For mouse	<0.0001**	<0.0001**	<0.0001**	<0.0001**	<0.0001**	

Observer means and standard deviations were calculated after summing over mice. The p-values for treatment, observer, and mouse were assessed using permutations after fitting a two-factor and three-factor ANOVA model.

NV = neovascularization.

\*p < 0.05, but not significant after a multiple test correction.

\*\*significant test results.



[0069] Data from the three observers was first averaged for each eye, and then the average and standard error for each condition and time point were plotted (see FIG. 4B). Consistent with the fluorescence microscopy results, at two days post-injection there was no significant reduction in the area of subretinal neovascular buds for AAVrh.10BevMab-injected eyes; but from 14 to 168 days post-injection, eyes injected with AAVrh.10BevMab exhibited a significantly less area of subretinal neovascular buds as compared with retinas from eyes injected with PBS (see FIG. 4B). The reduction ratio was calculated as:

$$\frac{(\text{mean neovascular bud area in PBS-injected eye at indicated time point}) - (\text{neovascular bud area in AAVrh.10BevMab-injected eye at indicated time point})}{(\text{mean neovascular bud area in PBS-injected eye})}$$

[0070] The reduction ratio showed no reduction at two days post-injection, but significant reduction was observed at 14 days (49%) to 168 days (90%) post-injection (see FIG. 4C).

[0071] The results of this example confirm that a single intravitreal administration of AAVrh.10BevMab can persistently suppress subretinal neovascularization in a mouse in accordance with the inventive method.

[0072] All references, including publications, patent applications, and patents, cited herein are hereby incorporated by reference to the same extent as if each reference were individually and specifically indicated to be incorporated by reference and were set forth in its entirety herein.

[0073] The use of the terms "a" and "an" and "the" and similar referents in the context of describing the invention (especially in the context of the following claims) are to be construed to cover both the singular and the plural, unless

otherwise indicated herein or clearly contradicted by context. The terms "comprising," "having," "including," and "containing" are to be construed as open-ended terms (i.e., meaning "including, but not limited to,") unless otherwise noted. Recitation of ranges of values herein are merely intended to serve as a shorthand method of referring individually to each separate value falling within the range, unless otherwise indicated herein, and each separate value is incorporated into the specification as if it were individually recited herein. All methods described herein can be performed in any suitable order unless otherwise indicated herein or otherwise clearly contradicted by context. The use of any and all examples, or exemplary language (e.g., "such as") provided herein, is intended merely to better illuminate the invention and does not pose a limitation on the scope of the invention unless otherwise claimed. No language in the specification should be construed as indicating any non-claimed element as essential to the practice of the invention.

[0074] Preferred embodiments of this invention are described herein, including the best mode known to the inventors for carrying out the invention. Variations of those preferred embodiments may become apparent to those of ordinary skill in the art upon reading the foregoing description. The inventors expect skilled artisans to employ such variations as appropriate, and the inventors intend for the invention to be practiced otherwise than as specifically described herein. Accordingly, this invention includes all modifications and equivalents of the subject matter recited in the claims appended hereto as permitted by applicable law. Moreover, any combination of the above-described elements in all possible variations thereof is encompassed by the invention unless otherwise indicated herein or otherwise clearly contradicted by context.

SEQUENCE LISTING

```

<150> NUMBER OF SEQ ID NOS: 2
<210> SEQ ID NO 1
<211> LENGTH: 369
<212> TYPE: DNA
<213> ORGANISM: Artificial Sequence
<220> FEATURE:
<223> OTHER INFORMATION: Synthetic
<400> SEQUENCE: 1
gaagtgagga cgtctggagc tggcggagga cctctcagaa ctgggggggc actgagactc 60
tcctgtgag cctctggata cactcttact aactatgggx tgaaactgggt ccgcwaaagt 120
ccagggaagg cctctggatg gctcggatgg atcaatccct atcagggaga cctcacttat 180
gtagcagatt ctaaaaggag atcaacttcc tctctagaaa ctgcaagag taccggctat 240
ctgcgaatga acagctctgag agctgaggaa ccggcggctgt attatctgta aaaaatcccc 300
cattactcag ctgagctgca ttggtatctt gatgtctggg gccagggaac cctggtccac 360
gtctctctca
<210> SEQ ID NO 2
<211> LENGTH: 321
<212> TYPE: DNA
<213> ORGANISM: Artificial Sequence
<220> FEATURE:
<223> OTHER INFORMATION: Synthetic
    
```

-continued

<400> SEQUENCE: 2  
 gatatccaga tgcaccagtc ccgaagatcc ctgtccgect ctgtgggaga tagggtaact 60  
 atccaccgca ggcaccagtc ggcaccagtc aactatctga actgggtatca acgagaaccc 120  
 ggaaaagctc cgaaaagctc gatttaacttt accagtagtc tccatagttg agtcccttct 180  
 cgtctctctg gatccgcttc tgggacggat ttcactctga ccctccagcg tctgcagcca 240  
 gaagacttcg caaattatta ctgtccagcg tacagccagg ttccctggac atttggacag 300  
 ggtacraagg tggagatcaa \*

<410> SEQ ID NO 3  
 <211> LENGTH: 4191  
 <212> TYPE: DNA  
 <213> ORGANISM: Artificial Sequence  
 <220> FEATURE:  
 <410> OTHER INFORMATION: Synthetic

<400> SEQUENCE: 3  
 ggtaccaccc tggagtttgg actgagctgg gtttctcttg ttgctatctt aasaggtgac 60  
 cagttgcgag tgaagctcgt gggctctcgg ggggctcttg tcaagcttgg ggggtccctg 120  
 agactctctt gtcagagctc tggataccac ttacttaact atgggcatgaa ctgggtccgg 180  
 caagctccag ggaagggctt ggggtgggct ggtatgatta atccctatcc gggagaaact 240  
 atttccgag ccgattctaa aaggccgatt accctctctc tggaccctag caagagctac 300  
 gggctctctg caatgaaacg tctggagctt gaggacacgg ccggtcttta ttgtgcaaaa 360  
 taccccact actangctag tagtcaattg tactttgatg ttctggggca gggaaacccg 420  
 gttaccctgt cctccagctc caccacagggc cctctcggct tccctctggc accctctctc 480  
 aagagcaact ctggggggcc agggggcttg ggcctgcttg tcaagggata ctctcccgaa 540  
 ccggtgacgg tgccttggaa ctccagctcc ctgacacagc gctgtgacac ctccctggct 600  
 gttctaccgt cctccagctc ccaactctctc agcagcttgg tgaacgtgac ctccagcagc 660  
 ttgggcaccc agacctaac ctgcaacgtg aatcccaagg ccagcaaac ccaggctggc 720  
 aagaagctg agcccaactc ttgtgacaaa acccaaacat gcccaacgtg cccagcaact 780  
 gggctctctg ggggacctgc agtctctctc ttcccccxa aaccccaagg caccctcttg 840  
 atctcccgga cccctgaggt caactccttg gttgtggatg tggctccagc agacctctag 900  
 gtcaggctca accgttccgt ggcagctcctg ggggtgcata atgcaaacac aaggtctggg 960  
 gaggagctgt accaacagcc gttccctctg gttcagcttc tccactctt gttccctggc 1020  
 ttgctgaaat gcaagggatc caagtgcag gttcccaacc aagccctccc agccccctc 1080  
 ggaacaaacc tctccaaagg caagggctcg cccctgagaa caccagctga caccctgccc 1140  
 cctctccggg atgagctgac caagaaatcc gttcagctga cctccctctt caagagcttc 1200  
 tctctccagc caatctcctt ggggtgggag agtcaatggc agtctggaga caactcaag 1260  
 accagctctc cctgtctgga ctccagcagg tctctctctc tctccagcga gctccctctg 1320  
 gcaaacagca ggtggcagca ggggaacgtc ttctcaagct ccgtgagca tggggctctg 1380  
 caaacccact caacgcagaa gggccctctc ctgtctccgg gtagcaagag gggagcaact 1440  
 gtagaacaga ctctgaactt tgacctctc agttggcgg gagagctaga gttcaaacct 1500  
 gggctccgta cccagatgac ctagtcccca agctctctgt cccctctctg gggcctagg 1560



-continued-

```

gtcaccatca cctgcagcgc cagtcaggac atcagcaact atctgaaactg gtatcaacag 1620
aaacccggaa aagctccgaa agtactgatt taccttaaca gtatctccca tagtggagt 1630
cctctctcgt tctctggacc cggctctggg accgattcca ctctgacctc cagcagctcc 1740
cagccagaaag acttcgacac tctattactgt cagcagtaaa gacaggttcc ctggacattt 1800
ggacagggta ctacggggg gatcaaaaga aatgtggctg cacacactgt ctccaccttc 1860
ccgcatcng atgagragct gaactctgga acgcttcng tctgtgtcct gctgaataac 1920
tctatccca gagagccaa agtaccgtg aggtctgata acgacctcca atcgggtaac 1980
ctccagggg gtctccagc gaagggcagc aagggcagca ctatccagct cagcagcagc 2040
ctgactctga gcaagccaga ctccagaaa cacaaagctc acgctctgga agtccacctc 2100
cagggctga gttccgctt caaaaagcgc ttcacaggg gagagtgta aggaactgag 2160
g 2161
    
```

1. A method of inhibiting ocular neovascularization in a mammal, which method comprises administering a composition comprising an adeno-associated virus (AAV) vector and a pharmaceutically acceptable carrier directly to the eye of a mammal, wherein the AAV vector comprises a nucleic acid sequence encoding bevacizumab, or an antigen-binding fragment thereof, whereupon the nucleic acid sequence is expressed in the eye and ocular neovascularization is inhibited in the mammal.

2. The method of claim 1, wherein the nucleic acid sequence encodes bevacizumab.

3. The method of claim 2, wherein the nucleic acid sequence encodes an antigen-binding fragment of bevacizumab.

4. The method of claim 1, wherein the mammal is a human.

5. The method of claim 1, wherein the mammal is a mouse.

6. The method of claim 1, wherein the ocular neovascularization is associated with age-related macular degeneration (AMD) or diabetic retinopathy (DR).

7. The method of claim 1, wherein the composition is administered to the mammal intravitreally.

8. The method of claim 1, wherein the composition is administered once to the eye of the mammal.

9. The method of claim 1, wherein the AAV vector is generated using a non-human adeno-associated virus.

10. The method of claim 9, wherein the AAV vector is generated using a rhesus macaque adeno-associated virus.

\* \* \* \* \*